Immunological implications of feto-maternal microchimerism in HLA-haploidentical stem cell transplantation

Dissertation

zur Erlangung des Grades
eines Doktors der Naturwissenschaften (Dr. rer. nat.)

Fachbereich Chemie
der Fakultät für Mathematik, Informatik und Naturwissenschaften,
Universität Hamburg

vorgelegt von

Lena-Marie Martin
aus Lüneburg

Hamburg 2020

Vorgelegt am: 24.09.2020

Gutachter

1. Gutachter
   Prof. Dr. Ingo Müller
   Department of Pediatric Hematology and Oncology, Head of Pediatric Stem Cell Transplantation and Immunology, University Medical Center, Hamburg-Eppendorf

2. Gutachter
   Prof. Dr. Wolfram Brune
   Department of Virus-Host-Interactions, Heinrich Pette Institute (HPI), Leibniz Institute for Experimental Virology, Hamburg

Tag der Disputation: 20.11.2020

Prüfungskommission

1. Vorsitz:	Prof. Dr. Sebastian Wicha
2. Stellvertretender Vorsitz:	Prof. Dr. Ingo Müller
3. Mitglied mit Betreuungsrecht im FB Chemie:	Prof. Dr. Ralph Holl

Bearbeitungszeitraum: Juni 2017 - September 2020

Diese Arbeit wurde unter der Leitung von Prof. Dr. Ingo Müller am Forschungsinstitut Kinderkrebs-Zentrum in Hamburg in der Sektion für Pädiatrische Stammzelltransplantation und Immunologie, Klinik für Pädiatrische Hämatologie und Onkologie des Universitätsklinikums Hamburg-Eppendorf angefertigt.

I. Table of contents

II. List of abbreviations

Abbreviation	Name
°C	Degree Celsius
ALL	Acute lymphoblastic leukemia
AML	Acute myeloid leukemia
ASCT2	Sodium-dependent neutral amino acid transporter
BM	Bone marrow
CAR	Chimeric antigen receptor
CB	Cord blood
CD	Cluster of differentiation
Cer	Cerulean
CMV	Cytomegalovirus
ddH_2O	Double distilled H_2O
ddPCR	Digital droplet PCR
DMEM	Dulbecco's modified eagle medium
DNA	Deoxyribonucleic acid
dNK	Decidual NK cells
E.coli	*Escherichia coli*
eGFP	Enhanced green fluorescent protein
et al.	Et alii
EtBr	Ethidium bromide
FACS	Fluorescence activated cell sorting
FBS	Fetal bovine serum
FM	Fetal microchimerism
FM cells	Fetal cells in the maternal blood system
FP	Fluorescent protein
GvHD	Graft-versus-host disease
GvL	Graft-versus-leukemia
h	Hour
Haplo	Haploidentical
HCK	Hematopoietic cell kinase
hHSCT	Haploidentical hematopoietic stem cell transplantation
HLA	Human leukocyte antigen
HLH	Hemophagocytic lymphohistiocytosis
HSA	Human serum albumin
HSC	Hematopoietic stem cell
HSCT	Hematopoietic stem cell transplantation
IFNγ	Interferon γ
IL	Interleukin
InDel	Insertion/deletion polymorphism
Iono	Ionomycin
IPEX	Immune dysregulation polyendocrinopathy enteropathy X-linked syndrome
IRES	Internal ribosome entry site
KIR	Killer cell immunoglobulin- like receptor

LAMP-1	Lysosomal-associated membrane protein-1
LDLR	Low density lipoprotein receptor
LILR	Leukocyte Ig-like receptors
lin	Lineage
LTi	Lymphoid-tissue-inducers
mg	Milligram
MHC	Major histocompatibility complex
min	Minute(s)
mL	Milliliter
MM	Maternal microchimerism
MOI	Multiplicities of infections
MPSI	Mucopolysaccharidosis type I
NB	Neuroblastoma
NCR	Natural cytotoxicity receptors
NIMA	Non inherited maternal antigens
NIPA	Non inherited paternal antigen
NK cell	Natural killer cell
NRM	Non-relapse mortality
PBMCs	Peripheral blood mononuclear cells
PBS	Phosphate buffered saline
PBSC	Peripheral blood mobilized stem cells
PCR	Polymerase chain reaction
PFA	Paraformaldehyde
PI	Propidium iodide
PMA	Phorbol 12-myristate 13-acetate
PrSf	Protamine sulfate
RD114/TR	RD114 feline leukemia virus protein
RNA	Ribonucleic acid
RT	Room temperature
RT-PCR	Real-time quantitative polymerase chain reaction
SFFV	Spleen focus-forming virus promotor
SIN	Self-inactivating
SSP-PCR	Sequence specific primers polymerase chain reaction
T-NHL	T cell non-Hodgkin lymphoma
Tm	Melting temperature
TNFα	Tumor necrosis factor α
T_{reg}	Regulatory T cells
TRM	Transplant-related mortality
VF-1	Vectofusin-1
VSV-G	Envelope proteins glycoprotein of vesicular stomatitis virus
wb	Whole blood
wt	Wild type
µg	Microgram
µL	Microliter

III. List of figures

IV. List of tables

1. Abstract

A persisting fetal microchimerism (FM^+) in the maternal peripheral blood is associated with a significantly increased survival of up to 42% of children after haploidentical hematopoietic stem cell transplantation (hHSCT) compared to father-to-child transplantations and transplantations from mothers without detectable fetal cells (FM^-). FM means that filial cells are still detectable in the maternal blood system postpartum. These persisting filial cells are termed FM cells. The biological function of FM cells is still controversial. There is a lack of exact quantification and phenotypical characterization, and there are no studies that have identified genetic features that might affect the continued presence of FM cells in some but not all mothers. To more precisely quantify the filial cells, a digital droplet PCR protocol was established. With this protocol, an FM was detected in 37% of all analyzed mothers. Moreover, the FM cells were phenotypically characterized. FM cells had a stem cell-like phenotype marked by expression of $CD34^+$ $CD38^{+/-}$. Additionally, detection of $CD34^+$ and/or $CD133^+$ suggests the presence of FM cells with a long-term stem cell phenotype.

Interactions of killer immunoglobulin-like receptors (KIRs) with their ligands, the human leukocyte antigen (HLA) molecules, have been important for rejection of foreign tissue. In 51 analyzed mother-child pairs, three independent maternal genetic parameters correlated with the persistence of an FM: presence of an HLA-C1 allele, absence of KIR2DL3, and a centromeric KIR B/B motif. When mother and child were HLA-C matched, an FM was favored. In studies analyzing mismatched HSCT, a beneficial effect of KIR-ligand mismatch between donor and recipient had been detected. Therefore, beyond genetic factors, the effect of FM and different KIR phenotype/HLA combinations on the alloreactivity of parental NK cells against filial blasts was analyzed. NK cells from FM^+ mothers showed an up to 45% higher activation compared to NK cells from FM^- mothers against their children's leukemic blasts. Particularly, a significantly higher activation of KIR2DS1 and KIR2DS5 expressing NK cells was detected in FM^+ mothers compared to FM^- mothers after co-culture with their children's leukemic blasts. These activated cells were potentially educated to recognize and tolerate the filial cells and can therefore distinguish between filial healthy and leukemic cells. However, an effect of an FM on the cytotoxicity of maternal NK cell against filial leukemic blasts was not detected *in vitro*, suggesting an important role of other immune effector cells, e.g. alloreactive T cells.

A cohort of sibling transplantations was analyzed for the occurrence of a trans-maternal microchimerism (TM). A TM was detected in 62% of the siblings, but occurrence of TM was independent of donor or recipient HLA or KIR and did not affect the outcome.

In the second part of this study, the feasibility to equip human NK92-MI cells and primary NK cells with distinct KIR receptors to modulate their effector function was shown. Single KIR expressing NK92-MI cell lines (NK92-MI-KIR^+) were successfully generated with the following

KIRs: KIR2DL1, KIR2DS1 and KIR2DS2. Functionality of NK92-MI-KIR$^+$ cell lines against single KIR ligand expressing target cell lines or primary leukemic blasts, analyzed by degranulation and cytotoxicity, was not significantly affected by the expressed KIR. This suggest that the cells are potentially inhibited by other (not KIR) receptors expressed on their surface. In addition, NK92-MI cells do not need polarization to exert their effector function, indicating that NK92-MI cells are not a suitable model cell line for functional analysis of KIR receptor insertion. Subsequently, primary NK cells were successfully transduced to express distinct KIRs using alpharetroviral particles that were pseudotyped with RD114/TR. Their functionality was not impaired by the viral challenge, and analysis of their functionality in a small cohort indicated that modification of primary NK cells with distinct KIRs might affect their reactivity, building the basis for further functional analyses of modified primary NK cells. These modified NK cells equipped, with an optimized effector function, could be used to treat patients post-HSCT in cases of viral infections or relapse.

2. Zusammenfassung

Ein fetaler Mikrochimärismus (FM^+) im peripheren Blut von Müttern ist mit einer um bis zu 42% besseren Überlebensrate nach T-Zell-depletierter haploidenter Stammzelltransplantation (hHSCT) von Mutter-zu-Kind assoziiert. Dies wurde im Vergleich zu hHSCTs beobachtet, in denen Kinder Stammzellen von einer Mutter ohne Nachweis von kindlichen Zellen im Peripherblut (FM^-) erhalten haben oder aber die Stammzellen von ihrem Vater. Bei einem FM handelt es sich um kindliche Zellen, die noch nach der Geburt in dem Peripherblut von Müttern nachweisbar sind, sogenannte FM Zellen. Die biologische Funktion der FM Zellen ist umstritten. Zudem mangelt es an genauer Quantifizierung und phänotypischer Charakterisierung. Derzeit sind keine Studien bekannt, in denen der Einfluss mütterlicher und/oder kindlicher genetischer Merkmale auf einen FM untersucht wurde.

In dieser Arbeit wurde ein Protokoll für eine digitale droplet PCR etabliert, welches die genaue Quantifizierung der kindlichen Zellen ermöglicht. In 37% der analysierten Mütter konnte ein FM detektiert werden. Die FM Zellen wiesen einen Stammzell-ähnlichen Phänotypen auf und zeigten sich $CD34^+$ $CD38^{+/-}$. Zudem konnten $CD34^+$ und/oder $CD133^+$ FM Zellen detektiert werden, was auf langzeitrepopulierenden Stammzellen in dieser Population hindeutet.

Die Interaktion von Killer Zell Immunglobulin-ähnlichen Rezeptoren (KIRs) mit ihren Liganden, den humanen Leukozyten Antigen (HLA) Molekülen, spielt eine entscheidende Funktion in der Abstoßungsreaktion fremden Gewebes. In 51 untersuchten Mutter/Patienten Paaren korrelierten drei unabhängige mütterliche Merkmale mit der Persistenz eines FM: das Vorhandensein eines HLA-C1 Allels, eines zentromerischen KIR B/B Motives, sowie die Abwesenheit von KIR2DL3. Darüber hinaus wurde ein FM begünstig, wenn Mutter und Kind HLA-ident waren.

Studien in HSCT, mit teilweiser HLA Ungleichheit, zeigten, dass eine KIR-Liganden Ungleichheit die Reaktivität von NK Zellen begünstigt. Daher wurde im Folgenden die Wirkung eines FM sowie von KIR Phänotyp/HLA Kombinationen auf die Reaktivität der elterlichen NK Zellen untersucht. Die NK Zellen von FM^+ Müttern zeigten eine um bis zu 45% stärkere Aktivierung nach der Kultivierung mit den leukämischen Blasten ihres Kindes im Vergleich zu NK Zellen von FM^- Müttern. Zudem waren signifikant mehr KIR2DS1 und KIR2DS5 exprimierende NK Zellen aktiviert, wenn diese NK Zellen aus FM^+ Müttern stammten. Dies lässt vermuten, dass die mütterlichen NK Zellen gelernt haben die kindlichen Zellen zu erkennen und zu tolerieren. Aufgrund dessen könnten sie zwischen gesunden kindlichen und leukämischen Zellen unterscheiden. Ein direkter Einfluss eines FM auf die Zytotoxizität der mütterlichen NK Zellen gegen die kindlichen Blasten konnte nicht gezeigt werden, was vermuten lässt, dass hier andere Effektorzellen eine wichtige Funktion ausüben, z.B. alloreaktive T-Zellen.

Eine Gruppe von Geschwistertransplantationen wurde auf das Vorhandensein eines trans-maternalen Mikrochimärismus (TM) untersucht. Ein TM wurde in 62% der Geschwister detektiert. Weder der HLA- noch der KIR-Genotyp des Spenders oder Empfängers beeinflussten das Auftreten eines TM und es konnte kein Einfluss auf das Überleben der Kinder nach Stammzelltransplantation nachgewiesen werden.

Im zweiten Teil dieser Arbeit konnte gezeigt werden, dass die humane Zelllinie NK92-MI, sowie primäre NK Zellen modifiziert werden können, um bestimmte KIR Rezeptoren zu exprimieren. Einzel-KIR exprimierende NK92-MI Zelllinien (NK92-MI-KIR$^+$) konnten für die folgenden KIRs erfolgreich hergestellt werden: KIR2DL1, KIR2DS1 und KIR2DS2. Die Funktionalität der NK92-MI-KIR$^+$ Zellen wurde gegen Einzel KIR-Liganden exprimierende Zielzellen oder primäre leukämische Blasten in Form von Degranulation und Zytotoxizität untersucht. Die Funktionalität der NK92-MI-KIR$^+$ Zellen wurde durch die Expression bestimmter KIR Rezeptoren nicht signifikant beeinflusst. Das lässt vermuten, dass die Zellen potentiell durch andere (nicht KIR) Rezeptoren inhibiert werden. Zudem benötigen NK92-MI Zellen keine Polarisierung und Akkumulation verschiedener Signale für die Ausübung ihrer Effektorfunktion, was darauf hindeutet, dass NK92-MI Zellen nicht die ideale Zelllinie sind, um den Einfluss von KIR Rezeptoren zu untersuchen. Daher wurden im Folgenden humane primäre NK Zellen erfolgreich mit alpharetroviralen Partikeln transduziert, um bestimmte KIRs zu exprimieren. Die viralen Partikel wurden mit RD114/TR pseudotypisiert. Die Behandlung mit den viralen Partikeln hatte keinen Einfluss auf die generelle Funktionalität der NK Zellen. Funktionelle Analysen in einer kleinen Gruppe deuten darauf hin, dass diese Modifikation die Reaktivität von primären NK Zellen beeinflusst. Das stellt die Basis für weitere funktionelle Analysen von modifizierten NK Zellen dar. Optimierte NK Zellen könnten folglich für eine Behandlung nach Transplantation, z. B. im Falle einer viralen Infektion oder eines Rückfalles, eingesetzt werden.

3. Introduction

3.1 Hematopoiesis

In a healthy individual, the hierarchical process termed *hematopoiesis*, continuously replenishes all cells of the hematopoietic system. The pathway for all hematopoietic cell development begins with the multipotent lineage-unrestricted (lin^-), $CD34^+$hematopoietic stem cells (HSCs) that have the ability of self-renewal and differentiation into multiple progenitor cells and further into all other blood forming cells (*1*). Furthermore, a primitive population of lin^- $CD133^+$ $CD34^-$ HSCs has been detected in cord blood (CB) (*2*). HSCs have the potential to completely replenish the immune system in a recipient after a hematopoietic stem cell transplantation (HSCT) (*3*). Lineage committed progenitors differentiate into either the common myeloid or lymphoid lineage and lose their self-renewal capability. The myeloid lineage generates three types of cells: erythrocytes (red blood cells), megakaryocytes (platelets and thrombocytes) and myeloblasts, which further differentiate into granulocytes, macrophages, and monocytes. They help to defend the body against pathogens. Recent research has shown that monocytes can also evolve from the lymphoid lineage (*4*). B, T, and natural killer (NK) cells are the key controllers of infections and arise from the lymphoid lineage (*5*). In addition, some subgroups of dendritic cells arise from the lymphoid lineage. Dendritic cells are antigen-presenting cells (APC) and thereby modulators of the immune response (*6*). HSCs are mainly located in the stem cell niche in the bone marrow (BM), where the hematopoiesis starts. The hematopoiesis is balanced by various cell types like mesenchymal stem cells, adipocytes, glia cells and their production of chemokines, cytokines, and adhesion molecules, e.g. CXCR12 or stem cell factor (SCF). The process of hematopoiesis is strictly regulated (*1*). If a cell escapes the regulatory processes and regains the ability of self-renewal, due to mutations or other genetic abnormalities, this can result in leukemia.

3.2 Leukemia

Leukemia is a malignant progressive disease in which the BM produces elevated numbers of immature or abnormal leukocytes, called blasts. Production of these blasts suppresses the production of healthy blood cells, leading to anemia, thrombocytopenia, and other symptoms. Worldwide, leukemia is the most common malignant disease in children with an incidence of 3 in 100,000 children between the ages of 0 - 19 years (*7*).

Leukemia is believed to arise from a single transformed cell. Often, this leukemic cell is poorly differentiated and carries genetic mutations that drive a clonal expansion of the cell. Because of the extensive proliferation, additional mutations accumulate (*8*). Based on the cell of origin, leukemias are divided into myeloid or lymphoid lineages. Myeloid leukemias include acute myeloid leukemia (AML) and chronic myeloid leukemia (CML). Lymphoid leukemias include

acute lymphoblastic leukemia (ALL) and chronic lymphoblastic leukemia (CLL), whereby CML is rare and CLL has not been observed in pediatric patients (*9*).

Leukemias are classified for diagnosis and treatment by either the French-American-British classification (FAB) or the World Health Organization (WHO) classification (*10, 11*). The FAB classification is primarily based on morphology and cytochemical staining, whereas the newer WHO classification includes more recently identified factors, such as molecular and cytogenetic changes. Accordingly, the WHO classification already includes genetic abnormalities, whereby after FAB classification genetics are only considered for ongoing treatment and risk grading, e.g. occurrence of relapse.

Table 1: Phenotypical ALL classification. B-ALL: B cell acute lymphoblastic leukemia, T-ALL: T cell acute lymphoblastic leukemia, TdT: terminal deoxynucleotidyl transferase, cCD3: cytoplasmic CD3, sCD3: surface CD3.

	Subtype		Marker	Optional marker
B-lineage ALL	B-I	pro B-ALL	$CD19^+$, $CD79a^+$, TdT^+	$CD24^+$, $4G7^+$, often $CD15^+$, $CD20^+$, $CD22^+$
	B-II	common ALL	$CD19^+$, $CD79a^+$, TdT^+, $CD10^+$	$CD24^+$, $4G7^+$, $CD34^+$, $CD38^+$, $CD25^+$ and $CD13/33^+$
	B-III	pre B-ALL	$CD19^+$, $CD79a^+$, $CD22^+$, $CD34^+$, $CD10^+$, TdT^+, cytoplasmic heavy mu chain	-
	B-IV	mature B-ALL	$CD19^+$, $CD79a^+$, $CD22^+$, $CD34^+$, $CD10^+$, surface immunoglobulin light chains	$CD117^+$, $CD15^+$
T-lineage ALL	T-I	pro T-ALL	$cCD3^+$, $CD7^+$	-
	T-II	pre T-ALL	$cCD3^+$, $CD7^+$, $CD5/CD2^+$	-
	T-III	cortical T-ALL	$cCD3^+$, $CD1a^+$, $sCD3^{+/-}$	-
	T-IV	mature T-ALL	$cCD3^+$, $sCD3^+$, $CD1a^-$	-
	-	early T-Precursor	$CD1a^-$, $CD8^-$, weak $CD5^+$	$CD34^+$ and/or $CD13/33^+$
NK cell ALL	-	NK ALL	$CD56^+$, $CD7^+$, $CD2^+$, $CD5^+$	$cCD3^+$

Prognosis is based on the cell type (B, T or NK cell), the stage of differentiation and genetics. Therefore, cells are phenotypically characterized according to the surface markers depicted in Table 1. For B-ALLs, the cell surface markers CD10, CD19, CD20, CD22, CD24, CD34, CD79a and the terminal deoxynucleotidyl transferase (TdT) are used to define subgroups. B-ALLs are usually negative for T cell markers (*12*). T-ALLs are identified by surface or cytoplasmic CD3 (cCD3) and are further classified by expression of the markers CD1a, CD2, CD3, CD4, CD5, CD7, and CD8. In 25% of patients, leukemia cells express CD10 and additionally CD34, as well as the myeloid cell markers CD13 and/or CD33 (*12*). In some patients, leukemia occurs with a mixed phenotype (*13*). The NK cell ALL, very rare in both adults and children (*14*), is characterized by expression of the NK specific CD56 antigen. Besides CD56, NK ALLs often express early T-cell antigens CD7, CD2, CD5, and, occasionally, cCD3 (*10*). Each subgroup of leukemia is correlated with a different prognosis

and as a result, an adapted treatment protocol is used. Details in treatment protocols vary between countries and even treatment centers. If the first therapy is insufficient or if there is a high risk for relapse, a hematopoietic stem cell transplantation (HSCT) is a well-established treatment.

3.3 Hematopoietic stem cell transplantation (HSCT)

Often, HSCT is a curative treatment for patients suffering from malignant hematological disease as well as for patients suffering from severe genetically inherited disorders, e.g. sickle cell diseases, thalassemia, and storage diseases (*15*). These genetically inherited disorders account for 46% of pediatric patients receiving an HSCT (*16*). In allogenic HSCT, multipotent stem cells from a healthy donor are transplanted into a genetically matched patient. For autologous HSCT, the patient receives their own stem cells, collected before a conditioning treatment (which will be explained later in this section) (*17*).

That donor-derived BM cells engraft in lethally BM irradiated dogs and mice was first reported in the late 1950s (*18, 19*). Thomas *et al*. described the first BM transplantation in humans in 1958, however all patients died because of disease progression or major complications (*20*). The first successful human transplantation was achieved in 1965 with a mixed BM source from six family members (*21*). These early studies identified a significant post-transplant complication termed graft-versus-host disease (GvHD). In GvHD a mismatch between donor and recipient in the human leukocyte antigens (HLAs) results in activation of donor-derived cytotoxic lymphocytes. The mismatched, donor-derived cells recognize the recipient's tissue as foreign and attack them. Detailed genetic insights into the HLA system (*22, 23*) highlighted the important role of HLA-typing and donor choice (section 3.3.1) and ultimately led to the establishment of HSCT.

Additionally, the graft-versus-leukemia effect (GvL) was described as a potentially useful weapon to fight residual leukemic blasts. Besides HSCs, the stem cell product contains low levels of other cells, e.g. NK, T and B cells. In the GvL, the transplanted cytotoxic effector cells (T and NK cells) detect and eliminate the remaining degenerated leukemic cells (*21*).

The first successful transplantation in a pediatric patient was performed in 1968 with BM from a sibling (*24*). Another milestone was the successful transplantation of a matched-unrelated donor (MUD) in 1980 (*25*). Over the last decades, HSCT has been optimized to reduce transplant-associated morbidity and mortality, which will be described in more detail in section 3.3.2.

HSCT includes three different phases (Figure 1). Initially, patients receive a so-called *conditioning therapy*, complete obliteration of native BM, to achieve an aplastic state of severe neutropenia, which is essential to enable implantation of the infused HSC. During the aplastic phase, the risk for fungal or viral infections and organ toxicities is markedly increased. After

the first phase, engraftment and immune reconstitution are ongoing. During the first phase of immune reconstitution, there is a high risk for viral infections and acute GvHD. Later, the risk for chronic GvHD increases, whereas the risk for viral infections decreases. Dependent on the stem cell source, some patients receive immune suppression throughout phases I to III of the HSCT to prevent acute and chronic GvHD.

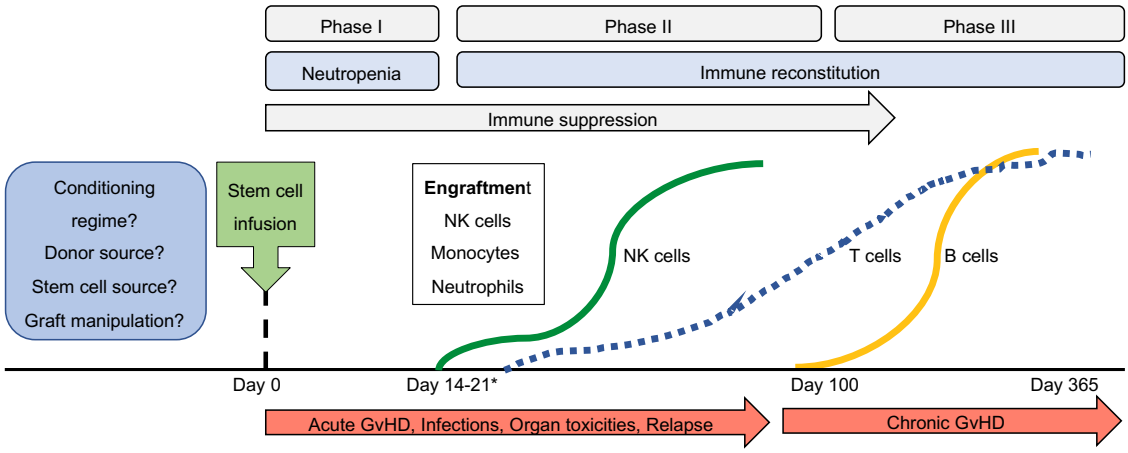

Figure 1: Phases of an HSCT and reconstitution. Modified from (*26*) with information from (*27*). *Engraftment starts between day 14 - 21, depending on the stem cell source. GvHD: graft-versus-host disease.

Currently, a successful HSCT is dependent on three important factors that must be considered and carefully planned: I. conditioning regime, II. stem cell source, and III. stem cell donor. As a factor of how the first three aspects are chosen, there may be a need for graft manipulation (e.g. TCR α/β and $CD19^+$ cell depletion or $CD34^+$ cell enrichment). It is important to note that these points differ between children and adults, mostly because children are smaller and not full-grown (*28*).

With the conditioning treatment, the patient is prepared for the upcoming HSCT. Irradiation, chemotherapeutic drug treatments called myeloablative conditioning (MAC), lymphodepleting agents and a serotherapy such as anti-thymocyte globulin (ATG) or combinations are used. Here, the amount of leukemic blasts and recipient HSCs are reduced, which is essential on the one hand to provide space in the stem cell niche for the transplanted cells (*29*). On the other hand, it gives the reconstituting cells a chance to fight the remaining malignant cells. In addition, the number of potentially alloreactive recipient T cells, which could cause graft rejection, is reduced (*30*). The type, dose, and schedule of administration depends on the type of donor and indication.

For pediatric leukemia patients, the most common condition treatment right now is a MAC condition with total body irradiation (TBI) (*31*). Nevertheless, TBI increases the risk for late effects (*32*). Non-malignant diseases often do not require an intensive conditioning regime, hence newly developed protocols include a reduced intensity regime (RIC) or non-MAC. They are associated with reduced non-relapse mortality (NRM) and non-hematological toxicities and additionally foster the GvL (*33*).

Sources for stem cells are BM, peripheral blood stem cells (PBSCs), or cord blood (CB). Although BM is the original source of HSCs on account of its easy accessibility, it showed slower engraftment rates compared to PBSCs (*34*). CB has the advantage of naive donor cells, which tolerate more HLA disparities. Consequently, less acute GvHD disease is observed in recipients of CB. However, a delayed reconstitution and increased transplant-related mortality (TRM) were observed compared to unmanipulated unmatched BM (*35, 36*). In cases where there is no matched sibling donor available, CB has proven to be a good alternative in pediatric AML patients (*37*). However, the limited number of cells available results in a prolonged engraftment time, which enhances the risk for infection and engraftment failure. Consequently, a CB transplantation is feasible for pediatric patients only (*35*). BM is the preferred stem cell source for pediatric patients, resulting in lower chronic GVHD and TRM than PBSC (*38*).
Donor choice is another challenging aspect that depends on donor suitability, availability, will and a good health condition. Here, the HLA similarity is important to reduce GvHD and graft rejections (section 3.3.1). First choice for possible donors is HLA matched sibling donors (MSDs), which are available for 25% of the patients (*31*). The high degree of HLA matches results in a reduced risk for GvHD, less severe infections and a faster myeloid engraftment and immune reconstitution in the patients (*39*). The second choice is MUDs, limited by presence and availability. Another alternative is haploidentical donors, which are always the parents or children for their parents, and in some cases HLA haploidentical siblings.
Further criteria include the human cytomegalovirus (CMV) status, as positive recipients should receive cells from a CMV positive donor. BM is preferred as the HSC source and younger donors are preferable to older ones (*28*).

3.3.1 Human leukocyte antigen (HLA) system and its role in HSCT

The HLA system, located on chromosome 6, is the most polymorphic genetic region in humans, with its main function being to present and process peptide antigens, thereby regulating the immune response (*40*). These genes are within the major histocompatibility complex (MHC) present in all vertebrates and is called HLA in humans. HLA genes are closely linked and inherited as an HLA haplotype according to the mendelian rules (*41*). For some HLA haplotypes a so-called linkage disequilibrium exist, meaning that some genes at some loci are associated, which results in the occurrence of some HLA genotypes more frequently than others (*40*). Additionally, there is a high recombination rate >1% between the HLA genes (*42*). Two siblings have a 25% chance of being HLA-identical or not sharing one HLA haplotype and a 50% change of being HLA-haploidentical (*28*). Parents always share one HLA haplotype with their children and are therefore HLA-haploidentical.
HLA molecules can be divided into classical and non-classical (Figure 2). Classical HLA molecules can be subdivided into class I and class II molecules. Class I molecules include

HLA-A, -B and -C. These are expressed on the surface of all nucleated cells, whereas the class II molecules, which include HLA-DR, DQ, DP, are only expressed on the surface of B lymphocytes, APCs, which include monocytes, macrophages, Langerhans cells, and dendritic cells, and on activated T cells (*40*).

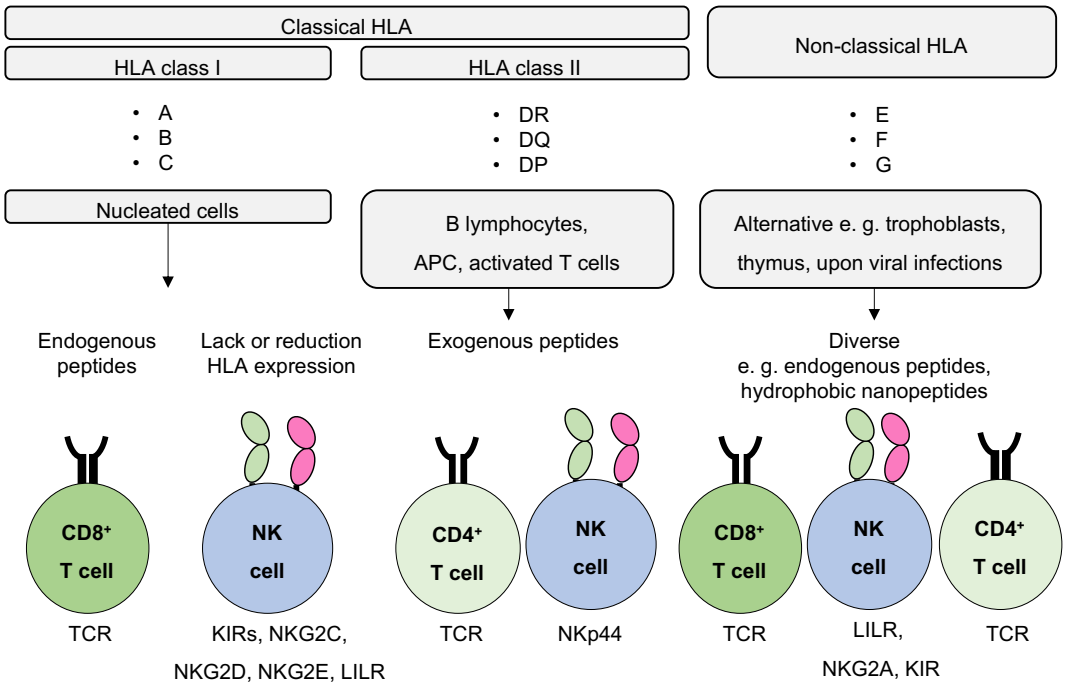

Figure 2: Overview HLA and interactions. The HLAs can be divided into the classical and non-classical HLA. Classical HLA consists of HLA class I and II. HLA class I is presented on the surface of nucleated cells and expresses endogenous peptides to $CD8^+$ T cells, whose TCR interacts with the HLA/peptide complex. NK cells recognize a lack or reduction of HLA class I by KIRs. Also, the receptors NCR, NKG2C, NKG2D, NKG2E and LILR, on the membrane of NK cells, interact with HLA class I and recognize presented peptides, which are usually intracellular. HLA class II presents endogenous peptides to $CD4^+$ T cells and the NK cell receptor NKp44 interacts with HLA-DP. Non-classical HLA molecules are alternatively expressed and are supposed to exert an immune regulatory function by interaction with either the TCR or various receptors on NK cells, e.g. LILRs, NKG2A, NCR and some KIRs. APC: antigen-presenting cells, KIR: killer cell immunoglobulin-like receptors, TCR: T cell receptor, LILR: leukocyte Ig-like receptors, NKp44 belongs to the group of natural cytotoxicity receptors (NCR).

Both molecules present peptides of different origin. Class I presented peptides are of endogenous origin, meaning either from virus-infected cells or resulting from a cellular transformation in degenerated cells. Recognition of MHC-peptide complexes by the T-cell receptor (TCR) expressed on class I restricted $CD8^+$ T cells leads to their activation (*43*). Besides T cells, NK cells can be activated. NK cells are not MHC-restricted but recognize a loss of HLA class I molecules. As a consequence, cells with low or no HLA class I expression are killed by NK cells (sections 3.5) (*44*). Class II molecules present exogenously expressed peptides, which are taken up by endocytosis and presented to $CD4^+$ T lymphocytes after degradation. The CD4 molecule interacts with the class II molecule (*45*). Upon TCR engagement $CD4^+$ T cells are activated to produce cytokines for helper or regulatory functions (*46*). Non-classical HLA molecules, which include HLA-E, HLA-F and HLA-G, are similar to the classical HLA molecules in sequence and structure but show a smaller polymorphism.

Furthermore, the non-classical HLAs have an alternative expression pattern and binding specificity, resulting in an alternative functionality (*47*). For example, HLA-G is highly expressed at the maternal/fetal interface, highlighting its role for peptide presentation during pregnancy (section 3.5.4). Some receptors expressed on NK cells are known to interact with non-classical HLAs and are further described in sections 3.5 and 3.5.1 (*48*).

For an HSCT, HLA typing is indispensable, because T cells can be alloreactive. They can recognize non-self or allogeneic tissues or cells either directly, indirectly or semidirectly (*49*). T cells can either directly recognize the entire mismatched HLA peptide complexes expressed on allogenic cells or are being activated indirectly by presentation of mismatched HLA peptides on the surface of self-HLA complexes. Another indirect alloreactivity is the activation of T cells by foreign peptides of other polymorphic genes presented on self-HLA (*50*). The semidirect T cell alloreactivity is mediated by cell-cell transfer of HLA molecules owing to cell-cell contact or secretion and uptake of exosomes (*49*).

Some HLA mismatches are better tolerated than others (*41*). General recommendations for HLA matches for donor choice are a 10/10 match in five HLA loci A, B, C, DR, DQ for MUD followed by 9/10 in MUD, or a haploidentical donor if an HLA-identical sibling is not available.

3.3.2 Haploidentical hematopoietic stem cell transplantation (hHSCT)

In the absence of an HLA-matched donor or an HLA-identical sibling, the HLA-haploidentical stem cell transplantation (hHSCT) has become well established (*51*). This donor source has various advantages as the donor can be chosen from family members. Thus, the donor is usually immediately available, willing to donate and is also available for possible post-transplantation donor cell collections, which can be used for e.g. donor-lymphocyte infusion (*52*).

The first successful hHSCT was performed in the late 1970´s, but the partial HLA mismatch between recipient and donor led to severe GvHD (*53*). In 1985, a study of 105 patients receiving hHSCT showed that more patients developed early acute GvHD, delayed engraftment, granulocytopenia or graft rejection compared to a group of HLA-identical sibling donations (*54*). The observed GvHD were assumed to be mediated by T cells that remained in the graft. Various strategies to manipulate the transplant were subsequently applied, all with the aim of reducing GvHD and rejection by affecting the number of remaining T cells in the transplant. The first T-cell-depleted hHSCT was performed in 1981, which resulted in full recovery of the donor-derived blood system without GvHD. However, the patient eventually relapsed (*55*). The importance of a well-defined T cell balance in HSCT was affirmed by the occurrence of an increased risk of relapse in 405 CML patients, who received T-cell-depleted hHSCT (*56*). Donor-derived T cells, on the one hand, might attack healthy recipient cells and tissue, resulting in GvHD (*41*). On the other hand, these donor-derived T cells exert the

beneficial GvL to control the remaining leukemic cells, which, in case of an HLA mismatch, is supported by NK cells (*57*).

Various optimizing steps were performed by intensifying the conditioning regime and optimizing the *ex vivo* T-cell depletion with T cell-specific antibodies. This was further combined with the so-called $CD34^+$ mega dose approach. Here, high numbers of $CD34^+$ cells were infused. Nevertheless, the immune reconstitution was slow and increased the risk for infections (*51, 58, 59*). Other approaches used *in vivo* T-cell depletion with serotherapies, e.g. anti-thymocyte globulin (ATG) or alemtuzumab (*60, 61*), because alloreactive recipient-derived T cells could cause graft rejection. Nevertheless, both approaches resulted in a higher risk of relapse compared to T-cell-replete HSC grafts (*62*). In T-cell-replete HSCT a pre and post transplantation GvHD prophylactic treatment is used and combined with a MAC condition regime and allows the usage of unmanipulated grafts (*63, 64*). The basics of current hHSCT approaches that have been evolved in different transplantations centers are summarized in Table 2. However, protocols are continuously optimized and some centers even combine different platforms, e.g. post-transplantation cyclophosphamide (PT-Cy) and ATG (*65*).

Table 2: Basics of hHSCT approaches and the protocol used in Hamburg. TBI: total body irradiation ATG: anti-thymocyte globulin, BM: bone marrow, PBSC: peripheral blood stem cells, CsA: cyclosporine A, MMF: mycophenolate mofetil, MTX: methotrexate, G-CSF: granulocyte-colony stimulating factor, Cy: cyclophosphamide, PT-Cy: post-transplantation cyclophosphamide, Ara-C: cytosine arabinoside.

Pioneers	Perugia group, Italy (*51, 59, 66*)	Baltimore group, USA (*67, 68*)	Bejing group, China (*69, 70*)	Protocol used in Hamburg
Conditioning	• Fludarabine, thiotepa, TBI, ATG	• Fludarabine, Cy and TBI	• Ara-C, ATG, Cy, busulfan, simustine	• Fludarabine, thiotepa, melphalan or treosulfan, ATG
Source HSC	• High cell dose $CD34^+$ from G-CSF primed PBSC	• BM • or G-CSF primed PBSC	• G-CSF primed BM or PBSC	• $CD34^+$ from G-CSF primed PBSC
Graft manipulation	• T-cell-depleted	• T-cell-replete	• -	• T-cell-replete
Post trans-plantation treatment	• -	• High dose PT-Cy • MMF, tracrolimus	• CsA, MMF, short term MTX • Daclizumab	• MMF

Besides manipulation of the stem cell source, another important question is: Which haploidentical donor is the best donor, the mother or the father?

In hHSCT, there is always an HLA mismatch resulting either from the paternal or maternal side of non-inherited maternal antigens (NIMA) and non-inherited paternal antigens (NIPA). About 50% of patients do not produce antibodies against the NIMA antigens, while they show a high reactivity against the NIPAs. The lack of these antibodies is beneficial in the transplantation setting. A NIMA mismatch as in sibling or maternal donors results in less GvHD compared to

paternal and NIPA mismatched sibling donors (*71*). Reduced TRM was associated only with NIMA mismatched sibling donors.

T-cell-replete transplantations from the father or younger brothers resulted in less NRM, acute GvHD and better survival of the recipient (*72*). However, others reported less acute GvHD (*71*) and significantly better survival rates after mother-to-child transplantation (*73*). In T-cell-depleted hHSCT, better survival, reduced incidence of relapse and reduced TRM was observed in patients, when maternal HSCs were used (*74*).

The main difference between mother and father is the pregnancy. Maternal cells have already encountered and tolerated the filial cells during pregnancy, where a bidirectional cross-placental cell trafficking occurs (section 3.4). In some mothers, filial cells remain detectable in the maternal blood circulation. Accordingly, the maternal cells still tolerate the persistence of the filial cells at a low level (*75, 76*). The impact of persisting fetal cells in the maternal blood system on the outcome of hHSCT was analyzed (*77*). A persisting fetal microchimerism (FM) in the maternal peripheral blood (FM^+ mothers) is associated with a significantly increased survival of the child after HSCT compared to father-to-child transplantation and transplantation from mothers without detectable fetal cells (FM^- mothers). Consequently, the remaining FM cells in the maternal blood system seem to have a beneficial role on the outcome after hHSCT (*77*). The mechanisms behind this rationale are not known and are further discussed in section 3.5.5.

3.4 Feto-maternal microchimerism

A recipient of stem cells or an organ transplantation is always an acquired chimera containing two genetically distinct cell populations from the same species (*19*). In addition to these acquired chimeras, natural chimeras exist. Mother and child during pregnancy are natural chimeras. Both have low levels of each other's cells detectable in their body, called a microchimerism. Maternal cells detectable in the fetal blood system or tissues are designated as a maternal microchimerism (MM). Fetal cells in mothers are called an FM or FM cells. The persistence and tolerance of an MM in filial cadaveric tissues was observed in different tissues, e.g. thymus, skin, thyroids, liver, pancreas, lung, kidney and spleen (*78, 79*).

In women carrying a male fetus, microchimeric cells can be detected as early as six weeks from the beginning of gestation (*80*) and have been found in corpses of pregnant women in lung, spleen, liver, kidney, and heart tissue, in descending frequencies in the stated order (*81*), and in the brain (*82*). Thus, there is bidirectional cross-placental trafficking between maternal and fetal cells, whereby this traffic is asymmetrical with more fetal cells being transferred into the maternal blood stream and with an increase of these FM cells as gestation progresses (*83, 84*). Most of the fetal cells are eliminated as a consequence of induction of apoptosis by the maternal cells after parturition (*85*), but in some women the fetal cells persist up to 35 years

after pregnancy (*75, 86*). These FM cells can either become resident or persist in different tissues (*87*). Some have a $CD3^+$ or $CD34^+$ phenotype (*81*) or circulate in the maternal blood system with a lymphoid or myeloid progenitor phenotype marked by expression of either CD34 or CD34 and CD38 (*75*).

The first encounter of maternal and fetal cells occurs at the placenta. The placenta is a normal physical barrier between mother and child with the main function of nutrition and gas exchange without mixing the maternal and fetal circulation (*88*). Decidual NK cells (dNKs), which highly differ from their peripheral blood counterparts, are present in the decidua (*89*). Their role during pregnancy is explained in detail in 3.5.4. Besides NK cells, the decidua consists of myeloid cells and low numbers of maternal T and regulatory T (T_{reg}) cells (*88*) that, under normal circumstances, would attack and reject the semi-allogenic fetus carrying inherited paternal antigens (*90*). There must be a unique adaption in mothers to maintain tolerance towards the foreign paternal-derived fetal antigens. A systemic increase in immunosuppressive $CD4^+$ maternal T_{regs} and an accumulation in the decidua was observed (*91*) when the amount of FM cells in the maternal blood system increased (*84*). Deficiencies in T_{reg} expansion and accumulation are associated with various pregnancy complications (*92*). Experiments in mice have shown that most fetal-specific $CD8^+$ T cells do not gain cytotoxic effector function but instead undergo clonal deletion (*93*). Here, a cis-acting pathway is important where placental antigens are shed by $CD8^+$ dendritic cells. This changes them to be non-immunogenic independent of T_{reg} cells (*94*). Furthermore, distinct immune cells are excluded from the maternal-fetal interface by epigenetic silencing of ligands in the maternal decidual stroma cell (e.g. CXCL9 and CXCL10). Normally these ligands promote adhesion of other immune cells (*95*). During pregnancy fetal-specific T_{regs} accumulate and persist at increased levels after pregnancy to retain tolerance to the existing fetal antigens. During subsequent pregnancies, these cells rapidly re-accumulate, indicating a T_{reg} memory formation (*96*). Moreover a partner-specific protective benefit is observed in case of complications for subsequent pregnancies (*97*).

Besides migration of fetal cells into the maternal body, maternal cells have also been detected in the fetus with an accumulation over time. When the fetal thymus and peripheral lymphoid tissue maturation occurs, maternal cells start to seed into the fetus. It is suggested that these maternal cells transfer NIMAs into the fetus in order to prime filial cell tolerance towards the maternal tissue (*98*). Upon NIMA stimulation, the fetal $CD4^+$ T cells differentiate into T_{reg} cells to suppress NIMA-specific effector cells (*99*). Consequently, the fetus is not damaged or attacked by the maternal effector cells.

The fetal maternal cell transfer is not only described for mother-child pairs. The mother can additionally have microchimeric cells from her mother, which can be transferred into the fetus (*100*). Furthermore, FM cells from a first pregnancy can be transferred to a second or third

child during subsequent pregnancies (*101, 102*), resulting in a trans-maternal microchimerism (TM). With subsequent pregnancies a reduction of maternal microchimeric cells, which a woman obtained from her mother (MM), is observed (*103*). This suggests a competition between the microchimeric cells within a woman (*100*). The biological role and function of this traffic and persistence of microchimerism is still controversial. The association of microchimeric cells with diseases and disorders observed in women after pregnancies (*100, 104*) is described in section 3.4.2.

3.4.1 Detection of a microchimerism

Microchimeric cells persist at a small number in the host, which makes their detection challenging. In 1969, Walknowska *et al.* were the first who detected Y-chromosomes by karyotyping activated peripheral blood mononuclear cells (PBMCs) of pregnant women carrying a male fetus (*105*). Various groups have verified this finding (*106, 107*). Fluorescence-activated cell sorting techniques (FACS), which utilize HLA disparities to distinguish between maternal and fetal cells, were used and filial origin of enriched cells was verified by Y-chromatin analysis (*108*). Later, a PCR was developed to amplify Y-chromosome specific DNA in mothers carrying a male fetus *(76, 80).* The PCR results correlated with the results from fluorescence *in situ* hybridization (FISH) (*109*). Novel approaches for FM determination were driven by the field of HSCT.

Besides the natural microchimerism in mother and child, a microchimerism can be acquired after blood or organ transplantation. Thus, during development of HSCT, the detection of chimerism became of huge importance to monitor engraftment and reconstitution of the transplant. Moreover, the detection of low-level-residual degenerated cells, named minimal residual disease (MRD), is important in case of early relapse recognition and to improve the treatment options. The detection of MRD requires high sensitivity and resolution power for exact quantification (*110*). First, restriction fragment length polymorphisms (RFLP) to distinguish patients and donor cells were used for MRD detection (*111*). A PCR-based method was used for analysis of variable numbers of tandem repeats (VNTR) or characterization of short tandem repeats (STR), which was further paired with fluorescent labeling of probes, followed by analysis of the products after capillary electrophoresis. This increased sensitivity to 1 - 5% (*112*). Real-time quantitative PCR (RT-PCR) for chimerism and, moreover, microchimerism determination further increased sensitivity (*113, 114*). Both detection of insertion/deletion polymorphisms (InDels), known as deletion/insertion polymorphism (DIPs), and single nucleotide polymorphism (SNPs) both increased the sensitivity up to 0.1% compared to STR-analysis (≥1%) (*115, 116*). The human genome consists of 1.42 million SNPs that differ from each other at just a single nucleotide, resulting in an SNP every 1.9 kb (*117*). In comparison, the prevalence of InDels is lower (*118*). Nevertheless, STRs are

detectable in all patients, while SNPs and InDels are found in only 90%. Thus, STRs amplification, including the Y-chromosome, has remained the “gold standard” for chimerism analysis until now. Moreover, RT-PCR does not allow for exact quantification and needs standard dilution series for quantification, which provides a source of error especially in detection of genes occurring at low frequencies.

An alternative to the commonly used RT-PCR is the digital droplet PCR (ddPCR), as it allows exact quantification over several magnitudes and has been reported to be highly reproducible with excellent sensitivity (0.01%) (*119*). With this technique, each PCR reaction is separated into up to 20,000 single droplets using a water-oil-emulsion technology. After the PCR run, each droplet is analyzed for fluorescence. Duplex reactions and Poisson statistics enable exact quantification. Additionally, high amounts of input DNA are possible, up to 1 µg/reaction. This method was optimized with primer/probe pairs for 29 InDels for chimerism analysis after HSCT resulting in high sensitivity and precise quantification (*120*). The main disadvantage of ddPCR is that it requires a lot of laboratory hands-on work and thereby is time consuming. However, the advantage is that per sample of microchimerism analysis only few reactions are necessary because of the increased amount of DNA. Consequently, the ddPCR provides a high potential for use in microchimerism analysis (*120, 121*).

3.4.2 The role of FM cells in disease

The role of a persisting microchimerism in mother and child is still controversial. The fact that persistence of FM is highly conserved between all mammalian species leads to the assumption that these cells have a beneficial effect (*122*). On the other side, a lot of diseases are observed at a higher frequency in women during their childbearing years, suggesting a negative influence of the FM cells on the mothers health (*100*).

Beneficial roles of FM cells are their support of maternal wound healing, observed particularly after a Caesarean section. Additionally, these filial cells support the postpartum fetal care by seeding in the respective organs (*122*). FM cells are supposed to infiltrate various tissues and replace injured cells as observed in different murine experiments and female tissues (*100*). During pregnancy, the symptoms of autoimmune diseases like rheumatoid arthritis or multiple sclerosis are mitigated, potentially mediated by the suppressive systemic changes in the maternal immune system (*123, 124*) and expansion of maternal T_{reg} cells (*91*).

On the other hand, seeded cells of fetal origin provide a target for alloreactive maternal immune cells, leading to inflammatory responses of maternal cells (*125*). A significantly higher amount of male DNA, potentially derived from FM cells, was observed in women suffering from scleroderma compared to their healthy sisters or a healthy control. This observation suggests that FM cells might influence the pathogenesis of scleroderma (*126*). It is not distinguishable if the maternal alloreactivity is against autologous cells (autoimmunity) or the fetal cells (*100*).

Nevertheless, an increased number of pregnancies reduces the risk of developing autoimmune diseases such as scleroderma, rheumatoid arthritis and multiple sclerosis, and is postulated to be a result of a higher heterogeneity due to accumulation of microchimeric cells (*100*). It is not yet known which environmental or biological stimuli might determine microchimeric cell fate, and what the implications of microchimeric cells are on graft survival after HSCT or organ transplantation.

3.5 Natural Killer (NK) cells

NK cells are large granular lymphocytes that belong to the innate immune system and they are members of the innate lymphoid cell family (ILCs) (*127*). Based on their development and function, ILCs are divided into the five subgroups NKs, ILC1, ILC2, ILC3 and lymphoid-tissue-inducers (LTis). They all arise from the same common progenitor, but compared to the other ILC groups, NK cells require Interleukin 15 (IL-15) and ILCs IL-7 mediated signaling for differentiation into NK cells (*128*). Each ILC has a distinct immune function (*129*).

In the mid 1970´s, NK cells were discovered as immune effector cells able to kill virus-infected and tumor cells without prior priming (*130, 131*). NK cells comprise 10 - 20% of the lymphocytes in the peripheral blood (*132*). Besides in the peripheral blood, NK cells are found in secondary lymphoid organs, lung, liver, intestine, skin and uterus during pregnancy (*133*). Under pathophysiological conditions, they accumulate at tumor-bearing or inflammatory sites (*134, 135*). NK cells are not a static population as they can recirculate between different organs since they are recruited by a wide array of chemokines to inflammatory sites (*136, 137*). However, the organ-specific migration pattern of NK cells is still only partly characterized and their functionality depends on cytokines and chemokines(*133*).

Best characterized are the two main subpopulations in the peripheral blood, the immature $CD3^-$ $CD56^{bright}$ $CD16^-$ and the mature $CD3^-$ $CD56^{dim}$ $CD16^+$. The $CD3^-$ $CD56^{bright}$ $CD16^-$ NK cells represent 10% of the peripheral blood NK cells and are activated in response to IL-15, IL-2 and IL-12 to primarily produce interferon γ (IFNγ) and tumor necrosis factor α (TNFα). IFNγ and TNFα, in turn, result in activation of macrophages and other APCs. In contrast, the mature $CD3^-$ $CD56^{dim}$ $CD16^+$ NK cells represent 90% of the peripheral blood NK cells and exert a cytotoxic function to eliminate infected cells upon stimulation (*132*). Upon *in vitro* stimulation with IL-15 or IL-2, $CD56^{bright}$ NK cells can also exert cytotoxic function (*138*). *Vice versa* mature NK cells can produce cytokines in response to activating signals as well (*139*).

NK cells can mediate killing of target cells in different ways. The perforin-dependent cytotoxic response of NK cells starts with recognition of the affected target cell (*140*). The NK cell forms an immunological synapse with the target cell. Inside this synapse activating and inhibitory receptors regulate NK cell functionality. After remodeling of the actin skeletons and polarization of a microtubule organization, secretory lysosomes are mobilized towards the synapse. These

lysosomes fuse with the NK cell plasma membrane and as a consequence cytotoxic effector molecules are released into the intracellular space (*141*). Released perforins polymerize and form a pore that enables the entry for proteases called granzymes (*142*). These molecules, where granzyme B is the best characterized, have various cleaving targets like caspase-3, Bid, DNA-PCK, all inducing apoptosis in the target cell (*143*). The entire process of effector molecule release is called degranulation. Upon vesicle fusion with the NK cell plasma membrane, the lysosomal-associated membrane protein-1 (LAMP1 also known as CD107a) and LAMP-2 (CD107b) are converted to the surface. CD107a/LAMP1 expression can be measured and is used as a marker for degranulation (*144*). Additionally, CD107a/LAMP1 has a protective effect for NK cells during cytolysis of target cells. Knock-out of CD107a/LAMP1 in primary human NK cells results in a higher amount of apoptotic NK cells upon target cell induced degranulation (*145*).

Another way to induce cell death in target cells involves death receptors CD95L or TNF-related apoptosis-inducing ligand (TRAIL) expressed on the cell surface of NK cells. Receptor/ligand engagement (CD95/Fas and TRAIL/R1-R2) on the target cell surface results in conformational changes of the receptors and generation of a death-inducing-signal complex (DISC) (*146*). In the end a caspase cascade is initiated, resulting in cell death of the target cell (*141*).

Afterwards, the NK cell actively disengages from the target cell and mediates killing of other target cells (*147*), called serial killing. Exhaustion of NK cells can be restored by IL-2 and the frequency of activated NK cells can be enhanced by IL-2, IL-15 or by antibodies, e.g. through the anti-CD20 antibody rituximab (*148*). Additionally, NK cells release exosomes expressing NK cell-specific surface markers that contain the cytotoxic mediators granzyme and perforin and exert cytotoxic functions against human tumor cell lines and activated immune cells, but not against resting immune cells (*149*).

To fight tumor cells, NK cells first use the fast perforin-granzyme-dependent killing. In subsequent target cell encounters, NK cells switch to the receptor-mediated induced killing, which is regulated by the upregulation of CD95L (*150*). The latter often needs multiple NK-cancer cell activating receptor interactions (*151*). Regulation of both mechanisms is independent of each other. Perforin absence increases CD95L expression, but CD95 absence on tumor targets does not impair perforin-mediated killing (*150*).

Additionally, NK cells can exert antibody-dependent cytotoxicity (ADCC) mediated by recognition of antibody-coated target cells by their surface receptor CD16. CD16 binds to the constant region of antibodies and thereby activates the NK cell. Activation of NK cells can be mediated by CD16 receptors alone, whereas all other signals mentioned in the following section require an accumulation of signals (*152*).

In contrast to other immune effector cells, NK cells do not rearrange or express T cell or B cell receptor genes (*153*). NK cells' functionality is regulated by an enormous array of germline-

encoded inhibitory and activating receptors resulting in diverse phenotypes. Activation of an NK cell requires synergistic stimulation of several receptors until a threshold is reached (*141*). This includes various HLA specific, non-HLA specific, co-stimulatory as well as chemokine and cytokine receptors (*154*).

The leukocyte immunoglobulin (Ig)-like receptors (LILRs) recognize both HLA and non-HLA molecules (*155*). The non-HLA specific receptors are the natural cytotoxicity receptors (NCRs), comprising NKp46, NKp44, and NKp30 (*156*). The NCRs are type I transmembrane molecules belonging to the Ig-like family. Their extracellular domains interact with virus-derived molecules that mainly exert an activation but in some cases can be inhibitory (*157*). Recently, the HLA class II molecule HLA-DP has been identified as an interaction partner for NKp44 (*158*).

The HLA-specific receptors harbor the killer cell immunoglobulin-like receptors (KIRs) (*159, 160*), which will be further discussed in section 3.5.1, and the natural-killer group 2 members (NKG2). NKG2 receptors belong to the group of C-type lectin-type II transmembrane proteins. Some of the receptors exert activating signals, e.g. NKG2C, NKG2D and NKG2E, mediated by intracellular interaction with adaptor molecules. Other receptors like NKG2A intracellularly contain an immunoreceptor-tyrosine inhibitory motif (ITIM), whose activation results in inhibition of the cell (*161*). NKG2A recognizes the non-classical MHC HLA-E (*162*), whereas ligands for activating receptors are various structural homologues of MHC class I molecules (*141*). Nevertheless, it is known that NK cells need co-expression of activating ligands for efficient activation (*163*). These co-stimulatory receptors are either activating (2B4, DNAM1), inhibitory (PD1, KLRG1, TIM3, LAG3, CD96 and TIGIT) or cytokine receptors (IL-2 ,-4, -10, -12, -15, -18, -21) (*164*).

In the peripheral blood of a healthy individual, 6,000 - 30,000 subsets of NK cells with >100,000 phenotypes can be detected. Many subsets are presumed to display maturation steps and do not belong to the fully matured pool (*165*). At birth, the diversity is lower than in adults. Upon viral infection, the diversity increases towards more mature cytokine producing NK cells with lower ability of cell division and degranulation (*166*). The expression of inhibitory receptors is determined by the individual genetics, whereas expression of activation receptors is environmentally influenced. This results in a functional adaption of NK cells towards fighting tumors and pathogens by activating receptors and co-stimulatory signals while maintaining self-tolerance mediated by inhibitory receptors, as explained in sections 3.5.1 and 3.5.2 (*165*). Even though NK cells are short-lived, with a turnover time of two weeks in the peripheral blood (*167*), the individual receptor expression within the NK cell populations remains stable over time. This is mediated by homeostatic mechanisms, whereas cytokine treatment, e.g. administered therapeutically, or increased cytokine secretion by activated immune cells during infections alters the receptor repertoire (*166*). Up to now, there is still a lack of understanding

of the overall relationships between genotype, phenotype, and functionality of the individual NK cell repertoire.

3.5.1 Killer cell immunoglobulin-like receptors (KIRs)

KIRs, which interact with HLAs, are expressed on NK cells and regulate their tolerance and functionality. The KIR family consists of the 15 KIR genes: 2DL1, 2DL2/L3, 2DL4, 2DL5 A and B, 2DS1, 2DS2, 2DS3, 2DS4, 2DS5, 3DL1/S1, 3DL2, 3DL3, and two pseudogenes: 2DP1 and 3DP1, which are mapped on chromosome 19q13.4 within the leukocyte receptor complex (LCR) (*168, 169*). Each KIR gene spans 10 - 16 kb and they are tightly arranged in a head-to-tail orientation (*170*). All consist of a uniform exon-intron organization with four to nine exons and highly conserved exon boundaries (*169*). In addition, KIR genes show an extremely allelic polymorphism and a high variation in KIR gene content (*171*). Despite this, most KIR haplotypes can be divided in either the A haplotype or the B haplotype (Figure 3, A) (*171*). The A haplotype has a fixed KIR gene content consisting of KIR2DL1, KIR2DL2, KIR2DL3, KIR3DL1, KIR3DL2, KIR2DL4 and KIR2DS4. The latter is the only gene coding for an activating receptor. All remaining KIR haplotypes are defined as B haplotype and characterized by the presence of at least one of the remaining KIR genes or by the absence of one of the haplotype A genes (*172, 173*).

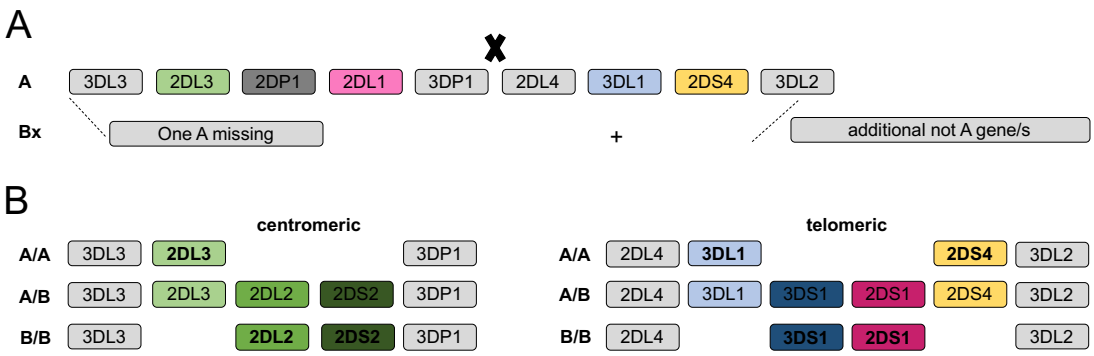

Figure 3: KIR gene organization. A. KIR genes in haplotype A and haplotype Bx. x represents a hotspot of recombination. B. Genes determining centromeric and telomeric gene regions. Each color represents one KIR gene. Inhibitory KIR genes are in light color, activating counterpartners are displayed in dark. Framework genes are in light gray. Centromeric and telomeric region determining genes are in bold.

With few exceptions, KIR genes can be divided based on the chromosomal region where they are located: the centromeric or the telomeric (Figure 3, B) (*174*). These regions have a framework of three conserved blocks: I. KIR3DL3, II. KIR3DP1, KIR2DL4, and III. KIR3DL2, which are interrupted by variable segments. These segments differ in type and number of KIR genes. Between the centromeric and the telomeric gene region lies a hot spot of recombination (*170*), meaning that recombination between these regions occurs more often than expected and generates multiple centromeric and telomeric combinations. The centromeric gene region

is determined by either the presence or absence of KIR2DL3, whereas the telomeric region is defined by KIR3DL1 and KIR2DS4 and/or KIR3DS1 and KIR2DS1 (*173*).

KIR genesis is explained partly by mono- and multigenic tandem duplications of KIR genes, deletions, and intergenic non-reciprocal sequence recombination (*170, 173*), which explain the high variation, the observed truncated or extended haplotypes and hybrid gene formation (*175, 176*). Polymorphic and polygenic KIR genes segregate independently from their HLA ligands (*177*). A strong linkage disequilibrium exists among some KIR genes (e.g. KIR2DL2 and KIR2DS2 or KIR2DS1 and KIR3DS1), which hampers examination of the role of the individual KIR (*178*). The function of KIR genes, ligand affinity and signal transduction/strength is also affected by the high polymorphisms in the KIR genes. For instance different KIR3DL1 and KIR2DL1 alleles are associated with low or high receptor surface expression (*179, 180*).

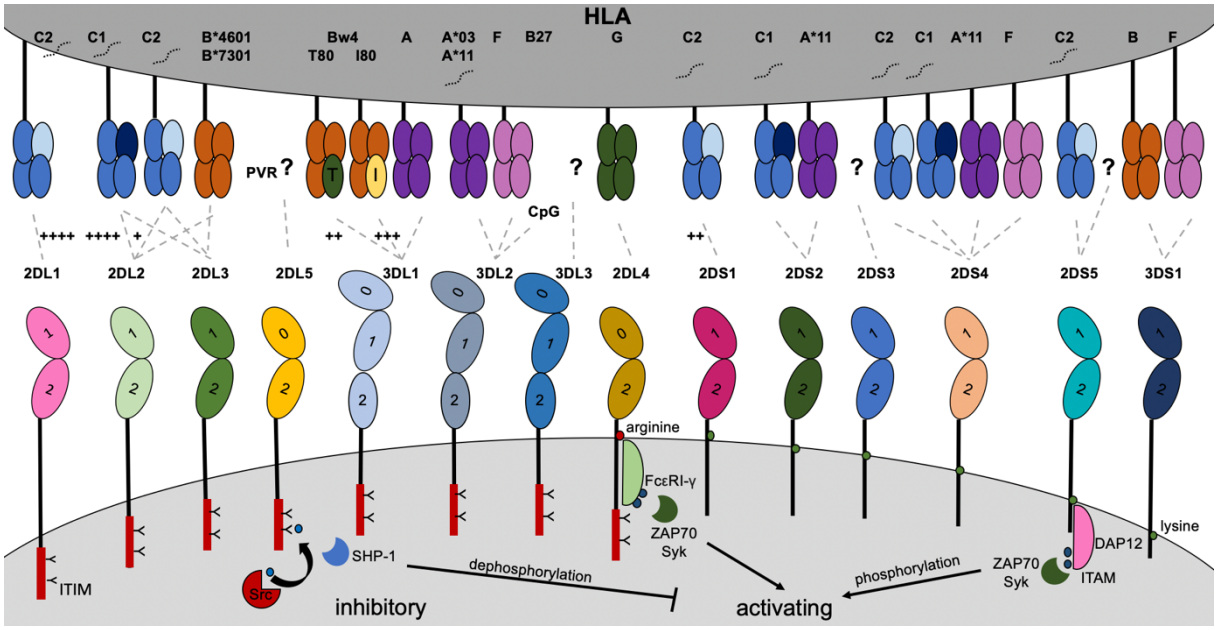

Figure 4: KIR receptors with their ligands and signaling pathways. KIR receptors, their HLA ligands and exemplarily signaling pathways are depicted. Oval structures represent the homologous domains. ITIMs are depicted in red and ITAMs are the blue dots. A charged transmembrane domain is represented by a circle either in red (arginine) or in green (lysine). PVR: polio virus receptor, ITIM: immunoreceptor tyrosine-based inhibitory motif, ITAM: immunoreceptor tyrosine-based activating motif. ⋰ symbol indicates, additionally a peptide dependent interaction is described.

Allelic polymorphism, methylation, promotor variation, copy number variation, HLA ligand background and prior infection with CMV have all been identified as variables contributing to KIR surface expression (*179*).

The extracellular, transmembrane and cytoplasmic domains of KIRs are highly conserved (*170*). The extracellular domain, responsible for ligand recognition, comprises two to three closely related immunoglobulin-like domain structural units. The number of these domains is reflected in the name of the KIR. KIR2D receptors contain D1 and D2, KIR3D receptors D0, D1 and D2, whereas KIR2DL4 and KIR2DL5 contain D0, D2, and lack D1. KIR/HLA binding is dependent on hydrogen bonds and charge complementarity. The D1 and D2 domains affect

the receptor's avidity (*181, 182*). Furthermore, the affinity and the interaction of receptor and ligand are affected by peptides bound to HLA-C (*181*).

As mentioned earlier, KIRs are divided into inhibitory and activating receptors. Single clone analysis of NK cells revealed a normal distribution of inhibitory receptors expression from two to nine on a single NK cell (*183*). Some activating and inhibitory KIR pairs contain a highly homologous extracellular sequence, e.g. KIR2DL1 with KIR2DS1, KIR2DL2 with KIR2DS2, and KIR3DL1 with KIR3DS1 (*184*). The name contains information about the length of the intercellular domain - either "L" for the long-tailed inhibitory receptors or "S" for the short-tailed activating receptors (*185*). The structure of KIRs, signaling pathways and ligands are depicted in Figure 4. The transmembrane domain of all activating KIRs contains a charged residue that is essential for association with adaptor molecules and consequently receptor functionality (*186*). KIR2DS and KIR3DS1 receptors contain a lysine providing an interaction site for DAP12, while KIR2DL4 contains an arginine for interaction with the FcεRI-γ (*187, 188*). Both adaptors contain an immunoreceptor tyrosine-based activation motif (ITAM) in their cytoplasmic domains that, upon non-covalently receptor association, leads to tyrosine phosphorylation of cellular proteins and activation of the cell. The following activation pathway is similar to T and B cells and involves phosphorylated DAP12 proteins that bind ZAP70 and Syk protein tyrosine kinases (*187*). The inhibitory receptors have a long cytoplasmic tail with ITIMs. Upon KIR/HLA engagement, the ITIM tyrosines are phosphorylated by Src family kinases creating docking sites for SH2 domain-containing protein tyrosine phosphatases (SHP-1 and SHP-2). These inhibit NK cells by dephosphorylation of tyrosine phosphoproteins that mediate activation (*189, 190*).

The ligands for some but not all KIRs are well known and are summarized in Figure 4 (*160, 168, 191-203*). In brief, the distinct KIR/HLA interactions are described that are important after HSCT and during pregnancy.

KIR/HLA interactions of KIR2DL1, KIR2DL2/L3 and KIR3DL1 are important after HSCT. Residues 76 - 83 within the HLA class I heavy chain determine the specificity of KIR binding to HLA class I molecules (*204*). HLA-C2 is characterized by a lysine at position 80 and HLA-C1 by an asparagine at this position. KIR2DL1 specifically binds to HLA-C2, but not to HLA-C1. The inhibitory receptors KIR2DL2/L3 bind with a high affinity to HLA-C1 and with low affinity to HLA-C2. Next to HLA-C, they interact with the two HLA-B epitopes (B*46:01 and B*73:01). In these HLA-B epitopes the C1 specific binding epitope is conserved (*205, 206*). Additionally, all three receptors show the ability to bind various peptide/HLA combinations, whereas a higher selectivity is observed for KIR2DL2 and KIR2DL3 compared to KIR2DL1 (*207*). KIR3DL1 binds to HLA-A and some HLA-Bw4 bearing allotypes, while an Isoleucine at position 80 is supposed to lead to a high-affinity binding compared to a threonine at this position. Recently it has been shown for KIR3DL1 and its ligand that expression and avidity of both shape NK cell function

(*208*). KIR2DL4 is constitutively expressed (*209*) and interacts with the non-classical HLA-G, expressed on the surface of invading fetal trophoblasts. This receptor is important during pregnancy (section 3.5.4). Furthermore, this is the only KIR receptor that contains both an intracellular ITIM motif and a charged residue in the TM region, leading to a switch in signal transduction. The inhibitory potential of KIR2DL4 is weak, whereas soluble ligand engagement results in a strong cytokine release without cytotoxic function (*210, 211*). It is noteworthy that, in the past, many peptide-specific engagements of NK cell receptors, especially the activating KIR receptors, with their ligands have been reported. This highlights the potential adaption and control of NK cells towards infections and environmental influences (*184, 212-214*).

3.5.2 NK cell education/licensing and alloreactivity

NK cells develop from $CD34^+$ progenitor cells that have been detected in liver (*215*), tonsils, thymus (*216*), and decidua (*217, 218*). Development of NK cells starts from $CD34^+$ $CD7^-$ $CD56^-$ hematopoietic precursors into pre-NK cells, which are $CD34^-$ $CD7^-$ $CD56^-$. From this stage, they turn into $CD56^{bright}$ immature and finally mature $CD56^{dim}$ NK cells with KIR expression (*219*). NK cells' primary function is to maintain tolerance to self, e.g. during an immune response against cancer, pathogen control and pregnancy. A functional NK cell has to learn to recognize self-HLA class I molecules in a process called licensing or education (*220, 221*). Therefore, NK cells express receptors (especially KIRs and NKG2A) on their surface for interaction with self-HLA molecules. During development, the inhibitory and activating receptors are balanced, resulting in an inhibited NK cell mediated by class I molecules expression on healthy cells (*222, 223*). Infection or disease often cause cells to reduce or lose their HLA class I expression (*224*). Encountering NK cells recognize the "missing self," lose their inhibition and attack the degenerated cells (*221*). NK cells without expression of inhibitory receptors often fail to respond to HLA-class I deficient cells (*183, 225*). The educated NK cells are responsive, whereas uneducated NK cells are hyperresponsive against missing self. Individual NK cells exhibit graded levels of responsiveness, which correlate with their sensitivity for inhibitory self-molecules (*226*). A single KIR receptor is only expressed on a fraction of NK cells and can be co-expressed with varying numbers of other KIR receptors, resulting in a modified education profile for each individual NK cell (*227*). Different education models have been proposed.

In the licensing/arming model the inhibitory receptor engagement activates a molecular machinery in the NK cell that leads to an educated phenotype (*228*). In detail, education leads to reorganization of the lysosomal compartment in self-KIR^+ NK cells (*229*). The NK cell needs the inhibitory signal to become activated, and a lack of an inhibitory signal results in a uneducated NK cell (*228*).

In contrast, the disarming model includes the activating signals and postulates that initially all NK cells are highly reactive, but this results in a state of anergy. Only signals from an inhibitory receptor rescue the NK cell and lead to an educated NK cell. Thus, NK cell reactivity is preserved by dampening of activation induced by inhibitory signals (*230*).

The tuning theory underlines that the capacity of an individual NK cell to respond to stimuli is quantitatively regulated by the type and extent of HLA class I alleles present during NK cell education (*231*). Additionally, the rheostat model considers that the strength of inhibition regulates effector function potential and environmental HLA regulates NK cell responsiveness (*232*). Here, KIRs interacting in cis with their receptors on the same cell maintain a permanent adaption of the NK cell. Inclusion of environmental HLA changes in the educational process results in a continuing adaption of NK cells, which helps to sustain tolerance, avoid autoimmunity, and reproduce successfully. Nevertheless, the total educational process is not completely understood.

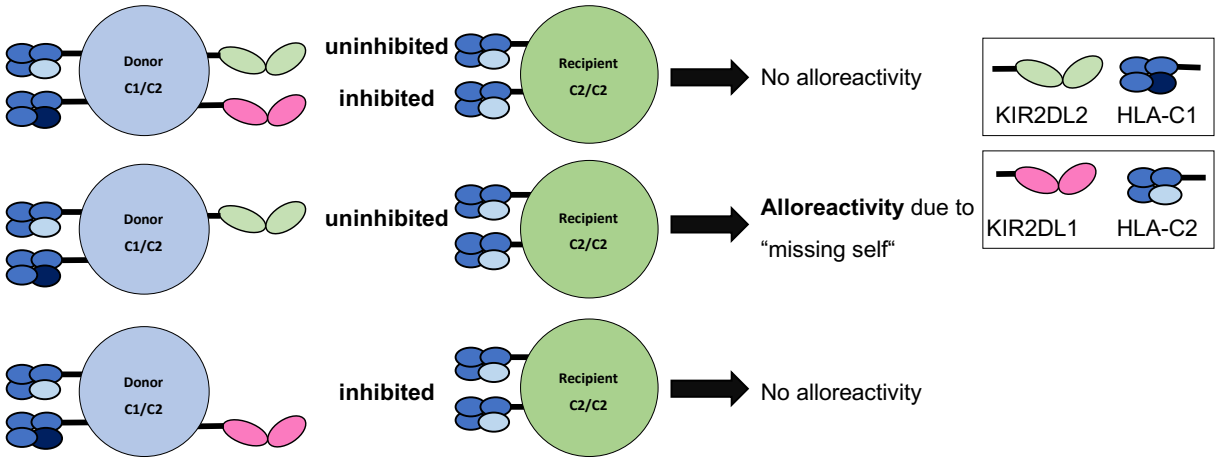

Figure 5: Visualization of NK cell alloreactivity in the setting of hHSCT. Donor NK cells are depicted in light blue, recipient cells in green.

In a healthy individual, different populations of educated and uneducated NK cells exist. The educated NK cell expresses at least one inhibitory receptor, whose ligand is present. In contrast, if an NK cell expresses only one or more inhibitory receptors for those the ligands are absent, the NK cell remains uneducated. Each individual has a distinct HLA/KIR combination, due to separated inheritance of both loci (*233*). Some receptors are expressed even though the ligand is not, but these cells are less reactive. Under inflammatory conditions, this "unresponsiveness" can be reverted to NK cell alloreactivity.

HSCT, especially HLA mismatched or hHSCT, provides a powerful tool to study the education of NK cells. It is unknown whether NK cells are educated by donor-derived self-HLA or by the recipients' remaining stromal cells. Functional analyses of reconstituting NK cells have provided details about the education of NK cells but so far, this question is not completely elucidated. However, NK cell education seems to be affected by both the recipient and the donor cells (*234, 235*).

In HSCT, donor NK cells that have been educated by the donor's immune system remain in the graft. If these cells are transferred into an MUD or MSD, the educated NK cells recognize a downward regulation in HLA. Consequently, detected remaining leukemic cells are eliminated by the donor-derived NK cells in a GvL reaction. In case of an HLA mismatch, NK cell alloreactivity can be predicted (Figure 5). An HLA-C heterozygous donor donates stem cells for an HLA-C2 homozygous donor. The donor's NK cells that express KIR2DL1 and/or KIR2DL2 are both educated and recognize the lack of each HLA-C1 and HLA-C2 molecule, respectively. In the recipient, these donor NK cells expressing both KIRs are inhibited by KIR/ligand interaction of KIR2DL1 and HLA-C2 (Figure 5, upper panel). KIR2DL1 only expressing NK cells are inhibited in the same way (Figure 5, lower panel). An NK cell lacking KIR2DL1 is not inhibited, as the ligand for KIR2DL2 is not presented. This results in an alloreactive NK cell (Figure 5, middle panel). This alloreactive NK cell exerts a beneficial role in GvL (*57*), which will be explained in the following chapter. The prediction of NK cell alloreactivity can be performed for presence and absence of the following combinations: KIR2DL1/HLA-C2, KIR2DL2/L3/HLA-C1, KIR3DL1/HLA-Bw4 (*236*).

3.5.3 NK cells after hHSCT

After HSCT, T cells remaining in the graft are important for enhanced engraftment and GvL, but alloreactive T cells cause severe and life-threatening GvHD (*237*). Nevertheless, depletion of T cells results in a higher risk of graft rejection and relapse, since donor T cells are necessary to eliminate remaining leukemic blasts (*238*). In addition to T cells, in HLA-mismatched HSCT, NK cell alloreactivity was identified as an effective GvL tool to kill allogenic leukemic cells with avoidance of GvHD and increased engraftment (*57, 239*). Furthermore, NK cells are the first lymphocytes to reconstitute after HSCT (*240*). An increase in the number of NK cells is associated with less TRM. Acute GvHD and viral infections are major causes of TRM. The higher amount of NK cells results in enhanced control of viral and bacterial infections during the aplastic phase. (*241*). A beneficial role of NK cell alloreactivity was observed with regard to the outcome of AML patients (*237*). Leukemia-free survival correlated with a high proportion of alloreactive NK cells post-transplantation in the majority of patients (*242*). Various studies analyzed the influence of KIR and HLA on transplantation outcome in the HLA-mismatched setting.

A donor KIR B haplotype, especially cen-B motif homozygosity, is associated with better outcome in unrelated HSCT in patients with AML (*243, 244*), suggesting a protective effect of the activating KIR genes in the B haplotype. Especially the presence of KIR2DS1 correlates with better outcome and protection against relapse (*243, 245*). However, if the donor is homozygous for HLA-C2, the beneficial effect of KIR2DS1 is lost. This phenomenon is thought to be a result of induction of hyporesponsiveness in the KIR2DS1^{+} NK cell subset according

to their education (*246*). Additionally, KIR3DS1 is associated with reduced mortality in AML patients (*245*). In pediatric ALL patients, relapse risk is reduced, if the centromeric B motif is present in donors, but the telomeric B motif is absent. In contrast to AML patients, no influence on GvHD or TRM was observed (*247*).

In HLA-identical sibling transplantation, a survival benefit was observed by presence of cen-B genes in the donor (*248*). In hHSCT, a significantly reduced risk of relapse and better event-free survival (EFS) is observed in pediatric ALL patients receiving KIR B haplotype donor cells, compared to those transplanted from a KIR A haplotype donor (*249*). Additionally, the benefit of KIR-ligand mismatch was observed in a cohort of hHSCT patients (*250*). Presence of both KIR2DS1 and KIR3DS1 in the donor is protective against NRM (*251*).

Not only the alloreactivity prediction, but also the conditioning before HSCT and therapy during reconstitution influence NK cell reactivity. In a recently published analysis of MUD in pediatric patients receiving MAC and T-cell-replete grafts, no effect of KIR, KIR gene regions/content or KIR ligand match was detected (*252*). When post-transplantation cyclophosphamide treatment was used in combination with an MAC or RIC, the protective effect of donor KIR genes was diminished, too (*253*). Alloreactive NK cells are potentially targeted by the treatment, eradiating their positive effect (*254*).

3.5.4 NK cells during pregnancy

dNKs constitute up to 70% of the leucocytes present in the first trimester decidua (*255*) and greatly differ from their peripheral blood counter partners in gene expression, phenotype and function (*89*). Compared to peripheral blood NK cells, proportions are inverted, resulting in a decrease of $CD56^{dim}$ cytolytic NK cells and an increase of $CD56^{high}$ cytokine producing NK cells with an altered secretion profile. In the first trimester, fetal trophoblasts deeply invade the placenta and its blood vessels, the spiral arteries, to interact with dNK cells and monocytes. The purpose is to promote uterine vascular remodeling towards a high-flow and low-resistance circulation, forming the basis for the blood supply of placenta and fetus during pregnancy (*256*). Here, the polymorphic maternal and paternal HLA-C molecules are highly expressed (*257*) on proliferative extravillous trophoblasts (EVT), indicating a protective role for the semi-allogenic fetus during early pregnancy (*258*). Non-classical HLA molecules, HLA-G, HLA-E and HLA-F are highly expressed on the invasive, actively migrating EVTs, suggesting a more pronounced role in interaction with the dNK cells. HLA-A, HLA-B or HLA-DR expression is absent on these EVTs (*258*).

dNK cells control EVT invasion by secretion of cytokines and chemokines, e.g. IL-8 and the interferon-inducible-protein 10 (IP-10) that bind to the trophoblast surface. Due to their interaction with EVTs, activated dNKs promote uterine vascular remodeling and growth by secretion of angiogenic factors, e.g. vascular endothelial growth factor (VEGF) and placental

growth factor (PLGF) (*259*). The dNK cell-EVT interaction is further regulated by activating and inhibitory surface receptors, e.g. KIRs, NCRs and LILRs, expressed on the surface of dNK cells, with their ligands on EVTs (*260*). The maternal KIR receptors and fetal HLA-C molecules are highly variable. Therefore, each pregnancy has unique genetic KIR/HLA combinations (*261*). Whereas engagement of KIR2DL1 positive cells with their ligands reduces secretion, KIR2DS4 positive dNKs cells are activated by ligand stimulation and secrete increased amounts of vascular promoting factors, e.g. granulocyte-macrophage colony-stimulating factor (GM-CSF) (*262*). Pro-angiogenesis factor secretion by LILR-1^{+} dNKs is more strongly inhibited by interaction with non-classical HLA-G, compared to the interaction with the classical HLAs. This is supposed to be an effect mediated by a higher receptor affinity for HLA-G (*263*). The ligands for the NCRs, NKp30 and NKp44 are detected on maternal decidual stroma cells and fetal trophoblast, regulating NK cells' secretory function (*259*). Insufficient spiral artery remodeling as a result of defects in trophoblast invasion leads to a reduced blood flow and a potentially deadly disease in the late onset of pregnancy called preeclampsia (*264*). Increased inhibition of NK cells is associated with an increased risk for preeclampsia, poor fetal growth, and recurrent miscarriage (*261*).

An increase in the early miscarriage rate was observed in *in vitro* fertilizations of mothers with a KIR A haplotype (*265*). Additionally, the above mentioned pregnancy complications occurred more frequently in KIR A and HLA-C1 homozygous mothers with a C2 fetus (*266-268*). Presence of the HLA-C2 activating receptor KIR2DS1 in the maternal telomeric KIR B region was proven to be protective in this situation in a European cohort (*266*). Moreover, increase of fetal birth weight is associated with maternal activating KIR2DS1, and a decrease with maternal inhibitory KIRs, if HLA-C2 is paternally inherited (*269*). In an African cohort, the same correlation of maternal KIR A haplotype and fetal HLA-C was observed. Interestingly, the protective activating gene is KIR2DS5, here present in an unique centromeric B region (*270*). In non-African populations, KIR2DS5 is linked to KIR2DS1, though the observed effect from KIR2DS1 could be attributed to KIR2DS5. Yet, the ligand for KIR2DS5 is still controversial (*271*).

Taken together, NK cells and KIR interactions play a huge role during pregnancy. Consequently, it is presumed that NK cells and distinct KIR interactions are important for the establishment of an FM as well.

3.5.5 Influence of FM on hHSCT

In T-cell-replete hHSCT from an IPA/NIMA mismatched donor, a lower number of severe GvHD was observed (*71, 272*). In mothers, this can be explained by an IPA/NIMA-specific tolerance by deletion of specific reactive T cells during pregnancy that have formed a memory in the mother's immune system. Many individuals show low immune response against the

NIMAs they have encountered during pregnancy, and some mothers even show a protective immune response to the IPAs of their child (*273*).

Furthermore, a chimerism in organs can be established by lymphocyte infusion prior to organ transplantation. This chimerism results in enhanced tolerance of the transplanted organ in the recipient, whereby this effect is independent of a microchimerism in the peripheral blood (*274*). HSC donations from mothers with a persisting FM resulted in a higher overall survival (up to 40%) and a trend towards a lower risk of relapse compared to HSC donations from FM^- mothers (*77*). Thus, a persisting FM in the mother potentially results in the same effect. Since the FM cells are persistent, there must be an origin of the cells with self-renewal potential. It is likely that the cells have settled in the BM or other tissues, where they are tolerated by the surrounding cells. Consequently, maternal cells are on the one hand primed to tolerate the filial cells, but additionally have the potential to distinguish between healthy and degenerated filial leukemic cells. Another hypothesis is that deletion of alloreactive T cells that occurred during pregnancy (*94*) resulted in a memory formation in the T cell population. From this assumption, two scenarios evolve: First, the maternal cells exert an alloreactivity against the filial cells. During pregnancy, the maternal immune system was inhibited to not attack the semi allogenic fetus (*91, 92*). After HSCT, the donated stem cells from the mother are not in an immunosuppressed environment as during pregnancy. Thus, the maternal alloreactive cells could cause severe GvHD, which might result in TRM or graft rejection. Second, the maternal cells still tolerate the filial cells in their own circulatory system. As a result, the maternal cytotoxic cells have a higher potential to differentiate between healthy and degenerated cells and exert a higher reactivity against the remaining leukemic blasts. Furthermore, the maternal cells are better tolerated in the child, which might result in less TRM and increased engraftment. This could result in the main advantage of maternal HSC compared to the paternal “unbiased” cells. It is still unclear which of the described scenarios holds true for the influence of an FM on hHSCT. Besides, it is not known if distinct KIR and HLA combinations affect the influence of an FM on HSCT.

3.6 Genetic modification of NK cells for combinational therapy of hHSCT and immunotherapy

NK cells express a huge repertoire of surface receptors essential for their effector function regulation (*141, 154*). Also, in mismatched HSCT a beneficial role has been attributed to the alloreactive NK cells, meaning that NK cells have a huge potential to be used therapeutically (*275*). Infusion of haploidentical KIR-ligand mismatched alloreactive NK cells has been shown to be feasible and safe in childhood AML patients (*276*) and also in elderly high-risk AML patients (*277*). However, up to now the outcome is not satisfactory and there is an urgent need for improvement (*278*). One factor influencing NK cells’ potential is the microenvironment

(*275*). Different genetic modifications of NK cells and pre-treatment or combined treatments are currently under investigation. These include combination with checkpoint inhibitors or cytokines. Still, infusion of haploidentical NK cells combined with human IL-15 infusion resulted in toxic side effects (*279*).

An alternative strategy is to equip NK cells with a chimeric antigen receptor (CAR) targeting a cancer specific antigen. Various clinical trials are currently in process using either *ex vivo* expanded and pre-activated NK cells or the human NK cell line NK92 (*280*). Another approach to increase their functionality is to block innate inhibitory receptors on the NK cell surface. Clinical usage of the KIR2DL1 and KIR2DL2/L3 blocking antibody IPH2101 showed promising results in a phase 1 trial in myeloma and AML patients (*281, 282*). Unfortunately, the phase II trial was terminated at an early stage because of a lack of efficiency. A rapid reduction of KIR2D surface expression was observed, which was correlated with a reduction in NK cell responsiveness. This reduction is caused by trogocytosis, a mechanism in which surface molecules from one cell are shed and uptaken by an interacting cell. An effect of KIR2DL-null NK cells could not be observed because of the general reduction in KIR2DL-expressing NK cells (*283*). A good alternative to alter NK cell functionality is to genetically equip NK cells with a certain inhibitory or activating KIR receptor.

The majority of approaches for genetic modification of effector cells use viral transfer systems to deliver the effector molecules (e.g. CARs or fusion proteins containing an activating receptor) into the target cells (*284*). Most commonly used are retroviral vector systems, e.g. gammaretroviral, lentiviral or alpharetroviral vectors (*285, 286*). The gammaretroviral vectors integrate into dividing cells, whereas the lenti- and alpharetroviral vectors are able to infect non-dividing cells (*287*). Thus, for low proliferating cells as NK cells, lenti- and alpharetroviral vectors are the best choice. Besides the lentiviral vector, the alpharetroviral vector shows a high potential to be used for gene therapeutic approaches by virtue of its integration pattern. The alpharetroviral vectors show only a low preference to integrate into active genes and no preference to integrate close to transcription start sites, which could induce overexpression of the downstream gene and could result in oncogene activation (*288*).

Transduction of T cells has been shown to be feasible, whereas transduction of NK cells is challenging (*289*). This is expected since NK cells are the first responders to viral infections (*290*) and thus are equipped with a high endurance during viral infection (*291*). Nevertheless, different attempts showed promising results to genetically modify primary NK cells (*286, 289*). Lentiviral vectors combined with protamine sulfate in IL-21 and IL-2 activated NK cells showed good transduction efficiencies (*289*), whereas for alpharetroviral vectors, a combination with vectofusin-1 (VF-1) seems promising (*292*).

Since most studies use CAR-modified NK cells, less is known about how insertion of a germline-encoded receptor could change the NK cell reactivity. Insertion of the activating

receptor NKG2D^{+} and DNAM^{+} in NK92 cells provides a potential tool to treat sarcoma and other malignancies (*293*). Modification of primary NK cells with a fusion construct of the NCR NKG2D-CD3ζ-DAP10 resulted in prolonged and enhanced killing of tumor cell lines *in vitro* and in a xenograft model compared to the NK cells that were not modified, whereas reactivity against non-transformed cells remained low (*294, 295*).

After HSCT, distinct KIR receptor/ligand interactions exert protective effects and can exert an alloreactivity against non-self HLA-mismatched cells, resulting in avoidance of GvHD and increased engraftment (*57, 239*), Modification of NK cells with certain receptors that affect NK cell alloreactivity would provide an excellent tool to treat patients with more effective donor- derived NK cells post-transplantation, e.g. in case of viral infections or relapse. Another benefit is that, if functionality of NK cells can be affected by certain KIR receptors, this would be transferable to other fields of research and applications.

3.7 Aims of the project

hHSCT is a well-established treatment for pediatric patients lacking a MUD or an HLA-identical sibling stem cell donor. The presence of a persistent FM in a mother donating the HSCs for her child has been shown to be beneficial for the child's survival (*77*). The mechanism behind this phenomenon is unknown. Although FM cells have been found in many organs and tissues, less is known about the phenotype of these circulating microchimeric cells. In addition, there is a lack of precise quantification of the FM cells. Why some, but not all, mothers tolerate fetal cells has also not been addressed so far. Furthermore, the presence of a TM has been described, but little is known about the impact on the outcome of receiving a sibling-derived transplantation.

During pregnancy, wherein the establishment of an FM occurs, NK cells and distinct KIR/HLA interactions are important for placentation and a successful pregnancy. After HSCT, as the maternal cells rebuild the immune system in the recipient, NK cells are the first lymphocytes that reconstitute. Distinct KIR receptor/ligand interactions exert protective effects and can exert an alloreactivity against non-self HLA-mismatched cells. Aims of the study:

1. Establishment of a digital PCR-based approach for exact quantification and detection of FM cells
2. Determination of the phenotype of circulating FM cells
3. Investigation of the influence of distinct KIR/HLA combinations on the establishment and persistence of an FM
4. Analysis of whether the functionality and reactivity of maternal NK cells against filial blasts is affected by a persisting FM or distinct KIR/HLA combinations
5. Investigation of the influence of distinct KIR/HLA combinations on the establishment of a TM

In current clinical trials, the infusion of *ex vivo* expanded and activated alloreactive NK cells has been investigated. Here, NK cell administration has been shown to be feasible and safe, but NK cells lack optimal reactivity. Therefore, the idea is to equip NK cells with the KIR receptors KIR2DL1, KIR2DS1, KIR2DL2 and KIR2DS2, to then be able to analyze whether insertion of these receptors leads to alteration of NK cell reactivity into a more sensitive reactive state. Therefore, further aims were to

6. Generate lentiviral and alpharetroviral vectors containing the respective KIR sequences
7. Generate NK92-MI cells expressing a single KIR followed by functional testing of their cytotoxicity and degranulation
8. Modify primary human NK cells with certain KIR receptors and analyze their cytotoxicity and degranulation against distinct target cells

4. Results

4.1 Detection of a microchimerism

The role of FM cells in the maternal tissues and blood system is still controversial (*77, 125, 126, 274, 296, 297*). A variety of methods has been used to identify a microchimerism, but all differ regarding their detection capability, face low sensitivity because of a lack of suitable markers and all lack precise quantification (*76, 80, 105, 106, 108*). Therefore, a method is needed that I. allows for an exact quantification, II. has a broad panel of usable markers to distinguish donor and recipient, and III. can be easily adapted to other research groups and fields. Various groups validated ddPCR for chimerism analysis after HSCT with high sensitivity, exact quantification and excellent reproducibility (*120, 121*). Here, a ddPCR protocol was developed and optimized for exact quantification of FM within DNA from maternal blood cells.

4.1.1 Droplet digital PCR for determination of microchimerism

Maternal and filial DNA were distinguished with a panel of primer/probe pairs, specific for InDels. Additionally, a Y-chromosome-specific primer/probe pair was included (*113, 115*). In the following, the different InDels are referred to as markers. To make ddPCR applicable for all markers and to run different analyses in parallel, general reaction conditions (inserted DNA, reaction temperature, reaction buffer) were maintained equally.

Human-derived cell lines (HEK293T, K562, NK92-MI, MHH-MHH-Call3, MHH-Call3, CCRF-CEM, Jurkat) were screened for the presence or absence of the respective markers. Subsequently, these were used for assay establishment and determination of the background level. To achieve precise quantification, a straight separation of droplets by salt concentration was used (*120*). Therefore, optimal PCR conditions with and without the addition of $MgCl_2$ were determined for each marker using a cell line positive for the respective marker. Exemplarily, separation influenced by $MgCl_2$ is depicted for the marker 7b (Figure 6, A). In this case, the best separation of droplets is reached with the addition of 4 mM $MgCl_2$. Optimal ddPCR conditions for each marker are depicted in section 6.3.3, Table 28. In the next step, the sensitivity of each marker was determined.

Healthy volunteer female donors might have a persistent microchimerism (from earlier pregnancies, e.g. a maternal or trans-maternal microchimerism), which could result in false positive droplets. To avoid false positive signals, artificial dilution series were generated with human cell lines (Figure 6, B and C). In ddPCR, at least 300,000 diploid cells must be analyzed to detect one target cell in 100,000 background cells. This equals 2 µg of genomic DNA. To overcome this limit of detection, 4 µg of DNA per dilution step was analyzed. The experimental set-up for microchimerism determination is depicted in Figure 6, B. To detect rare events, two separate reactions were employed. I. An analysis reaction with an increased amount of

inserted DNA of 500 ng/well, in which the increased amount impedes Poisson statistics and II. A quantification reaction. In the quantification reaction, 100 ng/well of DNA were analyzed using the marker and the housekeeping gene HCK in a duplex-reaction. HCK positive copies represented the total amount of inserted cells in this reaction and enabled calculation of the inserted DNA in all reactions. The sum of marker positive copies in the analysis reactions was used to directly quantify the amount of marker positive copies in relation to all HCK positive copies.

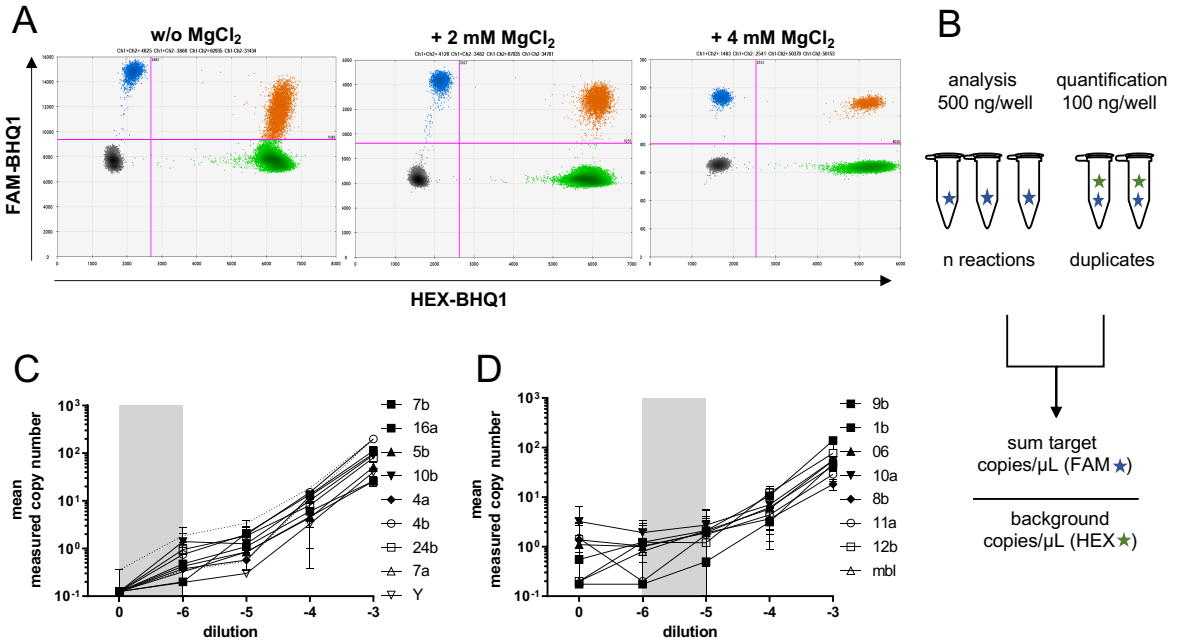

Figure 6: Optimization and sensitivity determination of ddPCR. PCR conditions for each marker were optimized with the addition of $MgCl_2$ for better separation of droplets. (A) Improved separation of the droplets for the marker 7b (FAM-BHQ1) and HCK (HEX-BHQ1) is reached with increased amount of $MgCl_2$ (from left to right). (B) Experimental set-up for sensitivity and microchimerism determination. N analysis reactions containing 500 ng DNA/well were prepared with the markers and duplicates of a quantification reaction with 100 ng DNA/well. The quantification reaction is a duplex reaction including the housekeeping gene HCK, where the probe is labeled with HEX-BHQ1 (green star), and the probe for the marker of interest is labeled with FAM-BHQ1 (blue star). Total analyzed DNA copies are determined and directly used to quantify the amount of copies from the gene of interest in the total amount of input background copies. (C + D) Artificial dilution series were generated using cell lines. ddPCR was performed in eight analysis reactions (in total 4 µg of DNA) of each dilution series and duplicates of the quantification reaction. Markers with a high sensitivity up to 10^{-6} and no background signal are shown in C. D summarizes markers with a lower sensitivity limit at 10^{-5}, which is caused by higher background at 0. Zero are samples of undiluted marker negative DNA. Markers show a different limit of sensitivity between 10^{-5} - 10^{-6}. Gray bars mark the range of detection. Depicted are mean ± SD. w/o: without; n: number, HCK: hematopoietic cell kinase.

The false positive rate, referred to as background level, was determined for each marker in a cell line that was negative for the respective marker. Each analyzed marker had a different background level, reflecting differences in marker sensitivity. Markers were grouped into markers with and without background level detection (Figure 6, C and D). Markers with no background level had a high sensitivity that resulted in detection of one microchimeric cell in up to 10^6 background cells (Figure 6, C). Markers with a strong background level had a lower sensitivity that resulted in the detection of one microchimeric cell in 10^5 background cells (Figure 6, D). To avoid detection of false positive samples in subseqeunt experiments, the

same number of reactions was prepared with DNA from a cell line negative for the respective marker. Results from the marker negative cell line were used to determine the background level. Consequently, samples were only considered as positive, if the detected level of microchimeric cells exceeded the background level.

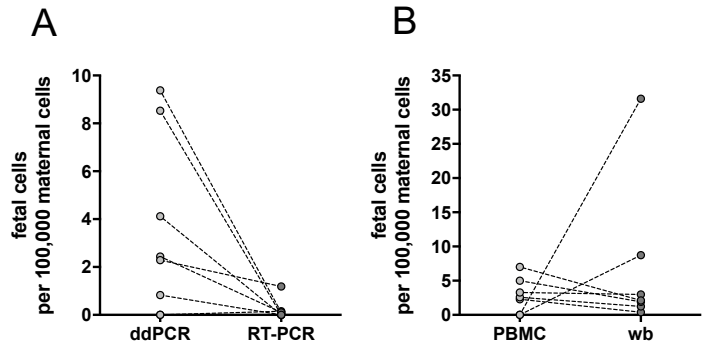

Figure 7: Validation of ddPCR analysis in FM samples. Maternal DNA was isolated and analyzed for the occurrence of an FM. (A) Eight samples from PBMCs were analyzed using both methods ddPCR and RT-PCR. (One dot at 0 combines two samples negative in both methods). (B) Detection of FM in DNA isolated from PBMCs or wb. ddPCR: digital droplet PCR, RT-PCR: real-time PCR, PBMCs: peripheral blood mononuclear cells; wb: whole blood.

ddPCR and the previously used RT-PCR were used to analyze eight samples of maternal DNA in parallel (Figure 7, A). Two samples were negative in both methods. Two samples negative in RT-PCR were positive in ddPCR. In six samples both methods revealed the same results, whereby the mean level of FM cells was increased in ddPCR analyses (mean of FM cells: ddPCR 3.5 vs. RT-PCR 0.2).

Another factor that could influence the detection of a microchimerism is the pre-treatment of cells. Therefore, FM was determined in DNA extracted from the same donor either directly from the whole blood (wb) or from NK cell negative PBMCs (Figure 7, B). For the latter, PBMCs were isolated using density centrifugation. Afterwards, NK cells were depleted from PBMCs, using magnetic activated cell sorting (MACS) and used for functional analyses (section 4.3). DNA was isolated from PBMCs lacking NK cells. In six donors a lower number of fetal cells was detected in the samples from whole blood compared to the samples from PBMCs (mean of FM cells: PBMCs 7.0 vs. wb 2.9). In two samples an FM was only detected in whole blood and not in PBMCs.

Overall, the established ddPCR protocol was suitable to analyze DNA either from whole blood or from purified PBMCs for the occurrence of FM.

4.1.2 FM determination in maternal samples

A group of 60 mothers, whose children were treated for a malignant hematological disease at the University Medical Center Hamburg-Eppendorf, was analyzed for the detection of FM. This group will be referred to as FM group. Additionally, a second group of mothers was analyzed, whose children suffered other diseases. In the second group, all children received an hHSCT from their mother. Because no leukemic blasts were available for functional analyses, this

group was considered for analyses of genetic factors only. This group will be hereafter referred to as Haplo group. Patient characteristics are depicted in Table 3.

Table 3: Patient characteristics. Others include: T cell non-Hodgkin lymphoma (T-NHL), neuroblastoma (NB), hemophagocytic lymphohistiocytosis (HLH), mucopolysaccharidosis type I (MPSI), and immune dysregulation polyendocrinopathy enteropathy X-linked syndrome (IPEX). c-ALLs are a subgroup of B-ALLs and considered separately. Depicted are counts and frequencies in the subgroups. FM: prospective group of mother-child pairs that was analyzed for occurrence of an FM and in which functional assays were performed. Haplo: group of mother-child pairs in which the child received a haploidentical stem cell transplantation from the mother.

N = 70		FM		Haplo	
		N	%	N	%
Patients, N		60	86	10	14
Sex	Female	28	47	7	70
	Male	32	53	3	30
Age (years)	Median (range)	6.28	(0.1 - 17.6)	2.58	(0.1 - 5.52)
Disease	c-ALL	35	58	-	-
	T-ALL	8	13	-	-
	B-ALL	13	22	-	-
	AML	2	3	-	-
	Others	2	3	10	100

The FM group included 60 patients. The number of male and female patients was almost equal (53% vs. 47%). The median age was 6.28 (range 0.1 - 17.6) years, 58 of the children suffered from leukemias (c-ALL, T-ALL, B-ALL, AML) and two had a T cell non-Hodgkin lymphoma (T-NHL). These two are grouped into “others.” The Haplo group contained 10 patients with more female than male patients (70% vs. 30%), and the median age was 2.58 (range 0.1 - 5.52) years. Children suffered from hemophagocytic lymphohistiocytosis (HLH), neuroblastoma (NB), mucopolysaccharidosis type I (MPSI) or immune dysregulation polyendocrinopathy enteropathy X-linked syndrome (IPEX), classified into “others.”

Table 4: Overview FM determination in two groups. Mothers, whose children were treated for hematological diseases (FM) and mothers of children who received an hHSCT (Haplo) were analyzed for the occurrence of an FM using ddPCR. Depicted are counts and frequencies of FM determinations.

Samples	N total (%)	FM determination possible (% of samples)	FM^+ (% of analyzed)	FM^- (% of analyzed)
FM	60 (86)	42 (70)	13 (31)	29 (69)
Haplo	10 (14)	9 (90)	6 (67)	3 (30)
Total	70 (100)	51 (73)	19 (37)	32 (63)

FM determination was compared between both groups (Table 4). In 42 (70%) mothers of the FM group an FM analysis was possible. In 20 (30%) mother-daughter pairs, no suitable marker was found. An FM was detected in 13 (31%) of the mothers. In the Haplo group, for nine (90%) of the mothers a suitable marker was identified, and an FM was detected in six (67%) of the

analyzed mothers. Consequently, FM determination was possible in 51 (73%) and a persisting FM was detected in 19 (37%) mothers.

Subsequently, the level of FM was compared between the groups (Figure 8). In the FM group, the level of detected FM cells ranged from 1 to 10 filial cells per 100,000 maternal cells except one outlier with 90 FM cells per 100,000 maternal cells. In the Haplo group the level ranged from 5 to 25 FM cells per 100,000 maternal cells. In general, in the FM group the level of FM was significantly lower, compared to the Haplo group (FM group 3.4 vs. Haplo group 10.2). For the following analyses (section 4.2) these groups were pooled.

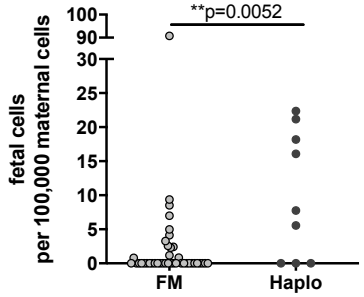

Figure 8: FM level determination. Maternal PBMCs were isolated and DNA was extracted followed by a marker selection and ddPCR for FM determination. FM determination was possible in 42 mothers of the FM group (mothers of patients suffering from leukemia), and nine mothers of the Haplo group (mothers who donated stem cells for their children). Statistical analysis was performed using the Mann-Whitney test. Significance level $p<0.05$.

4.1.3 Phenotype of circulating FM cells

FM cells are detected in different compartments, cell populations (*81, 87*) and with different phenotypes (*75, 81*). It is still a mystery why only some and not all fetal cells are cleared and why only some mothers tolerate these filial cells. If filial cells survive for decades postpartum, there must be a population of fetal cells with the ability of self-renewal settled in the mother's body. Information about the phenotype of these FM cells would help to understand their function and would allow to explain their persistence.

To elucidate the phenotype of the circulating FM cells in the analyzed mothers, PBMCs from one FM positive mother were sorted into the lymphocyte subgroups: B ($CD20^+$ $CD19^+$), T ($CD3^+$ $CD4^+$ and $CD3^+$ $CD8^+$), NK ($CD56^+$ $CD16^+$), and $CD34^+$ cells followed by FM analysis (Figure 9, A). FM cells were detected in the PBMCs, whole blood (wb), and in the $CD34^+$ subgroup (filial cells per 100,000 maternal cells: PBMCs 2 vs. wb 0.5 vs. $CD34^+$ 7000).

Most of the FM cells were found in the $CD34^+$ population, which is a marker for HSC. To determine whether FM cells belong to a distinct progenitor population, cells were sorted into the following four lin^- stem cell progenitor sub-populations: I. $CD38^-$ $CD133^+$ $CD34^+$, II. $CD38^-$ $CD133^-$ $CD34^+$, III. $CD38^-$ $CD34^-$ $CD133^+$, and IV. $CD133^-$ $CD38^+$ $CD34^{+/-}$ (Figure 9, B; gating strategy is provided in appendix 8.3.1). In total four mothers were analyzed, one of which was pregnant at the time of blood donation. From one non-pregnant mother, BM was analyzed.

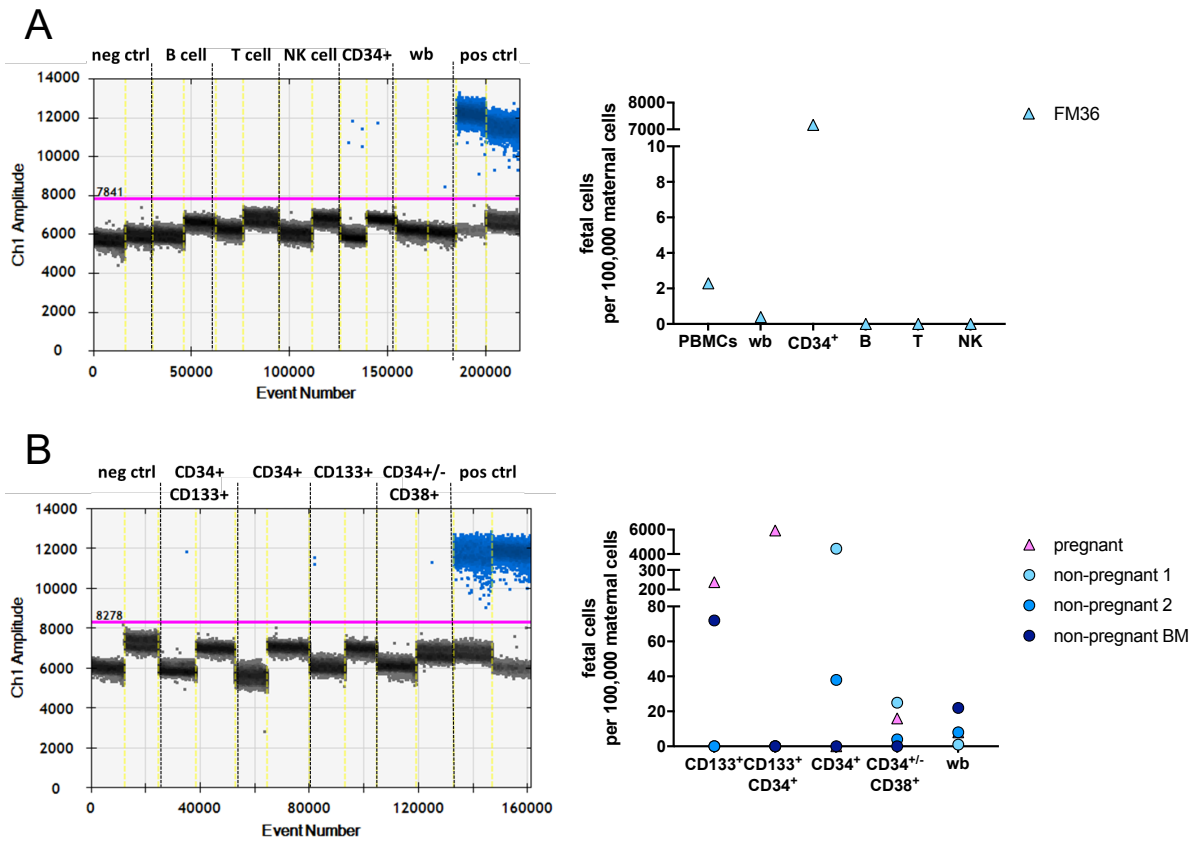

Figure 9: Phenotype of FM cells. Maternal PBMCs were isolated and sorted into different subgroups. DNA was analyzed for an FM. (A, left) 2D plot of sorted subgroups from one woman into B, T, NK, and $CD34^+$ cells. (A, right) Quantification of filial cells in maternal background cells. (B) Sorting of maternal cells into lineage negative (lin^-) and different hematopoietic precursor types: $CD34^+$ $CD133^+$, $CD34^+$ only, $CD133^+$ only, and $CD34^{+/-}$ $CD38^+$. Analysis was performed from wb of one woman that was pregnant at the time of blood donation and from three non-pregnant women. From two non-pregnant women DNA from wb was analyzed, and in one woman DNA from BM. (B, left) Exemplary 2D plot from one woman and (B, right) quantification of filial cells in maternal background cells. PBMCs: peripheral blood mononuclear cells. B cell: $CD19^+$ $CD20^+$; T cell: $CD3^+$; NK cell: $CD56^{dim/+}$ $CD16^+$; $CD34^+$ cell, wb: whole blood, BM: bone marrow, neg ctrl: negative control, pos ctrl: positive control. DNA from a cell line negative for the marker was used as negative control. DNA isolated from the leukemic blasts of the respective child was used as positive control.

FM was detected in the whole blood of all analyzed mothers ranging from 1 to 22 FM cells (here and in the following descriptions always in relation to 100,000 maternal cells). In the non-pregnant women, the FM cells were detected in the $CD34^+$ (38 FM cells) and $CD34^+$ $CD38^+$ subpopulation (25 and 4 FM cells). In one non-pregnant mother, the level of $CD34^+$ FM cells was very high with 4444 FM cells, compared to 38 FM cells in the second non-pregnant woman. In the pregnant woman, the FM cells had a $CD133^+$, $CD34^+$ $CD133^+$ and $CD34^+$ $CD38^+$ phenotype. Here, $CD133^+$ FM cells were detected at a high number of 238 FM cells, and $CD133^+$ $CD34^+$ FM cells at the highest number with 5926 FM cells. In the $CD34^+$ $CD38^+$ population the lowest level of FM cells was detected with 16 FM cells. Interestingly, in the BM sample, FM cells were detected only in the $CD133^+$ subgroup and at a moderate level of 72 FM cells.

In conclusion, the phenotype of FM cells differed during pregnancy, after pregnancy, and in BM.

4.2 Factors that influence an FM

4.2.1 Impact of genetic factors on the occurrence of an FM

The exact mechanism why an FM persists in only 37% of the women is not known. Moreover, no studies have analyzed genetic features that might affect the continued presence of FM in some but not all mothers. To examine which factors could influence the establishment and the persistence of FM, 70 parent-patient pairs were grouped into FM^+ and FM^- and analyzed for a correlation with the children's age, sex, disease, and the genetic factors centromeric or telomeric KIR genes, B content score, and HLA-C genotype or match/mismatch (Table 5).

Table 5: Correlation of genetic factors in child, mother, and father with the occurrence of an FM. Samples were grouped dependent on age, sex, disease, centromeric or telomeric KIR genes, B content score, HLA-C genotype and HLA-C match or mismatch of parent and child. Differences in FM^+ and FM^- groups were analyzed using Fisher's exact test for two groups or Chi^2 for more than two followed by Cramer-V to determine the strengths of association (0.1 small effect, 0.3 medium effect, 0.5 large effect). Significance level $p<0.05$.

	Factor	N	Value	p-value	Cramer-V
Child	Age	51	45.875	1	1
	Sex	51	3.989	0.080	0.280
	Disease	51	9.223	0.088	0.457
	Centromeric KIR	51	0.716	0.143	0.104
	Telomeric KIR	51	4.127	0.105	0.289
	B content score	51	4.660	0.148	0.308
	HLA-C	51	2.215	0.298	0.212
Mother	**Centromeric KIR**	**51**	**8.551**	**0.011**	**0.422**
	Telomeric KIR	51	0.944	0.702	0.112
	B content score	51	6.595	0.072	0.372
	HLA-C	**51**	**6.979**	**0.031**	**0.387**
	HLA-C match	**51**	**9.188**	**0.009**	**0.434**
Father	Centromeric KIR	17	0.032	1	0.044
	Telomeric KIR	18	0.692	1	0.177
	B content score	18	1.313	1	0.226
	HLA-C	20	0.672	1	0.169
	HLA-C match	20	0.020	1	0.032

FM was detected independent of children's age, sex, and disease. Occurrence of an FM significantly correlated with maternal centromeric KIR genes (8.551, n=51, p=0.011, Cramer-V =0.422), and maternal HLA-C (6.979, n=51, p=0.031, Cramer-V 0.387), both with a medium strength. Maternal and filial or paternal and filial HLA-C equality was analyzed. HLA-C match means mother or father and child have the same HLA-C, whereas mismatch indicates a disparity. Occurrence of an FM correlated strongly with mother to child HLA-C match/mismatch (9.188; n=51, p=0.009, Cramer-V 0.434), indicating that maternal-filial HLA match is beneficial for an FM. No correlation was seen between an FM and any of the filial or paternal-derived factors.

Table 6: Correlation of KIR genes and haplotype in child, mother, and father with the occurrence of an FM. Fisher's exact test with risk calculation of odds ratio and 95% confidence analysis was performed. Odds ratios were calculated as follows: odds ratio = $((FM^-/KIR^+)/(FM^+/KIR^+))/(FM^-/KIR^-)/(FM^+KIR^-)$. Odd ratio >1 = occurrence or absence of gene affects FM. KIR2DL1, KIR2DL4, KIR3DL2 and KIR2DL3 are present in all donors and therefore were excluded. *Genes are constantly present and therefore were excluded. Significance level $p<0.05$.

KIR	Child			Mother			Father		
	N	p-value	Odds ratio (95% CI)	N	p-value	Odds ratio (95% CI)	N	p-value	Odds ratio (95% CI)
2DL2	51	0.765	1.388 (0.432-4.459)	51	0.202	0.358 (0.085-1.500)	18	1	0.9 (0.133-6.08)
2DL3	51	0.623	1.765 (0.228-13.685)	**51**	**0.04**	**6.923 (1.23-35.956)**	18	1	0.909 (0.754-1.096)
2DL5	50	0.145	0.368 (0.113-1.198)	51	0.065	0.241 (0.058-0.995)	18	0.627	0.500 (0.068-3.696)
2DP1	*			51	1	0.969 (0.91-1.031)	*		
2DS1	51	0.08	0.306 (0.094-0.998)	51	0.565	0.642 (0.204-2.017)	18	0.627	0.500 (0.068-3.696)
2DS2	51	0.771	0.75 (0.234-2.404)	51	0.543	0.595 (0.171-2.071)	18	1	1.111 (0.164-7.506)
2DS3	44	0.738	1.447 (0.365-5.735)	44	0.456	2.571 (0.475-13.913)	18	1	0.600 (0.031-11.473)
2DS4	51	0.373	1.056 (0.949-1.174)	51	0.373	1.056 (0.949-1.174)	*		
2DS5	51	0.106	0.317 (0.089-1.132)	51	0.563	0.667 (0.211-2.106)	18	1	2.250 (0.185-27.369)
3DL1	51	0.134	1.118 (0.958-1.304)	51	0.373	1.056 (0.949-1.174)	*		
3DP1	0	0.285	0.906 (0.811-1.013)	51	1	0.969 (0.91-1.031)	18	1	0.909 (0.754-1.096)
3DS1	51	0.07	0.311 (0.091-1.065)	51	0.561	0.616 (0.196-1.933)	18	1	1.333 (0.098-18.192)
Haplotype	51	0.128	6 (0.687-52.383)	51	0.236	4.154 (0.464-37.513)	18	1	1 (0.072-13.868)

As described earlier, maternal centromeric KIR genes are a factor that correlated with an FM. Thus, correlation of distinct KIR genes and haplotype was analyzed in FM^+ and FM^- groups of child, mother and, as a control, the father (Table 6). FM significantly correlated with the absence of maternal KIR2DL3 ($p=0.04$, odds ratio 6.923, 95%CI 1.23-35.956). No correlation was detected between FM and any of the other KIR genes or the haplotype.

Taken together, maternal HLA-C, further HLA-C match, and the centromeric KIR genes, especially KIR2DL3, were significantly correlated with an FM.

4.2.2 Influence of child's age, sex, and disease on an FM

Even though no significant correlation between the occurrence of an FM and the child's age, sex, and disease was observed (Table 5), these factors could influence the level of FM in the mothers. Hence, mothers were grouped depending on their child's, age, sex and disease, and the level of FM was analyzed (Figure 10).

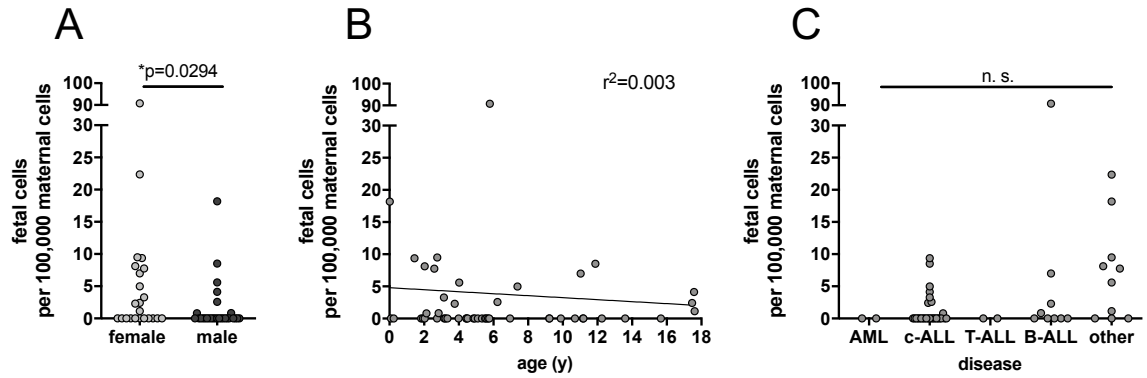

Figure 10: Influence of child's, age, sex, and disease on the level of FM cells. FM was determined in mothers using ddPCR. The level of microchimeric cells was compared between mothers grouped depending on their child's (A) sex, (B) age, and (C) disease. Exact n values are provided in appendix 8.4. For statistical analyses in (A) Mann-Whitney test, in (B) simple linear regression analysis, and in (C), the Kruskal-Wallis test followed by Dunn´s-multiple comparison test was used. Significance level $p<0.05$. n. s. not significant.

FM cells from daughters were detected at a significantly higher level compared to FM cells from sons (mean FM cells: female 7.35 vs. male 1.45; p=0.0294) (Figure 10, A). An FM was detected in mothers from children shortly after until up to 18 years after parturition (Figure 10. B). With increasing child's age, the level of FM cells slightly decreased. However, the level of FM was independent of child's age (r^2=0.003). Mothers were grouped depending on her child's disease. An FM was detected in mothers of children suffering from c-ALL, B-ALL and other diseases. The AML and T-ALL groups contained two patients each, and no fetal cells could be detected in the respective mothers (Figure 10, C). The mean values of FM cells were not significantly affected (AML 0 vs. c-ALL 1.3 vs. T-ALL 0 vs. B-ALL 11.2 vs. other 7.3). Taken together, FM cells from daughters persisted at a significantly higher level in the mother compared to FM cells from sons, but the level of a persisting FM was independent of the child's age and disease.

4.2.3 Influence of HLA-C genotypes on an FM

In pregnancy, distinct mother/filial HLA combinations are beneficial to a successful pregnancy. Moreover, in HSCT an HLA match is desirable to prevent GvHD and graft rejection (*266-268*). Consequently, an HLA match or disparities could affect the persistence and tolerance of FM cells. The influence of maternal and filial HLA-C genotype and their combination on an FM was analyzed.

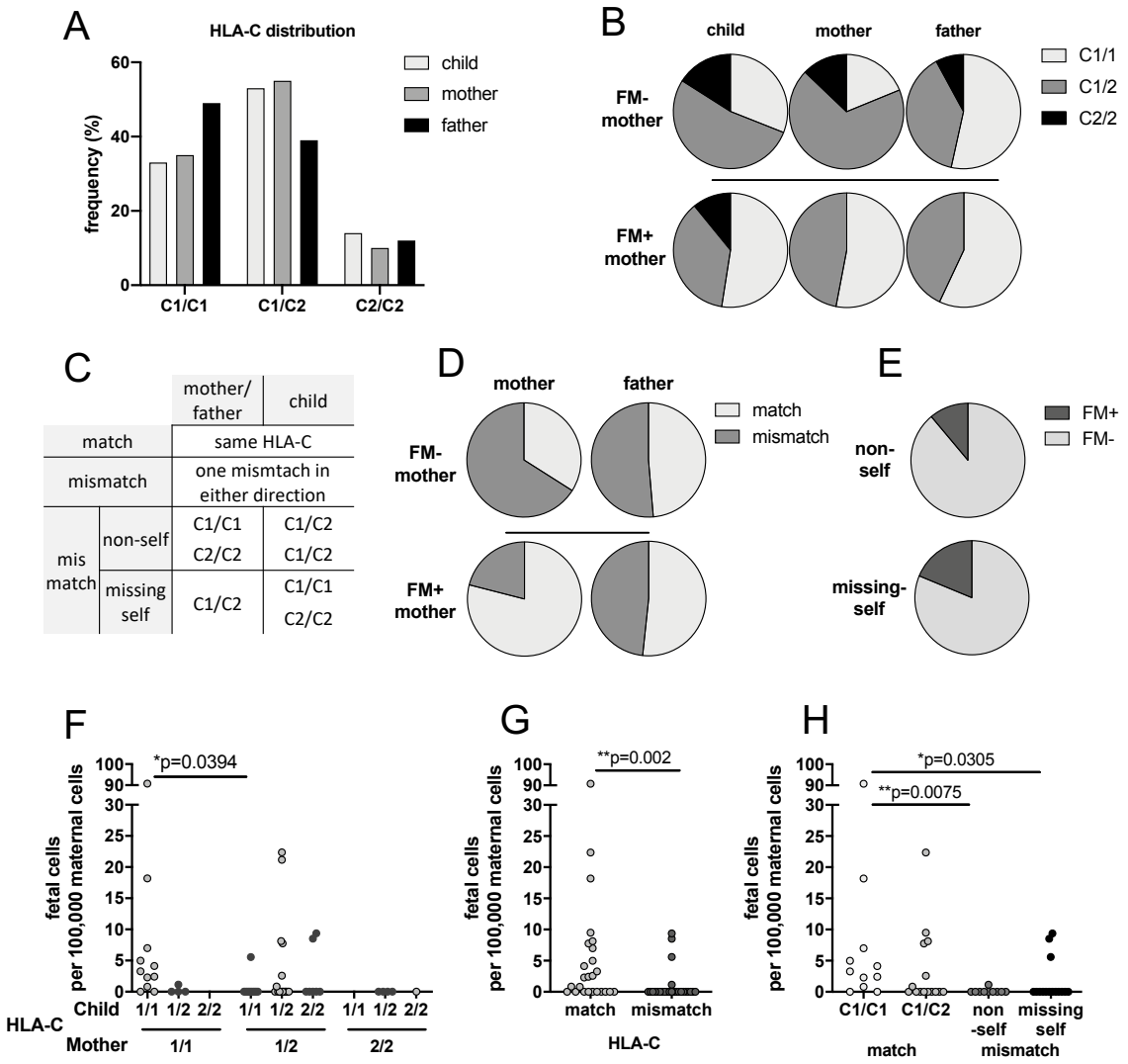

Figure 11: FM is favored in HLA-C matched mothers and children. Frequency and level of FM were analyzed in regard to filial or parental HLA-C genotypes. Child, mother, and father were grouped according to their HLA-C genotype into C1 or C2 homozygous or C1/C2 heterozygous. (A) HLA-C distribution in the analyzed groups. (B) Frequencies in child, mother and father grouped into FM^+ and FM^-. (C) Criteria for grouping into HLA-C match and mismatch. (D) Frequencies in HLA-C match or mismatch groups and (E) mismatch mothers grouped into mismatch non- or missing-self. FM was determined in mothers using ddPCR. Influence on the level of FM was analyzed of (F) maternal and fetal HLA-C, (G) HLA-C match or mismatch, (H) match, non-self, and missing-self mismatch from the maternal to filial direction. In total n=51. Exact n values are provided in appendix 8.4. Statistical analysis of frequencies was performed using Fisher's exact test for two groups or Chi^2 for more than two. The Kruskal-Wallis test followed by Dunn´s-multiple comparison test was used to analyze differences in FM levels. Statistical significance $p<0.05$.

First of all, child, mother, and as a control the father were grouped depending on their HLA-C genotype into C1 and C2 homozygous and C1/C2 heterozygous, and frequencies in the groups were compared (Figure 11, A). The distribution was equal between all three groups and in accordance with the described frequencies for the Caucasian population (*298*). Heterozygous individuals make up to 50 - 60%, while 30 - 50% are C1 homozygous individuals and the lowest fraction with 10 - 20% are C2 homozygous.

Previously, a correlation was observed between maternal HLA-C and the occurrence of FM ($p=0.031$, Table 5). To investigate the influence of an FM, child, mother, and father were

grouped depending on the detection of a persisting FM in the mother, and HLA-C genotype frequencies were compared (Figure 11, B). Fathers were considered as a control and grouped depending on the occurrence of an FM in the respective mother of their child. The FM^+ group consisted of mothers either C1 homo- or heterozygous. All C2 homozygous mothers were FM^-. Furthermore, the FM^+ group contained more C1 homozygous mother and children than the FM^- group (C1 homozygous mothers: FM^+ 52.6% vs. FM^- 18.8%; children: FM^+ 52.6% vs. FM^- 31.3%). HLA-C frequencies were similar in fathers from each group.

An HLA-C match or mismatch between mother and child could affect the establishment of an FM. To examine this, child and mother vs. child and father were grouped depending on their HLA-C matches (Figure 11, C). A significant correlation of an FM with HLA-C match was detected in the mother-child group (p=0.009, Table 5), but not in the father-child group (p=1,Table 5). Frequencies of HLA-C match and mismatch and the occurrence of an FM were compared (Figure 11, D). In the HLA-C matched mother-child pairs, an FM was observed more frequently (matched pairs: FM^+ 79% vs. FM^- 34%), while in the mismatched mother-child pairs, an FM was observed less often (mismatched pairs: FM^+ 21% vs. FM^- 66%). Frequencies in the father-child matched or mismatched pairs were not affected by grouping into FM^+ and FM^- mothers. Based on these findings, the type of mismatch between mother and child was further determined (Figure 11, E). The mismatched mother- child pairs were grouped into non-self or missing-self from the mother to child direction. Frequencies of FM in the two mismatched settings were equal (FM^+ non-self 11% vs. missing-self 19%).

In conclusion, FM was more often detected in mothers carrying at least one HLA-C1 allele and occurred more often in HLA-C matched mother and child pairs compared to mismatched pairs. Further, the type of mismatch did not affect the occurrence of an FM.

Then the influence of maternal HLA-C or a maternal and fetal HLA-C match on the level of FM was analyzed. Mothers were grouped depending on their HLA-C genotype and the level of FM was compared. As mentioned previously, in the C2 homozygous group no FM was detected. C1 homozygous and C1/C2 heterozygous mothers showed the same level of FM (data not shown). For the following analysis, the filial HLA-C was considered as well. Mothers and children were grouped depending on their HLA-C genotypes (Figure 11, F). A significantly higher level of FM was detected in C1 homozygous matched mothers compared to C1/C2 heterozygous mothers with a C1 homozygous child (mean FM cells: C1/C1 12.2 vs. C1/C2 0.6; p=0.0394). Consequently, the influence of a maternal HLA-C match or mismatch on the level of FM was determined (Figure 11, G). A significantly higher level of FM occurred in matched mother-child pairs compared to mismatched pairs (mean FM cells: match 7.40 vs. mismatch 0.98; p=0.002). Mothers and children were further grouped depending on the kind of mismatch, as described previously, to analyze the effect on the level of FM (Figure 11, H).

The level of FM was significantly increased in the HLA-C1 matched pairs compared to either non-self (mean FM cells: match 12.17 vs. non-self 0.12; p=0.0075) or missing-self (mean FM cells: match 12.17 vs. missing-self 1.57; p=0.0305) mismatched pairs. A heterozygous match had no significant impact on the level compared to a C1 homozygous match. Neither had any mismatch.

Taken together, the level of FM was influenced by maternal HLA-C1, and further increased in C1 homozygous matched mother-child pairs compared to mismatched mother-child pairs. This led to the assumption that the corresponding receptors the KIR receptors, which interact with HLA-C, might influence an FM.

4.2.4 Influence of KIR genotypes on an FM

An FM was favored in mothers carrying HLA-C1 and a higher number of FM cells was detected when both mother and child were homozygous for HLA-C1. Thus the receptors for HLA, the KIRs, might have an influence on the establishment and further could favor the persistence of an FM. Correlation analysis revealed a significant influence of KIR2DL3 on the occurrence of FM (p=0.04, Table 6). To further investigate the impact of KIR2DL3, mothers were grouped into FM^+ and FM^-. Analysis of frequencies showed that an FM was detected more often, if KIR2DL3 was absent (FM^+ 75% vs. FM^- 25%) (Figure 12, A).

Then the influence of presence or absence of a KIR gene on the level of an FM was analyzed. Therefore, mothers were grouped as either KIR positive (KIR^+) or KIR negative (KIR^-) and the level of FM was compared in the respective groups (Figure 12, B). Absence of KIR2DL3 significantly affected the level of FM (mean FM cells: $KIR2DL3^+$ 2 vs. $KIR2DL3^-$ 15; p=0.009). Presence or absence of any of the other KIR genes did not significantly affect the level of FM. Filial KIR genes had no effect on the level of FM in the mothers (data not shown). KIR2DL2, KIR2DL3 and KIR2DS2 receptors all share the same ligands with high affinity for HLA-C1 and with low affinity for HLA-C2. KIR2DL3-C1 interaction results in a lower inhibition than KIR2DL2-C1 interaction (*299*). The mothers were then grouped depending on the presence or absence of KIR2DL2 and KIR2DL3 (Figure 12, C). Absence of KIR2DL3 resulted in a significantly higher amount of FM cells compared to the group where only KIR2DL3 was present (mean FM cells: $KIR2DL3^+$ 0.52 vs. $KIR2DL3^-$ 14.97; p=0.0183).

Further, individuals can be grouped depending on their centromeric or telomeric KIR gene motifs. The centromeric KIR genes are mainly classified by either the presence of KIR2DL3 and absence of KIR2DL2 (A/A) or the absence of KIR2DL3 and presence of KIR2DL2 (B/B) (Figure 12, G, upper graphic). Correlation analysis showed a significant correlation between FM and maternal centromeric KIR genes (p=0.011; Table 5). Mother and child were grouped in FM^+ and FM^-. Frequencies within the centromeric KIR gene motifs were compared (Figure 12, D).

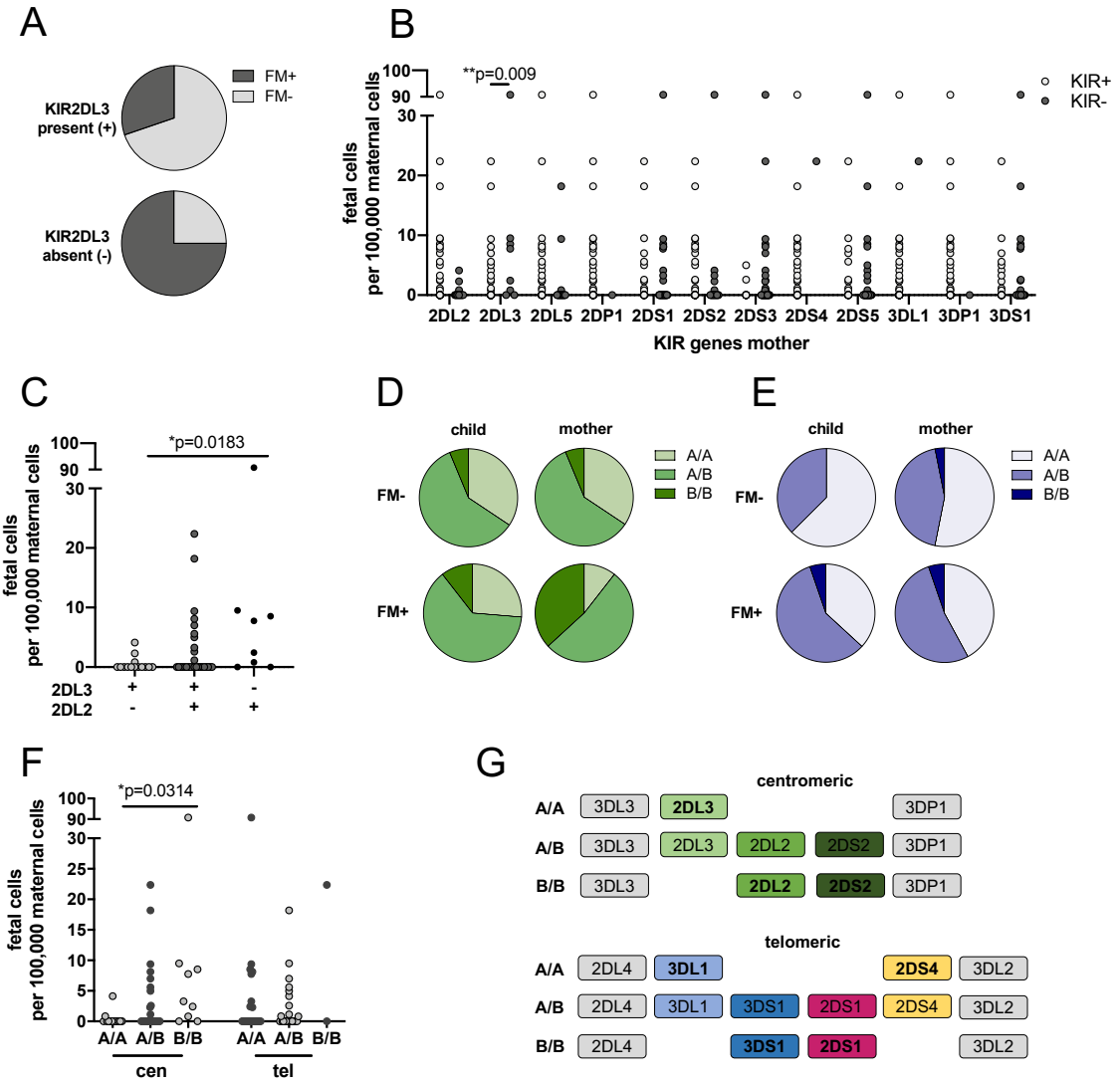

Figure 12: Influence of KIR genes on the occurrence and level of an FM. (A) Frequency of KIR2DL3 gene presence or absence in FM^- and FM^+ mothers. (B) Mothers were KIR genotyped and grouped depending on presence or absence of KIR genes. Level of FM was compared in KIR positive and KIR negative groups. (C) Mothers were grouped depending on their KIR2DL2 and KIR2DL3 combinations and the level of FM was compared between the groups. (D + E) Child and mother were grouped depending on their centromeric and telomeric KIR genes and the presence or absence of FM. (D) Centromeric motif and (E) telomeric motif frequencies classified as depicted in (G). (F) Influence of maternal centromeric and telomeric KIR gene motifs on the amount of FM cells. (G) Illustration of the centromeric and telomeric KIR gene regions. Exact n values are provided in appendix 8.4. Statistical analysis of frequencies was performed using Fisher's exact test for two groups or Chi^2 for more than two. Mann-Whitney test was used for comparison of two groups, Kruskal-Wallis test followed by Dunn´s multiple comparison test was used for more than two groups. Statistical significance $p<0.05$.

In the FM^- group, frequencies of centromeric KIR gene motifs were equal in mother and child (Figure 12, D). Most of the samples had a centromeric A/B motif, A/A occurred in 34% and the B/B motif was present in about 6%. In the FM^+ group, the frequency of mothers with a B/B motif was higher (B/B: FM^- 6% vs. FM^+ 37%), while frequencies of A/A and A/B were lower (A/A: FM^- 34% vs. FM^+ 6% and A/B: FM^- 60% vs FM^+ 53%). Grouping into FM^+ and FM^- had no effect on frequencies of filial centromeric KIR gene motifs.

Subsequently, telomeric gene motifs were compared according to the depicted criteria (Figure 12, G, lower graphic). The A/A motif is defined by the presence of KIR3DL1 and

KIR2DS4 and the absence of KIR3DS1 and KIR2DS1. The A/B motif has all four genes or lacks one of them, and the B/B motif consists of KIR3DS1 and KIR2DS1 and lacks KIR3DL1 and KIR2DS4. At first, frequencies of telomeric KIR gene motifs were compared in FM^+ and FM^- groups. The proportion shifted from more A/A mothers in the FM^- to more A/B mothers in the FM^+ group (A/A: FM^- 53% vs. FM^+ 42% and A/B: FM^- 44% vs. FM^+ 53%), but did not reach statistical significance (p=0.702; Table 5). Taken together, the occurrence of FM was influenced by the centromeric B/B motif, but it is still unknown if the level of FM was affected as well.

A

B content score	Cen	Tel
0	A/A	A/A
1	A/A	A/B
	A/B	A/A
2	A/A	B/B
	A/B	A/B
	B/B	A/A
3	A/B	B/B
	B/B	A/B
4	B/B	B/B

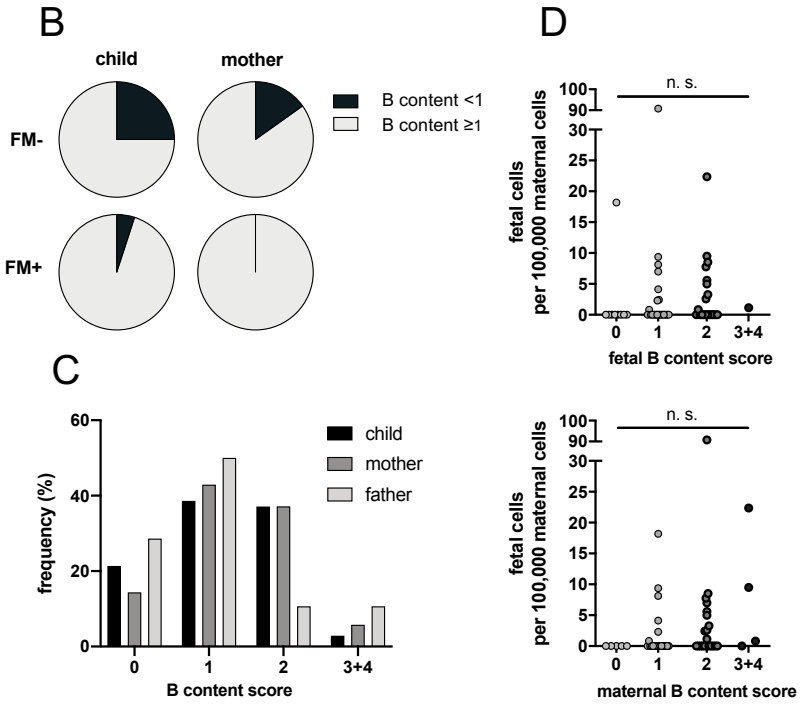

Figure 13: Influence of B content score on occurrence and level of an FM. Children and mothers were KIR genotyped and grouped depending on their centromeric and telomeric KIR motif and the B content score was determined as depicted in A. (B) Children and mothers were grouped depending on the presence or absence of an FM in the mother and frequencies of individuals with a B content <1 and a B content ≥1 were compared. (C) Influence of grouping in B content <1 and ≥1 was analyzed on the level of an FM. (C) The exact B content score was determined in child, mother, and father and the frequencies were compared. (D) Exact fetal and maternal B content score was correlated with the amount of microchimeric cells. Exact n values are provided in appendix 8.4. Statistical analysis of frequencies was performed using Fisher's exact test for two groups or Chi^2 for more than two groups. Mann-Whitney test was used for comparison of two groups, Kruskal-Wallis test followed by Dunn´s multiple comparison test was used for more than two groups. Statistical significance $p<0.05$. n. s: not significant.

Thus the impact of the centromeric and telomeric KIR gene motifs on the level of FM was determined. Mothers were grouped depending on their centromeric and telomeric gene motifs (Figure 12, F). A significantly higher level of FM was detected in mothers with a centromeric B/B motif compared to mothers with a centromeric A/A motif (mean FM cells: B/B 13.67 vs. A/A 0.38; p=0.0314). The telomeric KIR gene motifs did not significantly affect the level of FM cells. Absence of KIR2DL3 did not only correlate with the presence of an FM moreover, it affected the level of FM. A higher frequency of mothers with a centromeric B/B motif had a persisting FM even at a higher level.

Besides analysis of the centromeric and telomeric gene motifs, KIR genes can be grouped into two haplotypes. The A haplotype holds all inhibitory KIR genes and the only constantly present activating KIR gene KIR2DS4. The B haplotype can either have all the A genes and additionally activating genes, or it lacks some of the haplotype A genes. Thus the A haplotype is characterized by allelic variation, while the B haplotype varies in KIR gene content. Depending on the number of activating KIR genes, a B content score can be determined (Figure 13, A). For the haplotype A, the B content score is always 0 (B content <1) due to the lack of activating KIR genes. For the haplotype B, the B content score can vary between 1 to 4 (B content ≥1).
First, frequencies of mothers and children with B content ≥1 or <1 were compared in FM^+ and FM^- groups (Figure 13, B). The FM^- group held more mothers and children with a B content ≥1 than the FM^+ group. No significant correlation was observed between an FM and either fetal or maternal B content ≥1 or <1 (KIR haplotype, Table 6). Frequencies of exact KIR contents were compared in mothers, children and as control in fathers. Mothers and children showed an equal B content score distribution, while less fathers had a B content score of 2 and more had one of 4 (2: father 10.5% vs. mother and child 37% and 3+4: father 10.5% vs. mother and child 3 - 6%) (Figure 13, C). Then the impact of a maternal or filial B content score on the level of an FM was analyzed. Mothers and children were grouped depending on their B content score and the FM level was compared between the different groups (Figure 13, D). Neither maternal nor fetal B content significantly affected the level of FM (mean FM child: 0: 2.0, 1: 5.95, 2: 3.27, 3+4: 1.156; mother: 0: 0, 1: 2.05, 2: 6.39, 3+4: 8.16). However, an FM was only detected in mothers with a B content ≥1.
In conclusion, the occurrence of an FM and the number of FM cells were independent of maternal and fetal B content score but were influenced by the maternal centromeric KIR motif and the absence of KIR2DL3.

4.3 Influence of an FM on parental NK cell phenotype and effector function

4.3.1 Impact of an FM on NK cell KIR phenotype and degranulation

KIR gene expression is highly variable among individuals and determined by various factors, e.g. methylation, allelic variation and HLA-ligand background (*183, 300*). Over time the KIR repertoire is stable in an individual, but can adapt to environmental changes, such as in case of viral infection. After viral infection, imprints in the human KIR repertoire were detected (*214*). Out of this, the question arose if a persisting FM in the maternal blood system leaves an imprint in the maternal KIR repertoire. To detect potential changes in KIR receptor expression and activation of distinct KIR expressing NK cells, the KIR phenotype and degranulation of pre-activated maternal and paternal NK cells was determined after co-culture with either their children's leukemic blasts or the HLA-negative cell line K562. The gating strategy is provided in appendix 8.3.2. CD107a was used as a marker for activated cells. Normally, CD107a is

intracellular, but upon fusion of vesicle (which contains cytotoxic granular) with the cell membrane, it occurs on the cell surface and can be used as a degranulation marker (*144*).

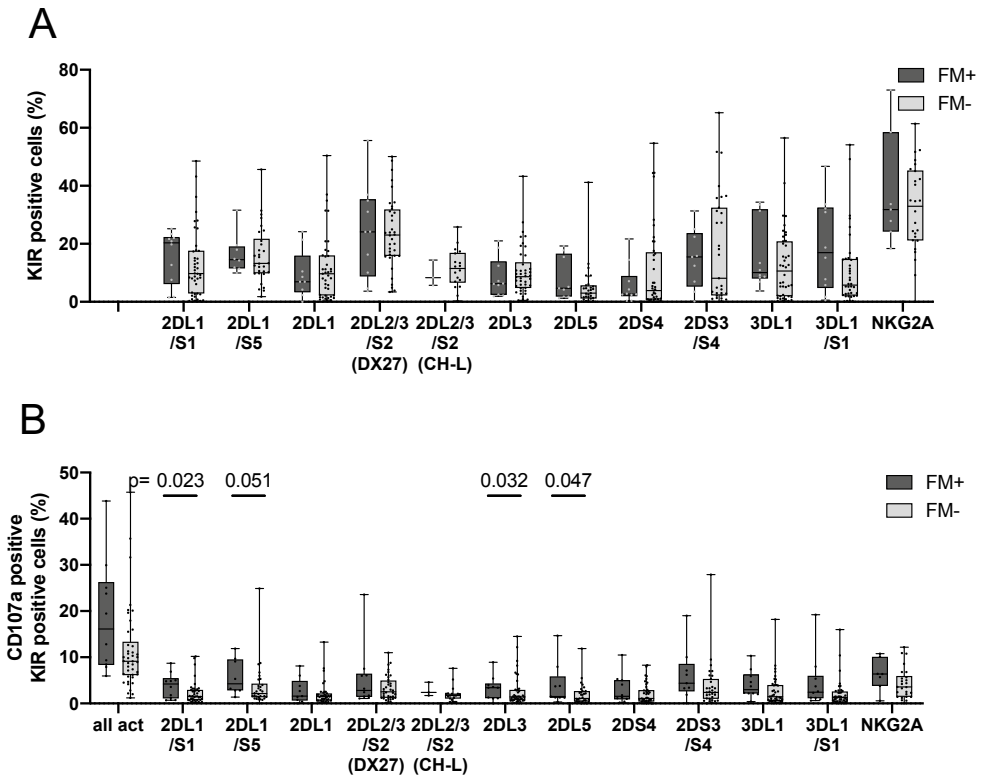

Figure 14: KIR expression in FM$^+$ and FM$^-$ mothers after co-culture with leukemic blasts. Maternal NK cells were isolated and IL-2/IL-15 pre-activated. The next day, cells were co-cultured with filial blasts in an effector to target (E:T) ratio of 1:1 for four hours with the addition of CD107a. Next cells were stained with anti-KIR antibodies to determine the NK cell KIR phenotype. Mothers were grouped into FM$^+$ and FM$^-$. (A) All cells positive for the respective KIR, (B) CD107a positive activated cells of the respective KIR. For KIR2DL2/L3/S2 two different clones were used DX27 and CH-L. Exact n values are provided in the appendix 8.4. Depicted are box and whiskers from min to max with each point standing for one sample. Statistical analysis was performed using Mann-Whitney test for comparison of FM$^+$ to FM$^-$ groups. Significance level $p<0.05$.

First, general phenotypes and proportions of activated NK cells from mothers and fathers, after co-culture with blasts or K562, were compared. No significant difference was observed (data not shown). One exception was that cells co-cultured with K562 showed a higher degranulation, which will be described later in this section. The frequencies of all KIR expressing cells (Figure 14, A) and activated CD107a positive KIR expressing cells (Figure 14, B) were compared between FM$^+$ and FM$^-$ mothers against their children's leukemic blasts. The general KIR expression pattern was similar in both groups (Figure 14, A), but the proportion of activated KIR expressing cells differed (Figure 14. B). In the FM$^+$ group significantly more KIR2DL1/S1, KIR2DL1/S5, KIR2DL3 and KIR2DL5 positive cells were activated compared to the FM$^-$ group (KIR2DL1/S1 FM$^+$ 4% vs. FM$^-$ 2%; KIR2DL1/S5 FM$^+$ 6% vs. FM$^-$ 4%, KIR2DL3 FM$^+$ 3% vs. FM$^-$ 2%, KIR2DL5 FM$^+$ 4% vs. FM$^-$ 2%).

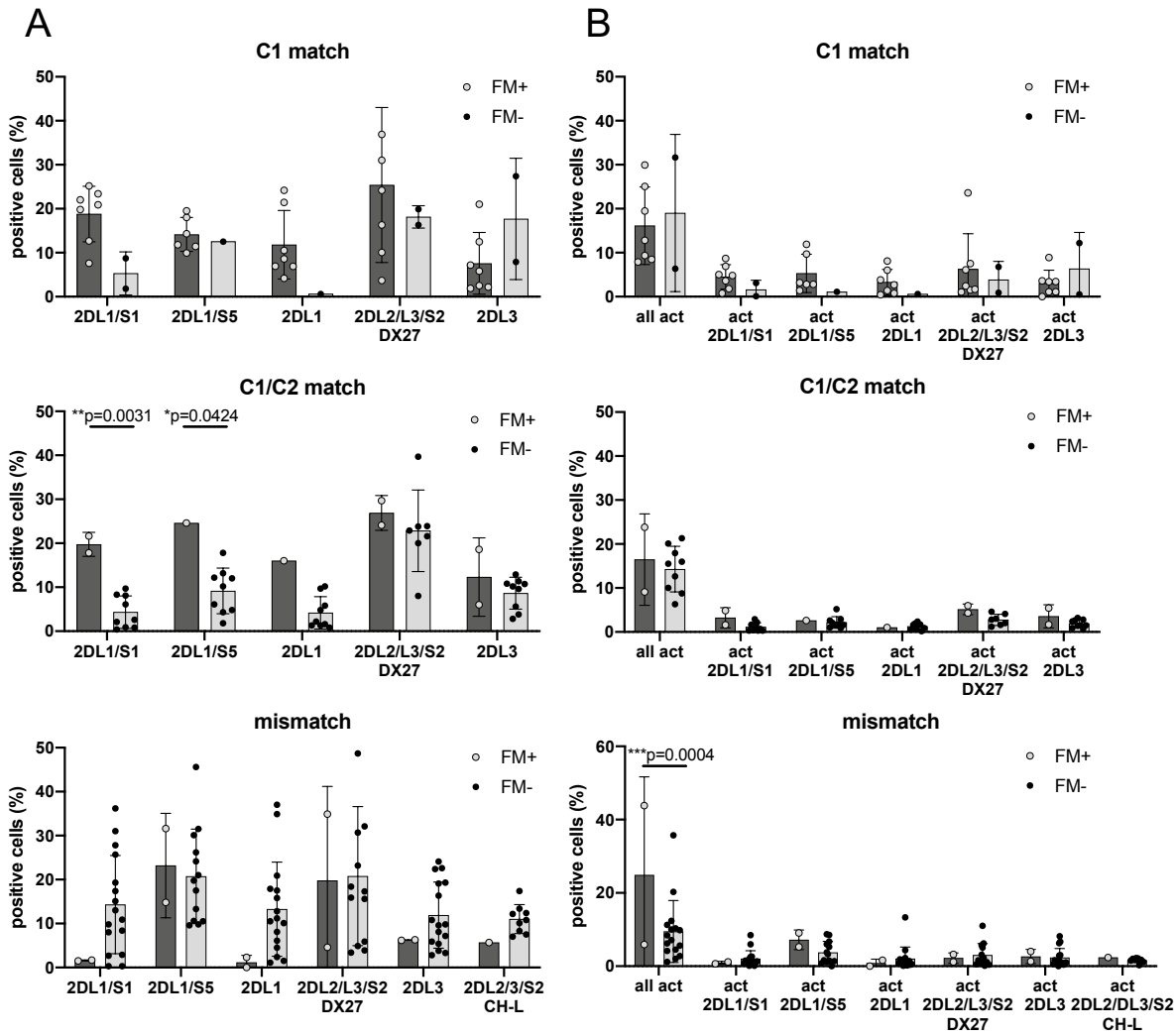

Figure 15: Effect of HLA-C match or mismatch on activation of maternal NK cells against filial leukemic blasts. Maternal NK cells were isolated and IL-2/IL-15 pre-activated overnight. The next day cells were co-cultured with filial blasts in an E:T ratio of 1:1 for four hours with the addition of CD107a. After incubation cells were stained with anti-KIR antibodies to determine NK cells KIR phenotype. NK cells were gated on the respective KIR^+ (A) and the proportion of activated $CD107a^+$ cells was determined (B). Mothers were grouped into FM^+ (dark bars) and FM^- (gray bars) and further grouped depending on maternal and filial HLA-C1/C1 or HLA-C1/C2 match or mismatch. The two clones DX27 and CH-L were used for detection of KIR2DL2/L2/S2. Statistical analysis was performed using Mann-Whitney test for comparison of FM^+ and FM^- groups. Significance level $p<0.05$.

The KIR receptors have highly homologous extracellular domains. For some KIRs no antibodies are available with a specificity for a single KIR receptor, because of a cross reactivity with other KIR receptors. Consequently, if both receptors are genetically present and expressed, some antibodies bind to more than one KIR receptor, e.g. KIR2DL1/S1 binds to KIR2DL1 and KIR2DS1. In those cases, genetic information about the presence of KIR genes is helpful in identifying the role of single KIR receptors. Interestingly, more KIR2DL1/S1 and KIR2DL1/S5 positive cells were activated, but only KIR2DL1 positive cells did not show a higher activation. This led to the assumption that cells expressing the activating receptor are activated and not the ones carrying the inhibitory receptor only. For detailed analysis of the receptors influence, the genotype of the respective KIR in the mother was considered, but no significant differences were detected (data not shown).

Another factor that could influence NK cells reactivity is their education. During this process, referred to as licensing or education, NK cells learn to distinguish between self and non-self (*220, 221*). As a result, KIR2DL1 positive NK cells are more reactive in an HLA-C2 carrying individual, while KIR2DL2 and KIR2DL3 positive NK cells are more reactive in an HLA-C1 homozygous individual. NK cells lacking a self-KIR are in a state of hyporesponsiveness. Out of this, it was analyzed if FM has an influence on the frequency of all KIR positive and activated KIR positive NK cells regarding maternal and filial HLA-C (Figure 11, C). Mother-child pairs were grouped depending on their HLA-C either in HLA-C match (C1 homozygous or C1/C2) or mismatch (Figure 15). Frequencies of all KIR positive (Figure 15, A) and activated KIR positive (Figure 15, B) NK cells were compared. The only C2 matched mother-child pair was excluded from the statistical analysis. In the C1 matched group, no significant difference was detected in KIR expression of any analyzed KIR between the two FM groups. In the C1/C2 matched group, a significantly higher frequency of KIR2DL1/S1 positive (FM^+ 19.73% vs. FM^- 4.33%) and KIR2DL1/S5 positive cells (FM^+ 24.6% vs. FM^- 9.15%) was detected in the FM^+ group, but these cells were not activated. The proportions of activated cells were equal. In the mismatched group, no significant difference in the frequency of KIR positive NK cells was discerned between the FM^+ and FM^- group, but the total frequency of activated cells was significantly higher in the FM^+ group compared to the FM^- group (FM^+ 24.88% vs. FM^- 9.49%). Previously in this study, it was described that an HLA-C match affects the frequency of an FM. Consequently, grouping into FM^+ and FM^- and further into match and mismatch resulted in only small groups (FM^- C1 match, FM^+ C1/2 match, and FM^+ mismatch n=2, respectively).
In conclusion, no striking difference in the frequency of KIR expression or a distinct KIR positive activated subgroup was seen between FM^+ and FM^- mother in regard to maternal-filial HLA-C match or mismatch.

Then the reactivity of parental NK cells, concerning their degranulation by detection of CD107a, was analyzed. Responsiveness of NK cells from FM^+ and FM^- mothers was compared against K562 and the leukemic blasts (Figure 16). The activation of NK cells in the FM^- group was significantly higher against K562 compared to leukemic blasts (28.63% vs. 13.05%; $p<0.0001$), which was abolished in the FM^+ group (22.76% vs. 18.63%; n. s.) (Figure 16, A). Because the degranulation against K562 was similar in FM^+ and FM^- groups (23% vs. 29%; n.s.), degranulation of mothers was normalized to their maximal degranulation against the positive control K562 (Figure 16, B). NK cells from FM^+ mothers showed a significantly higher normalized degranulation against their children's leukemic blasts compared to NK cells from FM^- mothers (FM^+ 88 vs. FM^- 48; $p=0.0098$).

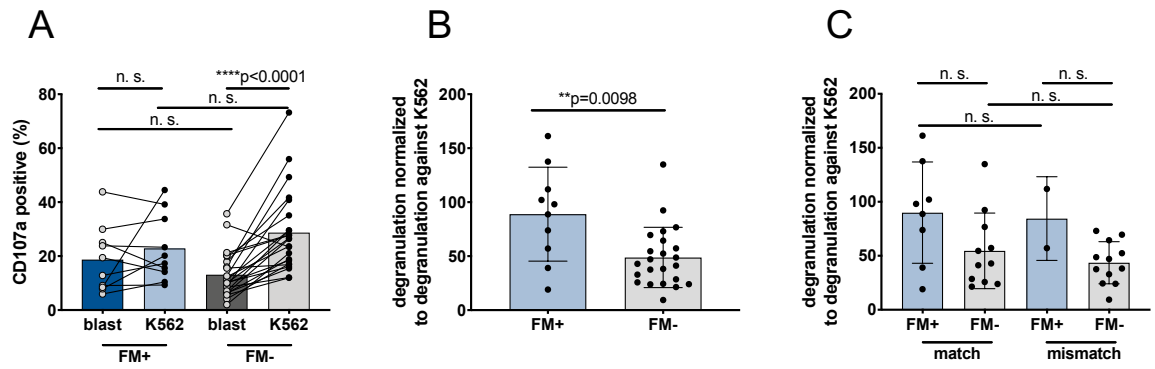

Figure 16: Frequencies of activated NK cells of FM$^+$ and FM$^-$ mothers after co-culture with leukemic blasts or K562. Maternal NK cells were isolated and IL-2/IL-15 pre-activated overnight. The next day, cells were co-cultured with filial leukemic blasts or K562 in an E:T ratio of 1:1 for four hours with addition of CD107a. Mothers were grouped into FM$^+$ and FM$^-$. (A) Proportion of activated NK cells from co-culture with blasts or with K562. Degranulation was normalized to degranulation against K562. (B) Normalized degranulation of FM$^+$ mothers and FM$^-$ mothers and (C) mothers grouped in match or mismatch between maternal and filial HLA-C. Lines connect values from co-cultures with blasts or K562 from one donor. Statistical analysis was performed using Wilcoxon test for paired samples and Mann-Whitney test for unpaired samples. Significance level $p<0.05$.

NK cell reactivity is balanced by inhibitory and activating receptors on the surface of the NK cell. As mentioned previously, the combination of maternal and fetal HLA-C could influence the reactivity of maternal NK cells. Hence, mothers were grouped depending on the maternal fetal HLA-C into either match or mismatch as previously described (Figure 11, C). In both groups, FM$^+$ and FM$^-$, no significant difference was observed in the degranulation of NK cells, neither in the matched nor in the mismatched group (match: FM$^+$ 90 vs. FM$^-$ 55 and mismatch: FM$^+$ 84 vs. FM$^-$ 43) (Figure 16, C).

In conclusion, NK cells from FM$^+$ mothers showed a higher normalized degranulation against their child's leukemic blasts compared to NK cells from FM$^-$ mothers.

4.3.2 Impact of an FM on parental NK cell alloreactivity

An increased degranulation was seen in NK cells from FM$^+$ mothers against their children's leukemic blasts. Therefrom the question arose as to whether the alloreactivity of NK cells is affected as well. In a healthy environment, NK cells are inhibited by inhibitory surface receptors interacting with self-HLA molecules. In hHSCT, an HLA-C mismatch between recipient and donor resulted in alloreactive donor NK cells. NK cell alloreactivity was identified as effective in GvL to kill allogenic leukemic cells with avoidance of GvHD (*57, 237, 243, 244*). Hence the influence of a persistent FM on parental NK cell alloreactivity was analyzed.

The alloreactivity of parental pre-activated NK cells against filial leukemic blast was determined in an FACS-based killing assay. Parental NK cell killing of blasts or K562 was analyzed in different effector to target (E:T) ratios and showed equal mean specific lysis (data not shown). In general, both showed a high specific lysis of K562 and a moderate specific lysis of leukemic blast (data not shown). Maternal and paternal NK cell-mediated specific lysis of leukemic blasts was statistically analyzed (Figure 17, A) but no significant difference was seen between

maternal or paternal NK cell specific lysis of leukemic blasts (mothers 28.55% vs. fathers 23.22%).

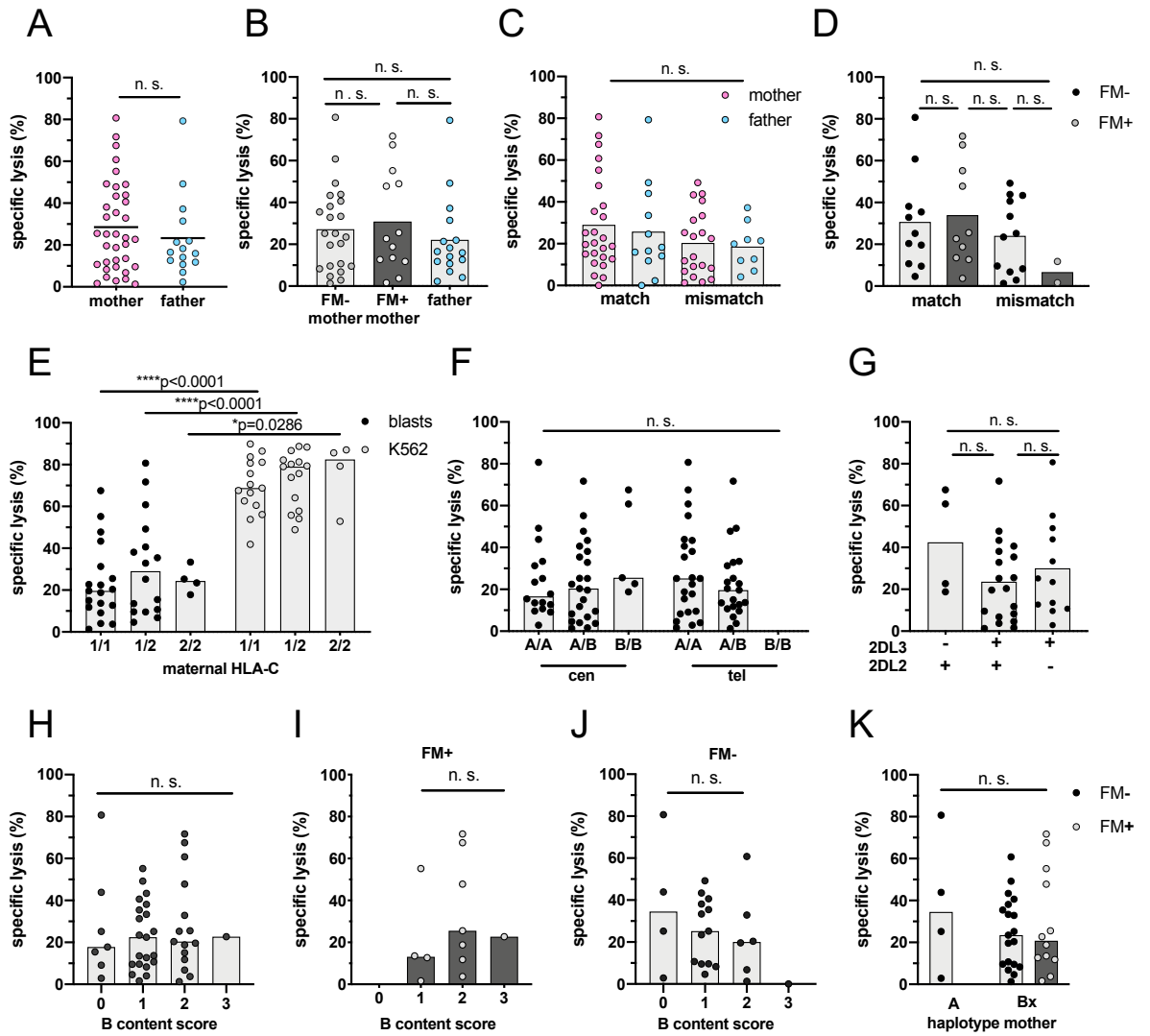

Figure 17: Parental cytotoxicity against filial leukemic blasts. Parental NK cells were isolated and IL-2/IL-15 pre-activated overnight. The next day their cytotoxicity was analyzed against filial blasts and the control cell line K562 in an FACS-based killing assay. (A) Analysis of maternal and paternal NK cell killing of leukemic blasts (E:T 10:1). Influence of (B) a persisting FM (FM^+) in mothers on NK cell cytotoxicity against filial blasts compared to fathers, (C) HLA-C match or mismatch between child and either mother or father, (D) an FM in match or mismatch mother-child groups. (E) Mothers were grouped depending on their HLA-C genotype and lysis of blasts or K562 was analyzed. Influence of (F) maternal centromeric (cen) or telomeric (tel) KIR gene motifs or (G) maternal KIR2DL2 and KIR2DL3 genotype on maternal NK cells specific lysis of leukemic blasts. (H) All mothers were grouped depending on their B content score and the lysis of leukemic blasts was compared between the groups. Mothers were further grouped into (I) FM^+ and (J) FM^- and the specific lysis was compared between the groups. (K) Mothers were grouped depending on their KIR haplotype and specific lysis of leukemic blasts was compared. Each dot represents one sample; bars show mean of the group. Exact n values are provided in appendix 8.4. Statistical analysis was performed using Mann-Whitney test for comparisons of two groups and Kruskal-Wallis test followed by Dunn's multiple comparison test for more than two groups. Significance $p<0.05$, n. s. not significant.

Then the influence of a persistent FM on maternal NK cell alloreactivity was analyzed. Mothers were grouped into FM^+ and FM^- and their specific lysis of leukemic blasts was compared to the lysis of paternal NK cells (Figure 17, B). No significant difference in the specific lysis among the three groups was detected (FM^+ 30.89% vs. FM^- 27.27% vs. father 22.12%).

HLA-C match or mismatch is indispensable for alloreactivity prediction. Thus a match or mismatch in HLA between child and parent could affect the alloreactivity of the parental NK cell against the filial leukemic blast. To examine this question, mothers and fathers were grouped depending on their HLA match or mismatch with their children from the parent to child direction and the specific lysis was compared (Figure 17, C). Parental NK cell specific lysis of leukemic blasts was equal in HLA-C match or mismatched groups (match vs. mismatch: mothers 29.03% vs. 20.03%; fathers 25.81% vs. 16.53%). Interestingly, mismatch in both mother-child and father-child pairs resulted in a slightly lower mean specific lysis of leukemic blasts by parental NK cells compared to matched parent-child pairs. Additionally, analysis was repeated with the specific lysis normalized to the maximal lysis of K562, because NK cells showed a difference in degranulation against K562 and blasts. But still, no significant differences were detected (data not shown).

Up to now it is unknown, if FM that has been shown to occur more frequently in matched mother-child pairs affects the specific lysis of maternal NK cells in matched or mismatched mother-child pairs. Therefore, mothers were grouped first into FM^+ and FM^- and then into HLA-C match or mismatch from the mother to child direction. The specific lysis of leukemic blasts was compared between the groups (Figure 17, D). FM had no influence on maternal NK cell specific lysis of leukemic blasts, neither under HLA-C match (FM^+ 33.93% vs. FM^- 30.74) nor under HLA-C mismatched conditions (FM^+ 24.01% vs. FM^- 6.71%). Interestingly, in the matched pairs, a slightly higher mean killing was seen.

The maternal HLA-C genotype per se might affect the ability to kill blasts or K562. Therefore, mothers were grouped depending on their HLA-C genes and the specific lysis of each group was compared (Figure 17, E). In all settings, a significantly higher specific lysis was evident against K562 (69% - 76%) compared to lysis of blasts (23% - 32%). The mean of the specific lysis was equal between the HLA-C groups.

KIR genes had an impact on an FM (section 4.2.4), but it is unknown whether they also affect the parental NK cell specific lysis of the children's blasts. For analysis, mothers were grouped depending on their centromeric and telomeric KIR gene motifs and the specific lysis of leukemic blasts was compared among the groups (Figure 17, F). A slightly higher mean specific lysis of mothers with a centromeric B/B motif (B/B 39% vs. A/B 24% and A/A 25%) was detected, but this was not statistically significant. Specific lysis was not influenced by the telomeric KIR gene motifs (A/A 29% vs. A/B 23%).

KIR2DL3 absence favors the establishment of an FM. Thus, it could also have a beneficial effect on the maternal NK cell alloreactivity against filial blasts. To validate this hypothesis, mothers were grouped depending on their KIR2DL2 and KIR2DL3 genotype (Figure 17, G). Absence of KIR2DL3 or absence of KIR2DL2 had no significant effect on NK cell reactivity

against filial leukemic blasts (KIR2DL3$^-$ 43% vs. KIR2DL3$^+$ 30%). In comparison, if both receptors were present, a slightly decreased specific lysis of leukemic blasts to 24% was detected in mothers, but this was not significant.

Besides these two inhibitory receptors, the activating receptors could have an impact on NK cell reactivity against filial leukemic blasts. To examine this, the B content score of mothers was determined as previously described (Figure 17, H). In general, maternal NK cell specific lysis of leukemic blasts was not affected by the maternal B content score. All four groups showed an equal specific lysis (0: 28%, 1: 23%, 2: 29%, 3: 23%). In addition whether an FM together with a certain B content score affects maternal NK cells specific lysis was examined. Mothers were first grouped into FM$^+$ (Figure 17, I) and FM$^-$ (Figure 17, J) and hereafter depending on their B content score. In the FM$^+$ group, mothers with a B content score of 2 showed a higher specific lysis compared to the other two groups (2: 35% vs. 1: 21% and 3: 23%). The FM$^+$ group did not contain a mother with a B content score of 0. In the FM$^-$ group, the mean specific lysis was slightly higher in the B content 0 group (0: 38% vs. 1: 26% and 2: 24%), but this group was absent in the FM$^+$ group. Finally, the influence of the maternal haplotype was analyzed in mothers grouped into FM$^+$ and FM$^-$ (Figure 17, K). The analyzed cohort did not contain an FM$^+$ mother with a KIR A haplotype, as mentioned previously, and within the KIR Bx haplotype, no difference was seen between the groups (A: FM$^-$ 38%, Bx: FM$^+$ 25% and Bx FM$^-$ 30%). Interestingly, the mean killing of the mothers with a KIR A haplotype was higher compared to the Bx haplotype mothers (A haplotype 38% vs. B haplotype 30%).

To sum up, no difference was detected between maternal and paternal NK cells' potential to lyse their children's leukemic blasts. A persisting FM did not affect maternal NK cells' lysis of filial leukemic blasts *in vitro* compared to paternal NK cells and mothers without FM. Presence of a centromeric B/B motif in mothers potentially led to a higher power to kill leukemic blasts in some mothers, but in general the ability of maternal NK cells to kill their children's leukemic blasts was independent of maternal B content score and haplotype.

4.4 Trans-maternal microchimerism in sibling transplantation

A younger sibling might have cells from the older sibling in his or her blood system, which is called a TM (*100, 102*). The genetic background for the occurrence or persistence of a TM has not been addressed so far. The persistence of a microchimerism in the younger sibling, who donates the stem cells for the older sibling, could have the same positive impact as observed for a persisting microchimerism in mother-to-child transplantation (*77*). Furthermore, a sibling donor is the preferred donor compared to an HLA-matched or haploidentical donor owing to the low risk of GvHD and relapse (*39*).

At first, it was determined if a TM can be detected with the ddPCR method, which was established during this study (section 4.1.1). DNA from 13 sibling pairs in which the older sibling had received an HSCT between 2010 and 2017 was analyzed for a TM. For all sibling pairs a suitable marker was found. Patient characteristics are summarized in Table 7. The female to male ratio was 3:2 (62% to 38%), the children suffered from different malignancies and one sibling pair was twins. Two patients died, one due to relapse and one patient because of severe GvHD.

Table 7: Trans-maternal microchimerism patient characteristics. Other includes beta thalassemia, anemia, MPS II: mucopolysaccharidosis type II, and MDS: myelodysplastic syndrome. GvHD: graft-versus-host disease.

		N	%
Patients		13	100
Sex	Female	8	62
	Male	5	38
Age (years)	Median (range)	10	(3 - 17)
Disease	Other	4	58
	Leukemia	3	13
	Sickle cell disease	6	22
Additional information	Twins	1	8
	Survival	11	85
	GvHD	1	8
	Relapse	1	8
Time of transplantation (year)		2010 - 2017	
TM analysis	Positive	8	62
	Survival of positives	6	75
	Negative	5	38
	Survival of negatives	5	100

DNA from younger siblings who donated the stem cells for their older siblings was analyzed for the occurrence of a TM. In eight (62%) of the analyzed samples, which included those who died, a TM was detected (Figure 18, A). Comparison of the level of FM and TM revealed the same mean level in both groups and no significant difference (TM^+ 5.3 vs. FM^+ 5.6) (Figure 18, B). Then the survival was analyzed in the TM^+ and the TM^- group (Figure 18, C). Presence of a TM had no significant influence on the survival of the children (TM^+ 75% vs. TM^- 100%). In the following, the impact of recipients' sex, age at HSCT, and disease was analyzed on the level of TM (Figure 18, D - F). TM was more often detected in males compared to females (6 vs. 2), but the level of TM was not significantly affected (male 5.5 vs. female 4.0). Furthermore, the level of TM was not significantly affected by children's age or disease. In sum, the level of TM was independent of children's sex, age, and disease.

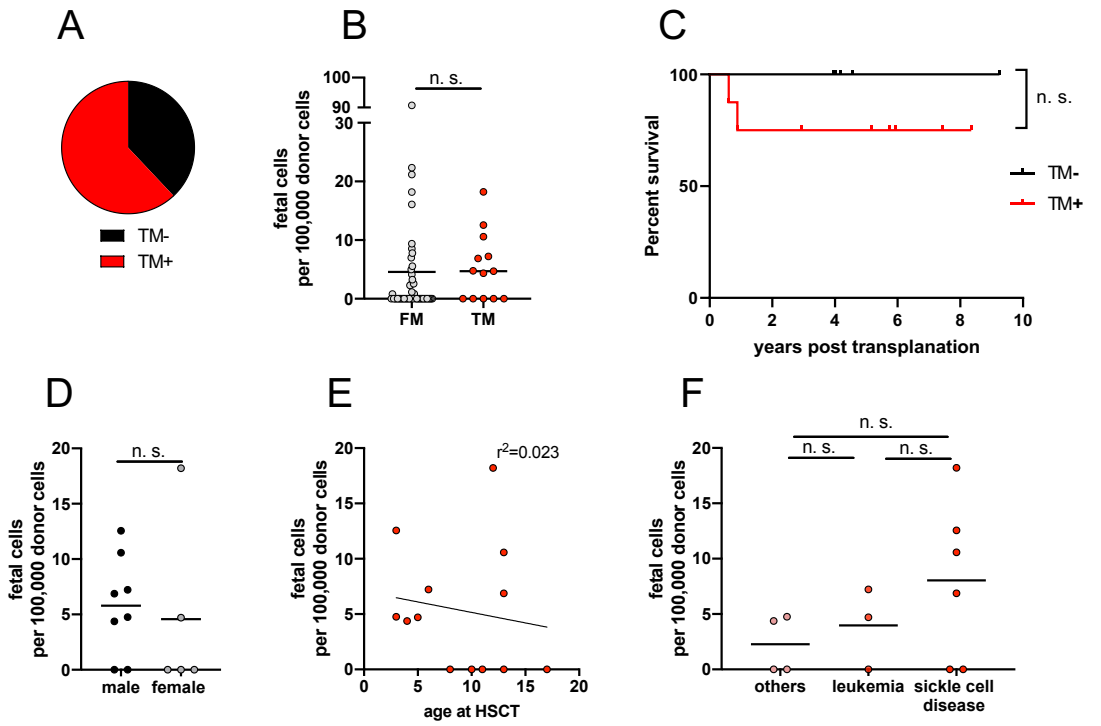

Figure 18: Factors influencing a trans-maternal microchimerism. Younger siblings that donated stem cells for their older siblings were analyzed for the occurrence of a TM. (A) Frequency of TM occurrence or absence. (B) Comparison of TM and FM level. Survival curve of TM^+ and TM^-. Influence of recipient's (B) sex, (C) age at HSCT, and (D) disease on the level of TM. Statistical analysis was performed using Mann-Whitney test for comparisons of two groups and Kruskal-Wallis test followed by Dunn's multiple comparison test for more than two groups. In (E) simple linear regression analysis was used. Significance $p<0.05$, n. s. not significant.

FM in the mother was associated with maternal HLA-C, maternal-filial HLA-C match and further, presence of at least one HLA-C1 in the mother favored an FM (section 4.2.3). All sibling pairs were HLA-C matched, and frequencies were as described for the Caucasian population (C1/C1 23%, C1/C2 62%; C2/C2 15%). Frequencies in HLA-C genotypes were compared between TM^+ and TM^- groups (Figure 19, A). The TM^+ group had a higher frequency of C1/C2 heterozygous pairs compared to the TM^- group (TM^+ 75% vs. TM^- 40%). Additionally, a higher level of TM was detected in the heterozygous group (C1/C2: 7.2 vs. C1/C1: 1.6 and C2/C2: 3.4 fetal cells per 100,000 donor background cells), but the difference was not significant (Figure 19, B).

FM was positively influenced by the centromeric B/B KIR gene motif. Thus, this could be important for a TM as well. To investigate this question, donors and recipients were grouped depending on their centromeric and telomeric KIR gene motifs (as explained in Figure 12, G) and frequencies were analyzed (Figure 19, C). All recipients had either a centromeric A/B or B/B motif (A/A 38% vs. A/B 62%), while some donors had a centromeric B/B motif (A/A 15% vs. A/B 62% vs. B/B 23%). Frequencies of telomeric KIR gene motifs were equal in both groups (A/A 70% vs. A/B 30%). Subsequently, donors were grouped into TM^+ and TM^- and frequencies in centromeric and telomeric KIR gene motif were compared (Figure 19, D). Only donors were further analyzed, because the donor cells are the potent effector cells during HSCT. No

difference was observed between the groups (cen: A/A TM^- 20% vs. TM^+ 12.5%, A/B TM^- 60% vs. TM^+ 62.5%, B/B TM^- 20% vs. TM^+ 25%; tel: A/A TM^- 80% vs. TM^+ 62.5%, A/B TM^- 20% vs. TM^+ 37.5%). A TM did not occur more often if any of the centromeric or telomeric KIR gene motif was present.

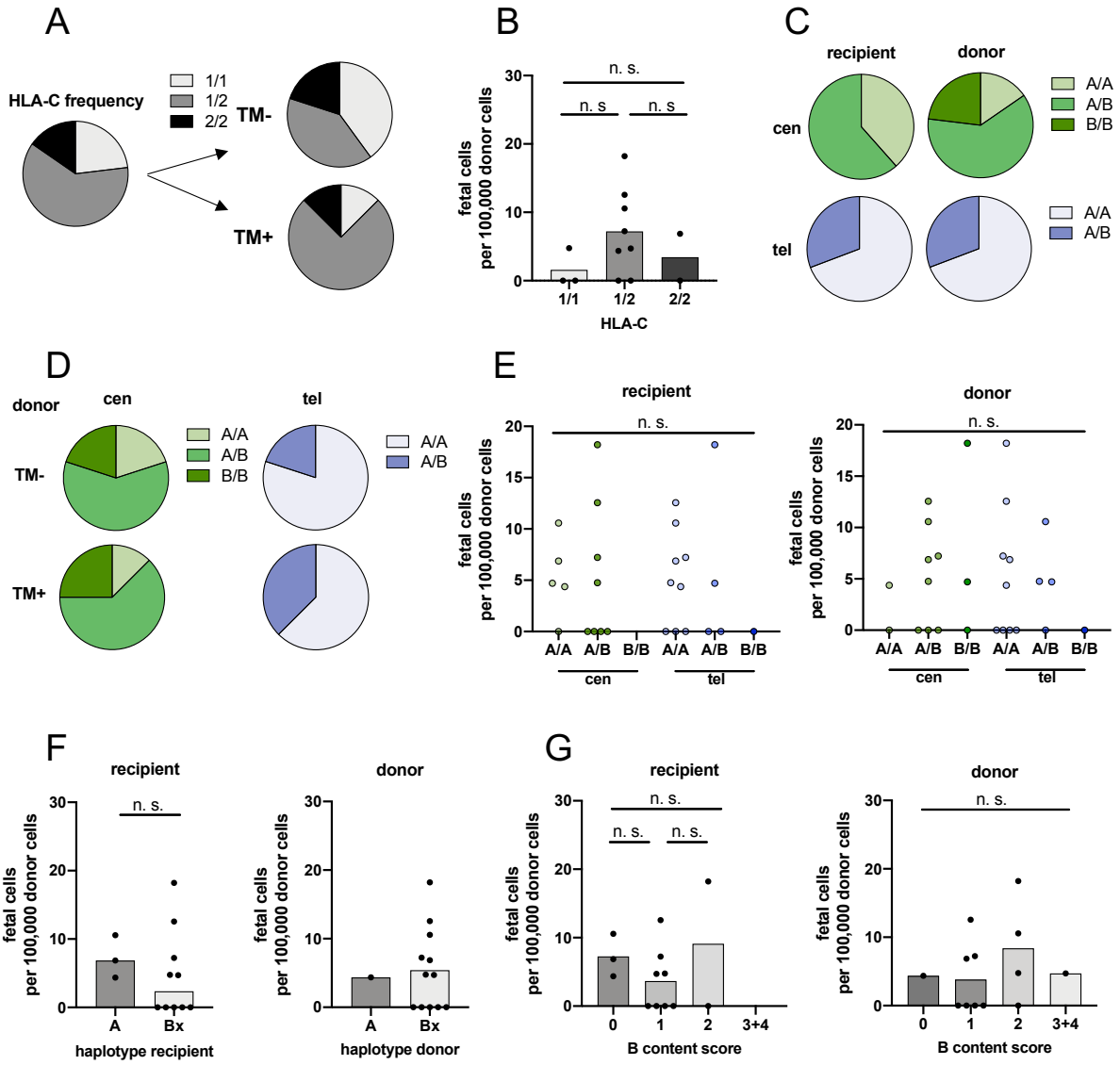

Figure 19: Influence of HLA and KIR genes on a trans-maternal microchimerism. Younger siblings who donated stem cells for their older siblings were analyzed for the occurrence of a TM. Influence of HLA and KIR genes on occurrence and level of TM was analyzed. (A) Frequency of HLA-C in the group (siblings were all HLA-C matched). (B) Influence of HLA-C on the level of TM. (C) Frequencies of centromeric and telomeric KIR gene motifs in donor and recipient. (D) Frequencies of centromeric and telomeric KIR gene motifs in donors grouped into TM^+ or TM^-. Influence of (E) either recipient or donor centromeric or telomeric motifs on the level of TM, (F) recipient or donor haplotype and (G) recipient or donor KIR content score. Bars show mean. Correlation of frequency was performed using Chi^2 test and comparison of TM levels was performed using Mann-Whitney or Kruskal-Wallis test followed by Dunn's multiple comparison test. Significance $p<0.05$, n. s. not significant.

Even if the centromeric or telomeric gene motifs did not favor the occurrence of a TM, they might have an influence on the level of TM. Therefore, donors and recipients were grouped depending on their centromeric or telomeric KIR gene motif and the level of TM was analyzed

(Figure 19, E). No significant differences were detected among any of the groups (mean TM cells: recipient 0 - 5.7 and donor 0 - 7.6).

The centromeric and telomeric KIR gene motifs had no influence, but variation in activating KIR genes still could affect a TM. Therefore, donors and recipients were grouped into their haplotypes and the level of TM was compared (Figure 19, F). In total, more TM positives were detected with a Bx haplotype (number of individuals with haplotype recipient: A 3 vs. Bx 5, donor: A 1 vs. Bx 7). Statistical analysis of the TM level was only possible for the recipient and revealed no difference (mean TM cells haplotype: A 7.2 vs. Bx 4.7; n. s.). So far, it seems like the donor's Bx haplotype might be beneficial for the occurrence of a TM. Nevertheless, the group of haplotype A donors contains only one donor. For statistical analysis, this group must be increased. Besides haplotype, the exact amount of activating KIR genes can affect a TM. Therefore, the impact of the B content score on the level of TM was determined (Figure 19, G). In both groups, the B content score had no significant influence on the level of TM (TM cells recipient vs. donor: 0: 7.2 vs. 4.3, 1: 3.7 vs. 3.9, 2: 0.1 vs. 8.4, 3: absent vs. 4.7).

Taken together, a TM was found more often in C1/C2 heterozygous siblings and was independent of donors and recipients KIR gene motifs. However, a tendency was observed that a TM occurred more frequently in Bx donors.

4.5 Equipment of NK cells with receptors for enhanced functionality

A main advantage of the haploidentical donor is that the donor is usually readily available for post-transplantation immune cell collections. This might be of interest in case of viral infections or relapse occurring post-hHSCT. Here, NK cells are promising effector cells to be collected from the donor and to be infused into the recipient. In the recipient, the NK cells can provide additional GvL effects to prevent relapse or fight viral infections (*301*). Infusion of NK cells into patients has been shown to be safe and feasible, but NK cells lack optimal functionality. Thus there is a need to optimized NK cells to enhance their effector function. The receptor/ligand combinations KIR2DL1/HLA-C2, KIR2DL2/HLA-C1 and KIR3DL1/HLA-Bw4 are essential for NK cell alloreactivity. Consequently, NK cell functionality might be modulated by insertion of distinct KIR receptors.

4.5.1 Generation of viral vectors

For modification of NK cells, the inhibitory KIR receptors KIR2DL1 and KIR2DL2 and the activating counterparts KIR2DS1 and KIR2DS2 were used (*184, 222*). Sequences for the inhibitory KIR genes KIR2DL1 and KIR2DL2 and the activating KIR genes KIR2DS1 and KIR2DS2 were cloned from cDNA from positive donors. The inhibitory KIR gene vectors were equipped with the fluorescent protein (FP) Cerulean as reporter (*302*), while the activating genes were equipped with the FP enhanced green fluorescent protein (eGFP) (*303*). Vector

constructs are depicted in Figure 20. The viral vectors were successfully cloned, and Sanger sequencing verified correct vector sequences. Then they were used for production of viral particles.

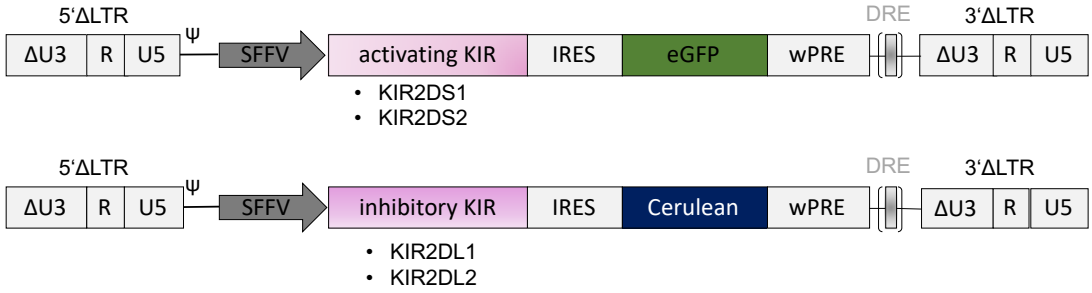

Figure 20: Schematic depiction of generated viral vectors. All sequences were cloned into alpharetroviral and lentiviral vectors downstream of the SFFV promotor and upstream of an IRES that separates the gene of interest and the fluorescent protein (FP). The sequences for the activating receptors KIR2DS1 and KIR2DS2 were cloned in vectors, which harbor the enhanced green fluorescent protein (eGFP) (*304*). The inhibitory KIRs, KIR2DL1 and KIR2DL2 were inserted into vectors, which harbor the FP Cerulean (*304*). 5'ΔLTR: N-terminal deleted long terminal repeats, ΔU3: deleted 133 bp in the U3 region to abolish emergence of replication competent recombinants, R: repeated regions, ψ: encapsulation signal, SFFV: spleen focus-forming virus promotor, IRES: internal ribosome entry site, wPRE: woodchuck hepatitis virus post-transcriptional regulatory element, DRE direct repeat element only present in alpharetroviral, but not in lentiviral vectors.

4.5.2 Generation of single-KIR expressing NK92-MI cells

The cell line NK92-MI was used to investigate whether insertion of a distinct KIR receptor influences its functionality. The cell line has been described to be without endogenous KIR receptor expression, except KIR2DL4 (*305*). Therefore, it might be ideal to study the effect of KIR receptor insertion. First, NK92-MI cells were examined for KIR expression. Phenotypical characterization by FACS analysis revealed that NK92-MI cells express CD56 (Figure 21, A). Twelve percent of the cells expressed KIR3DL1, 31% expressed NKG2A but all other KIR receptors were not expressed. Consequently, NK92-MIs are a suitable cell line to be transduced with the KIR receptor constructs.

To obtain adequate transduction efficiencies for functional analyses, different transduction strategies and conditions were compared. Two envelope proteins which are important for viral entry on the target cells were tested: glycoprotein of vesicular stomatitis virus (VSV-G) (*306*) and an optimized form of the RD114 feline leukemia virus (RD114/TR) (*307*). Furthermore, different multiplicities of infections (MOIs) from 5 to 100 of lentiviral particles were applied (Figure 21, B). With increasing MOIs more cells were transduced and RD114 led to a higher transduction efficiency in total, compared to VSV-G (MOI100: VSV-G 29% vs. RD114/TR 80%). Consequently, all NK92-MI cells were transduced with RD114/TR pseudotyped lentiviral particles.

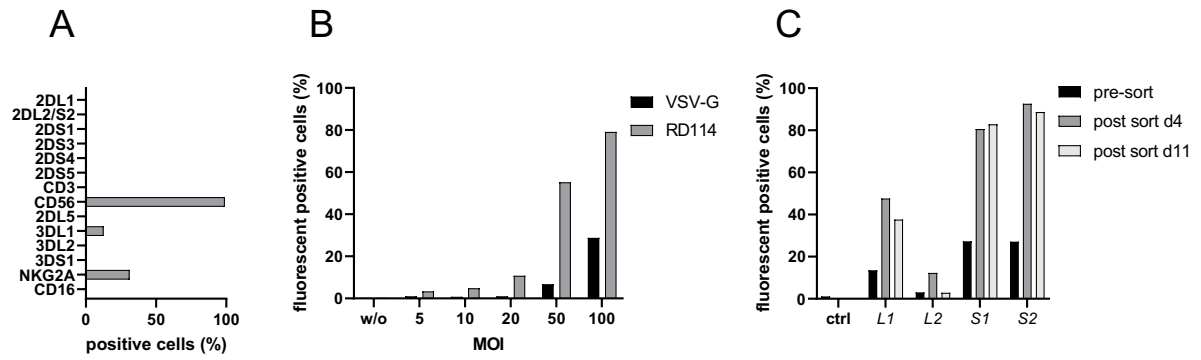

Figure 21: Generation of NK92-MI-KIR$^+$ cells. (A) Characterization of wildtype NK92-MI cells for receptor expression. (B) Optimal parameters for efficient NK92-MI transduction were determined using different MOIs and differently pseudotyped (VSV-G and RD114/TR) viral particles. (C) KIR expression in transduced NK92-MI cells after enrichment by FACS. KIR expression was analyzed by antibody staining. Name of transgene is depicted in italics.

Transduced and expanded NK92-MI cells were sorted by flow cytometry based on FP and KIR positive cells (Figure 21, C). Each transduced cell line expresses a certain KIR. In the following, the KIR expressing NK92-MI cells are referred to as NK92-MI-KIR$^+$. Likewise, the inserted transgene KIRs are abbreviated and written in italics as follows: KIR2DL1 = *L1,* KIR2DL2 = *L2*, KIR2DS1 = *S1* and KIR2DS2 = *S2*. The sorted NK92-MI cells were checked for transgene expression using fluorescently labeled antibodies against the inserted KIR on day four and day eleven post sorting. Expression of the activating KIR receptors *S1* and *S2* remained stable at 80% in the NK92-MI population. In contrast, the amount of inhibitory KIR expressing NK92-MI cells, *L1* and *L2*, decreased rapidly (*L1* 50% to 38% and *L2* 12% to 3%). Especially *L2* was not stable.

4.5.3 Generation of NK92-MI-KIR$^+$ single clones

After cell sorting, the KIR expression in NK92-MI-KIR$^+$ cells decreased within a few weeks. To examine whether unmodified cells have a growth advantage or if the receptor is internalized, single cell-derived clones were generated.

Single cells from NK92-MI-KIR$^+$ cells were sorted by flow cytometry and expanded. All growing clones were characterized for KIR and FP expression. For further experiments, two single-clone derived cell lines per receptor, which showed the highest KIR expressing cells, were selected (data not shown). For simplification, generated cell lines are named as follows: e.g. NK-*S1* 2.1 is a NK92-MI cell line transduced to express KIR2DS1, grown from a single clone with the number 2.1. Naming, inserted transgene (KIR), and FP are summarized in Figure 22, A. All clones grown from NK92-MI cells transduced with *L2* were negative, so no single KIR expressing cell lines could be generated. The following experiments were performed with single KIR expressing NK92-MI cell lines, except for *L2*.

A

Name generated cell line	Inserted receptor	FP
NK-*S1* 2.1	KIR2DS1	eGFP
NK-*S1* 1.5	KIR2DS1	eGFP
NK-*S2* 2.1	KIR2DS1	eGFP
NK-*S2* 3.5	KIR2DS2	eGFP
NK-*L1* 1.1	KIR2DL1	Cer
NK-*L1* 2.1	KIR2DL1	Cer
NK-*Cer* 2.1	-	Cer
NK-*Cer* 4.1	-	Cer
NK-*eGFP* 2.1	-	eGFP
NK-*eGFP* 4.1	-	eGFP

B

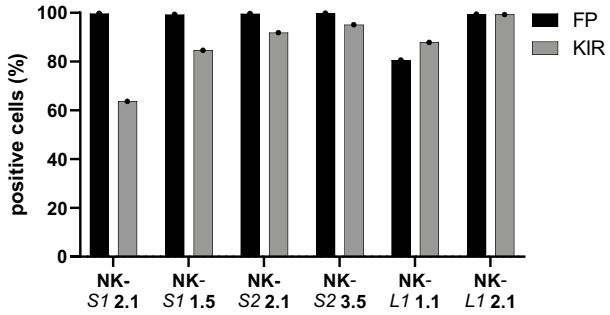

C

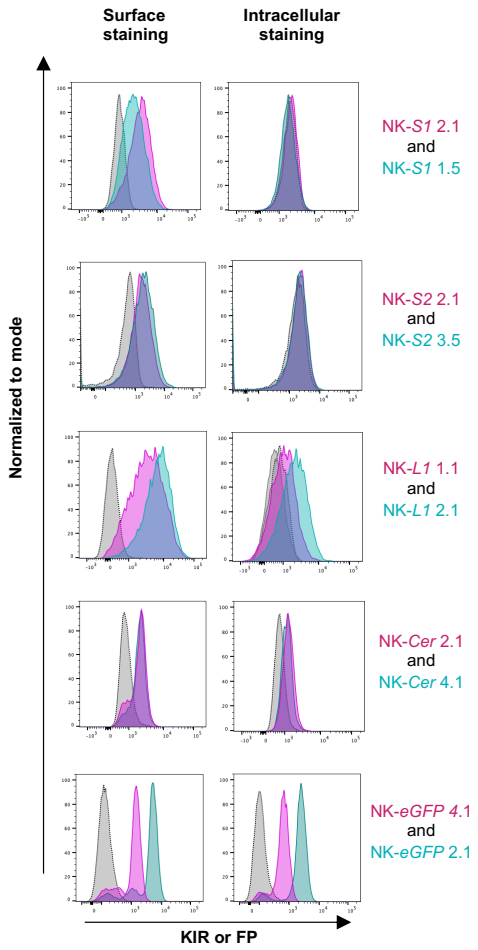

Figure 22: Generation of cell lines expressing a single KIR named NK92-MI-KIR$^+$. (A) Overview of generated cell lines. All generated cell lines express a single KIR. Thus they are comprehensively referred to as NK92-MI-KIR$^+$ cells. Exact naming of generated cell lines expressed KIR receptor and fluorescent protein (FP). Italic names represent abbreviation of transgene KIR. Grown clones were numbered, depicted number refers to a certain clone. Single cell clones were generated using FACS, based on KIR and FP double positive cells. (B) KIR and PF expression was analyzed on the surface of single clones using fluorescent labeled antibodies against the respective KIR. (B) Histograms of surface and intracellular expression for the respective KIR. Controls are enhanced green fluorescence protein (eGFP) and Cerulean (Cer) expressing cell lines that do not contain a transgene. Isotype controls are depicted in gray.

KIR and FP expression were analyzed on cell lines derived from single clones (Figure 22, B). Most of the selected cell lines showed a high KIR surface expression over 80% and a high FP expression (eGFP or Cerulean), except one: NK-*S1* 2.1. To reveal whether the lower KIR expression of NK-*S1* 2.1 might be a result of receptor internalization, an intracellular FACS staining was performed (Figure 22, B). CD107a was used as positive staining control and verified functionality of intracellular staining (data not shown). All receptors were only detectable on the cell surface, except for NK-*L1* 2.1 (middle plot, depicted in blue), which showed a weak shift. Cells remained PF positive during treatments. Thus, receptor internalization is unlikely to cause a reduction of the KIR expression on NK92-MI-KIR$^+$ cells.

4.5.4 Functionality of NK92-MI-KIR$^+$ single clones

Next KIR expression was analyzed to determine whether it influences the functionality of the generated NK92-MI-KIR$^+$ cell lines. A degranulation and a killing assay of NK92-MI-KIR$^+$ cells against different target cell was performed. The HLA-negative cell line 721.221 was used either unmodified (wt) or modified to express different HLA-C molecules on their surface. The modified target cells express either the HLA-C1 molecules C*0701 or C*0304 or the HLA-C2 molecules C*0401, which are the ligands for the KIRs (section 3.5.1). Relevant KIR/HLA interactions are depicted in Figure 22, C. NK92-MI-KIR$^+$ specific lysis of the target cells was analyzed after co-cultures in different E:T ratios of 10:1, 3:1 and 1:1 (Figure 23, A).

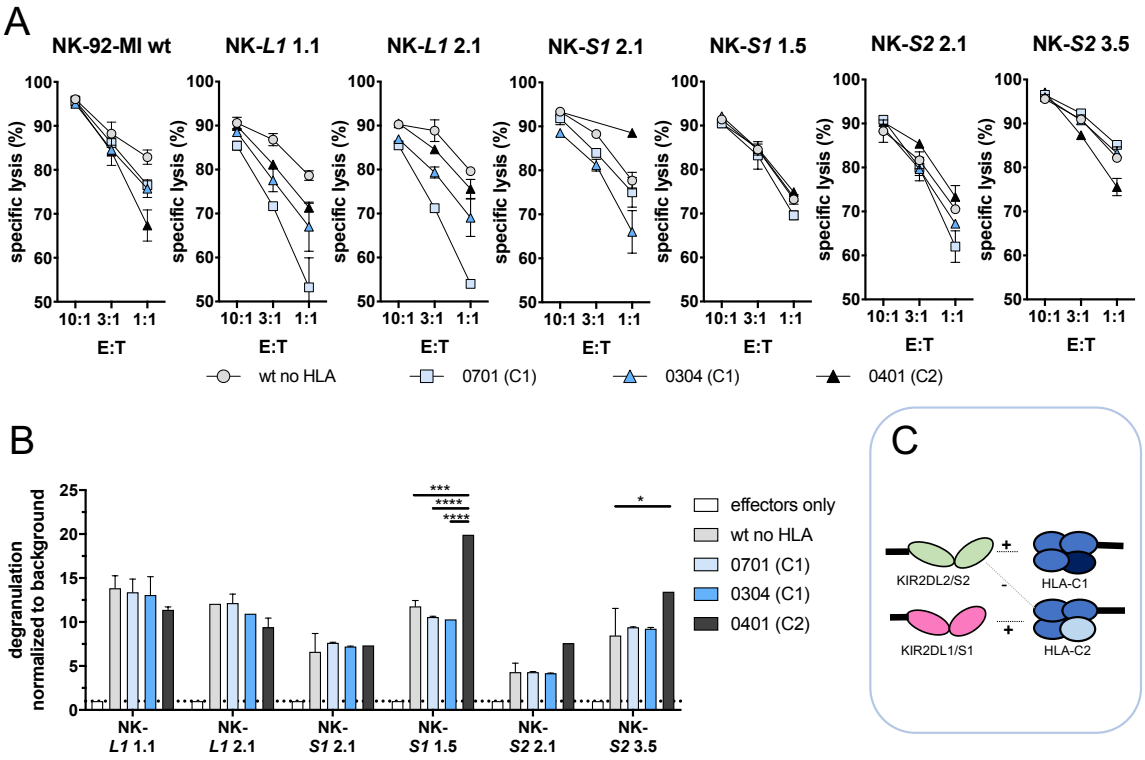

Figure 23: Functional analysis of NK92-MI-KIR$^+$ cells against HLA expressing 721.221 cells. NK92-MI wt and NK92-MI-KIR$^+$ cells were co-cultured with 721.221 that express either HLA-C1 (HLA-C*0701 or HLA-C*0304) or HLA-C2 (HLA-C*0401) or no HLA (wt) on their surface, in different E:T ratios of 10:1, 3:1, 1:1 for four hours. (A) Specific lysis of target cells was analyzed in an FACS-based killing assay. (B) NK92-MI-KIR$^+$ cells were co-cultured with the target cells in an E:T ratio of 1:1. Degranulation of NK92-MI-KIR$^+$ cells was analyzed by detection of the degranulation marker CD107a. Degranulation was normalized to background degranulation of unstimulated cells (effector cells only). (C) Schematic depiction of relevant KIR/HLA interaction partners. Dashed lines show interaction. KIR2DL2 and KIRDS2 have a weak interaction with HLA-C2. Depicted are mean ± SD or single values. Statistical analysis was performed using Two-way ANOVA followed by Tukey's multiple comparison test. Depicted are only significant differences in co-cultures with 721.221 cells. All differences between cells only and co-cultures are significant and therefore not depicted. Significance ****p<0.0001, ***p<0.001, *p<0.05, n. s. not significant.

Both inhibitory KIR expressing cells NK-*L1* 1.1 and NK-*L1* 2.1 showed a lower specific lysis compared to the other NK92-MI-KIR$^+$ and NK92-MI wt cells against the HLA-C*0401 expressing cells (E:T 1:1 52%, respectively compared to >60% by the other NK92-MI-KIR$^+$ and NK92-MI wt cell lines). NK-*S1* 2.1, but not the NK-*S1* 1.5 cells, showed higher reactivity against HLA-C*0701 expressing cells, but not against HLA-C*0304 expressing cells. Both HLA-C

variants belong to the HLA-C1 group. In general, NK-*S2* 3.5 had a higher reactivity compared to the other NK92-MI-KIR$^+$ and NK92-MI wt cells. Otherwise, no significant difference was detected in lysis of any of the other NK92-MI-KIR$^+$ cells against a specific target cell line. The question arose as to whether the inhibition observed by both NK-*L1* cells (1.1 and 2.1) could also be detected in the degranulation of the cells. Therefore, NK92-MI-KIR$^+$ cell lines were co-cultured with the target cells in an E:T ratio of 1:1 and degranulation was analyzed by the marker CD107a (Figure 23, B). A reduced degranulation was observed in both NK-*L1* cells (1.1 and 2.1) after co-culture with the HLA-C2 (C*0401) expressing cells, compared to both C1 (C*0701 and C*0304) expressing or the wt target cells, but the difference was not significant. The NK-*S1* 2.1 cells showed no difference in degranulation against any of the target cells. A significantly higher degranulation was detected in NK-*S1* 1.5 cells co-cultured with C2 expressing target cells, compared to the ones co-cultured with both C1 expressing and wt target cells (C2 targets: 20% vs. C1 targets 11% and 13%). Besides, these cells (NK-*S1* 1.5) showed a higher KIR expression compared to the NK-*S1* 2.1 cells (section 2.9.3). Interestingly, both NK-*S2* cell lines (2.1 and 3.5) showed a higher degranulation against C2 expressing cells as well, whereby a significant difference was only detected for NK-*S2* 3.5 cells co-cultured with C2 expressing cells compared to the wt target cells (NK-S2 3.5 15% vs. wt 7%).

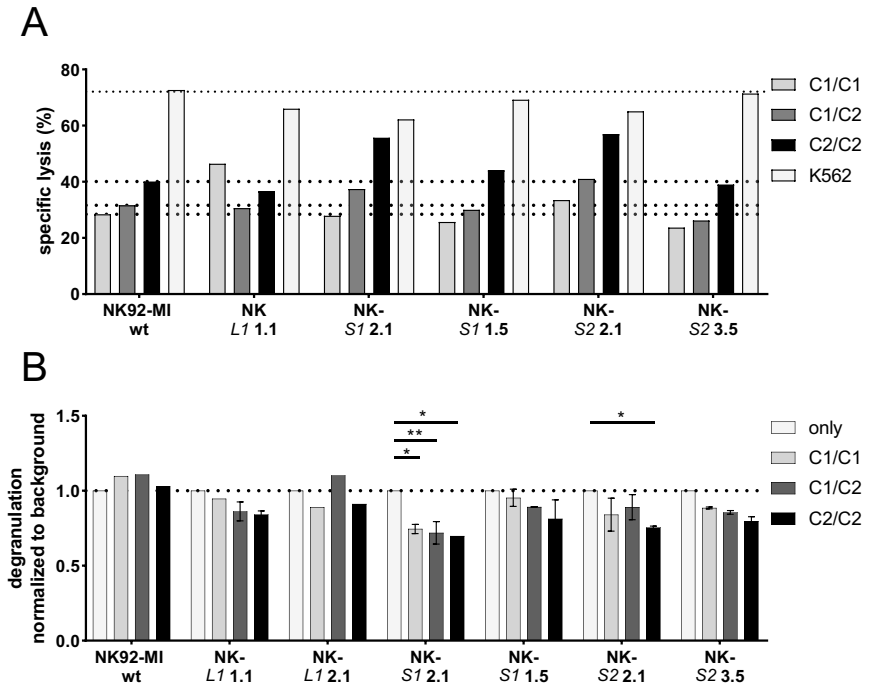

Figure 24: Functional analysis of NK92-MI-KIR$^+$ cell lines against primary leukemic blasts. NK92-MI and NK92-MI-KIR$^+$ cells were co-cultured with primary human leukemic blasts that differ in HLA-C genotype, and K562 as positive control. (A) Specific lysis of target cells was analyzed in an FACS-based cytotoxicity assay from co-cultures after four hours. Depicted is an E:T ratio of 1:10. (B) Degranulation of NK92-MI and NK92-MI-KIR$^+$ cells was determined as the number of CD107a$^+$ cells from co-cultures with the target cells in an E:T ratio of 1:1. Degranulation was normalized to background degranulation of unstimulated cells (only). Depicted is one representative experiment. Depicted are mean ± SD or single values. Statistical analysis was performed using Two-way ANOVA followed by Tukey's multiple comparison test. Significance *p<0.05, **p<0.01, n. s. not significant. Dashed lines show specific lysis or degranulation of in (A) wildtype (wt) NK92-MI cells and in (B) unstimulated cells only.

Functionality of NK92-MI-KIR$^+$ cells was not clearly affected by expression of distinct HLA-Cs on target cells. They might need additional signals to become activated or inhibited.

Then the reactivity of NK92-MI and NK92-MI-KIR$^+$ cells against primary human-derived leukemic blast was analyzed (Figure 24). For this purpose, NK92-MI-KIR$^+$ cells were co-cultured with different c-ALL leukemic blasts, either HLA-C1 or HLA-C2 homozygous or HLA-C1/C2 heterozygous, and against K562. The specific lysis of target cells was determined from co-cultures at an E:T of 1:10 (Figure 24, A).

All NK92-MI-KIR$^+$ cell lines showed a high cytotoxicity against K562 of 60 - 80%. In general, the reactivity against leukemic blasts was lower. Against C1 homozygous blasts, all NK92-MI-KIR$^+$ cells showed an equal lysis of blasts, except NK-*L1* 1.1 cells that exhibited a higher specific lysis (46% vs. 24 - 33%). Against C1/C2 heterozygous blasts, the cell line NK-*S2* 2.1 showed a higher reactivity (41% vs. 30% wt), but not the second cell line expressing the same KIR NK-*S2* 3.5 (26% vs. wt 30%). In comparison against C2 homozygous blasts, NK-*S1* 2.1 and NK-*S2* 2.1 cells showed a slightly higher cytotoxicity (NK-*S1* 2.1: 56% and NK-*S2* 2.1: 57% vs. wt 40%), while cytotoxicity of NK-*L1* 1.1 cells was reduced (37% vs. wt 40%). Besides cytotoxicity, degranulation of the NK92-MI-KIR$^+$ cell lines was analyzed after co-cultured with leukemic blasts (Figure 24, B). Degranulation of NK-*S1* 2.1 cells was significantly reduced after co-cultured with any of the target cells (0.7 vs. 1). Degranulation of NK-*S2* 2.1 was also reduced, but only the reduction from co-culture with C2 homozygous blasts was significant (0.7 vs. 1). No significant difference was seen in degranulation of any of the other NK92-MI-KIR$^+$ cells after co-culture with the leukemic blasts.

In conclusion, reactivity of some NK92-MI-KIR$^+$ cells was slightly affected by expression of HLA-C on 721.221, but inconsistent for cell lines expressing the same KIR. In general, the functionality of NK92-MI-KIR$^+$ cells against primary leukemic blasts was very weak and not clearly affected by expression of a certain KIR.

4.6 Modification of primary human NK cells

4.6.1 Lentiviral particles for transduction of primary human NK cells

Reactivity of human NK cells is balanced by a fine-tuned KIR receptor signaling and NK cells mostly need an accumulation of different signals to become activated. By contrast, NK92-MI cells are highly activated and reported to mainly kill in a perforin-granzyme-dependent manner, independent of polarization (*151*). Consequently, in the per se highly activated NK92-MI cells the signal provided by the inserted KIR might be masked by other (stronger) signals or might be insufficient, which might result in the lack of clear effects. Therefore, the effect of KIR insertion was additionally analyzed in primary human NK cells. A major disadvantage of primary NK cells is the expression of endogenous KIRs on a fraction of NK cells. For simplification of the following experiments, the nomenclature depicted in Table 8 is used to

discriminate between endogenous KIR expression, transgene KIR expression and the antibodies used for detection. As mentioned before, some KIRs have highly homologous extracellular domains, resulting in a cross reactivity of antibodies, detecting the respective KIRs. Therefore, antibodies are named according to the detected KIRs, e.g. L1/S1 binds to KIR2DL1 and KIR2DS1, whereas L1 is specific for KIR2DL1.

Table 8: Nomenclature of KIRs to simplify following experiments.

Receptor	Nomenclature	Example
Endogenous KIR	Complete name	KIR2DL1, KIR2DS1, KIR2DL2, KIR2DS2
Inserted exogenous KIR	Abbreviated without KIR2D in italics and in text underlined	KIR2DL1 = *L1*, KIR2DS1 = *S1*, KIR2DL2 = *L2*, KIR2DS2 = *S2*
Detection antibody for flow cytometry	Abbreviated without KIR2D and all targets	anti-KIR2DL1/S1 = L1/S1, anti-KIR2DL1 = L1 anti-KIR2DL2/S2 = L2/S2

The generated viral vectors (section 4.5.1), were pseudotyped with VSV-G and used to equip primary human NK cells with distinct KIR receptors. At first, lentiviral particles were tested, because others had achieved good transduction efficiencies, when lentiviral particles were combined with protamine sulfate (PrSf) (*289*). NK cells from three healthy voluntary donors were isolated, then IL-2/IL-21 activated and transduced with the different KIR containing viral particles. During this experiment, the suitability to insert one or more KIR receptors was tested. Therefore, donor NK cells were transduced either with lentiviral particles for one KIR (*L1*, *S1*, *L2*) or with a mixture of two types of lentiviral particles for different KIRs (*S1* and *S2* or *L2* and *S1*).

Four days after transduction the KIR expression was analyzed by flow cytometry using fluorescent labeled antibodies against the respective KIR (Figure 25, A). In all donors, exogenous KIR expression was analyzed in non-viral particle treated control cells (ctrl). In donor 1, 22% of the NK cells expressed KIR2DL1 and/or KIR2DS1 detected by L1/S1, 10% expressed KIR2DL1 only detected by L1, and 18% expressed KIR2DL2 and/or S2 detected by L2/S2. Donor 2 showed a generally lower percentage of KIR expressing cells: 10% expressed KIR2DL1 and/or KIR2DS1detected by L1/S1, 2% expressed KIR2DL1 detected by L1, and 22% expressed KIR2DL2 and/or KIR2DS2 detected by L2/S2. The third donor had a high fraction of 56% of KIR2DL2 and/or KIR2DS2 expressing cells detected by L2/S2, a lower fraction of 17 - 18% of KIR2DL1 and/or KIR2DS1 expressing cells (detected by L1/S1) and KIR2DL1 only (detected by L1) expressing cells, respectively.

In two donors, transduction with *L1* containing viral particles resulted in an increase of 10% of L1 positive cells. Transduction with *S1* viral particles only led to an increase of 3% of L1/S1 positive cells (donor 1), and combination with *S2* viral particles had no effect and more likely seemed to reduce the frequency of L2/S2 positive cells. Transduction with *L2* viral particles did not affect the frequency of L2/S2 positive cells in two donors (donor 1 and donor 2). In the

third donor, no difference in the fraction of either L1/S1, L1 only or L2/S2 positive cells was observed. Interestingly, a reduction of L2/S2 expressing cells was detected in all cells that were transduced with *L1* or with *S1* containing lentiviral particles.

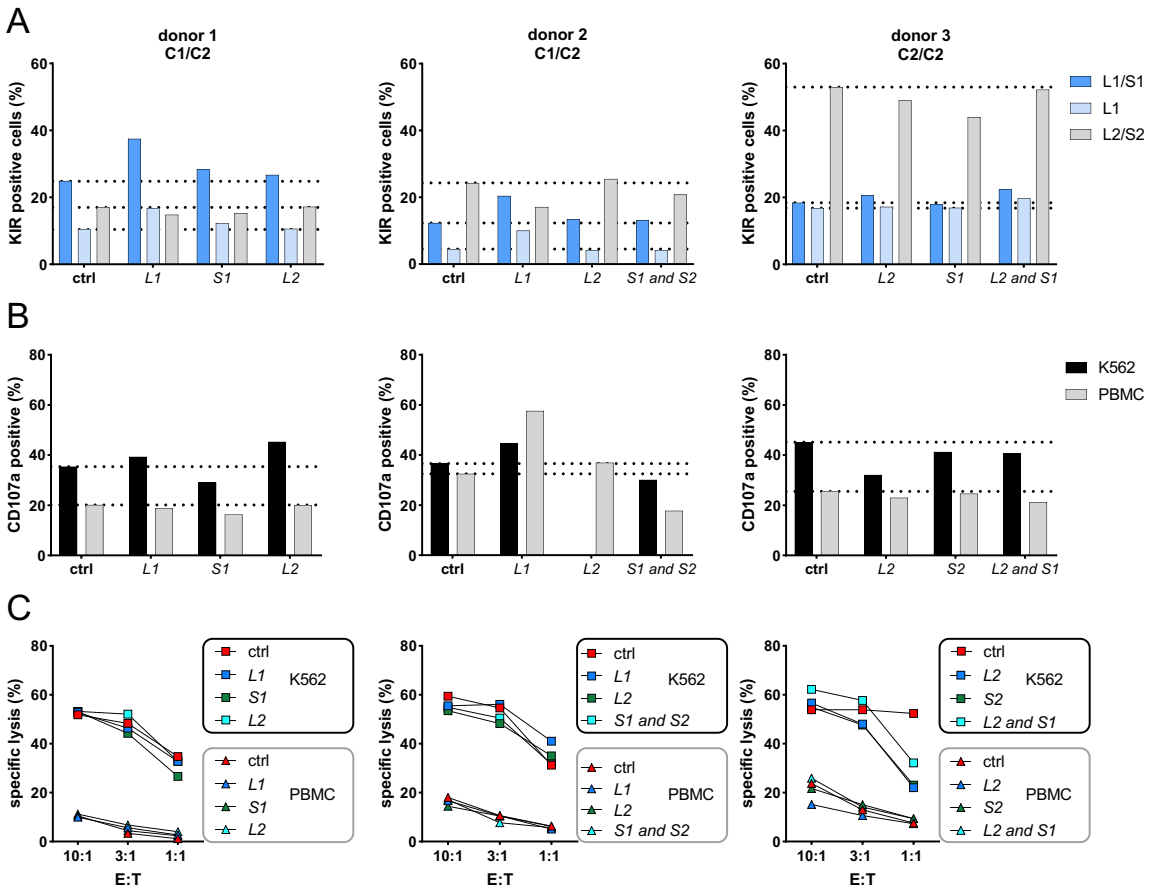

Figure 25: Transduction and modification of primary human NK cells using lentiviral particles. Three donors were HLA-C genotyped and NK cells were isolated. These isolated primary human NK cells were activated for four days with IL-2/IL-21 followed by transduction with either lentiviral particles for one KIR (KIR2DL1 (*L1*), KIR2DL2 (*L2*), KIR2DS1 (*S1*) respectively), or with a mixture of two types of viral particles for different KIRs (KIR2DS1 (*S1)* and KIR2DS2 (*S2)* or KIR2DL2 (*L2)* and KIR2DS1 (*S1)*). Lentiviral particles were pseudotyped with VSV-G. Transduction was performed with addition of protamine sulfate (as described (*289*)). (A) Three days after transduction KIR expression was analyzed using the different antibodies L1/S1, L1, and L2/S2 that recognize the respective KIRs. Functionality of transduced NK cells was determined against K562 and autologous freshly thawed PBMCs. (B) Degranulation, analyzed as CD107a positive NK cells, was determined after co-cultures with either K562 or PBMCs in an E:T ratio of 1:1. (C) Specific lysis of either K562 or autologous freshly thawed PBMCs by transduced primary NK cells was determined in different E:T ratios of 10:1, 3:1 and 1:1 in an FACS-based cytotoxicity assay. Each column represents measurements from one donor. In B, 2nd plot *L2* values against K562 are missing because of the limited cell number. In (A) dashed lines show baseline of endogenous KIR expression defined in untreated controls and in (B) dashed lines show degranulation level of NK cells only without target cells.

Despite low transduction rates, it was investigated if the challenge with viral particles affects NK cells reactivity and NK cells maintain tolerance towards self. Therefore, cells were co-cultured with either the HLA-negative cell line K562 or with autologous PBMCs (Figure 25, B). Transduction with different KIRs did not affect NK cell degranulation after co-culture with autologous PBMCs. Only donor 2 showed an increased degranulation when cells were treated with *L1* viral particles (ctrl 45% vs. *L1* 58%). Besides the degranulation, the reactivity of modified NK cells against K562 and autologous PBMCs was determined in a

cytotoxicity assay (Figure 25, C). All cells killed most of the K562 and showed a low killing of autologous PBMCs. In addition, donors were HLA-C genotyped to assess whether the donor's HLA-C genotype affects KIR gene expression. Two donors were HLA-C1/C2 heterozygous and one was HLA-C2 homozygous. All observations were independent of the respective donor's HLA-C genotype.

Despite the low transduction efficiency from 5 - 10%, expression of the FP was not detected in any of the transduced cells. The question then arose as to whether low receptor expression increase is accompanied by lack of FP expression, resulting from the low transduction efficiency or involvement of the IRES sequence. To overcome this, primary NK cells from three different donors were transduced with lentiviral particles VSV-G pseudotyped, encoding either for eGFP or an IRES followed downstream by eGFP. Additionally, cells were transduced either with the addition of protamine sulfate (PrSf) or the transduction enhancer vectofusin-1 (VF-1) that is described to increase the transduction efficiency in primary human-derived cells (*292, 308, 309*). Cells were analyzed for detection of fluorescence on day four after transduction (Figure 26, A). Transduction with viral particles encoding *eGFP* led to a higher frequency of eGFP expressing cells with PrSf, compared to transduction with VF-1 (PrSf 10% vs. VF-1 3%). Using the *IRES eGFP* viral particles, only low transduction efficiencies were achieved with both reagents (4 - 5%). Both transductions were performed with the same MOI. Thus equal transduction efficiencies were expected. Hence the vector copy number (VCN) was determined, which means the number of inserted viral vectors per cell.

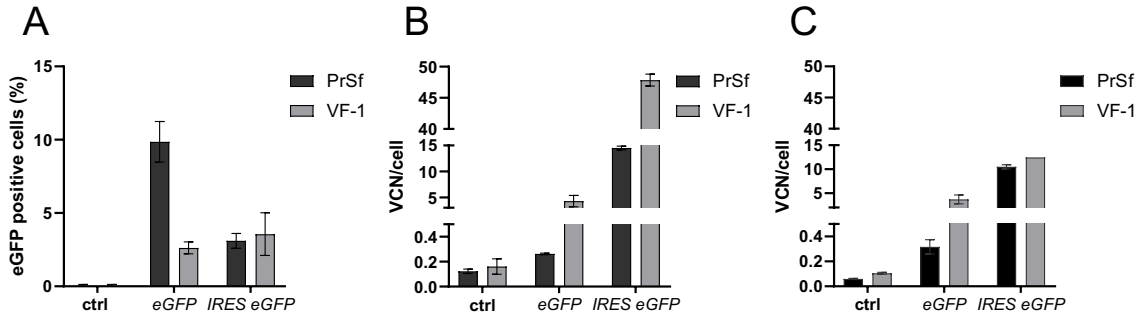

Figure 26: Functionality of IRES in transduced human primary NK cells. NK cells were isolated and activated for four days with IL-2/IL-21. Activated NK cells were transduced using either protamine sulfate (PrSf) or vectofusion-1 (VF-1) and the lentiviral construct LeGo-eGFP (*eGFP*) or LeGo-IRES-eGFP (*IRES eGFP*) with a multiplicity of infection (MOI) of 30. Lentiviral particles were VSV-G pseudotyped. (A) Analysis of eGFP expression on day four after transduction (n = 3 donors, duplicates of each condition). Vector copy number (VCN) was analyzed using ddPCR in duplicates. In (B) DNA isolated from cells directly and in (C) samples that were treated with RNAse A prior to DNA isolation. Depicted are mean ± SEM. ctrl: controls are cells treated with PrSf or VF-1 only without viral particles.

DNA was isolated and the VCN per cell was determined with primers/probes specific for eGFP in a ddPCR (Figure 26, B). The VCN was increased in cells transduced with *eGFP* coding viral particles and VF-1 compared to PrSf (VCN/cell: VF-1 5 vs. PrSf 0.2) and was further increased, if cells were transduced with the *IRES eGFP* viral particles (VCN/cell: VF-1 48 vs. PrSf 14).

The increased VCN per cell might have resulted from the presence of viral particles that had not been integrated but were still present. Therefore, cells were lysed and treated with RNAse A (Figure 26, C). After treatment, the similar VCN per cell was detected for cells transduced with the *eGFP* viral particles and PrSf (VCN/cell: not RNAse A treated 0.2 vs. RNAse A treated 0.3). Treatment with VF-1, still resulted in an increased VCN as seen for non RNAse A treated cells (VCN/cell: both 5) (Figure 26, B). The detected increase of VCN per cell disappeared when cells were transduced with *IRES eGFP* viral particles in combination with VF-1 after RNAse A treatment (VCN/cell: not RNAse A treated 45 vs. RNAse A treated 14).
In conclusion, usage of VF-1 did not increase the transduction efficiency, detected by the FP. A higher VCN per cell was detected, if cells were transduced with *IRES GFP* viral particles, but only few cells showed FP expression. Consequently, FP expression downstream from the IRES cannot be considered as reliable marker for transgene insertion in primary human NK cells. In subsequent experiments, the transgene upstream from the IRES was used to assess transduction efficiency.

4.6.2 Alpharetroviral particles for transduction of primary human NK cells

Up to now, only a low transduction efficiency was reached in primary NK cells using lentiviral particles. However, efficient transduction of NK92-MI cells has verified functionality of lentiviral particles. Consequently, a crucial factor is improvement of the transduction efficiency, because cultivation, cell sorting, and expansion of NK cells is challenging and potentially affects NK cell reactivity. Recently, it was described that increased transduction efficiencies in primary NK cells could be reached, when cells were transduced with RD114/TR pseudotyped alpharetroviral particles in combination with the transduction enhancer VF-1 (*292*).
The question arose as to whether the transduction enhancer (VF-1 or PrSf) per se affects the KIR expression of the NK cell. Therefore, KIR expression was analyzed after treatment of primary NK cells either with PrSf or VF-1 without viral particles. NK cells from three healthy donors (1 - 3) were isolated, activated and, the fraction of KIR positive cells was analyzed four days after transduction. The following previously mentioned antibodies were used: L1/S1 and L2/S2, except L1. L1 was excluded because this receptor is already recognized by L1/S1 (Figure 27, A). In two donors (1 and 2) treatment did not influence the fraction of L1/S1 positive cells (donor 1: L1/S1 all 5 - 7%, donor 2: all 4 - 5%), but in donor 3 the fraction increased after PrSf treatment (23% to 31%). The fraction of L2/S2 positive cells was not affected in donor 1 (all 12%) but increased in donor 2 after both treatments (21% to PrSf: 29% and VF-1: 27%). In donor 3, the fraction of L2/S2 positive cells increased only after PrSf treatment (26% to 34%). Additionally, donors were HLA-C genotyped to determine an influence of donor's HLA-C genotype on KIR gene expression. Two donors were HLA-C1 homozygous and one was HLA- C1/C2 heterozygous. Influences of both VF-1 and PrSf were only detected in the

homozygous donors. Accordingly, in some, but not in all donors, treatment with either PrSf or VF-1 per se slightly affected the fractions of KIR positive cells.

So far, it was not analyzed if the activation per se influences the KIR expression. To determine this, NK cells from three healthy donors (donor 4 - 6) were isolated. A KIR phenotyping was performed to compare the KIR expression before and after treatment (including activation and transduction). NK cells were activated for four days, then cells were treated with freshly concentrated alpharetroviral particles in combination with VF-1. Four days after transduction, NK cells were analyzed for KIR expression. Cells were stained with the antibodies used in section 4.6.1, Table 8 (L1 or L1/S1 and L2/S2). As a control, some cells were left untreated or were treated only with VF-1. Endogenous KIR expression before activation was compared to activated untreated and activated VF-1 treated cells (Figure 27, B).

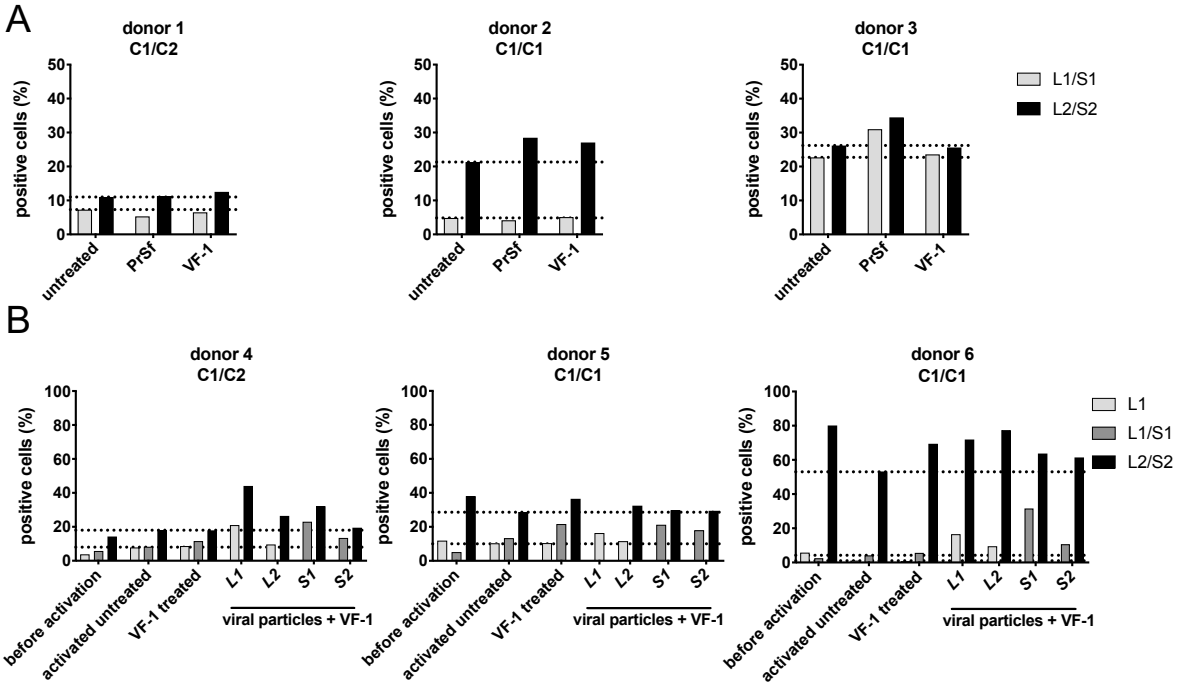

Figure 27: Transduction of primary NK cells using alpharetroviral particles and vectofusin-1. Human NK cells were isolated from six different donors. Donors were HLA-C genotyped. (A) Isolated primary human NK cells from three donors (1 - 3) were activated for four days with IL-2/IL-21 followed by transduction with either vectofusin-1 (VF-1) or protamine sulfate (PrSf) without viral particles. Four days post treatment, cells were stained with the antibodies (L1/S1 and L2/S2) against the respective KIR. (B) From three donors (4 - 6) NK cells were isolated and the KIR expression was analyzed (before activation) with the mentioned antibodies and additionally with an antibody specific for KIR2DL1 (L1). NK cells were activated for four days with IL-2/IL-21. After activation, NK cells either were left untreated (activated untreated), were treated with VF-1 (VF-1 treated) or with VF-1 and additionally freshly generated concentrated KIR containing alpharetroviral particles: KIR2DL1 (*L1*), KIR2DL2 (*L2*), KIR2DS1 (*S1*) or KIR2DS2 (*S2*). Four days post treatment, KIR expression was determined by staining NK cells with antibodies against the respective KIRs (L1, L1/S1, L2/S2). Each graph represents analysis of samples from one donor. Dashed lines show baseline based on control (ctrl) cells that were treated without viral particles. PrSf: protamine sulfate, VF-1: Vectofusion-1.

In donor 4, all frequencies of KIR expressing cells slightly increase after activation (L1: 4% to 7%, L1/S1: 6% to 8%; L2/S2: 14% to 18%). Using only VF-1 treatment further increased frequencies of L1/S1 positive cells (before 6% to activated 8% to VF-1 treated 11%). In donor

5 frequencies of L1 positive cells remained stable (all 11%), but frequencies of L1/S1 positive cells were increased (before 5% to activated 13% to VF-1 treated 22%). Fractions of L2/S2 positive cells were reduced after activation but remained at the same level if VF-1 was added (before 38% vs. activated 28% vs. VF-1 treated 36%). In donor 6, treatment reduced frequencies of L1 positive cells (before 5% to activated and VF-1 treated 1%). Frequencies of L1/S1 positive cells slightly increased (before 3% to activated and VF-1 treated 5%). The same variation observed for L2/S2 frequencies in donor 5 was seen in donor 6. Frequencies of L2/S2 positive cells decreased, when cells were activated only, but remained stable if VF-1 was added (before 80% to 53.1% to 70%). Consequently, in addition to VF-1 treatment, as already observed in donor 1 - 3, the activation per se slightly affected frequencies of KIR expressing NK cells.

Additionally, cells were transduced with alpharetroviral particles encoding the KIRs: *L1, L2, S1, S2*. Frequencies of KIR positive cells were analyzed four days after transduction with the antibodies mentioned before. In donor 4 and 6 an increase of KIR positive cells was detected when cells were transduced either with *L1* encoding viral particles (L1 positive cells: donor 4: 7% to 21%, donor 6: 1% to 17%), *S1* encoding viral particles (L1/S1 positive cells: donor 4: 12% to 23%, donor 6: 6% to 32%) or *L2* encoding viral particles (L2/S2 positive cells: donor 4: 18% to 26%, donor 6: 70% to 77%). In donor 5, an increase of KIR positive cells was detected only when cells were transduced with *L1* encoding viral particles (11% to 16%). Frequencies of KIR expression were not affected if cells were treated with the other alpharetroviral particles (*L2*, *S1* or *S2*) compared to frequencies of KIR expressing cells in VF-1 treated cells. Consequently, a high increase of inserted receptor expressing cells was not detected in any of the donors. An average transduction efficiency of 10 - 15% was achieved. In addition, donors were HLA-C genotyped, to assess whether the donor's HLA-C genotype affects KIR gene expression. Two donors were HLA-C1/C1 homozygous and one was HLA-C1/C2 heterozygous. All observations were independent of the respective donor's HLA-C genotype.

One drawback of the alpharetroviral vectors are the low titers of viral particles obtained after virus production (data not shown). Reduction of the cell number for transduction could lead to an increased transduction efficiency and was therefore tested. Additionally, combination of VSV-G pseudotyped lentiviral particles and PrSf was directly compared to RD114/TR pseudotyped lentiviral particles combined with VF-1.

To optimize the transduction efficiency, NK cells from three healthy donors were isolated activated and either transduced at 2.5 x 10^5 cells with VSV-G pseudotyped lentiviral particles and PrSf or RD114/TR pseudotyped lentiviral particles and VF-1. Additionally, 2.5 x 10^4 cells were transduced with RD114/TR pseudotyped alpharetroviral particles and VF-1 (Figure 28). Four days after transduction, cells were analyzed for KIR expression by staining with

antibodies against the respective inserted KIR. Here, the two antibodies recognizing L1/S1 and L2/S2 were used as follows: Control, *L1* and *S1* viral particle treated cells were stained with the antibody L1/S1. Control, *L2* and *S2* viral particle treated cells were stained with the L2/S2 recognizing antibody. In donor 7, transduction of 2 x 10^5 cells with lentiviral particles and either PrSf or VF-1 resulted in an increase between 5 - 15% of positive cells for the respective KIR receptor, except for the cells treated with *S2* encoding lentiviral particles and VF-1. In donor 8, treatment with lentiviral particles and PrSf increased frequencies of KIR expressing cell for the respective KIR about 5%, whereas treatment with VF-1 and viral particles encoding *L1* and *L2* resulted in a rise of up to 22%, respectively. In donor 9, transduction of 2 x 10^5 cells with VF-1 and with PrSf resulted in an increase of KIR expressing cells of only about 5%.

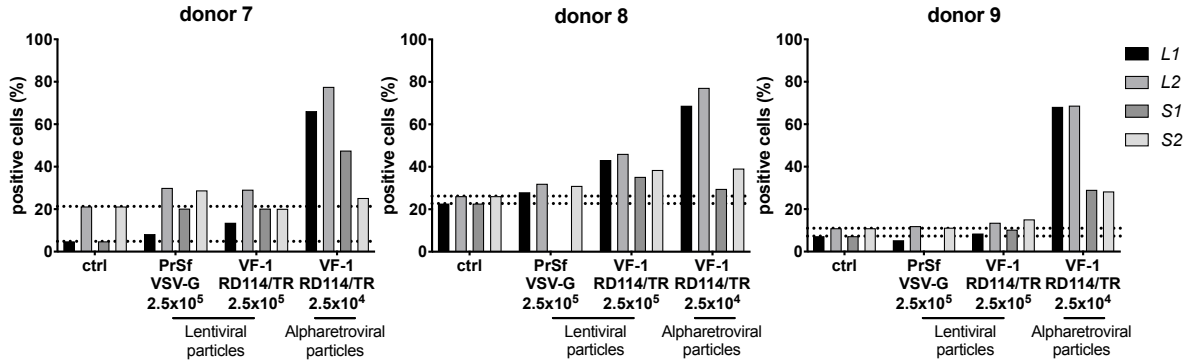

Figure 28: Optimizing viral transduction of primary human NK cells by reduction of the cell number. NK cells from three donors were isolated and activated followed by transduction. Either 2.5 x 10^5 or 2.5 x 10^4 cells were transduced. Transduction of 2.5 x 10^5 cells was performed with lentiviral particles pseudotyped with VSV-G and with protamine sulfate (PrSf) or with lentiviral particles RD114/TR pseudotyped and with vectofusion-1 (VF-1). 2.5 x 10^4 cells were transduced with RD114/TR pseudotyped alpharetroviral particles with VF-1. Four days after transduction cells were stained with antibodies against the respective KIR. Dashed lines show baseline expression in untreated control (ctrl) cells.

Reduction of the cell number to be transduced to 2.5 x 10^4 cells clearly increased the transduction efficiency. In all three donors a considerable increase of *L1* and *L2* positive cells was detectable (60% increase) with the alpharetroviral particles. In donor 7, treatment with *S1* encoding viral particles resulted in an increase from 5% to 50% of S1 positive cells, whereas treatment with *S2* viral particles did not affect the fraction of S2 positive cells (20% to 22%). In donor 8, the fraction of S2 positive cells was slightly increased from 25% to 40% after transduction with the *S2* encoding viral particles, but the fraction of S1 positive cells was not affected after transduction with the *S1* encoding viral particles (21% to 23%). In donor 9, the fractions of both *S1* and *S2* positive cells were increased for *S1* from 15% to 30% and for *S2* from 10% to 30% after treatment with the respective viral particles encoding *S1* or *S2*. A higher enhancement was reached by transduction with the inhibitory KIR encoding viral particles *L1* and *L2.* Treatment with *L1* viral particles resulted in an increase of L1 expression from 15% to 70% and treatment with *L2* viral particles resulted in an increase of L2 positive cells from 10% to 70%. In conclusion, reduction of the cell number and usage of alpharetroviral vectors dramatically increased transduction efficiency.

4.6.3 Killing and degranulation ability of receptor equipped NK cells

A high transduction efficiency was reached for some KIRs in primary NK cells using the alpharetroviral particles pseudotyped with RD114/TR (Figure 28). Subsequently, these NK cells equipped with a distinct KIR were tested for their functionality.

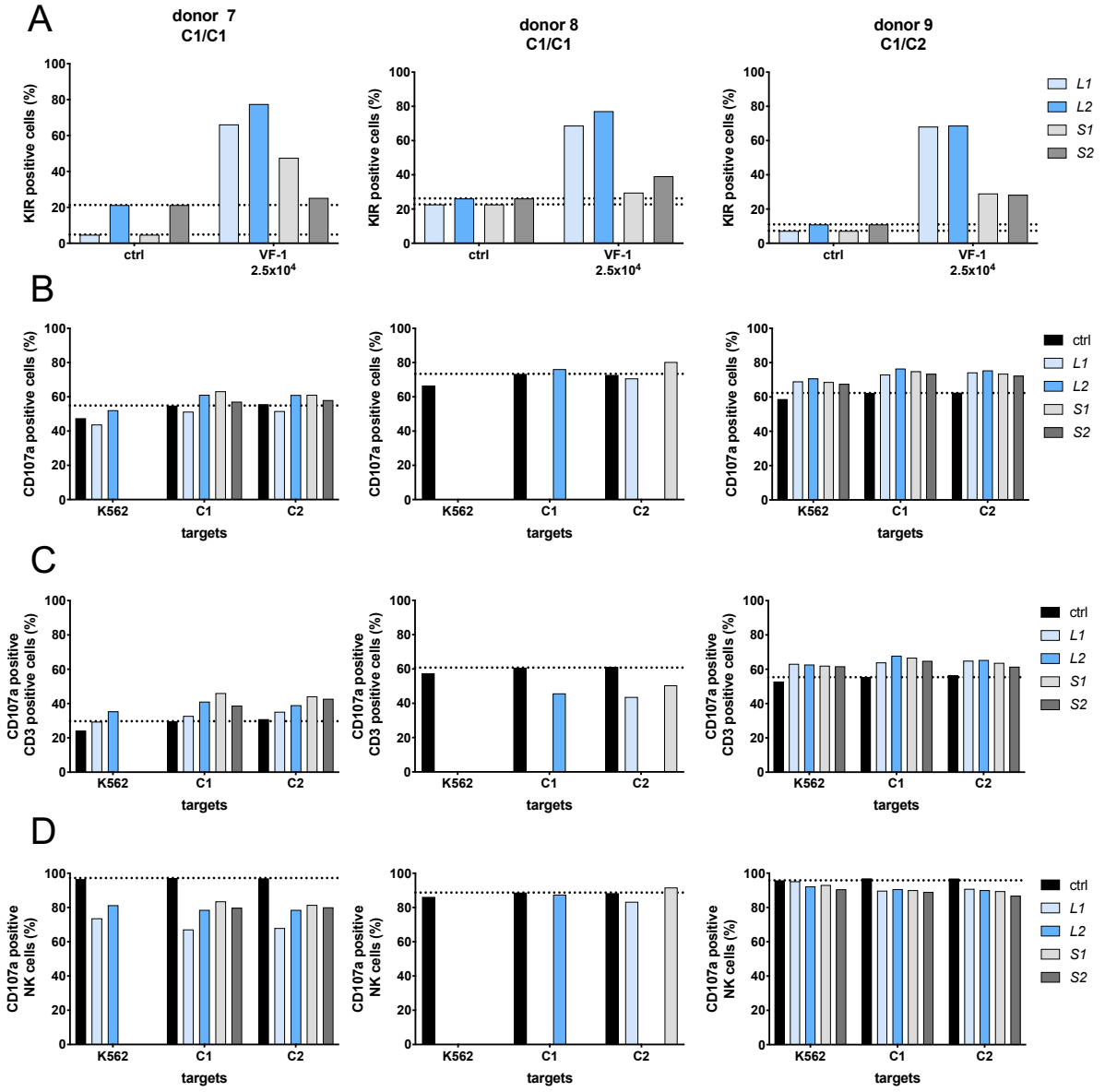

Figure 29: Functional analysis of KIR modified primary NK cells. NK cells from three donors were isolated and activated followed by transduction. 2.5 x 10^4 cells were transduced with alpharetroviral RD114/TR pseudotyped viral particles. (A) Four days after transduction, cells were stained with antibodies against the respective KIR and fraction of KIR expressing cells was determined. Modified cells were cultured for additional seven days. Degranulation of NK cells was determined in co-cultures with either K562 or HLA-C1 or HLA-C2 homozygous leukemic blasts in an E:T ratio of 1:1 for four hours. After incubation, cells were stained with antibodies against CD3, CD16, and CD56. Degranulation was analyzed in subgroups gated on (B) all cells, (C) $CD3^+$ cells and (D) NK cells. Each column represents data from one donor. Dashed lines show baseline adjusted on non-virus treated cells (ctrl). ctrl: control cells only without target cells.

Frequencies were as mentioned before all donors showed an increase of the inhibitory KIR receptor positive cells (Figure 29, A). Donor 7 had no increase of S2 positive cells and donor 9 none of *S1* positive cells. Expression of all inserted KIRs was increased in donor 8, but

transduction with the inhibitory receptors resulted in a higher increase of KIR expressing cells, compared to transduction with the activating receptors (L1 60% L2 60% S1 20% S2 20%). NK cells were expanded for seven days after transduction and functionality was tested in a degranulation assay and degranulation was determined by surface expression of CD107a. KIR modified NK cells were co-cultured with either K562 or HLA-C1 or HLA-C2 homozygous leukemic blasts. After incubation cells were stained with antibodies against CD3 and the NK cell marker CD16 and CD56. CD3 was included to differentiate between NK cells and T cells. These T cells might result from a less efficient NK cell isolation. Percentages of all activated cells (Figure 29, B), activated CD3 positive cells (Figure 29, C) and activated NK cells (Figure 19, D) were analyzed after co-cultures with the different target cells.

In donor 7 the fraction of CD107a positive cells was reduced when cells were equipped with the *L1* receptor compared to the other receptors. Modification with *L*2 and *S1* led to a slightly increased degranulation (56% to 62%). Degranulation of *S2* modified cells, as expected due to the low transduction efficiency, was unaffected (control and S2 modified cells both 58%). Interestingly, in the CD3 population that resulted from impurity of the isolated NK cells, modification with activating KIRs *S1* and *S2* and the inhibitory *L2* resulted in a higher degranulation against all target cells (30% to 40 - 50%), while degranulation was decreased in all modified NK cell subgroups after co-cultures (99% to 70 - 90%). In donor 8, the fraction of all CD107a positive cells was not affected by different target cells (Figure 29, B). Here, an inhibitory effect was seen, if the ligand was present for the inhibitory receptors in the CD3 fraction (60% to 42%) and for *L1* modified NK cells (90 to 82%), but not for *L2* modified cells (Figure 29, C and D). In the third donor (9), no difference was seen. All cells were per se highly activated and showed a high degranulation above 60%. In donor 8 a slight influence of the inhibitory KIR/ligand interaction was detected. Donor 9 was highly over-activated and from donor 7 all NK cells showed a reduced degranulation compared to untreated cells, highlighting a huge donor variance in case of NK cell activation, transduction ability and expansion, which all affect post transduction functional analysis.

Taken together, a protocol to transduce primary NK cells with different KIR receptors was established by using alpharetroviral particles that were pseudotyped with RD144/TR. With this protocol a high transduction efficiency in primary NK cells was achieved that enabled functional analyses of modified primary NK cells.

5. Discussion

Detection and identification of microchimerism is still challenging and a variety of methods has been used (*76, 80, 105, 106, 108*) to elucidate the still controversial role of FM cells in different biological aspects (*77, 125, 126, 274, 296, 297*). In the first part of this study, a ddPCR protocol was developed to directly detect FM and TM cells in maternal or younger sibling background cells. This assay was used to analyze two cohorts for an FM and one cohort for occurrence of a TM. In addition, the phenotype of the FM cells was determined. Further, the impact of parental KIR genotype, phenotype and HLA-C genotype on FM was analyzed as well as their influence on parental NK cell alloreactivity.

A significant advantage of the haploidentical donor is that the donor is available for post-transplantation immune cell collections and certain effector cells can be infused into the patient. Here, NK cells are promising effector cells that can be used to provide additional GvL effects and thereby fight or prevent relapse without causing GvHD (*301*). However, NK cells need to be optimized for enhanced functionality, which can be done by insertion of distinct receptors. Here, the influence of ectopical expression of KIR receptors KIR2DL1, KIR2DL2, KIR2DS1 and KIR2DS2 was examined. In the second part of this work, single-KIR expressing NK92-MI cells were generated and their functionality was tested. Finally, the most conductive conditions for modification of primary NK cells were determined followed by functional analysis.

5.1 Suitability of ddPCR for detection of microchimeric cells

Current methods for the detection of a microchimerism have different advantages (high reducibility, applicable and approved for routine diagnostics, various panels of detection markers available) and disadvantages (lack of sensitivity, exact quantification, time consuming), the major disadvantage being that all methods lack comparability and equivalent controls.

So far, ddPCR has been used for chimerism analysis (*119, 120*), MRD detection (*310*) and detection of circulating fetal DNA in maternal cell-free plasma (*311*), but it has not been described for microchimerism detection. Here, a ddPCR protocol was established for detection of microchimerism. One main advantage of ddPCR is the more precise quantification. In RT-PCR, for example, the level of FM was quantified based on the amount of genomic DNA employed. A reaction was considered positive or negative based on the cycle threshold. The FM level was determined from the positive reactions and the amount of DNA used, e.g. 2 µg of genomic DNA (which equates to 300,000 cells) was employed and distributed on eight reactions. If one reaction was positive this was reported as an FM level of three FM cells in 100,000 maternal cells, which is equivalent to an FM level of 3×10^{-5} (*77*). Hence, the RT-PCR method is based on measured DNA content. This measurement poses a huge source of error and is avoided in ddPCR through the direct detection of background copies by use of a

housekeeping gene. The level of FM is directly calculated in relation to the measured background copies. This results in a precise quantification of the level of FM. Furthermore, control reactions were included to exclude false positive samples. With these control reactions, the assay can be easily adopted by other scientific issues involving microchimerism. It was demonstrated that ddPCR can be used for detection of FM in mothers and TM in siblings. Furthermore, it facilitates detection of low levels of MM in DNA. This increases the spectrum of the method and makes it applicable to a wide range of scientific issues. A widely used method will result in comparable results from different research fields that can be compared and elucidate the role of microchimerism in a broad overlapping context.

In this study, a microchimerism was detected in 37% of mothers (section 4.1, Table 4) and in 62% of younger siblings (section 4.4, Table 7). The same results were revealed in 6/8 samples in RT-PCR and ddPCR, but ddPCR allowed for exact quantification. The exact quantification enables a precise calculation of the level of FM, which, together with the higher sensitivity reached by ddPCR, resulted in an increased level of detected FM in ddPCR compared to RT-PCR (Figure 7, A). Two samples that were tested negative by RT-PCR were positive by ddPCR, pointing out a higher sensitivity of the ddPCR. The high sensitivity with a limit of 0.01% in ddPCR presented during this work has already been described for chimerism analysis after HSCT (*119, 120*) and for detection of circulating cell-free DNA in plasma (*312, 313*).

In addition, pretreatment of the cells did not impair microchimerism detection. An FM was detected in maternal DNA isolated either from whole blood or from purified PBMCs (Figure 7). Additionally, FM was detected in DNA isolated from cells after sorting by flow cytometry (Figure 9). However, we observed that the fixation of cells with formalin for sorting affects downstream PCR reactions (data not shown). Formalin leads to DNA lesions, which can result in sequence artefacts (*314*), leading to incorrect results.

The relative number of FM cells was reduced in samples from whole blood compared to PBMCs, indicating that FM cells are enriched within mononuclear cells. The extraction of other mononuclear cells, e.g. granulocytes during PBMC isolation, results in the increased proportion of detected FM cells in the PBMCs. Because of the increased number of maternal mononuclear cells in DNA from whole blood, the level of FM cells might be below the detection limit.

Surprisingly, in two samples an FM was detected in DNA from whole blood only, but not in PBMCs. Here, the detected FM might result from the detection of circulating cell-free filial DNA. Potentially, FM cells persist in tissues or the BM, undetected by the maternal immune cells in some individuals. These persisting FM cells might influence their surrounding immune cells to become tolerated. In contrast, differentiated circulating FM cells might be detected and eliminated by maternal effector cells resulting in cell-free filial DNA. During treatment (PBMC isolation followed by MACS isolation of NK cells), this filial cell-free DNA is washed out,

resulting in detection of intact FM cells only. Hence, it is possible to differentiate between circulating cell-free filial DNA and persisting intact filial cells. Filial circulating cell-free filial DNA has already been detected in maternal plasma using ddPCR (*312, 313*).

In the Haplo group, DNA from whole blood was analyzed, because DNA from PBMCs was not available. In the FM group, DNA from both sources (whole blood and PBMCs) was available only from some mothers, which impeded comparison of all samples. The higher detection of an FM in the Haplo group compared to the FM group (Figure 8), and the higher frequency of an FM (Haplo 67% vs. FM 31%) could be explained by detection of cell-free filial DNA. Furthermore, this explains the reduced frequency of an FM compared to the previously described detection of an FM in 50% of the mothers *(77)*. In the former study, DNA from whole blood was analyzed and during this study DNA from PBMCs was analyzed. In addition, in TM analysis, where a TM was detected in 62% of analyzed samples, DNA was isolated from whole blood as well. In order to differentiate between intact FM cells and filial-derived circulating cell-free DNA, for subsequent studies, the pre-treatment of cells before isolation of DNA should be kept equal and ideally the FM levels should be compared in DNA isolated from both whole blood and from PBMCs.

A challenge of our protocol remains the dependence on marker panels. In this study, a relatively large number of samples (27%, Table 4) lacked a suitable marker. In case of sons, a Y chromosome specific marker can be used, but mother-daughter pairs lack this alternative. However, the detected Y-positive cells could result from earlier pregnancies, thus an alternative marker was preferred. Regarding clinical application, the marker panel needs to be extended. An alternative can be the inclusion of SNPs, which represent the most frequent variations in the human genome (*315*). They are already in use for chimerism analysis after HSCT using RT-PCR (*116*). Combination of SNP-typing and NGS has been applied to detect donor cell-free DNA after organ transplantation (*316*) and to determine chimerism and MRD after HSCT (*317*). One main advantage is the possibility to analyze large marker sets simultaneously, which results in an enormous opportunity to distinguish two genomes. Furthermore, this allows for concurrent analyses of disease-specific markers, abnormalities, chimerism and microchimerism. However, an NGS approach is expensive. An analysis pipeline has to be built that includes a lot of bioinformatic input and up to now lacks standardizations (*318*). Therefore, the described ddPCR is currently the best alternative for microchimerism analysis in comparison to RT-PCR, with a high sensitivity and precise quantification.

5.1.1 Occurrence of a microchimerism

FM was detected in mothers and TM was detected in younger siblings. In addition to FM or TM, an woman might have a persisting MM from her mother. MM was detected in 39% of

women and was found to be less prevalent than FM in the following lymphocyte subsets: T cells (MM 25% vs. FM 58%), B cells (MM 14% vs. FM 75%), monocytes/macrophages (MM 6% vs. FM 50%) and NK cells (MM 16% vs. FM 62%) (*319*). An increase in these MM cells in a healthy pregnant woman is seen with ongoing gestation, but not in women suffering pregnancy complications such as preeclampsia, suggesting a beneficial effect of the MM cells. An increase in MM cells is a marker for healthy adaption to pregnancy (*320*). Interestingly, a decrease in MM cells in pregnant women is observed with increased parity (*103*). Thus, the mixed microchimerism of FM and MM in a woman is on the one hand beneficial for pregnancy progression, but on the other hand these cells compete for the same niche within the female body. One drawback of analyzing FM is that the cells declared as FM can originate from another sibling or the grandmother who is positive for the used marker. An ideal comparison would be to analyze a whole family for the occurrence of a microchimerism. However, it would be challenging to find a single marker for each analyzed individual in a family for which only one family member is positive. The detection of SNPs using NGS might be useful to examine this question (*317*) and should be considered for further analysis.

5.2 Phenotype and origin of microchimeric cells

Filial cells can persist for decades in the maternal blood system (*75*). Thus there must be a population of fetal cells capable of self-renewal. During this research, the cellular subgroup that holds the FM cells was determined. FM cells were detected in the $CD34^+$ cells of a mother, but not in the differentiated subgroups T, B or NK cells (Figure 9, A). This observation is in line with the reported $CD34^+$ phenotype of FM cells (*75*). In contrast, Loubiére *et al.* detected an FM in T, B, NK cells, and monocytes/macrophages (*319*). In their study, the reported subpopulations were pooled from all analyzed individuals, highlighting that the compartment of microchimeric cells differs between individuals. A crucial point of Loubiére *et al.*'s report is that no further information on earlier transfusions is given that could also lead to a persistent microchimerism. In our study, because of limited availability, only one mother was analyzed for the presence of an FM in the lymphocyte subsets. So far it cannot be ruled out that FM cells differentiate and persist below the detection limit.

The precise phenotype of the microchimeric cells might help to discover their origin, explain their persistence, and explain their positive influence on the outcome of an hHSCT. FM cells were detected in the $CD34^+$ and $CD34^+$ $CD38^+$ subpopulations of non-pregnant women (Figure 9, B). In one woman, who was pregnant at the time of sample collection, the detected FM cells were in the $CD133^+$ and $CD34^+$ $CD133^+$ subgroup. FM cells of all donors tested showed an HSC phenotype as described previously (*75, 321*), whereas within this study we could further demonstrate that most of the cells are HSC marked by CD34 and/or CD133 expression and the absence of CD38 (*322-325*). Interestingly, in the sample from BM and the

pregnant woman, FM cells were detected in the $CD133^+$ subgroup. CD133 is an alternative stem cell marker that is expressed in both $CD34^+$ and $CD34^-$ cells (*326*). In humans, CD133 is a marker for more immature CB-derived $CD34^-$ HSCs compared to $CD34^+$ CB-HSCs (*2*). Hence, an alternative differentiation pathway is presumed. In this alternative model, the $CD133^+$ $CD34^-$ cells are very early precursors, with the ability to directly differentiate in a "Bypass route" into megakaryocytes/erythrocytes, but also maintain the ability to follow the conventional hematopoiesis pathway (*327*). *In vitro*, megakaryocyte progenitors have been shown to function as APCs due to MHC class II surface expression. Furthermore, when involving non-cognate interactions with memory cells, the TH_{17} response is activated (*328*). This observation highlights a role of megakaryocytes as immune cells, next to their major function of platelet production. Thus $CD133^+$ FM-derived megakaryocytes could affect the immune response after HSCT by secretion of immune modulatory cytokines and microparticles (*329*). The secreted effector molecules might positively influence the interplay between HSCs, HSC accompanying effector cells, and the remaining recipient stromal cells.

Additionally, the presence of filial cells with an immature early HSC phenotype explains the long persistence of the FM cells, their beneficial role in maternal tissue repair after injury (*330*) and their potentially protective role in thyroid cancer (*331*) and breast cancer (*332*).

It is described that FM cells with stem-cell like properties (*321*) settle in the maternal BM (*333*). This leads to the assumption that these FM cells might be enriched during BM or PBSC collection. In T-cell-deplete hHSCT, PBSCs are always collected to obtain a sufficient cell dose for infusion. Consequently, during mobilization of HSC for PBSC collection, the FM cells might be mobilized, too, and this results in increased amounts of FM cells that are infused into the child within the graft. These FM cells could enhance the beneficial effect on the outcome of an hHSCT (*77*).

Two possible mechanisms evolve: I. Maternal HSCs already tolerate increased levels of the persistent filial cells. Thus the donor-derived effector cells in the graft tolerate them as well. Consequently, the maternal effector cells have the ability to differentiate between healthy and non-healthy filial cells. II. The increased level of fetal HSCs leads to an increase of newly developing cells, originating from the FM cells, that differentiate quickly into megakaryocytes. These newly differentiated megakaryocytes are beneficial for the tolerance towards the graft, mediated by secretion of immunomodulatory molecules, which could lead to better tolerance and reduced graft rejection. However, the number of FM cells in an HSC source for HSCT has not been addressed so far.

5.3 Factors influencing the establishment and persistence of an FM

The reason why FM persists only in some, but not all mothers, is still unknown. The controversial biological role of FM cells and the genetic background for a persisting FM are still

unidentified. In this project, it was observed that an FM was not related to the children's age and did not significantly decrease in mothers with older children (Table 5). Thus if an FM occurs, it is stable.

Why can these FM cells survive in the mothers without being attacked by the maternal immune system? In a healthy individual, the immune system detects foreign or degenerated cells by the lack of HLA molecules mediated by NK cells, or HLA disparities, mediated by T cells, and eliminates them. One hypothesis was that the maternal cells do not recognize the filial cells due to the partial match in HLA-C. HLA similarity of mother and child significantly correlated with the occurrence of FM (Table 5). Besides favoring occurrence of an FM, an HLA-C match and the presence of at least one HLA-C1 allele in the mother resulted in an increased level of FM (Figure 11). All analyzed sibling pairs were HLA-C matched (Table 7). Therefore, the uniform HLA-C match and the fact that all donors carried at least one HLA-C1 allele might explain the high frequency of detected TM compared to FM (TM^+ 62% vs. FM^+ 37%).

Nevertheless, the maternal immune cells must be able to recognize the filial cells, because most of the filial cells are cleared by the maternal immune system after parturition (*85*). During pregnancy, the maternal immune system is suppressed to prevent an attack on the partially HLA-mismatched fetus. This is maintained by production of immunosuppressive molecules, activation of immunosuppressive cells, exclusion of immune cells and silencing of potentially reactive T cells (*91-96*). After pregnancy, the maternal immune system returns to normal levels. Consequently, most of the FM cells are detected and probably cleared by previously silenced alloreactive T cells (*85*). Hence, the presumption arose that the filial cells are detected, but somehow tolerated or even protected by maternal immune cells. Distinct KIR/HLA interactions and combinations play important roles for pregnancy progression and are beneficial for a successful pregnancy (*266-269*). These may be important for the tolerance of FM cells as well.

Therefore, mothers were analyzed for the influence of the different genetic factors: KIR genes, centromeric and telomeric KIR gene motifs, haplotype, B content score and their effect on the level as well as occurrence of an FM. Neither presence nor absence of any of the maternal activating KIR receptors affected either the occurrence or the level of an FM (Table 6 and Figure 12). Accordingly, no influence was detected on a TM in sibling pairs (section 4.4). Consequently, presence or absence of certain activating KIR genes is not elementary for microchimerism. This was unexpected, because a higher level of FM was observed in $KIR2DS1^+$ mothers compared to $KIR2DS1^-$ mothers in a previously analyzed cohort described by our group (*77*). One reason might be the difference in the DNA source or the different methods used for FM determination discussed in 5.1.

During pregnancy, a protective effect was observed by KIR2DS1 in a Caucasian population (*261*). In an African cohort, the protective effect is related to the activating KIR receptor

KIR2DS5 (*270, 271*). The mechanism behind this is explained by a strong inhibition of KIR2DL1 with its ligand HLA-C2. NK cells function is impaired by this inhibition but can be rescued by activating signals (*261*). Either inhibitory signals can surpass the protective effect mediated by the activating signals, or combinations of activating signals that are important are masked by the strong linkage equilibrium of some KIR genes (*178*). Interestingly, when the fraction of activated KIR expressing cells was analyzed, a significant higher fraction of KIR2DS1 and KIR2DS5 expressing cells was activated in NK cells from FM^+ mothers compared to cells from FM^- mothers. However, this effect was only present after co-culture with leukemic blasts (Figure 14, B). The fraction of KIR2DL1-only expressing cells was not affected, suggesting a role for KIR2DS1 and KIR2DS5 in the reactivity against the filial leukemic blasts. KIR2DS1 has a low affinity interaction with HLA-C2 (*197*). Additionally a peptide-specific interaction was observed with HLA-C*0602 presenting an HIV peptide (*334*). KIR2DS5 binds to HLA-C2 only, but allelic variation affects the binding ability (*271*). A peptide-specific activation of KIR2DS5 is not known, but a peptide-specific NK cell response protects infants from maternal HIV transmission during pregnancy (*335*). After HSCT, the risk for viral infections increases highlighting a protective role of NK cells, which are the first lymphocytes to recover. Here, a yet unidentified peptide-specific activation of both receptors could activate the KIR expressing NK cells and contribute to the superior outcome after hHSCT from FM^+ mothers. Because this activation was independent of HLA-C match or mismatch (Figure 15), it might be mediated by the persisting FM. A CMV infection leaves an imprint in the KIR repertoire of infected patients, which mainly involves activating KIR genes (*214*). Presence of FM did not affect the frequency of KIR expressing NK cells, but affects the fraction of activated cells after short-term co-culture (Figure 14, A). The observed activation of KIR2DS1 and KIR2DS5 expressing cells from FM^+ mothers (Figure 14, B) might result from an imprint in the maternal KIR repertoire. In the future long-term co-culture experiments should be performed to analyze if such an imprint can be verified. Further, co-culture experiments in a healthy control cohort with NK cells from FM^+ mothers against healthy filial cells could reveal whether this observation is based to the leukemic blasts per se or the detection of filial cells. FM was more often detected in HLA-C matched mother-child pairs. Consequently, this resulted in only small groups when mother-child pairs were grouped by their HLA-C match or mismatch. Even if a significantly higher fraction of KIR2DL1/S1 and KIR2DL1/S5 expressing cells was detected in the C1/C2 FM^+ group compared to the FM^- group (Figure 15, A), the FM^+ group must be increased to statistically verify these results (FM^+ n=1 - 2 vs. FM^- n=9).

Within the inhibitory KIR genes, a significant correlation was seen between FM and the maternal inhibitory KIR2DL3 (Table 6). An FM was more often detected in mothers lacking KIR2DL3 (Figure 12). Up to now, one can only speculate on the functional relevance of KIR2DL3 absence. Most of the analyzed mother-child pairs with an FM carry one HLA-C1.

Moreover, KIR2DL3 binds C1 with a lower avidity compared to KIR2DL2. The maternal NK cells are more strongly inhibited by KIR2DL2 if it is the only receptor present. The lower inhibition by KIR2DL3 might reduce the tolerance of maternal NK cells, resulting in an insufficient inhibition when maternal NK cells meet filial cells. Consequently, filial cells are eliminated, presuming a protective effect for an FM by KIR2DL2. Besides, KIR2DL2/L3$^+$ NK cells can barely distinguish between HLA-C1 and HLA-C2 target cells. In most cases, the alloreactivity depends on KIR2DS1 co-expression, because KIR2DS1 can directly recognize HLA-C2 (*242*). The activated KIR2DL3 expressing maternal FM$^+$ NK cells might co-express KIR2DS1. Thus, the increased activation of KIR2DL3 positive cells might result from expression of KIR2DS1 (Figure 16, B). Here, the activating signal surpasses the low inhibition. Because this increased activation was not detected against K562, it is likely to be an effect specific against the filial leukemic cells. Potentially, KIR2DS1 and KIR2DS5 expressing NK cells from FM$^+$ mothers were educated by the persisting filial cells in the maternal blood system. Consequently, these educated maternal NK cells can distinguish healthy from leukemic filial cells.

In pregnancy, mothers with a KIR A haplotype carrying a fetus that has inherited HLA-C2 from the paternal side are at a higher risk for pregnancy complications compared to mothers with an HLA-C1 homozygous fetus (*266-269*). Because of this, mothers were analyzed considering their KIR haplotype. TM was only detected in one sibling donor with an A haplotype. No FM was detected in mothers with an A haplotype. This led to the hypothesis that a B haplotype could favor the persistence of FM or TM, which would mean that the presence of activating KIR genes is important. This observation still lacks significance due to the small group size. Hence, these results must be confirmed in a larger cohort.

Furthermore, an increase of activating KIR genes, determined by the analysis of maternal and sibling donor B content score, did not affect the occurrence or level of FM or TM (Figure 15, J and Figure 19, F). This suggests that instead of KIR genetics the KIR expression and interactions are more important for FM and TM.

Taken together, maternal cells presumably have a unique mechanism to tolerate filial cells in their blood system. NK cells can be re-activated by viral re-challenge, which suggests a memory formation or trained immunity response by NK cells (*336*). NK cells probably have been educated or primed during pregnancy. NK cells are also in a permanent process of adaption to environmental changes (*229, 231, 232*). Thus the tolerance of NK cells towards FM cells is maintained. Consequently, KIR2DS1 and KIR2DS5 expressing cells still memorize filial healthy cells but are activated upon engagement with leukemic cells. Besides NK cells, T_{regs} are important in women during pregnancy and are described to form a memory that is beneficial for subsequent pregnancies (*96, 97*). A protective effect of these T_{reg} cells could also

explain the tolerance of filial cells in the maternal blood system independent of maternal KIR receptors, but this must be investigated more in the future.

5.4 NK cell alloreactivity, KIR and HSCT

NK cell alloreactivity is effective to exert a GvL effect after mismatched HSCT (*57, 237, 239*). Many studies, mainly performed in adults and AML patients, have analyzed the impact of KIR genes and contents on the alloreactivity of donor NK cells in the recipients after mismatched HSCT (*57, 242*). A superior effect is repatriated to KIR B haplotype donors and the presence of centromeric and telomeric KIR B genes in these donors (*243, 337*), whereas no beneficial effect was observed by the donors' KIR B genes in pediatric MUD transplantations (*252*). In contrast, in pediatric ALL patients undergoing allo-HSCT, the presence of centromeric B and absence of telomeric B genes in the donor were independently associated with a reduced risk for relapse (*247*), whereas others had observed an effect in AML, but not in ALL patients (*243*). These observations highlight that, besides the disease itself, other factors such as KIR expression, type of donor, graft manipulation and post-transplantation treatment must be considered to affect the influence of KIR genes.

An increased EFS was observed by Overmann *et al.* in pediatric ALL patients that received T-cell-depleted hHSCT from KIR B haplotype donors (*249*). This observation suggests an influence of NK cells in the hHSCT. However, this report lacks *in vitro* data on NK cell functionality before and after HSCT. Unfortunately, for our study no data on survival, relapse or EFS were available, because most of the patients did not receive an hHSCT. However, parent-child pairs were analyzed for influences on parental NK cell alloreactivity against filial blasts *in vitro*.

In general, maternal NK cells did not show an increased specific lysis of leukemic blasts isolated from the offspring compared to paternal NK cells *in vitro* (Figure 17, A). Further, persistence or absence of an FM did not affect maternal NK cell killing of the leukemic blasts (Figure 17, B). Thus the observed improved outcome in hHSCT from FM^+ mothers (*77*) cannot be directly attributed to maternal NK cell cytotoxicity *in vitro*. Furthermore, maternal NK cell reactivity against leukemic blasts *in vitro* was independent of the mothers' KIR gene motifs (Figure 17, F). Lack of an effect *in vitro* suggests that *in vivo* an interplay of different immune cells is necessary to increase the cytotoxicity of NK cells or might result from alloreactive T cells remaining in the graft. Potentially, co-stimulatory signals and cytokines provided by other immune cells, e.g. remaining alloreactive T cells in the graft or APCs, are essential to boost NK cell reactivity. Alternately, it is possible that the main effector cells, which are responsible for the superior outcome, are alloreactive T cells that remain in the graft. The T cells can have two main functions: I. They can be harmful and cause GvHD, because they recognize HLA-mismatched recipient cells or II. They might be beneficial and exert an

alloreactivity against remaining leukemic blasts. A phenotypical characterization and identification of the activated effector cell, immediately after hHSCT and follow-up during reconstitution, might provide this information. This might be challenging though because of low cell counts during the first phase post stem cell infusion. An alternative might be *in vitro* co-cultures of donor-derived CTLs with leukemic blasts and APCs (e.g. donor-derived dendritic cells) that might lead to identification of important co-stimulatory molecules and identification of activated T cell clones.

The study by Overmann *et al.* lacks information about an FM and type of haploidentical donor. Nevertheless, the study showed the importance of donor centromeric B and telomeric A genes for the recipients' survival. It was observed that these gene motifs favor an increased level of FM (Figure 12, F). If the presence of KIR B motifs leads to an improved EFS and reduced relapse rate, an FM that is fostered in the same donors potentially intensifies the positive effect observed in the recipients.

Another important point is that NK cell alloreactivity is affected by expression of HLA class I on the target cell. In the mismatched setting, NK cell alloreactivity was improved against B-lineage leukemic blasts with high HLA expression, but was not affected by blasts with low HLA expression (*338*). During our study, blasts were tested for their phenotype and surface HLA expression exemplarily and HLA expression was verified (data not shown). However, we did not analyze the level of HLA on the leukemic blasts compared to cells from healthy donors. Analysis of alloreactivity in matched or mismatched pairs, i.e. either mother-child or father-child (Figure 17, C) or mothers grouped depending on the presence or absence of an FM (Figure 17, D), did not significantly affect NK cell cytotoxicity. The lack of differences in the ability to kill leukemic blasts could be explained by a different HLA class I expression on the surface of leukemic blasts. Furthermore, this could explain the missing effect of B content score or haplotype (Figure 17, H - K). An increased B content score was clearly associated with a reduced risk for relapse in ALL patients (*249*) which emphasized a beneficial effect of activating donor KIR genes in hHSCT. Absence or reduction of HLA class I could mask a potential alloreactivity of the NK cells *in vitro*, especially if MHC class I expression is reduced in the matched pairs. No alloreactivity is expected in matched pairs if HLA expression occurs at normal levels on leukemic cells. Downregulation of HLA expression on leukemic cells results in recognition by NK cells independent of alloreactivity prediction. Furthermore, a lack of alloreactivity might result from a low frequency of potential alloreactive NK cells (*339*).

Although the cytotoxicity of maternal NK cells was unaffected, NK cells from FM^+ mothers showed a significantly higher degranulation against their child's leukemic blasts compared to NK cells from FM^- mothers (Figure 16, A). This leads to the assumption that maternal FM^+ NK cells still recognize the filial leukemic blasts and exert a higher reactivity. It can be ruled out that the maternal NK cells are in principle less reactive, because no significant difference was

seen in the reactivity of FM^+ and FM^- maternal NK cells against K562 (Figure 16, A). A reason for the higher degranulation but lack of difference in the specific lysis might be that filial leukemic blasts are more resistant to NK cell mediated killing. Either it takes longer for the NK cells to effectively kill leukemic blasts *in vitro* or the leukemic blasts inhibit NK cells by other mechanisms. Insufficient or defective NK cell activation that is independent of inhibitory signals is assumed to be responsible for resistance of B-ALLs to NK cell mediated killing (*340*), whereby the exact mechanism is still unknown.

Potentially, alloreactive T cells recognize and eliminate the remaining leukemic cells. An improved outcome was also detected in T-cell-depleted grafts (*249, 252*), though it seems that potentially either very low levels of T cells already have a higher impact or it is an interplay of different effector cells. To unravel a mechanism that could explain the interplay of different effector cells in the elimination of the remaining blasts, it would be necessary to analyze the fraction of activated NK and T cells after HSCT and further characterize these cells.

Memory NK cells formed during pregnancy (*341, 342*) could be reactivated and be effective in detecting the leukemic blasts, which have a different HLA expression compared to healthy filial cells. Besides memory NK cells, memory T_{regs} that developed during pregnancy (*96*) might be present in the stem cell source. Induction of an immunosuppressive environment by these T_{regs} could mediate the reduction of GvHD and benefits the GvL effect (*343*). A focused T_{reg} TCR repertoire, which was traced back to an increase in specific T_{reg} clones, was observed in patients receiving allogenic HSCT without acute GvHD (*344*). Thus, activation of specific maternal memory T_{regs} might be one factor that contributes to the improved outcome, thence as a side effect benefits the GvL of NK cells.

5.5 Receptor modified NK92-MI and primary NK cells

NK cells are a promising cell type to be used for post-transplantation effector cell administration, e.g. in case of viral infections or relapse. Here NK cells can be effective in prevention of relapse and support for the GvL reaction. Adoptive transfer of haploidentical NK cells into patients has been shown to be safe and feasible (*276, 277, 345, 346*), but the anti-leukemia effect needs to be optimized (*278*). The functionality of NK cells is maintained by activating and inhibitory signals, especially the KIR receptors (*222, 223, 228*). Manipulating NK cells by changing their activating and inhibitory signals might affect this functionality. Usage of the anti-KIR antibody IPH2101 resulted in hyporesponsiveness of NK cells (*283*). An alternative would be to use a viral vector gene transfer to either equip NK cells with distinct KIR receptors or knock out these receptors and thereby affect NK cell effector function. Regarding NK cells as an immunotherapeutic therapy, NK cells expressing an optimized KIR repertoire, e.g. a specific KIR/ligand mismatch from donor to recipient, could be infused into a recipient after HSCT. In the recipient, these modified NK cells potentially exert an increased

GvL reaction. Therefore, lentiviral and alpharetroviral vectors containing the KIRs KIR2DL1, KIR2DL2, KIR2DS1, and KIR2DS2 were generated (Figure 20).

First, to identify optimal transduction conditions, the envelope proteins VSV-G and RD114/TR were used for pseudotyping, whereby usage of RD114/TR resulted in an increased transduction efficiency (Figure 21, B). VSV-G pseudotyped viral particles use the low density lipoprotein receptor (LDLR) as the entry site to the cell (*347*). Low expression of LDLR seems to be responsible for the decreased transduction efficiency. Recently it was described that treatment with statins that induce LDLR expression on target cells increases the transduction efficiency in primary NK and NK92 cells (*348*) and might provide an alternative to be tested in the future. RD114/TR pseudotyped viral particles use the sodium-dependent neutral amino acid transporter (ASCT2) for their entry (*349*). ASCT2 is increased in NK cells upon IL-2 stimulation (*350*), thus making it an ideal envelope for transduction of NK92-MI cells and primary NK cells. ASCT2 is expressed on NK92 cells (*351*), leading to the observed increased transduction efficiency (Figure 21, B). Another alternative for lentiviral vectors that could be tested in the future is the baboon envelope, which showed promising transduction efficiencies in primary NK cells (*352*).

In IL-2/IL-21 activated primary NK cells, a high increase of the transduction efficiency was achieved using alpharetroviral particles that were pseudotyped with RD114/TR (Figure 28 and Figure 29) compared to VSV-G pseudotyped lentiviral particles (Figure 25, A). The high transduction efficiency with alpharetroviral particles is in accordance with the published literature (*286*). One difference is that Suerth *et al.* used primary NK cells which were expanded with IL-2 for 14 - 21 days. Furthermore, they used retronectin (*286*), whereas in our study VF-1 was used. Nevertheless, both resulted in equal transduction efficiencies. One drawback of the alpharetroviral RD114/TR pseudotyped viral particles is that the viral titer obtained from virus production was very low. We were not able to replicate the high titers generated by Suerth *et al.* (*286*). In our experiments, a high transduction efficiency was only reached with a reduced number of cells (Figure 28), which made it challenging to transduce enough cells for following functional analyses.

Another important factor is the reagent (e.g. PrSf or VF-1) used to increase the transduction efficiency. Transduction with PrSf slightly affected KIR expression in some donors (Figure **28**, C). Therefore, VF-1 which only slightly affects the KIR expression, is the better choice for transduction of primary NK cells. Additionally, retronectin was revealed to not affect NK cells phenotype (*286*) and might provide an alternative to VF-1. The differences detected in KIR expression mediated by PrSf and VF-1 in only some of the donors might result from a higher activation and expansion of a distinct subgroup of NK cells and seem to be donor dependent.

Another challenge in transduction of primary NK cells was the lack of FP expression if transduced with constructs expressing the FP downstream of an IRES sequence (Figure 26, A). Usage of an IRES eGFP vector resulted in a very high VCN per cell (Figure 26, B). RNAse A treatment (Figure 26, C) was performed to degrade viral particles that were still present, but did not affect the VCN per cell. Consequently, the FP is not adequately expressed in the NK cells. Either the promotor or the IRES are potentially responsible for the lack of expression. Here, the IRES eGFP vector has an SFFV promotor. In induced pluripotent stem cells, usage of a SFFV promotor resulted in a weaker eGFP expression compared to an EFS promotor (*353*). In mice, a strong methylation of the SFFV promotor was observed, which makes it inapplicable (*354*) and might manage the lack of expression in primary human NK cells. Accordingly, the promotor might be accountable for the lower expression or diminished expression to an undetectable level. Otherwise, the IRES that originates from the encephalomyocarditis virus (*355*) might have mutated during cloning or is not recognized by NK cells ribosomes. The latter is more likely, because transduction of NK92-MI with the same viral vectors resulted in excellent reporter expression and detection (Figure 22). A main advantage of the IRES is that it leads to an internal ribosome binding independent of a cap structure. Alternatively, a T2A or P2A site should be tested (*356*). These sites are characterized by a polycistronic nature, small size, and a high cleavage efficiency. Complete sequences, including the gene of interest and the reporter, are translated and the 2A that separates gene of interest and reporter mediates a self-cleavage. Ideally, this results in co-expression of multiple genes at the same level (*357*).

The human-derived cell line NK92-MI, in which most of the KIRs were not expressed (Figure 21, A), was successfully transduced, but the KIR expressing population decreased over time (Figure 21, C). Especially KIR2DL2 expression vanished and no single-KIR expressing NK92-MI-KIR$^+$ cells could be generated (Figure 21). The NK92-MI cell line is C1 homozygous (*in house* verified by HLA-C genotyping). The permanent and strong inhibition by interaction of KIR2DL2 with its ligand HLA-C1, in the absence of any activating signal, could promote the detected reduction in KIR2DL2 expressing cells. For KIR2DS1 it was shown that receptor internalization is not responsible for the reduction of receptor expression (Figure 22). Thus KIR2DL2 expressing cells are more likely go into apoptosis because of a permanent inhibition. Subsequent functional analysis of single-KIR expressing NK92-MI cells against HLA-C expressing target cells revealed that clones expressing the same activating KIR differ in functionality (Figure 23). Only one cell line NK-*S1* 1.5 had a significantly higher degranulation against HLA-C2 expressing target cells compared to HLA-C1 or wild type target cells, but the cytotoxicity was not affected. The inhibitory KIR expressing cell lines (NK-*L1* 1.1 and 2.1) showed a trend towards reduced killing and, accordingly, facilitated a reduced

degranulation against ligand expressing target cells, even though the differences were not significant (Figure 23). Only the NK-*S2* 3.5 cells showed a higher degranulation and slightly higher killing of HLA-C2 expressing target cells, but not the cells from the other KIR2DS2 expressing cell line NK-*S2* 2.1. Besides, KIR2DS2 has been proven to not affect the target cell lysis (*242*). According to this, other parameters for functional analysis, e.g. secreted cytokines or activation of intracellular adaptor molecules, should be considered. Others have used the NK cell line NKL for surface studies on KIR receptor expression. The cell line KHYG1-1 was used for functional analysis of KIR2DL2/L3 variants (*358*). Here, functionality was analyzed by cytokine secretion, e.g. IFNγ and TNFα.

In general, the NK92-MI-KIR$^+$ cell lines showed a lower specific lysis of primary leukemic blasts compared to K562, and the degranulation was reduced as well (Figure 24). Consequently, primary leukemic blasts might have an unknown mechanism to inhibit NK92-MI-KIR$^+$ cells' effector function. This mechanism outweighs the potential effect mediated by the inserted KIR receptors. NKG2A, which is expressed on some NK92-MI cells, might be responsible. Blockade of NKG2A resulted in a slightly increased killing of ALL and AML blasts by primary NK cells, whereas combination with the LILR-1 blockade significantly increased the specific lysis of the blasts (*359*). Further experiments should be conducted if the inhibition mediated by the leukemic blast can be revoked by NKG2A and LILR-1 blockade.

In conclusion, NK92-MI cells were not the best model to study the influence of KIRs on their functionality. NK92-MI cells are reported to be highly activated and do not require accumulation of signals to exert effector function (*151*), as known for primary human NK cells (*152*). This might explain the lack of reactivity observed by NK92-MI-KIR$^+$ cells. Consequently, primary NK cells were transduced with the viral vectors containing the KIRs (section 4.6). First, it was analyzed whether primary NK cells remain functional upon viral challenge. Preliminary data showed that the challenge with lentiviral vectors did not affect NK cells' functionality against K562 and did not induce alloreactivity against self (Figure 25). Nevertheless, only low transduction efficiencies were achieved (Figure 25 and Figure 27). Modification of primary NK cells using viral particles was challenging, but conducive conditions have been established using alpharetroviral particles in combination with VF-1. This combination led to equal transduction efficiencies in three independent donors (Figure 29, A). However, a high impact of donor variability in NK cell activation was detected (Figure 29, B - D). Consequently, more donors must be analyzed, and expansion conditions must be adopted. Expansion conditions might be optimized by short-term pre-activation with a reduced amount of IL-2 and IL-15. With this the highly IL-2 activated NK cells will have time to rest and to become re-activated upon target cell encounter. One donor showed promising effects by insertion of certain KIRs. Here, NK and T cells modified to express KIR2DL1 showed a decreased degranulation when co-cultured with HLA-C2 homozygous targets. Nevertheless, this observation must be verified

in the future. If this holds true, NK cells could be optimized for many clinical aspects related to presence of distinct KIRs, especially in control of viral infections.

5.6 Conclusion and outlook

In the first part of this study, it was shown that maternal HLA-C1 and an HLA-C match are important for the persistence and the level of FM. Maternal cells showed a higher degranulation against leukemic blasts. Consequently there is evidence that NK cells from FM^+ mothers can better detect leukemic cells. A direct effect of FM on cytotoxicity was not detected, highlighting the essential role of other immune effector cells, e.g. T cells. The role of T cells should be analyzed in the future. Consequently, the reason for the better outcome after HSCT cannot be attributed to NK cells alloreactivity. However, it is possible that the amount of FM cells has a beneficial effect.

In a small group of donors, it was shown that NK cells can be efficiently modified to express a particular KIR. Functional analysis pointed out a relevance of recombinant KIR receptor expression on NK cells reactivity, but this must be confirmed in the future. An alternative would be to generate fusion constructs to increase the impact mediated by the KIR. NK cells, equipped with an NKG2D-DAP10-CD3ζ fusion construct, showed an improved anti-tumor response against different tumor entities (*294*). Consequently, fusion constructs of extracellular KIR domains with a strong intracellular signaling domain might be an alternative.

During pregnancy, distinct KIR interactions prevent pregnancy complications. During viral infections, presence of e.g. KIR2DL3 and KIR3DS1 in HIV infection (*360*), KIR3DS1 in H1N1 infection (*361*) and KIR2DS1, KIR3DS1 and KIR2DL5 in hepatitis B virus infection (*362*) benefits the viral control. Thus the adoptive transfer of NK cells equipped with lacking receptors might help to prevent pregnancy complications or shape the NK cell response towards viral infections. Furthermore, it might be possible to promote the GvL effect for post-HSCT treatments.

In addition, NK cells equipped with the best KIR receptor repertoire could be combined with CARs against a distinct target, immune checkpoint regulators or bispecific antibodies to overcome inhibitions mediated by the microenvironment. All in all, the modification of primary NK cells with certain KIRs for a specific disease would be an excellent tool to exert new treatment options for a wide range of diseases.

6. Material and methods

6.1 Materials and equipment

Common laboratory material, chemicals and equipment was used as provided in the Research Institute Children's Cancer Center Hamburg. Special material and equipment are mentioned in the following sections.

6.1.1 Materials

Table 9: Used material.

Material	Order no.	Company
DG8 Cartridges for QX200/QX100 Droplet Generator	1864008	Bio-Rad, Laboratories, Hercules, CA, USA
DG8 Gaskets for QX200/QX100 Droplet Generator	1863009	Bio-Rad, Laboratories, Hercules, CA, USA
Eppendorf twin.tec® PCR Plate 96, semi-skirted, 250 µL, PCR clean	30128613	Eppendorf, Hamburg, Germany
LS Columns	130-042-401	Miltenyi, Bergisch Gladbach, Germany
PCR Plate Heat Seal, foil, pierceable	1814040	Bio-Rad, Laboratories, Hercules, CA, USA

6.1.2 Chemicals, reagents, cytokines

Table 10: Chemicals, reagents, cytokines.

Chemicals, reagents, cytokines	Order no.	Company
2-Propanol	CP41.4	Carl Roth, Karlsruhe, Germany
Alpha Medium	F 0915	Biochrome/Sigma-Aldrich, Munich
Anti-Mouse Ig, κ/Negative Control Compensation Particles Set	552843	BD Biosciences, San Jose, CA, USA
BD Cytofix/Cytoperm™ Fixation and Permeabilization Solution	554722	BD Biosciences, San Jose, CA, USA
BD Golgi Stop™ Protein Transport Inhibitor (containing Monensin)	554724	BD Biosciences, San Jose, CA, USA
BD Perm/Wash™ Perm/Wash Buffer	554723	BD Biosciences, San Jose, CA, USA
BD Propidium Iodide Staining Solution	556463	BD Biosciences, San Jose, CA, USA
Calcium chloride ($CaCl_2$)	CN92.2	Carl Roth, Karlsruhe, Germany
CellGenix® GMP SCGM, w/o phenol red	20806-0500	CellGenix, Freiburg im Breisgau, Germany
Chloroquine 25mM	C6628	Sigma-Aldrich, Munich, Germany
ddPCR™ Droplet Reader Oil	1863004	Bio-Rad, Laboratories, Hercules, CA, USA
Dimethyl sulphoxide (DMSO)	A994.2	Carl Roth, Karlsruhe, Germany
Droplet Generator Oil for Probes	1863005	Bio-Rad, Laboratories, Hercules, CA, USA
Dulbecco's Modified Eagle Medium (DMEM)	41965039	Thermo Fisher Scientific, Schwerte, Germany
Dulbecco's phosphate-buffered saline (DPBS)	141490-094	Thermo Fisher Scientific, Schwerte, Germany

eBioscience™ Cell Proliferation Dye eFluor™ 670	65-0840-85	eBioscience, San Diego, CA, USA
Ethanol, extra pure	5054.1	Carl Roth, Karlsruhe, Germany
Ethidium bromide solution, 1%	2218.1	Carl Roth, Karlsruhe, Germany
Fetal Bovine Serum (FBS), Qualified	10270-106	Thermo Fisher Scientific, Schwerte, Germany
Fluoresbrite YG Microspheres 6.00 µm	17156-2	Polysciences, Hirschberg an der Bergstraße, Germany
Formaldehyde (37%)	P733.2	Carl Roth, Karlsruhe, Germany
HEPES Buffer Solution (1M)	15630-056	Thermo Fisher Scientific, Schwerte, Germany
Horse Serum	H1270-500ML	Sigma-Aldrich, Munich, Germany
Human IL-15, premium grade	130-095-764	Miltenyi, Bergisch Gladbach, Germany
Human Serum Type AB (male) from male AB	H4522-20mL	Sigma-Aldrich, Munich, Germany
Interleukine-2 (Proleukin S)		Novartis Pharma, Basel, Switzerland
Ionomycin, calcium salt	I24222	Thermo Fisher Scientific, Schwerte, Germany
L-Glutamine 200mM (100X)	25030-024	Thermo Fisher Scientific, Schwerte, Germany
MACS Comp Bead Kit, anti-REA	130-104-693	Miltenyi, Bergisch Gladbach, Germany
Magnesium Chloride ($MgCl_2$) Solution 50 mM	B0510A	New England Biolabs GmbH, Frankfurt am Main, Germany
Penicillin-Streptomycin (10,000 U/mL)	15140-122	Thermo Fisher Scientific, Schwerte, Germany
PMA	P1585-1MG	Sigma-Aldrich, Munich, Germany
Polybrene (Hexadimethrine bromide)	H9268	Sigma-Aldrich, Munich, Germany
Protamine sulfate from salmon	P4020	Sigma-Aldrich, Munich, Germany
Recombinant Human Interleukin-2 (rhIL-2)	11340027	ImmunoTools, Friesoythe, Germany
Recombinant Human Interleukin-21 (rhIL-21)	11340213	ImmunoTools, Friesoythe, Germany
RPMI 1640 Medium w/0 Phenol red	F 1275	Biochrome, Berlin, Germany
RPMI Medium 1640 (1X)	21875-034	Thermo Fisher Scientific, Schwerte, Germany
Sodium Pyruvate 100mM (100X)	11360-039	Thermo Fisher Scientific, Schwerte, Germany
Triton X-100	3051.3	Carl Roth, Karlsruhe, Germany
TRIzol™ Reagent	15596026	Thermo Fisher Scientific, Schwerte, Germany
Trypsin-EDTA (0.05%), phenol red	25300-054	Thermo Fisher Scientific, Schwerte, Germany
UltraPure™ Agarose	16500-500	Thermo Fisher Scientific, Schwerte, Germany
Vectofusion-1	130-111-163	Miltenyi, Bergisch Gladbach, Germany

6.1.3 Kits, buffers, and enzymes

All restriction enzymes used were FastDigest™ from Thermo Fisher Scientific, Schwerte, Germany. Otherwise mentioned below.

Table 11: Kits, buffers, and enzymes.

Kit	Order no.	Company
Brilliant II QPCR Master Mix (2X)	600804-51	Agilent Technologies, La Jolla, CA, USA
Brilliant Multiplex QPCR Master Mix (2X)	600553-51	Agilent Technologies, La Jolla, CA, USA
CloneJET PCR Cloning Kit	K1232	Thermo Fisher Scientific, Schwerte, Germany
Direct-zol RNA Miniprep	R2050	ZymoResearch, Freiburg im Breisgrau, Germany
DNA Loading Dye (6X)	R0611	Thermo Fisher Scientific, Schwerte, Germany
DNAeasy Blood and Tissue Kit	69504	Qiagen, Hilden, Germany
DreamTaq DNA Polymerase (5 U/µL)	EP0702	Thermo Fisher Scientific, Schwerte, Germany
DreamTaq Green PCR Master Mix (2X)	K1081	Thermo Fisher Scientific, Schwerte, Germany
FastDigestion Green Buffer (10X)	B72	Thermo Fisher Scientific, Schwerte, Germany
FastStart Essential DNA Green Master	6402712001	Roche, Basel, Switzerland
GeneRuler™ 100 bp DNA Ladder	SM0242	Thermo Fisher Scientific, Schwerte, Germany
GeneRuler™ 1 kb DNA Ladder	SM0311	Thermo Fisher Scientific, Schwerte, Germany
Illustra Genomiphi™ V2 DNA Amplifikation Kit	25-6600-31	GE Healthcare, Munich, Germany
iTaq™ Universal Probes Supermix, 5mL	172-5135	Bio-Rad, Laboratories, Hercules, CA, USA
Maxima H Minus First Strand cDNA Synthesis Kit	K1652	Thermo Fisher Scientific, Schwerte, Germany
Mix & Go! E.coli Transformation Kit	3001	ZymoResearch, Freiburg im Breisgrau, Germany
NEBuilder® HiFi DNA Assembly Cloning Kit	E5520S	New England BioLabs, Frankfurt am Main, Germany
NK Cell Isolation Kit, human	130-092-657	Miltenyi, Bergisch Gladbach, Germany
NucleoBond Xtra Midi Kit for transfection grade plasmid DNA	740410.100	Macherey-Nagel, Düren, Germany
NucleoSpin Tissue, Mini Kit for DNA from cells and tissue	740952.50	Macherey-Nagel, Düren, Germany
Q5® High-Fidelity DNA Polymerase	M0491S	New England BioLabs, Frankfurt am Main, Germany
QIAprep Spin Miniprep Kit	27106	Qiagen, Hilden, Germany
QIAquick Gel Extraction Kit	28706	Qiagen, Hilden, Germany
RevertAid First Strand cDNA Synthesis Kit	K1621	Thermo Fisher Scientific, Schwerte, Germany
RNAse A, DNase and Protease-free	EN0531	Thermo Fisher Scientific, Schwerte, Germany
T4 DNA ligase	EL0011	Thermo Fisher Scientific, Schwerte, Germany
T4 DNA ligase buffer	B69	Thermo Fisher Scientific, Schwerte, Germany
TAE buffer (50X)	A1691,1000	A. Hartenstein, GmbH, Würzburg, Germany

6.1.4 Laboratory equipment

Standard laboratory equipment was used as provided by the Research Institute Children's Cancer Center Hamburg. Special equipment and Location/ Core Facility are mentioned in the following section.

Table 12: Special equipment.

Equipment	Company	Location/ Core Facility
BD FACSAria™ Fusion Cell Sorter	BD Biosciences, San Jose, CA, USA	Heinrich Pette Institute, FACS Core Facility
BD FACSCanto™ Cell Analyzer I	BD Biosciences, San Jose, CA, USA	Research Institute Children's Cancer Center Hamburg
BD FACSCanto™ II Cell Analyzer	BD Biosciences, San Jose, CA, USA	Heinrich Pette Institute, FACS Core Facility
BD LSRFortessa™ Flow Cytometer	BD Biosciences, San Jose, CA, USA	Heinrich Pette Institute, FACS Core Facility
MACS Multistand	Miltenyi, Bergisch-Gladbach, Germany	Research Institute Children's Cancer Center Hamburg
MACS Quant® Analyzer 10	Miltenyi, Bergisch Gladbach Germany	PSI Diagnostic Research Lab
NanoDrop™ 1000 Spectrophotometer	Thermo Fisher Scientific, Schwerte, Germany	Research Institute Children's Cancer Center Hamburg
QX200™ Droplet Generator	Bio-Rad, Laboratories, Hercules, CA, USA	Heinrich Pette Institute, Department Antiviral Strategies, Prof. Joachim Hauber
QX200™ Droplet Reader	Bio-Rad, Laboratories, Hercules, CA, USA	Heinrich Pette Institute, Department Antiviral Strategies, Prof. Joachim Hauber
Sorvall™ RC-5C Plus with the SS-34 Rotor	Thermo Fisher Scientific, Schwerte, Germany	Research Institute Children's Cancer Center Hamburg

6.1.5 Primary cells, cell lines, and their cultivation

Table 13: Primary cells, cell lines, and their cultivation.

Cells	Origin	Characteristics	Manufacturer/ kindly provided by
721.221 and HLA-C variants	B lymphocyte; Epstein-Barr virus transformed	Suspension, round large single cells	Dr. Christian Körner, Prof. Dr. Altfeld, Virus Immunology, Heinrich Pette Institute
CCRF-CEM	Human peripheral blood T lymphoblast from acute lymphoblastic leukemia (T-ALL)	Adherent epithelioid cells monolayer and single round cells in suspension	DSMZ ACC240
HEK293T	Human embryonic kidney cells from fetus	Adherent, fibroblastic epithelial cells growing as monolayer	DSMZ ACC635

Jurkat	Human peripheral blood T lymphocyte from acute T cell leukemia (T-ALL)	Suspension, round cells single or in small clumps	PD Dr. Peter Brossart, former University Medical Center, Tübingen
K562	Human bone marrow lymphoblast from chronic myelogenous leukemia (CML)	Suspension, round large single cells	Dr. Gunter Kerst, former University Medical Center, Tübingen
MHH-Call-2	Human B cell precursor leukemia from acute lymphoblastic leukemia (cALL)	Suspension, single, small round cells	DSMZ ACC341
MHH-Call-3	Human B cell precursor leukemia from pre-B cell acute lymphoblastic leukemia (ALL)	Suspension, single, small round cells	DSMZ ACC339
NK92-MI	Human peripheral blood cell natural killer cell from malignant non-Hodgkin's lymphoma	Suspension, grow in multicell aggregates, modified to express IL-2	NK-92® MI (ATCC® CRL-2408™)
Primary NK cell	Human peripheral blood natural killer cell	Large granular cells	Healthy volunteers*
REH	Human B cell precursor leukemia	Suspension, small, round single cells	DSMZ ACC22

* either from buffy coats or from parental donors in compliance with the regulations of the Institutional Review Board decision PV4296

6.1.6 Medium and buffer composition

Utilized media consisted of the indicated ingredients. Indicated supplements were added to the basis medium. Cell culture was performed in a laminar air flow cabinet under sterile conditions.

Table 14: Media composition and usage.

Medium name	Basis medium	Supplements	Used for
721.221	RPMI 1640	10% FBS h. i.* 1% P/S**	Cultivation of 721.221 cells
CCRF-CEM, REH and Jurkat	RPMI 1640	10% FBS h. i.*	Cultivation of CCRF-CEM, REH and Jurkat
FACS buffer	PBS	2% FBS h. i.*	Section 6.4.9
Freezing	FBS (h. i.)*	20% DMSO	Freezing of cells section
HEK293T	DMEM	10% FBS h. i.* 1% HEPES 1% Sodium pyruvate, 1% P/S**	Cultivation of HEK293T
K562	RPMI 1640	10% FBS h. i.* 1% L-Glutamine 1% P/S**	Cultivation of K562

MACS buffer	PBS	5% autologous plasma 0.2% EDTA	MACS isolation of primary human NK cells
MHH-Call2, MHH-Call3	RPMI 1640	20% FBS h. i.*	Cultivation of MHH-Call2 and MHH-Call3
NK assay	RPMI w/o phenol red	5% FBS h. i.* 1% L-Glutamine 1% Na-pyruvate	Degranulation and killing assay
NK cell overnight activation	RPMI w/o phenol red	5% autologous plasma 1% L-Glutamine 1% P/S**	Overnight activation of primary NK cells
NK92-MI	Alpha-Medium	12.5% FBS h. i.* 12.5% horse serum h. i.* 1% L-Glutamine 1% P/S**	Cultivation of NK92-MI
Primary NK cell cultivation	Cell Genix SCGM	10% human male AB serum or 5% autologous plasma h. i.*	Cultivation of primary NK cells
Stop solution	RPMI w/o phenol red	10% FBS h. i.*	Section 6.4.8

*FBS was heat inactivated (h. i.) 30 min at 56°C, ** P/S = Penicillin/Streptomycin

Table 15: In house prepared buffer and composition.

Buffer	Components	Order no.	Manufacturer
HBSS (2X) precipitation buffer	275.8 mM $CaCl_2$	HN04.1	Carl Roth, Karlsruhe, Germany
	10.2 mM KCl	104936	Merck, Darmstadt, Germany
	1.41 µM Na_2HPO_4	K300.2	Carl Roth, Karlsruhe, Germany
	42 mM HEPES	91053	Carl Roth, Karlsruhe, Germany
	1.1 mM Glucose	X997.2	Carl Roth, Karlsruhe, Germany
	pH 7.05, adjusted using NaOH		

Buffer was prepared using ddH_20

6.1.7 Antibodies for FACS staining

Antibodies were used for the respective FACS experiments: KIR phenotyping panel 1[1], KIR phenotyping panel 2[2], degranulation[3], cytotoxicity assay[4], characterization of fetal cells background[5].

Table 16: Antibodies for FACS staining.

Antigen/label	Clone	Order no.	Company	Volume 100 µL	Used for
Alexa Fluor® 700 Mouse Anti-human CD3	UCHT1	561027	BD Biosciences, San Jose, CA, USA	2.5	2
anti-KIR2DL3/CD158b2	180701	15763023	R&D Systems™, Minneapolis, MN, USA	1	1
APC anti human CD133 Antibody	clone 7	372805	Biolegend, San Diego, CA, USA	5	5

BB515 mouse anti human CD158b	CH-L	566053	BD Biosciences, San Jose, CA, USA	2	2
BB515 mouse IgG2b,k Isotype control	27-35	564510	BD Biosciences, San Jose, CA, USA	2	2
BUV395 Mouse Anti Human CD16	3G8	563785	BD Biosciences, San Jose, CA, USA	0.5	3
BV605 Mouse Anti-Human CD158b	CH-L	743453	BD Biosciences, San Jose, CA, USA	3	3
BV605 Mouse Anti-Human CD158e1 (NKB1)	DX9	742981	BD Biosciences, San Jose, CA, USA	1	3
BV650 Mouse Anti-Human KIR-NKAT2	DX27	745296	BD Biosciences, San Jose, CA, USA	1	3
BV711 Mouse Anti-Human CD56	NCAM16.2	563169	BD Biosciences, San Jose, CA, USA	0.5	3
CD107a (LAMP-1)-PE-Vio770, human	REA792	130-111-622	Miltenyi, Bergisch Gladbach, Germany	1	4
CD158a/h (KIR2DL1/DS1) -VioBlue, human	11PB6	130-095-233	Miltenyi, Bergisch Gladbach, Germany	3	1,3
CD158b (KIR2DL2/DL3)-APC-Vio770, human	REA1006	130-116-956	Miltenyi, Bergisch Gladbach, Germany	1	2
CD158b (KIR2DL2/DL3)-PE	DX27	130-099-397	Miltenyi, Bergisch Gladbach, Germany	1	1
CD158b (KIR2DL2/DL3)-PerCP	DX27	130-099-700	Miltenyi, Bergisch Gladbach, Germany	3	2
CD158b2 (KIR2DL3)-PE	REA 147	130-100-122	Miltenyi, Bergisch Gladbach, Germany	1	2
CD158b2 (KIR2DL3)-PerCP-Vio700, human	REA 147	130-100-120	Miltenyi, Bergisch Gladbach, Germany	1	3
CD158e (KIR3DL1), human, PE	DX9	130-092-473	Miltenyi, Bergisch Gladbach, Germany	1	1
CD158e/k (KIR3DL1/DL2) -PE-Vio615, human	REA970	130-116-286	Miltenyi, Bergisch Gladbach, Germany	2.5	3
CD158e/k (KIR3DL1/DL2)-FITC, human	REA970	130-116-280	Miltenyi, Bergisch Gladbach, Germany	2.5	2
CD158e1/e2 KIR3DS1/L1 unconjugated	Z27.7.3	PN IM2748	Immunotech, Marseille, France	1	1
CD158e1/e2-APC-Vio770	REA168	130-100-122	Miltenyi, Bergisch Gladbach, Germany	1	3
CD158f (KIR2DL5)-APC-VIO770	UP-R1	130-105-583	Miltenyi, Bergisch Gladbach, Germany	0.5	2

CD158i (KIR2DS4)-FITC	REA840	130-114-771	Miltenyi, Bergisch Gladbach, Germany	2	1
CD158i (KIR2DS4)-PE-Vio615, human	REA860	130-114-780	Miltenyi, Bergisch Gladbach, Germany	2.5	3
CD158i (KIR2DS4)-PE-Vio770, human	JJC11.6	130-099-963	Miltenyi, Bergisch Gladbach, Germany	2.5	3
CD158i (KIR2DS4), anti-human, PE	JJC11.6	130-092-680	Miltenyi, Bergisch Gladbach	1	1
CD159a (NKG2A)-PE-Vio770, human	REA110	130-114-093	Miltenyi, Bergisch Gladbach	1	3
CD16-APC, human	REA423	130-106-763	Miltenyi, Bergisch Gladbach	2	-
CD3-Vioblue, human	REA	130-114-519	Miltenyi, Bergisch Gladbach	2	-
CD56-FITC, human	REA196	130-114-740	Miltenyi, Bergisch Gladbach	1	-
CD58i (KIR2DS4)-PE	JJC11.C	130-099-698	Miltenyi, Bergisch Gladbach	2	1
FITC anti-human CD107a	LAMP-1/H4A3	328606	Biolegend, San Diego, CA, USA	1	3+4
FITC anti-human Lineage Cocktail (CD3, CD14, CD16, CD19, CD20, CD56)	UCHT1, HCD14, HIB19, 2H7, HCD56	348701	Biolegend, San Diego, CA, USA	5	5
Human KIR2DL1/KIR2DS5 PE	143211	FAB1844P-025	R&D Systems™, Minneapolis, MN, USA	5	5
Human KIR3DL2/CD158k PE	539304	FAB2878P-025	R&D Systems™, Minneapolis, MN, USA	3	1
mouse IgG2a-PerCP	-	130-099-190	Miltenyi, Bergisch Gladbach	1.5	1
PE/Cy7 anti-human CD107a	LAMP-1	328618	Biolegend, San Diego, CA, USA	2	4
PE/Cy7 anti-human CD3	HIT3a	300316	Biolegend, San Diego, CA, USA	2	5
Pe/Cy7 anti-human CD56	NCAM	318318	Biolegend, San Diego, CA, USA	2	5
PE/Cyanine7 Anti-mouse IgG1 Antibody	RMG1-1	406613	Biolegend, San Diego, CA, USA	1	1
PerCP anti-human CD16	3G8	302030	Biolegend, San Diego, CA, USA	2	5
REA control (S)-FITC	-	130-104-610	Miltenyi, Bergisch Gladbach	2	1
REA control (S)-PE	-	130-104-612	Miltenyi, Bergisch Gladbach	2	1
Zombie Yellow™ Fixable Viability Kit	-	423103	Biolegend, San Diego, CA, USA	0.01	2

*Phenotyping of FM samples was performed with the following panels: FM samples 1 - 28 with panel 1 and samples 29 - 62 with panel 2.

6.2 Molecular biology

6.2.1 Primers

All primers were ordered lyophilized at Metabion and reconstituted at 100 µM in ddH_2O. Ten µM working solution was prepared. All primers were stored at - 20 °C.
Lists of primer sequences for the respective methods: KIR genotyping (8.2.1), cloning KIRs from cDNA and sequencing primers (8.2.3), HLA-C PCR (8.2.2), marker selection, and digital PCR primers and probes (8.2.4) are provided in appendix 8.

6.2.2 Plasmids

Table 17: Plasmids.

Plasmid	Provided by
LeGO-iG2-wpre	(*304*)
LeGO-iCerulean-wpre	(*304*)
pAlpha.SIN(noTATA)SFFV.eGFP	PD Dr. Kerstin Cornils. University Medical Center Hamburg-Eppendorf
pA.SIN(noTATA)SFFV.2DL1.iCer-wpre	Cloned during this work
pA.SIN(noTATA)SFFV.2DL2.iCer-wpre	Cloned during this work
pA.SIN(noTATA)SFFV.2DS1.ieGFP-wpre	Cloned during this work
pA.SIN(noTATA)SFFV.2DS2.ieGFP-wpre	Cloned during this work
pcDNA3.Alpha.gagpol.co (alpharetroviral gag/pol)	PD Dr. Kerstin Cornils, University Medical Center Hamburg-Eppendorf
p.LeGo.SFFV.2DL1.iCer-wpre	Cloned during this work
p.LeGo.SFFV.2DL2.iCer-wpre	Cloned during this work
p.LeGo.SFFV.2DS1.iCer-wpre	Cloned during this work
p.LeGo.SFFV.2DS2.iCer-wpre	Cloned during this work
pMDLg-pRRE (lentiviral gag/pol)	Stock Research Institute Children's Cancer
pRSV-Rev	Stock Research Institute Children's Cancer
pCMV-VSV-G	Stock Research Institute Children's Cancer
phCMV-RD114/TR	Stock Research Institute Children's Cancer

6.2.3 Cloning KIRs from cDNA into lenti and alpharetroviral vectors

KIRs were cloned from human cDNA. Donors were characterized for their KIR genotype (section 4.2.4) and phenotype (section 8.3.2). NK cells from donors genotypically and phenotypically positive for the respective receptor were isolated (section 6.4.6) and RNA was extracted (section 6.2.4). cDNA was generated using the Maxima H Minus First Strand cDNA Synthesis Kit following the manufacturer's instructions and used for a nested PCR. Nested PCR was used to increase the PCR product. For each KIR, two sets of primers were designed that flank the respective KIR (primer sequences are provided in section 8.2.3). Two consecutive PCR reactions are performed with a first primer pair binding outside and the

second pair binding closer to the gene of interest. The PCR composition and conditions are depicted in Table 18. After the first PCR, a second PCR was performed. In the second reaction, one µL from the first reaction was used as template.

Table 18: Nested PCR reaction 1 and 2 composition and conditions. (A) PCR composition and (B) PCR conditions.

A. Reaction 1 and 2

Component	Final concentration	25 µL reaction
Q5 reactions buffer (5X)	100 µM	5 µL
dNTPs (10mM each)	200 µM	0.5 µL
Forward primer (10 µM)	0.5 µM	1.25 µL
Reverse primer (10 µM)	0.5 µM	1.25 µL
Q5 High GC enhancer (5X)	1X	5 µL
Q5 High-fidelity polymerase	0.2 U/µL	0.25 µl
*	-	1 µL
Nuclease-free water	-	to 25 µL

B. PCR conditions

Initial denaturation	98°C	30 sec	
Denaturation	98°C	10 sec	35x
Annealing	**50 - 72°C	30 sec	
Denaturation	98°C	10 sec	
Extension	72°C	30 sec	
Final Extension	72°C	10 min	
Hold	4°C	∞	

*Reaction 1: 1 µL cDNA, reaction 2: 1 µL from nested PCR reaction 1

**Annealing temperature was adjusted for each primer pair

PCR products were analyzed on a 1% agarose gel with EtBr and lanes with the expected sizes were cut out and purified using the QIAquick Gel Extraction Kit from Qiagen following the manufacturer's instructions. PCR products were eluted in 20 - 30 µL ddH20. DNA concentration was determined using a NanoDrop™ Microvolume Spectrophotometer. PCR products were subcloned into the pJET1.2/blunt vector following the manufacturer's instructions for the CloneJET PCR Cloning Kit followed by transformation into JM107-competent *E.coli (see 6.2.3.2*). Bacteria colonies were grown and analyzed for the insert as described in the following sections. For insertion of the gene of interest into either the LeGo-iG2-wpre or the LeGo-Cerulean-wpre vector Gibson Assembly was used. For this purpose, overlapping oligo primers were designed according to the manufacturer's instructions and used to amplify the insert from the pJET1.2 vector, which contains the insert. LeGo vectors were linearized with the restriction enzyme *Not*I (see 6.2.3.4). Gibson Assembly was performed following the manufacturer's instructions.

6.2.3.1 Colony PCR

Colony PCR was performed to analyze colonies for the presence of insert. A master mix was prepared (Table 19, A) and distributed to PCR stripes provided on ice or in a cooled block. Either a primer pair provided by the CloneJET PCR Cloning Kit or a self-designed primer pair, flanking the gene of insert, was used. Subsequently, 4 - 6 colonies were picked with a pipette tip, dipped in the provided tubes and transferred into 12 mL bacteria culture tubes containing

3 mL of LB medium and 1 mg/mL ampicillin followed by incubation over night at 37°C shaking. Following PCR, (conditions are depicted in Table 19, B,) the product was analyzed on a 1% agarose gel containing EtBr.

Table 19: PCR composition and conditions for colony PCR. (A) PCR composition and (B) PCR conditions.

A. PCR composition		
Component	pJET primer	Self-designed primer
DreamTaq Master (2X)	10 µL	10 µL
Forward primer (10 µM)	0.4 µL	1 µL
Reverse primer (10 µM)	0.4 µL	1 µL
DNA from bacteria colony	-	-
Nuclease-free water		to 20 µL

B. PCR conditions			
Initial denaturation	95°C	30 sec	
Denaturation	94°C	30 sec	
Annealing	*60°C	30 sec	25x
Extension	72°C	1 sec	
Final extension	72°C	5 min	
Hold	4°C	∞	

*60°C was used for primers provided by the CloneJET PCR Cloning Kit otherwise annealing temperature was calculated using an online tool (Table 32).

6.2.3.2 Transformation, re-transformation, inoculation of Mini and Maxi preparations

Re-transformation was performed to insert circular plasmid DNA for amplification into chemical competent bacteria. Chemical competent bacteria were prepared in house following the manufacturer's instructions of the *Mix & Go! E.coli* Transformation Kit and stored in 80 - 100 µL aliquots at - 80°C. Chemical competent bacteria were thawed on ice. For re-transformation 100 - 500 ng plasmid DNA, for transformation 2 - 10 µL of the ligation mixture, was added and the tubes were flicked and incubated for 30 min, on ice. After incubation, bacteria were either plated on agar plates containing 1 mg/mL ampicillin or transferred directly into 13 mL bacteria tubes containing 2 - 3 mL LB medium with 1 mg/mL ampicillin and incubated overnight at 37°C shaking. For Maxi preparations, either 1 - 3 mL medium from the Mini culture was transferred into Maxi flask containing 100 mL LB medium with 1 mg/mL ampicillin or a re-transformation was performed. The culture was incubated for 4 - 6 hours and then transferred into the Maxi flasks followed by incubation overnight, at 37°C, shaking.

6.2.3.3 DNA extraction from Mini and Maxi cultures

DNA was extracted either from Mini cultures of 2 - 3 mL LB medium or from Maxi cultures which consisted of 100 mL LB medium. DNA extraction from Mini cultures was performed following the manufacturer's instructions of the QIAprep Spin Miniprep Kit (Qiagen). DNA was eluted in 50 µL ddH20. Maxi preparations were performed following the manufacturer's instructions of the NucleoBond Xtra Midi Kit for transfection grade plasmid DNA (Macherey-Nagel). An additional centrifugation step was included after neutralization of cell breakup, to decrease the amount of cell debris on the filter tip. After precipitation, DNA was reconstituted

in 200 µL ddH20, DNA content was determined using a NanoDrop™ Microvolume Spectrophotometer and adjusted to 500 or 1000 ng/µL and stored at - 20°C.

6.2.3.4 Digestion and control digestion

A digestion was performed to cut out a fragment from a vector or open a vector backbone for insertion of a fragment. A control digestion was performed to analyze samples for the presence of insert. For control digestion, 500 - 1000 ng plasmid DNA was mixed with 0.5 µL of the respective FastDigest™ enzyme and 5 µL 10x FastDigestion buffer in a total volume of 20 µL adjusted with ddH_2O. For digestion of a vector, 3 - 5 µg plasmid DNA were used and reagents were scaled up. Samples were incubated at 37°C for 15 - 30 min, if necessary, digestion enzymes were inactivated at 65°C for 10 min. Afterwards, samples were analyzed on a 1% agarose gel containing EtBr.

6.2.3.5 Sequencing

DNA samples were sequenced for verification of correct base pair sequences of the insert. Therefore, one µg plasmid DNA was mixed with 30 ng sequencing primer and adjusted to 15 µL with ddH_2O. Sequencing was performed by Microsynth Seqlab, Göttingen, Germany. Sequencing results were aligned to *in silico* generated sequences using the software SnapGene®.

6.2.4 DNA and RNA extraction from primary cells and cell lines

DNA from primary human cells and cell lines was extracted using the DNA Blood and Tissue Kit (Qiagen) or the NucleoSpin® Tissue Kit (Macherey-Nagel) following the manufacturer's instructions. RNAse A treatment was performed with 10 mg/mL RNAse A following the manufacturer's instructions. DNA was eluted in 50 µL Aqua Braun and to increase DNA concentration re-eluted using 30 µL of the flow-through. DNA content was determined using a NanoDrop™ Microvolume Spectrophotometer.

For RNA isolation, 1 - 5 x 10^6 cells were transferred into an Eppendorf microcentrifuge tube and reconstituted in 650 µL TRIzol™ Reagent and stored at - 80°C. Further along the line, RNA was extracted using the Direct-zol RNA Miniprep Kit (ZymoResearch) following the manufacturer's instructions. RNA was eluted in 50 - 100 µL RNAse-free H_2O, analyzed at the NanoDrop™ Microvolume Spectrophotometer and stored at - 80°C.

6.2.5 cDNA synthesis

Purified RNA was used as template for *in vitro* cDNA synthesis. One to five µg RNA were used as template and cDNA was generated using the Maxima H Minus First Strand cDNA Synthesis

Kit following the manufacturer's instructions. cDNA was either used directly or was stored at - 20°C.

6.2.6 KIR genotyping

To determine the KIR receptors repertoire, KIR genotyping with sequence specific primers was performed (*363, 364*). Each primer pair flanks a specific region for one distinct KIR. KIR genotyping was performed by TaqMan-based real-time PCR (RT-PCR) using 18 sequence-specific primer pairs (appendix 8.2.1). For RT-PCR, SYBR Green I was used that binds unspecific to any double stranded DNA by intercalating between the DNA bases. These include the KIR specific amplicons, low level unspecific amplicons and primer dimers. For discrimination of KIR genes and unspecific binding the melting temperature (Tm) was determined and is depicted in the appendix Table 33. Each reaction was prepared in a 96-well plate as depicted in Table 20, A. The plate was mask with plastic foil, centrifuged at 900 x g, for 3 min, at RT and transferred into a RT-PCR cycler. PCR conditions are depicted in Table 20, B.

Table 20: RT-PCR composition and conditions for KIR genotyping. (A) PCR composition and (B) PCR conditions.

A. PCR composition	
Component	(µL)
2 ng genomic DNA	0.2
SYBR Green Master mix (2X)	5
1 nm of each SSP-Primer-pair (Working stock 10 nm)	1
V_{Total}	10

B. PCR conditions			
Initial denaturation	95°C	10 min	
Denaturation	95°C	15 sec	40x
Annealing	62°C	60 sec	
Melting curve	95°C	10 min	
Hold	4°C	∞	

After RT-PCR the plate was centrifuged at 900 x g, for 3 min, at RT and 1 µL 10x loading dye was added per well. The PCR products were analyzed on a 3% agarose gel containing EtBr. Expected size of the products for the respective KIR and the expected Tm and range of Tm after RT-PCR analysis are depicted in 8.2. Samples with obvious products at the desired size and Tm in the expected range were considered as positive for the respective KIRs. If a product was missing or Tm was out of range the KIR was considered as absent.

6.2.7 HLA-C genotyping

HLA-C typing was performed as described by Frohn *et al. (365).* Here, SSP-primer-pairs were used to amplify the specific region of interest. The reverse primer bound to an HLA-Cw specific sequence and the forward primer bound to the alternate sequence including amino acid position 80. HLA-C1 is characterized by alanine at position 80, while HLA-C2 has a lysine. Two PCR reactions were prepared for reach samples, one of which contained the NK1-specific

primer for HLA-C2 and the other the NK2-specific primer for HLA-C1. CRP was added as positive control. Primer sequences are depicted in 8.2. PCR composition and conditions are depicted in Table 21.

Table 21: PCR composition and conditions for HLA-C genotyping. (A) PCR composition. Two reactions were prepared for each sample: one with forward and reverse primers for NK1 and a second one with primer pairs for NK2. (B) PCR conditions.

A. PCR composition

Component	Stock	1x Reaction
Genomic DNA	10 ng/µL	3 µL
DreamTag master mix	10X	10 µL
NK1 or NK2 working stock	100 nM (each)	1 µL
CRP working stock	100 nM (each)	0.5 µL
H_20	to 20 µL	5.5 µL
V_{Total}	20 µL	20 µL

B. PCR conditions

95°C	10 min	
95°C	10 sec	10x
65°C	30 sec	
72°C	30 sec	
95°C	10 sec	25x
58°C	30 sec	
72°C	30 sec	
72 °C	5 min	
4°C	∞	

After PCR, products were analyzed on a 1% agarose gel containing EtBr. Expected size for the HLA-C products is 139 bp and for the CRP control 440 bp. Presence of the expected HLA-C product allows for determination of the HLA-C group.

6.3 Methods for microchimerism analysis

6.3.1 Genomiphi amplification of DNA

Maternal and filial DNA was a limited factor during this work. Since over 9,000 ng of DNA are necessary for the marker selection (6.3.2) DNA was amplified using the Illustra Genomiphi™ V2 DNA Amplifikation Kit. For generation of single-stranded DNA, 1 µL DNA (10 ng/µL) was mixed with 9 µL sample buffer and incubated for 3 min at 95°C in a thermocycler. Nine µL reaction buffer and 1 µL Phi29 DNA polymerase were added and the reaction was further incubated at 65°C for 90 min followed by heat inactivation of the enzyme at 95°C for 5 min. Amplified DNA was measured at the NanoDrop™ Microvolume Spectrophotometer, adjusted to 15 ng/µL with ddH_2O and stored at - 20°C until marker selection.

6.3.2 Marker selection

To distinguish between maternal and filial DNA, bi-allelic short insertion deletion polymorphisms were used as described (*113, 115*). These polymorphisms are named “markers” during this study. A suitable marker was identified using RT-PCR. For each marker, a probe was designed that specifically binds to the region of interest and was labeled with a fluorescence dye. This probe was flanked by specific forward and reverse primer. Amplification

of the region leads to hydrolysis of the probe and release of the fluorescence reporter. Marker selection was performed in six independent reactions each containing 5 - 6 markers (Table 22). Reaction composition and conditions are depicted in Table 23 - 25. All reactions were prepared in duplicates.

Table 22: Run order for marker selection.

Run	Marker						Instrument
1	7b (FAM) +HCK (VIC)	1b	7a	9b	mbl	4a	Stratagene, MX300, Agilent Technologies, La Jolla, CA, USA
2	06	5b	8b	03	10b	11a	7900HT Fast real-time PCR, Applied Biosystems™, Thermo Fisher Scientific, Schwerte, Germany
3	1a	10a	GSTT	8a	9a	9a	
4	12a	12b	13a	13b	24a	24b	
5	16a	16b	17a	17a	17b	22b	
6	5a	11b	14a	14b	Y	-	

Table 23: PCR composition marker selection run 1, except mbl.

Component	1x Reaction (µL)	7b with HCK (µL)	1b, 7a, 9b, 4a (µL)
2X Brilliant II QPCR Master Mix	12.5	12.5	12.5
Forward primer	0.25	0.25	0.25
Reverse primer	0.25	0.25	0.25
Probe (FAM labeled)	0.25	0.25	0.25
HCK forward	0.25	0.25	-
HCK reverse	0.25	0.25	-
HCK probe (VIC)	0.25	0.25	-
H_2O	1 / 1.75	1	1.75

Table 24: PCR composition marker selection run 1 mbl and PCR conditions for PCR run 1. (A) PCR composition and (B) PCR conditions.

A. PCR composition

Component	1x Reaction mbl (µL)
2X Brilliant Multiplex QPCR Master Mix	12.5
Forward primer	0.5
Reverse primer	0.5
Probe	0.25
H_2O	1.25

B. PCR conditions run 1

95°C	10 min	
95°C	15 sec	45x
60°C	60 sec	
4°C	∞	

After PCR, the cycle threshold (CT) was calculated. The CT was defined as cycle number in which a significant increase of the fluorescent signal was detectable for the first time (*115*). Samples with a CT between 25 - 30 were considered as positive, while samples with a CT above 30 were considered negative for the respective marker. To be suitable for determination of filial cells within maternal background cells, a marker needed to be positive for the child and

negative for the mother. For TM determination the marker needed to be positive for the older sibling and negative for the younger sibling. As soon as a suitable marker was identified the marker selection was terminated.

Table 25: PCR composition and conditions marker selection run 2 - 6. (A) PCR composition and (B) PCR conditions.

A. PCR composition

Component	1x Reaction (µL)
iTaq™ Universal Probes Supermix, 5mL	12.5
Forward primer	0.25
Reverse primer	0.25
Probe	0.25
H_2O	1.75

B. PCR conditions run 2 - 6

95°C	3 min	
95°C	15 sec	45x
60°C	60 sec	
4°C	∞	

6.3.3 Digital droplet PCR

With the QX200™ Droplet Digital PCR System, a TaqMan based digital droplet PCR (ddPCR) was performed to quantify the level of fetal cells in the maternal background cells. In ddPCR a single PCR reaction is separated into up to 20,000 nanoliter-sized droplets using a water-oil emulsion technology combined with a microfluidics system that results in each droplet containing ideally at least one template of target DNA. Amplification of the template occurs in each separate droplet. The PCR reaction contains a primer pair and a fluorescent labeled hydrolysis probe, which bind to the sequence of interest. The probe binds to the sequence intermediate the primers and contains a fluorescence reporter (either FAM or HEX) at the 5'-end, and a black hole quencher 1 (BHQ1) at the 3' end. In close proximity, the quencher suppresses the fluorophore's emission. During amplification, the 5' exonuclease activity of the TaqMan polymerase leads to hydrolysis of the fluorophore and the fluorescence can be detected. An exact quantification is possible due to inclusion of a housekeeping gene in a duplex reaction. With this duplex reaction, here named quantification reaction, the total copies of input DNA are counted. Following PCR an end point analysis is performed, in which each droplet is analyzed for fluorescence. Poisson statistics enables quantification of the absolute number of detected copies of interest (here, filial or older sibling's DNA) in the total amount of background copies (here, maternal or younger sibling's DNA)(*366*).

Table 26: 20x primer and probe master mix composition for ddPCR.

Component	Concentration 1x [µM]	20x master mix in V_{total} 250 µL [from 100 µM stock]
Forward primer	0.9	45
Reverse primer	0.9	45
Probe	0.25	12.5
H_20	-	147.5

For rare event detection it is necessary to set up two separate reactions. I. An analysis reaction and II. a quantification reaction, as depicted in Figure 6, B. In the analysis reaction at least 2 µg genomic DNA was distributed at 500 ng DNA/well. The quantification reaction, which was prepared in duplicates, consisted of 100 ng DNA/well and additionally a master mix detecting the diploid HCK gene for determination of the total amount of input DNA. A 20x master mix with respective probes and primers for each marker was prepared as depicted in Table 26. PCR composition is depicted in Table 27, A. Optimized parameters for the respective markers (section 4.1.1) are summarized in Table 28. The PCR mixture was compartmentalized using the QX200™ Droplet Generator following the manufacturer's instructions.

Table 27: PCR reaction composition and conditions for ddPCR. *0: no addition of $MgCl_2$, 0.88 µL: 2 mM $MgCl_2$ and 1.76 µL: 4 mM $MgCl_2$. (A) PCR composition and (B) PCR conditions.

A. composition			
Component	Stock	Analysis reaction (µL)	Quantification reaction (µL)
Genomic DNA	100 ng/µL	5	1
ddPCR Supermix for Probes (no dUTP)	2X	11	11
Master mix sequence of interest (FAM-BHQ1)	20X	1.1	1.1
Master mix reference gene (HEX-BHQ1)	20X	-	1.1
$MgCl_2$	50 nM	*	*
E*co*RI or *Hin*dIII	100,000 U/mL	0.5	0.5
H_20	-	ad 22	ad 22

B. PCR conditions		
Ramp rate 1.5 °C/s		
95°C	10 min	
94°C	10 sec	39x
60°C	60 sec	
98°C	10 min	
12°C	∞	

The generated water-oil emulsion droplets were transferred to a 96-well PCR plate, which was sealed followed by amplification in a thermal cycler with the PCR conditions depicted in Table 27, B. Afterwards, droplets were analyzed for fluorescence signals FAM and HEX simultaneously using the QX200™ Droplet Reader following the manufacturer's instructions. Data was processed using the QuantaSoft software, and the mean concentration of the target sequence (copies per 20 µL) was calculated from the software that incorporates Poisson statistics. To separate positive and negative HEX positive droplets a threshold was applied manually, and total background input copies were calculated from the quantification wells as follows:

$$\text{Total background copies} = \text{mean}\left(20\ \frac{\mu\text{L}}{\text{copies}}\right) HEX \times 5 * \times n$$

*dilution factor; n = number of analysis reactions

For analysis reactions, to separate FAM positive and negative droplets a threshold was applied manually. Then copies (per 20 µL) were totaled, the standard deviation was calculated and

added two times to the sum of FAM positive copies. This calculation includes the 95% confidence interval of false positives.

To determine the background level, the same number of wells and reactions was prepared with DNA from a cell line negative for the respective marker. The background level and FM level were calculated as follows:

1. $Background\ level\ marker = total\ background\ copies \div sum\ FAM\ \left(20\ \frac{\mu L}{copies}\right) + 2SD$
2. $Background\ level\ FM = total\ background\ copies \div sum\ FAM\ \left(20\ \frac{\mu L}{copies}\right) + 2SD$

Samples were only considered as positive, if the detected FM was higher as the measured background level from the marker in the negative cell line.

DNA from the child (or older sibling) was used as positive control. The positive control duplex reaction supplies the information, if the sequence of interest is haploid or diploid in the child/older sibling and is considered for the following FM/TM calculation. If the marker is haploid, the total background copies have not been divided by two. FM calculation is exemplarily depicted for a haploid marker. Microchimerism level was calculated as copies per 100,000 background copies.

$$microchimerism\ level = \frac{(total\ background\ copies\ \div 2)}{sum\ FAM\ \left(20\ \frac{\mu L}{copies}\right)}$$

Table 28: Parameters for ddPCR reaction.

Marker	Negative control	Positive cell line for dilution series	$MgCl_2$ (mM)	Digestion enzyme
03	MHH-Call2	K562	0	*Hind*III
10a	HEK293T	K562	4	*Eco*RI
10b	MHH-Call2	K562	0	*Eco*RI
11a	MHH-Call2	K562	2	*Eco*RI
12b	HEK293T	K562	0	*Eco*RI
16a	MHH-Call2	K562	0	*Eco*RI
17b	K562	HEK293T	2	*Eco*RI
1b	REH	K562	0	*Eco*RI
24b	K562	CCRF-CEM	2	*Eco*RI
4a	CCRF-CEM	K562	0	*Eco*RI
4b	K562	CCRF-CEM	2	*Eco*RI
5b	MHH-Call2	K562	0	*Hind*III
6	K562	CCRF-CEM	0	*Eco*RI
7a	NK92-MI	MHH-Call3	2	*Eco*RI
7b	REH	K562	4	*Eco*RI
8b	MHH-Call2	K562	2	*Eco*RI
9b	K562	CCRF-CEM	0	*Eco*RI
mbl	NK92-MI	MHH-Call3	2	*Eco*RI
Y	K562	Jurkat	2	*Eco*RI

6.4 Cell biology

6.4.1 General annotations

Incubator conditions: temperature 37°C, CO_2: 5%, humidity: 95%.
Centrifugations: general centrifugation was performed at 300 x g, 5 min, RT, if otherwise mentioned.

6.4.2 Cell counting

Cells were counted using a Neubauer hemocytometer. Cells were carefully resuspended to obtain a single cell suspension. Ten µL of cell suspension were diluted with trypan blue from this mixture 10 µL were transferred into a counting chamber and four big squares were counted. Cell number was calculated as follows:

$$total\ cell\ number\ = \frac{number\ of\ cells\ in\ 4\ big\ squares}{4} \times 10.000\ \times\ dilution\ factor \times total\ volume\ cell\ supension\ (mL)$$

6.4.3 Cryopreservation of cells

Cell lines were harvested, counted, centrifuged, and resuspended in the respective medium mentioned below. Primary leukemic blasts were isolated using Biocoll density centrifugation section 6.4.6. Cells were washed twice using PBS and counted. Five to ten aliquots containing 2 x 10^7 cells or more were prepared. The cell suspension was mixed 1:1 (v:v) with cryopreservation medium (FBS with 20% DMSO). Tubes were inverted and immediately frozen in isopropanol-containing cryopreservation boxes at - 80°C. This guarantees a gently cooling down at 1°C per min.

Table 29: Cryopreservation of cells.

Cell type	Medium	Cell density per tube
Cell line	Respective complete medium	1 - 5 x 10^6
PBMC	RPMI 1640	5 - 10 x 10^7
Primary NK cell	CellGenix SCGM	5 - 10 x 10^7
Primary blast	RPMI 1640	2 - 10 x 10^7

6.4.4 Thawing of cells

The respective culture medium of cells was prewarmed at 37°C in a water bath. Cryopreservation tubes containing cells were thawed at 37°C in a water bath until 80% of the cell suspension was thawed. The cell suspension was immediately transferred into a tube containing the prewarmed medium. Cells were centrifuged, resuspended in fresh culture medium and incubated in the incubator.

6.4.5 Virus production and titration

Viral particles were generated for stable transduction of target cells. The cell line HEK293T which was described as easy to transfect and a good production system, was used and transfected using calcium-phosphate. The general procedure is described briefly. Early in the day, HEK293T cells were seeded at 5 x 10^6 cells/ 10 cm dish and incubated for 4 - 6 h. After incubation, the adherent cells were attached to the surface. The medium was replaced with fresh prewarmed medium supplemented with 8 µg/mL chloroquine. Chloroquine is a lysomotrophic amine that inhibits lysosomal enzymes and thereby prevents DNA degradation, hence increasing the transfection efficiency (*367*). A side effect is that it also increases cell toxicity. Therefore, the medium had to be replaced after 4 - 6 h. Depending on the type of virus a master mix was prepared (Table 30).

Table 30: Composition virus production.

Component	Lentiviral particles	Alpharetroviral particles
Plasmid	10 µg	10 µg
pMDLg-pRRE (gag/pol)	10 µg	5 µg
pRSV-Rev	5 µg	-
Envelope either		
phCMV-RD114/TR or	4 µg	4 µg
pCMV-VSV-G	2 µg	2 µg
Aqua Braun	ad 450 µL	ad 450 µL
$CaCl_2$ (2.5M)	50 µL	50 µL
2X HBSS	500 µL	500 µL
Per 10 cm plate	1000 µL	1000 µL

The components were added in the indicated order. After vortexing, the master mix was added dropwise to the HBSS buffer, while air was blown into the HBSS buffer with a Pasteur pipette followed by incubation for 10 - 20 min. Afterwards, the mixture was added dropwise to the plates, while these were being smoothly shaken. After incubation for 6 - 12 h, the medium was replaced with fresh medium without chloroquine and plates were further incubated. Cells were checked for fluorescence in the microscope. Viral supernatant was harvested 24 h and 48 h after incubation. After 24 h fresh medium was added for the following 24 h. Viral supernatant was sterile filtered with a 0.45 µM filter and transferred into virus tubes following centrifugation at 20.000 x g, 4°C for 3 - 4 h without brake. After centrifugation, the supernatant was aspirated leaving 300 - 400 µL in the tube and the viral supernatant was resuspended in the remaining medium and stored in 30 - 40 µL aliquots at - 80°C.

To determine the number of viral particles in the concentrated supernatant, a titration was performed. 5 x 10^4 HEK293T cells/well were seeded with 8 µg/mL polybrene in a 24 well plate. After 4 - 6 h of incubation, freshly thawed viral supernatant was added in duplicates (0.1, 1, or

10 µL), following centrifugation at 1000 x g, RT, for 1 h. Three days after transduction, cells were harvested, fixed with FACS buffer containing 2% PFA and analyzed for fluorescence by flow cytometry. Titers were calculated from the wells containing 5 - 20% positive cells. Due to multiple integrations per target cells the titer would possibly be underestimated otherwise (*366*). Viral titers were determined using the following formula:

$T = N*P/V$

T: titer
N: number of plated cells
V: volume of added supernatant
P: proportion of transduced cells

6.4.6 Isolation and cultivation of primary cells

Primary human cells were isolated either from blood donations of from healthy volunteer donors after written approval or from buffy coats obtained from the cell separation facility at the University Medical Center Hamburg-Eppendorf. Lymphocytes were isolated using density centrifugation as follows. Whole blood was layered 1:1 (v:v) on Biocoll separation solution, buffy coat was mixed 1:1 (v:v) with PBS at RT and layered 2:1 (v:v) on Biocoll separation solution. The mixture was centrifuged at 900 x g, (acceleration 3, deceleration 3) at RT. After separation, the upper plasma layer was aspirated. The lymphocyte layer was transferred into a new tube and washed twice with 50 mL PBS + 2 mM EDTA. Cells were counted (section 6.4.2). NK cells were isolated from PBMCs using the Miltenyi NK Cell Isolation Kit according to the manufacturer's instructions. The flow-through containing the positive cells, was centrifuged, cells were counted and cultured at 1 x 10^6/mL under the respective conditions for the following assays as described in section 6.1.5.

6.4.7 Transduction of primary cells and cell lines

The cell line NK92-MI was transduced using vectofusin-1 as follows. 2 x 10^5 cells/ 50 µL were seeded in a 96 well round bottom plate in medium without supplements (plain medium). Viral supernatant was filled up to 197,5 µL with plain medium and 2,5 µL vectofusion-1 (10 µg/mL) was added. The mixture was vortexed and immediately added to the cells. Six µM BX795 was added per well and each well was mixed using a 1000 µL pipette. The plate was centrifuged at 400 x g, prewarmed to 32°C, for 2 h. After incubation for 4 - 6 h in the incubator, the plate was centrifuged. Approximately 80% of the supernatant was removed and replaced with fresh complete medium. Every 2 - 3 days cells were analyzed visually and if necessary, medium was added. After 4 days, cells were analyzed for fluorescence by flow cytometry.
Freshly isolated human NK cells were cultivated in CellGenix SCGM containing 10% human AB serum at 1 x 10^6 cells/mL. Cells were activated for 4 days with daily addition of 20 ng/mL

IL-21 and 1000 U/mL IL-2. On day four, cells were harvested, counted, and seeded at 2 x 10^5 or 2 x 10^4 cells per well in a 24 well plate. Cells were either transduced with lentiviral vectors and 8 µg/mL protamine sulfate or with alpharetroviral vectors and 10 µg/mL vectofusion-1. Viral supernatant and vectofusion-1 were premixed as described above and added to the cells. Six µM of the viral degradation inhibitor BX795 was added to each well. Plates were centrifuged for 1,5 - 2 h, at 32°C and 1000 x g in the prewarmed centrifuge followed by incubation for 4 - 6 h in the incubator. After incubation plates were centrifuged again for 1 h, at 32 °C and 1000 x g and 80% of the supernatant was removed and replaced with fresh medium containing 1000 U/mL IL-2. Every second day 1000 U/mL IL-2 was added and if the color of the medium started to change, fresh medium was added. On day four after transduction cells were checked for fluorescence and receptor expression. Therefore, cells were stained with the respective antibodies (6.4.9). Cells were further expanded for 6 - 8 days until usage for functional assays.

6.4.8 Cytotoxicity and degranulation assay

Primary NK cells were isolated as described in 6.4.6 and pre-activated in NK medium with addition of 100 U/mL IL-2 and 20 ng/mL IL-15. The next morning, cells were counted, centrifuged, and resuspended at 2 x 10^6 cells/mL. The target cell line K562 was harvested and primary blasts were thawed in prewarmed NK medium. All target cells were washed twice with PBS. After the second wash, cells were counted and adjusted to 20 x 10^6 cells/mL. An aliquot of 2 or 5 mM eFluor670 solution was thawed and diluted 1:1000 in PBS and then added 1:1 (v:v) to the cell suspension. Staining was performed at 37°C for 10 min in the incubator. The reaction was stopped by addition of the stop solution, followed by an incubation on ice for 5 min. Cells were washed twice with NK assay medium and adjusted to 2 x 10^6 cells/mL.
For the cytotoxicity assays, target cells were further diluted 1:10 and mixed in E:T ratios of 5:1, 10:1 and 20:1 in a total volume of 200 µL. Two additional wells with target cells only per cell type were prepared for determination of spontaneous and maximal cell dead.
After incubation, cytotoxicity assay samples were either analyzed at a BD FACSCanto™ Cell Analyzer I or at a MACS Quant® Analyzer 10. For analysis at the BD FACSCanto™ Cell Analyzer I, samples were supplemented with 20 µL counting beads (2 drops/mL). At the MACS Quant® Analyzer 100, 150 µL of co-culture was analyzed. At both instruments, 30 - 60 sec before measurement, PI was added 1:100. Target cells were gated on eFluor670 positive cells, which are detected in the APC channel. Dead cells are PI positive. The percent of specific lysis was determined as follows:

$$\%\ specific\ lysis = \frac{(\%\ lysis\ in\ sample) - (\%\ spontaneous\ lysis)}{(\%\ maximal\ \text{lysis}) - (\%\ spontaneous\ lysis)} * 100$$

For degranulation assays, a co-culture with an E:T ratio of 1:1 was prepared in either 96-well round button plates or in FACS tubes. Cells were spun down and incubated for 4 h at 37°C. After 1 h of incubation, 5 µL/mL BD Golgi Stop™ Protein Transport Inhibitor and 10 µL/mL CD107a antibody were added to the degranulation samples. For primary NK cells a KIR phenotyping was performed with the samples prepared for the degranulation assay. Samples were FACS stained (section 6.4.9) and analyzed either at a BD LSRFortessa™ Flow Cytometer or a BD FACSCanto™ I Cell Analyzer.

For analysis of degranulation and cytotoxicity of NK92-MI cells, the target cells were prepared as described above, except that cells were washed and adjusted in NK92-MI medium. NK92-MI cells were harvested, washed twice with NK92-MI medium counted and adjusted to 1 x 10^6 cells/mL. Maximal degranulation was determined by addition of 2.5 µg/mL PMA and 5 µg/mL ionomycin. For detection of background degranulation, untreated cells were seeded in medium only. Samples were prepared in duplicates or triplicates. After incubation, cells were stained as mentioned in section 6.4.9, fixed with FACS buffer containing 1% PFA and analyzed at the MACS Quant® Analyzer 10. NK cells were gated on eFluor670 negative cells and CD107a positive. Degranulation was determined as follows

$$\%\ degranulation = \frac{(\%\ degranulation\ of\ sample) - (\%\ degranulation\ of\ untreated\ cells)}{(\%\ maximal\ degranulation) - (\%\ degranulation\ of\ untreated\ cells)} * 100$$

6.4.9 FACS staining and compensation

Cells were stained with antibodies against surface receptors. All washing steps were performed with FACS buffer. A staining was performed either with a primary antibody directly labeled with a fluorophore or with a primary unlabeled antibody and a second one that was labeled. If a directly labeled antibody was used, cells were washed once and the antibody (Table 16) or the prediluted antibody master mix was added to the sample vortexed gently, and incubated for 20 min, at 4°C, protected from light. After incubation, cells were washed and fixed using FACS buffer containing 1 % PFA. Cells were either analyzed directly or stored up to 3 days, at 4°C, protected from light.

In case, the primary antibody was unconjugated, a two-step staining was performed. First, the cells were washed once followed by addition of the primary unconjugated antibody (Table 16) or prediluted antibody master mix. Cell were incubated for 20 min, at 4°C, protected from light. After incubation, cells were washed and the second fluorophore conjugated antibody that recognizes the constant domain of the primary antibody was added followed by an incubation for 15 min, at 4°C, protected from light. Afterwards, samples were washed, resuspended, and fixed in FACS buffer containing 1% PFA. Cells were either analyzed directly or stored up to 3 days, at 4°C, protected from light.

6.5 FM analysis

In compliance with the regulations of the Institutional Review Board decision PV4296 families were prospectively enrolled for the following analysis. Schematic depiction of FM sample pipeline (Figure 30). Fresh leukemic blasts were isolated (section 6.4.6) at initial diagnosis and stored at - 80°C for up to six months. For long term storage samples were stored in liquid nitrogen (section 6.4.3). After written consent, 20 mL peripheral blood was drawn from the parents. PBMCs were isolated followed by MACS isolation of NK cells (section 6.4.6). Primary NK cells were pre-activated with IL-2 and IL-15 overnight and used for the cytotoxicity and degranulation assays (section 6.4.8) against their child's leukemic blasts and the cell line K562. From remaining PBMCs after MACS and remaining leukemic blasts, DNA was extracted (section 6.2.4) and used for KIR and HLA-C genotyping (sections 6.2.6 and 6.2.7). Filial and maternal DNA was amplified (section 6.3.1) followed by marker selection (section 6.3.2) and microchimerism determination using ddPCR (section 6.3.3).

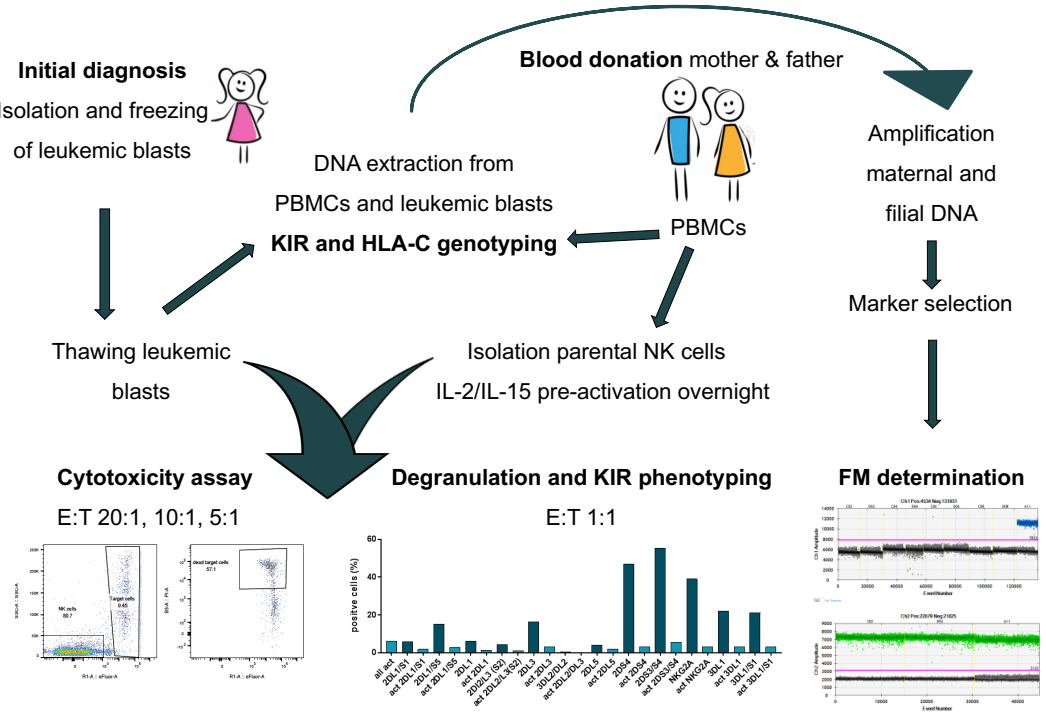

Figure 30: Experimental set-up FM analysis.

6.5.1 Software and online programs

Table 31: List of software.

Program	Version	Manufacturer	Used for
Microsoft Office 365	16.35	© 2020 Microsoft	Documentation, analysis, and data storage
QuantaSoft	1.7.4.0917	© Bio-Rad, Laboratories, Hercules, CA, USA	ddPCR analysis and experimental set-up
FlowJo	10.6.3	Becton, Dickinson and Company (BD)	FACS data analysis
BD FACSDiva™	8.0	Becton, Dickinson and Company (BD)	FACS data recording
Prism for macOS	8.4.1	GraphPad Software, LLC.	Visualization and statistical analysis
IBM SPSS Statistics	26	IBM Corp. ©	Statistical analysis
SnapGene®	5.1	Insightful Science	Sequence analysis during cloning

Table 32: List of free online tools.

Program	Link	Date, time (UTC+1)	Used for
NEB Gibson Assembly tool	http://nebuilder.neb.com/#!/	09.06.2020,14:50	Primer design
Primer blast	https://www.ncbi.nlm.nih.gov/tools/primer-blast/	09.06.2020, 14:52	Primer blast for specificity
TM calculation	http://tmcalculator.neb.com/#!/main	09.06.2020, 14:52	TM calculation of primers
Ligation ratio calculation	http://www.insilico.uni-duesseldorf.de/Lig_Input.html	09.06.2020, 14:56	Calculation of ligation ratios

7. References

1. S. Pinho, P. S. Frenette, Haematopoietic stem cell activity and interactions with the niche. *Nat Rev Mol Cell Biol* **20**, 303-320 (2019).
2. M. Takahashi *et al.*, CD133 is a positive marker for a distinct class of primitive human cord blood-derived CD34-negative hematopoietic stem cells. *Leukemia* **28**, 1308-1315 (2014).
3. L. O. Jacobson, E. L. Simmons, E. K. Marks, J. H. Eldredge, Recovery from radiation injury. *Science* **113**, 510-511 (1951).
4. S. Doulatov *et al.*, Revised map of the human progenitor hierarchy shows the origin of macrophages and dendritic cells in early lymphoid development. *Nat Immunol* **11**, 585-593 (2010).
5. A. Galy, M. Travis, D. Cen, B. Chen, Human T, B, natural killer, and dendritic cells arise from a common bone marrow progenitor cell subset. *Immunity* **3**, 459-473 (1995).
6. L. Wu, Y. J. Liu, Development of dendritic-cell lineages. *Immunity* **26**, 741-750 (2007).
7. E. M. Ferlay J, Lam F, Colombet M, Mery L, Piñeros M, Znaor A, Soerjomataram I, Bray F. (2018).
8. E. Laurenti, B. Gottgens, From haematopoietic stem cells to complex differentiation landscapes. *Nature* **553**, 418-426 (2018).
9. N. Hijiya, K. R. Schultz, M. Metzler, F. Millot, M. Suttorp, Pediatric chronic myeloid leukemia is a unique disease that requires a different approach. *Blood* **127**, 392-399 (2016).
10. J. W. Vardiman *et al.*, The 2008 revision of the World Health Organization (WHO) classification of myeloid neoplasms and acute leukemia: rationale and important changes. *Blood* **114**, 937-951 (2009).
11. J. M. Bennett *et al.*, Proposals for the classification of the acute leukaemias. French-American-British (FAB) co-operative group. *Br J Haematol* **33**, 451-458 (1976).
12. S. Chiaretti, G. Zini, R. Bassan, Diagnosis and subclassification of acute lymphoblastic leukemia. *Mediterr J Hematol Infect Dis* **6**, e2014073 (2014).
13. E. Matutes *et al.*, Mixed-phenotype acute leukemia: clinical and laboratory features and outcome in 100 patients defined according to the WHO 2008 classification. *Blood* **117**, 3163-3171 (2011).
14. S. G. DuBois, J. E. Etzell, K. K. Matthay, E. Robbins, A. Banerjee, Pediatric acute blastic natural killer cell leukemia. *Leuk Lymphoma* **43**, 901-906 (2002).
15. A. Sureda *et al.*, Indications for allo- and auto-SCT for haematological diseases, solid tumours and immune disorders: current practice in Europe, 2015. *Bone Marrow Transplant* **50**, 1037-1056 (2015).
16. M. K. Juric *et al.*, Milestones of Hematopoietic Stem Cell Transplantation - From First Human Studies to Current Developments. *Front Immunol* **7**, 470 (2016).
17. A. Bazinet, G. Popradi, A general practitioner's guide to hematopoietic stem-cell transplantation. *Curr Oncol* **26**, 187-191 (2019).
18. J. W. Ferrebee, H. L. Lochte, Jr., A. Jaretzki, 3rd, O. D. Sahler, E. D. Thomas, Successful marrow homograft in the dog after radiation. *Surgery* **43**, 516-520 (1958).
19. C. E. Ford, J. L. Hamerton, D. W. Barnes, J. F. Loutit, Cytological identification of radiation-chimaeras. *Nature* **177**, 452-454 (1956).
20. E. D. Thomas, H. L. Lochte, Jr., W. C. Lu, J. W. Ferrebee, Intravenous infusion of bone marrow in patients receiving radiation and chemotherapy. *N Engl J Med* **257**, 491-496 (1957).

21. G. MATHÉ *et al.*, Successful Allogenic Bone Marrow Transplantation in Man: Chimerism, Induced Specific Tolerance and Possible Anti-Leukemic Effects. *Blood* **25**, 179-196 (1965).
22. J. J. Van Rood, A. Van Leeuwen, Leukocyte Grouping. A Method and Its Application. *J Clin Invest* **42**, 1382-1390 (1963).
23. J. J. van Rood, The detection of transplantation antigens in leukocytes. *Semin Hematol* **5**, 187-214 (1968).
24. R. A. Gatti, H. J. Meuwissen, H. D. Allen, R. Hong, R. A. Good, Immunological reconstitution of sex-linked lymphopenic immunological deficiency. *Lancet* **2**, 1366-1369 (1968).
25. J. A. Hansen *et al.*, Transplantation of marrow from an unrelated donor to a patient with acute leukemia. *N Engl J Med* **303**, 565-567 (1980).
26. R. Danby, V. Rocha, Improving engraftment and immune reconstitution in umbilical cord blood transplantation. *Front Immunol* **5**, 68 (2014).
27. J. Ogonek *et al.*, Immune Reconstitution after Allogeneic Hematopoietic Stem Cell Transplantation. *Front Immunol* **7**, 507 (2016).
28. F. Ayuk, A. Balduzzi, in *The EBMT Handbook: Hematopoietic Stem Cell Transplantation and Cellular Therapies,* th, E. Carreras, C. Dufour, M. Mohty, N. Kroger, Eds. (Cham (CH), 2019), pp. 87-97.
29. A. Nagler, A. Shimoni, in *The EBMT Handbook: Hematopoietic Stem Cell Transplantation and Cellular Therapies,* th, E. Carreras, C. Dufour, M. Mohty, N. Kroger, Eds. (Cham (CH), 2019), pp. 99-107.
30. N. A. Kernan, N. Flomenberg, B. Dupont, R. J. O'Reilly, Graft rejection in recipients of T-cell-depleted HLA-nonidentical marrow transplants for leukemia. Identification of host-derived antidonor allocytotoxic T lymphocytes. *Transplantation* **43**, 842-847 (1987).
31. C. Peters, F. Locatelli, P. Bader, in *The EBMT Handbook: Hematopoietic Stem Cell Transplantation and Cellular Therapies,* th, E. Carreras, C. Dufour, M. Mohty, N. Kroger, Eds. (Cham (CH), 2019), pp. 539-545.
32. J. M. Mulcahy Levy *et al.*, Late effects of total body irradiation and hematopoietic stem cell transplant in children under 3 years of age. *Pediatr Blood Cancer* **60**, 700-704 (2013).
33. A. Nagler *et al.*, Mobilized peripheral blood stem cells compared with bone marrow as the stem cell source for unrelated donor allogeneic transplantation with reduced-intensity conditioning in patients with acute myeloid leukemia in complete remission: an analysis from the Acute Leukemia Working Party of the European Group for Blood and Marrow Transplantation. *Biol Blood Marrow Transplant* **18**, 1422-1429 (2012).
34. N. Schmitz *et al.*, Transplantation of mobilized peripheral blood cells to HLA-identical siblings with standard-risk leukemia. *Blood* **100**, 761-767 (2002).
35. A. Ruggeri *et al.*, Engraftment kinetics and graft failure after single umbilical cord blood transplantation using a myeloablative conditioning regimen. *Haematologica* **99**, 1509-1515 (2014).
36. V. Rocha *et al.*, Comparison of outcomes of unrelated bone marrow and umbilical cord blood transplants in children with acute leukemia. *Blood* **97**, 2962-2971 (2001).
37. A. K. Keating *et al.*, The influence of stem cell source on transplant outcomes for pediatric patients with acute myeloid leukemia. *Blood Adv* **3**, 1118-1128 (2019).
38. M. Simonin *et al.*, More chronic GvHD and non-relapse mortality after peripheral blood stem cell compared with bone marrow in hematopoietic transplantation for paediatric

acute lymphoblastic leukemia: a retrospective study on behalf of the EBMT Paediatric Diseases Working Party. *Bone Marrow Transplant* **52**, 1071-1073 (2017).

39. C. Peters *et al.*, Stem-cell transplantation in children with acute lymphoblastic leukemia: A prospective international multicenter trial comparing sibling donors with matched unrelated donors-The ALL-SCT-BFM-2003 trial. *J Clin Oncol* **33**, 1265-1274 (2015).
40. S. Y. Choo, The HLA system: genetics, immunology, clinical testing, and clinical implications. *Yonsei Med J* **48**, 11-23 (2007).
41. E. Spierings, K. Fleischhauer, in *The EBMT Handbook: Hematopoietic Stem Cell Transplantation and Cellular Therapies,* th, E. Carreras, C. Dufour, M. Mohty, N. Kroger, Eds. (Cham (CH), 2019), pp. 61-68.
42. M. Martin, D. Mann, M. Carrington, Recombination rates across the HLA complex: use of microsatellites as a rapid screen for recombinant chromosomes. *Hum Mol Genet* **4**, 423-428 (1995).
43. E. Pamer, P. Cresswell, Mechanisms of MHC class I--restricted antigen processing. *Annu Rev Immunol* **16**, 323-358 (1998).
44. P. Parham, Immunogenetics of killer-cell immunoglobulin-like receptors. *Tissue Antigens* **62**, 194-200 (2003).
45. J. M. Vyas, A. G. Van der Veen, H. L. Ploegh, The known unknowns of antigen processing and presentation. *Nat Rev Immunol* **8**, 607-618 (2008).
46. P. Cresswell, Assembly, transport, and function of MHC class II molecules. *Annu Rev Immunol* **12**, 259-293 (1994).
47. G. Kochan, D. Escors, K. Breckpot, D. Guerrero-Setas, Role of non-classical MHC class I molecules in cancer immunosuppression. *Oncoimmunology* **2**, e26491 (2013).
48. R. L. Allen, Non-classical immunology. *Genome Biol* **2**, REPORTS4004 (2001).
49. B. Afzali, R. I. Lechler, M. P. Hernandez-Fuentes, Allorecognition and the alloresponse: clinical implications. *Tissue Antigens* **69**, 545-556 (2007).
50. E. Spierings, Minor histocompatibility antigens: past, present, and future. *Tissue Antigens* **84**, 374-360 (2014).
51. F. Aversa *et al.*, Treatment of high-risk acute leukemia with T-cell-depleted stem cells from related donors with one fully mismatched HLA haplotype. *N Engl J Med* **339**, 1186-1193 (1998).
52. J. Apperley *et al.*, Haploidentical Hematopoietic Stem Cell Transplantation: A Global Overview Comparing Asia, the European Union, and the United States. *Biol Blood Marrow Transplant* **22**, 23-26 (2016).
53. P. M. Falk *et al.*, Bone marrow transplantation between a histocompatible parent and child for acute leukemia. *Transplantation* **25**, 88-90 (1978).
54. P. G. Beatty *et al.*, Marrow transplantation from related donors other than HLA-identical siblings. *N Engl J Med* **313**, 765-771 (1985).
55. Y. Reisner *et al.*, Transplantation for acute leukaemia with HLA-A and B nonidentical parental marrow cells fractionated with soybean agglutinin and sheep red blood cells. *Lancet* **2**, 327-331 (1981).
56. J. M. Goldman *et al.*, Bone marrow transplantation for chronic myelogenous leukemia in chronic phase. Increased risk for relapse associated with T-cell depletion. *Ann Intern Med* **108**, 806-814 (1988).
57. L. Ruggeri *et al.*, Role of natural killer cell alloreactivity in HLA-mismatched hematopoietic stem cell transplantation. *Blood* **94**, 333-339 (1999).

58. F. Aversa *et al.*, Successful engraftment of T-cell-depleted haploidentical "three-loci" incompatible transplants in leukemia patients by addition of recombinant human granulocyte colony-stimulating factor-mobilized peripheral blood progenitor cells to bone marrow inoculum. *Blood* **84**, 3948-3955 (1994).
59. F. Aversa *et al.*, Improved outcome with T-cell-depleted bone marrow transplantation for acute leukemia. *J Clin Oncol* **17**, 1545-1550 (1999).
60. F. Baron *et al.*, Anti-thymocyte globulin as graft-versus-host disease prevention in the setting of allogeneic peripheral blood stem cell transplantation: a review from the Acute Leukemia Working Party of the European Society for Blood and Marrow Transplantation. *Haematologica* **102**, 224-234 (2017).
61. R. Chakraverty *et al.*, Impact of in vivo alemtuzumab dose before reduced intensity conditioning and HLA-identical sibling stem cell transplantation: pharmacokinetics, GVHD, and immune reconstitution. *Blood* **116**, 3080-3088 (2010).
62. R. J. Soiffer *et al.*, Impact of immune modulation with anti-T-cell antibodies on the outcome of reduced-intensity allogeneic hematopoietic stem cell transplantation for hematologic malignancies. *Blood* **117**, 6963-6970 (2011).
63. K. Mochizuki *et al.*, Feasibility of tacrolimus, methotrexate, and prednisolone as a graft-versus-host disease prophylaxis in non-T-cell-depleted haploidentical hematopoietic stem cell transplantation for children. *Clin Transplant* **25**, 892-897 (2011).
64. S. Kobayashi *et al.*, T-cell-replete haploidentical stem cell transplantation is highly efficacious for relapsed and refractory childhood acute leukaemia. *Transfus Med* **24**, 305-310 (2014).
65. F. Ciceri, A. Bacigalupo, A. Lankester, A. Bertaina, in *The EBMT Handbook: Hematopoietic Stem Cell Transplantation and Cellular Therapies,* th, E. Carreras, C. Dufour, M. Mohty, N. Kroger, Eds. (Cham (CH), 2019), pp. 479-486.
66. F. Aversa *et al.*, Full haplotype-mismatched hematopoietic stem-cell transplantation: a phase II study in patients with acute leukemia at high risk of relapse. *J Clin Oncol* **23**, 3447-3454 (2005).
67. P. V. O'Donnell *et al.*, Nonmyeloablative bone marrow transplantation from partially HLA-mismatched related donors using posttransplantation cyclophosphamide. *Biol Blood Marrow Transplant* **8**, 377-386 (2002).
68. L. Luznik *et al.*, HLA-haploidentical bone marrow transplantation for hematologic malignancies using nonmyeloablative conditioning and high-dose, posttransplantation cyclophosphamide. *Biol Blood Marrow Transplant* **14**, 641-650 (2008).
69. X. J. Huang *et al.*, Haploidentical hematopoietic stem cell transplantation without in vitro T-cell depletion for the treatment of hematological malignancies. *Bone Marrow Transplant* **38**, 291-297 (2006).
70. X. J. Huang *et al.*, Treatment of acute leukemia with unmanipulated HLA-mismatched/haploidentical blood and bone marrow transplantation. *Biol Blood Marrow Transplant* **15**, 257-265 (2009).
71. J. J. van Rood *et al.*, Effect of tolerance to noninherited maternal antigens on the occurrence of graft-versus-host disease after bone marrow transplantation from a parent or an HLA-haploidentical sibling. *Blood* **99**, 1572-1577 (2002).
72. Y. Wang *et al.*, Who is the best donor for a related HLA haplotype-mismatched transplant? *Blood* **124**, 843-850 (2014).

73. S. Tamaki *et al.*, Superior survival of blood and marrow stem cell recipients given maternal grafts over recipients given paternal grafts. *Bone Marrow Transplant* **28**, 375-380 (2001).
74. M. Stern *et al.*, Survival after T cell-depleted haploidentical stem cell transplantation is improved using the mother as donor. *Blood* **112**, 2990-2995 (2008).
75. D. W. Bianchi, G. K. Zickwolf, G. J. Weil, S. Sylvester, M. A. DeMaria, Male fetal progenitor cells persist in maternal blood for as long as 27 years postpartum. *Proc Natl Acad Sci U S A* **93**, 705-708 (1996).
76. Y. M. Lo *et al.*, Prenatal sex determination by DNA amplification from maternal peripheral blood. *Lancet* **2**, 1363-1365 (1989).
77. A. Kruchen *et al.*, Donor choice in haploidentical stem cell transplantation: fetal microchimerism is associated with better outcome in pediatric leukemia patients. *Bone Marrow Transplant* **50**, 1367-1370 (2015).
78. B. Srivatsa, S. Srivatsa, K. L. Johnson, D. W. Bianchi, Maternal cell microchimerism in newborn tissues. *J Pediatr* **142**, 31-35 (2003).
79. A. M. Stevens, H. M. Hermes, M. M. Kiefer, J. C. Rutledge, J. L. Nelson, Chimeric maternal cells with tissue-specific antigen expression and morphology are common in infant tissues. *Pediatr Dev Pathol* **12**, 337-346 (2009).
80. Y. M. Lo *et al.*, Detection of single-copy fetal DNA sequence from maternal blood. *Lancet* **335**, 1463-1464 (1990).
81. E. C. Rijnink *et al.*, Tissue microchimerism is increased during pregnancy: a human autopsy study. *Mol Hum Reprod* **21**, 857-864 (2015).
82. W. F. Chan *et al.*, Male microchimerism in the human female brain. *PLoS One* **7**, e45592 (2012).
83. Y. M. Lo, T. K. Lau, L. Y. Chan, T. N. Leung, A. M. Chang, Quantitative analysis of the bidirectional fetomaternal transfer of nucleated cells and plasma DNA. *Clin Chem* **46**, 1301-1309 (2000).
84. K. M. Adams Waldorf *et al.*, Dynamic changes in fetal microchimerism in maternal peripheral blood mononuclear cells, CD4+ and CD8+ cells in normal pregnancy. *Placenta* **31**, 589-594 (2010).
85. A. Kolialexi, G. T. Tsangaris, A. Antsaklis, A. Mavroua, Rapid clearance of fetal cells from maternal circulation after delivery. *Ann N Y Acad Sci* **1022**, 113-118 (2004).
86. A. Ciaranfi, A. Curchod, N. Odartchenko, [Post-partum survival of fetal lymphocytes in the maternal blood]. *Schweiz Med Wochenschr* **107**, 134-138 (1977).
87. A. Bayes-Genis *et al.*, Identification of male cardiomyocytes of extracardiac origin in the hearts of women with male progeny: male fetal cell microchimerism of the heart. *J Heart Lung Transplant* **24**, 2179-2183 (2005).
88. A. Moffett, F. Colucci, Uterine NK cells: active regulators at the maternal-fetal interface. *J Clin Invest* **124**, 1872-1879 (2014).
89. L. A. Koopman *et al.*, Human decidual natural killer cells are a unique NK cell subset with immunomodulatory potential. *J Exp Med* **198**, 1201-1212 (2003).
90. G. Benichou *et al.*, Immune recognition and rejection of allogeneic skin grafts. *Immunotherapy* **3**, 757-770 (2011).
91. J. Heikkinen, M. Mottonen, A. Alanen, O. Lassila, Phenotypic characterization of regulatory T cells in the human decidua. *Clin Exp Immunol* **136**, 373-378 (2004).
92. T. T. Jiang *et al.*, Regulatory T cells: new keys for further unlocking the enigma of fetal tolerance and pregnancy complications. *J Immunol* **192**, 4949-4956 (2014).

93. A. Erlebacher, D. Vencato, K. A. Price, D. Zhang, L. H. Glimcher, Constraints in antigen presentation severely restrict T cell recognition of the allogeneic fetus. *J Clin Invest* **117**, 1399-1411 (2007).
94. C. S. Tay, E. Tagliani, M. K. Collins, A. Erlebacher, Cis-acting pathways selectively enforce the non-immunogenicity of shed placental antigen for maternal CD8 T cells. *PLoS One* **8**, e84064 (2013).
95. P. Nancy *et al.*, Chemokine gene silencing in decidual stromal cells limits T cell access to the maternal-fetal interface. *Science* **336**, 1317-1321 (2012).
96. J. H. Rowe, J. M. Ertelt, L. Xin, S. S. Way, Pregnancy imprints regulatory memory that sustains anergy to fetal antigen. *Nature* **490**, 102-106 (2012).
97. D. K. Li, S. Wi, Changing paternity and the risk of preeclampsia/eclampsia in the subsequent pregnancy. *Am J Epidemiol* **151**, 57-62 (2000).
98. J. E. Mold, J. M. McCune, Immunological tolerance during fetal development: from mouse to man. *Adv Immunol* **115**, 73-111 (2012).
99. J. E. Mold *et al.*, Maternal alloantigens promote the development of tolerogenic fetal regulatory T cells in utero. *Science* **322**, 1562-1565 (2008).
100. J. M. Kinder, I. A. Stelzer, P. C. Arck, S. S. Way, Immunological implications of pregnancy-induced microchimerism. *Nat Rev Immunol* **17**, 483-494 (2017).
101. C. Guettier *et al.*, Male cell microchimerism in normal and diseased female livers from fetal life to adulthood. *Hepatology* **42**, 35-43 (2005).
102. A. C. Muller *et al.*, Microchimerism of male origin in a cohort of Danish girls. *Chimerism* **6**, 65-71 (2015).
103. H. S. Gammill, K. A. Guthrie, T. M. Aydelotte, K. M. Adams Waldorf, J. L. Nelson, Effect of parity on fetal and maternal microchimerism: interaction of grafts within a host? *Blood* **116**, 2706-2712 (2010).
104. S. L. Klein, K. L. Flanagan, Sex differences in immune responses. *Nat Rev Immunol* **16**, 626-638 (2016).
105. J. Walknowska, F. A. Conte, M. M. Grumbach, Practical and theoretical implications of fetal-maternal lymphocyte transfer. *Lancet* **1**, 1119-1122 (1969).
106. J. de Grouchy, C. Trebuchet, [Fetomaternal transfusion of blood lymphocytes and identification of the sex of the fetus]. *Ann Genet* **14**, 133-137 (1971).
107. L. Grosset, V. Barrelet, N. Odartchenko, Antenatal fetal sex determination from maternal blood during early pregnancy. *Am J Obstet Gynecol* **120**, 60-63 (1974).
108. L. A. Herzenberg, D. W. Bianchi, J. Schroder, H. M. Cann, G. M. Iverson, Fetal cells in the blood of pregnant women: detection and enrichment by fluorescence-activated cell sorting. *Proc Natl Acad Sci U S A* **76**, 1453-1455 (1979).
109. H. Hamada, T. Arinami, T. Kubo, H. Hamaguchi, H. Iwasaki, Fetal nucleated cells in maternal peripheral blood: frequency and relationship to gestational age. *Hum Genet* **91**, 427-432 (1993).
110. V. Nunes, G. Cazzaniga, A. Biondi, An update on PCR use for minimal residual disease monitoring in acute lymphoblastic leukemia. *Expert Rev Mol Diagn* **17**, 953-963 (2017).
111. R. G. Knowlton *et al.*, Use of highly polymorphic DNA probes for genotypic analysis following bone marrow transplantation. *Blood* **68**, 378-385 (1986).
112. P. Bader, D. Niethammer, A. Willasch, H. Kreyenberg, T. Klingebiel, How and when should we monitor chimerism after allogeneic stem cell transplantation? *Bone Marrow Transplant* **35**, 107-119 (2005).

113. B. Fehse *et al.*, Real-time quantitative Y chromosome-specific PCR (QYCS-PCR) for monitoring hematopoietic chimerism after sex-mismatched allogeneic stem cell transplantation. *J Hematother Stem Cell Res* **10**, 419-425 (2001).
114. Y. M. Lo *et al.*, Quantitative analysis of fetal DNA in maternal plasma and serum: implications for noninvasive prenatal diagnosis. *Am J Hum Genet* **62**, 768-775 (1998).
115. M. Alizadeh *et al.*, Quantitative assessment of hematopoietic chimerism after bone marrow transplantation by real-time quantitative polymerase chain reaction. *Blood* **99**, 4618-4625 (2002).
116. F. Maas *et al.*, Quantification of donor and recipient hemopoietic cells by real-time PCR of single nucleotide polymorphisms. *Leukemia* **17**, 621-629 (2003).
117. R. Sachidanandam *et al.*, A map of human genome sequence variation containing 1.42 million single nucleotide polymorphisms. *Nature* **409**, 928-933 (2001).
118. S. B. Montgomery *et al.*, The origin, evolution, and functional impact of short insertion-deletion variants identified in 179 human genomes. *Genome Res* **23**, 749-761 (2013).
119. T. Stahl, M. U. Bohme, N. Kroger, B. Fehse, Digital PCR to assess hematopoietic chimerism after allogeneic stem cell transplantation. *Exp Hematol* **43**, 462-468 e461 (2015).
120. T. Stahl *et al.*, Digital PCR Panel for Sensitive Hematopoietic Chimerism Quantification after Allogeneic Stem Cell Transplantation. *Int J Mol Sci* **17**, (2016).
121. D. George, J. Czech, B. John, M. Yu, L. J. Jennings, Detection and quantification of chimerism by droplet digital PCR. *Chimerism* **4**, 102-108 (2013).
122. A. M. Boddy, A. Fortunato, M. Wilson Sayres, A. Aktipis, Fetal microchimerism and maternal health: a review and evolutionary analysis of cooperation and conflict beyond the womb. *Bioessays* **37**, 1106-1118 (2015).
123. C. Confavreux, M. Hutchinson, M. M. Hours, P. Cortinovis-Tourniaire, T. Moreau, Rate of pregnancy-related relapse in multiple sclerosis. Pregnancy in Multiple Sclerosis Group. *N Engl J Med* **339**, 285-291 (1998).
124. M. Ostensen, P. M. Villiger, The remission of rheumatoid arthritis during pregnancy. *Semin Immunopathol* **29**, 185-191 (2007).
125. J. L. Nelson, The otherness of self: microchimerism in health and disease. *Trends Immunol* **33**, 421-427 (2012).
126. J. L. Nelson *et al.*, Microchimerism and HLA-compatible relationships of pregnancy in scleroderma. *Lancet* **351**, 559-562 (1998).
127. H. Spits, J. H. Bernink, L. Lanier, NK cells and type 1 innate lymphoid cells: partners in host defense. *Nat Immunol* **17**, 758-764 (2016).
128. C. Seillet *et al.*, Deciphering the Innate Lymphoid Cell Transcriptional Program. *Cell Rep* **17**, 436-447 (2016).
129. E. Vivier *et al.*, Innate Lymphoid Cells: 10 Years On. *Cell* **174**, 1054-1066 (2018).
130. R. B. Herberman, M. E. Nunn, D. H. Lavrin, Natural cytotoxic reactivity of mouse lymphoid cells against syngeneic acid allogeneic tumors. I. Distribution of reactivity and specificity. *Int J Cancer* **16**, 216-229 (1975).
131. R. Kiessling, E. Klein, H. Wigzell, "Natural" killer cells in the mouse. I. Cytotoxic cells with specificity for mouse Moloney leukemia cells. Specificity and distribution according to genotype. *Eur J Immunol* **5**, 112-117 (1975).
132. M. A. Cooper, T. A. Fehniger, M. A. Caligiuri, The biology of human natural killer-cell subsets. *Trends Immunol* **22**, 633-640 (2001).
133. P. Carrega, G. Ferlazzo, Natural killer cell distribution and trafficking in human tissues. *Front Immunol* **3**, 347 (2012).

134. J. S. Schleypen *et al.*, Cytotoxic markers and frequency predict functional capacity of natural killer cells infiltrating renal cell carcinoma. *Clin Cancer Res* **12**, 718-725 (2006).
135. N. Dalbeth *et al.*, CD56bright NK cells are enriched at inflammatory sites and can engage with monocytes in a reciprocal program of activation. *J Immunol* **173**, 6418-6426 (2004).
136. C. Gregoire *et al.*, The trafficking of natural killer cells. *Immunol Rev* **220**, 169-182 (2007).
137. F. D. Shi, H. G. Ljunggren, A. La Cava, L. Van Kaer, Organ-specific features of natural killer cells. *Nat Rev Immunol* **11**, 658-671 (2011).
138. J. A. Wagner *et al.*, CD56bright NK cells exhibit potent antitumor responses following IL-15 priming. *J Clin Invest* **127**, 4042-4058 (2017).
139. J. S. Miller, L. L. Lanier, Natural Killer Cells in Cancer Immunotherapy. *Annual Review of Cancer Biology* **3**, 77-103 (2019).
140. D. Urlaub, K. Hofer, M. L. Muller, C. Watzl, LFA-1 Activation in NK Cells and Their Subsets: Influence of Receptors, Maturation, and Cytokine Stimulation. *J Immunol* **198**, 1944-1951 (2017).
141. S. Paul, G. Lal, The Molecular Mechanism of Natural Killer Cells Function and Its Importance in Cancer Immunotherapy. *Front Immunol* **8**, 1124 (2017).
142. J. Pardo, S. Balkow, A. Anel, M. M. Simon, Granzymes are essential for natural killer cell-mediated and perf-facilitated tumor control. *Eur J Immunol* **32**, 2881-2887 (2002).
143. D. Chowdhury, J. Lieberman, Death by a thousand cuts: granzyme pathways of programmed cell death. *Annu Rev Immunol* **26**, 389-420 (2008).
144. G. Alter, J. M. Malenfant, M. Altfeld, CD107a as a functional marker for the identification of natural killer cell activity. *J Immunol Methods* **294**, 15-22 (2004).
145. A. Cohnen *et al.*, Surface CD107a/LAMP-1 protects natural killer cells from degranulation-associated damage. *Blood* **122**, 1411-1418 (2013).
146. J. P. Medema *et al.*, FLICE is activated by association with the CD95 death-inducing signaling complex (DISC). *EMBO J* **16**, 2794-2804 (1997).
147. P. Netter, M. Anft, C. Watzl, Termination of the Activating NK Cell Immunological Synapse Is an Active and Regulated Process. *J Immunol* **199**, 2528-2535 (2017).
148. R. Bhat, C. Watzl, Serial killing of tumor cells by human natural killer cells--enhancement by therapeutic antibodies. *PLoS One* **2**, e326 (2007).
149. L. Lugini *et al.*, Immune surveillance properties of human NK cell-derived exosomes. *J Immunol* **189**, 2833-2842 (2012).
150. I. Prager *et al.*, NK cells switch from granzyme B to death receptor-mediated cytotoxicity during serial killing. *J Exp Med* **216**, 2113-2127 (2019).
151. Y. Zhu, B. Huang, J. Shi, Fas ligand and lytic granule differentially control cytotoxic dynamics of natural killer cell against cancer target. *Oncotarget* **7**, 47163-47172 (2016).
152. Y. T. Bryceson, H. G. Ljunggren, E. O. Long, Minimal requirement for induction of natural cytotoxicity and intersection of activation signals by inhibitory receptors. *Blood* **114**, 2657-2666 (2009).
153. P. Mombaerts *et al.*, RAG-1-deficient mice have no mature B and T lymphocytes. *Cell* **68**, 869-877 (1992).
154. S. Sivori *et al.*, Human NK cells: surface receptors, inhibitory checkpoints, and translational applications. *Cell Mol Immunol* **16**, 430-441 (2019).
155. L. Borges, D. Cosman, LIRs/ILTs/MIRs, inhibitory and stimulatory Ig-superfamily receptors expressed in myeloid and lymphoid cells. *Cytokine Growth Factor Rev* **11**, 209-217 (2000).

156. A. Moretta *et al.*, Activating receptors and coreceptors involved in human natural killer cell-mediated cytolysis. *Annu Rev Immunol* **19**, 197-223 (2001).
157. T. I. Arnon, G. Markel, O. Mandelboim, Tumor and viral recognition by natural killer cells receptors. *Semin Cancer Biol* **16**, 348-358 (2006).
158. A. Niehrs *et al.*, A subset of HLA-DP molecules serve as ligands for the natural cytotoxicity receptor NKp44. *Nat Immunol* **20**, 1129-1137 (2019).
159. A. Moretta *et al.*, Receptors for HLA class-I molecules in human natural killer cells. *Annu Rev Immunol* **14**, 619-648 (1996).
160. A. Moretta *et al.*, Existence of both inhibitory (p58) and activatory (p50) receptors for HLA-C molecules in human natural killer cells. *J Exp Med* **182**, 875-884 (1995).
161. M. Carretero *et al.*, The CD94 and NKG2-A C-type lectins covalently assemble to form a natural killer cell inhibitory receptor for HLA class I molecules. *Eur J Immunol* **27**, 563-567 (1997).
162. N. Lee *et al.*, HLA-E is a major ligand for the natural killer inhibitory receptor CD94/NKG2A. *Proc Natl Acad Sci U S A* **95**, 5199-5204 (1998).
163. D. H. Raulet, Missing self recognition and self tolerance of natural killer (NK) cells. *Semin Immunol* **18**, 145-150 (2006).
164. L. Chiossone, P. Y. Dumas, M. Vienne, E. Vivier, Natural killer cells and other innate lymphoid cells in cancer. *Nat Rev Immunol* **18**, 671-688 (2018).
165. A. Horowitz *et al.*, Genetic and environmental determinants of human NK cell diversity revealed by mass cytometry. *Sci Transl Med* **5**, 208ra145 (2013).
166. D. M. Strauss-Albee *et al.*, Human NK cell repertoire diversity reflects immune experience and correlates with viral susceptibility. *Sci Transl Med* **7**, 297ra115 (2015).
167. Y. Zhang *et al.*, In vivo kinetics of human natural killer cells: the effects of ageing and acute and chronic viral infection. *Immunology* **121**, 258-265 (2007).
168. K. C. Hsu *et al.*, Killer Ig-like receptor haplotype analysis by gene content: evidence for genomic diversity with a minimum of six basic framework haplotypes, each with multiple subsets. *J Immunol* **169**, 5118-5129 (2002).
169. J. Trowsdale *et al.*, The genomic context of natural killer receptor extended gene families. *Immunol Rev* **181**, 20-38 (2001).
170. M. J. Wilson *et al.*, Plasticity in the organization and sequences of human KIR/ILT gene families. *Proc Natl Acad Sci U S A* **97**, 4778-4783 (2000).
171. M. Uhrberg *et al.*, Human diversity in killer cell inhibitory receptor genes. *Immunity* **7**, 753-763 (1997).
172. M. Uhrberg, P. Parham, P. Wernet, Definition of gene content for nine common group B haplotypes of the Caucasoid population: KIR haplotypes contain between seven and eleven KIR genes. *Immunogenetics* **54**, 221-229 (2002).
173. A. M. Martin *et al.*, Comparative genomic analysis, diversity and evolution of two KIR haplotypes A and B. *Gene* **335**, 121-131 (2004).
174. C. W. Pyo *et al.*, Different patterns of evolution in the centromeric and telomeric regions of group A and B haplotypes of the human killer cell Ig-like receptor locus. *PLoS One* **5**, e15115 (2010).
175. J. A. Traherne *et al.*, Mechanisms of copy number variation and hybrid gene formation in the KIR immune gene complex. *Hum Mol Genet* **19**, 737-751 (2010).
176. D. Ordonez, N. Gomez-Lozano, L. Rosales, C. Vilches, Molecular characterisation of KIR2DS2*005, a fusion gene associated with a shortened KIR haplotype. *Genes Immun* **12**, 544-551 (2011).

177. P. Parham, MHC class I molecules and KIRs in human history, health and survival. *Nat Rev Immunol* **5**, 201-214 (2005).
178. P. Parham, A. Moffett, Variable NK cell receptors and their MHC class I ligands in immunity, reproduction and human evolution. *Nat Rev Immunol* **13**, 133-144 (2013).
179. S. E. Dunphy *et al.*, 2DL1, 2DL2 and 2DL3 all contribute to KIR phenotype variability on human NK cells. *Genes Immun* **16**, 301-310 (2015).
180. C. M. Gardiner *et al.*, Different NK cell surface phenotypes defined by the DX9 antibody are due to KIR3DL1 gene polymorphism. *J Immunol* **166**, 2992-3001 (2001).
181. J. C. Boyington, S. A. Motyka, P. Schuck, A. G. Brooks, P. D. Sun, Crystal structure of an NK cell immunoglobulin-like receptor in complex with its class I MHC ligand. *Nature* **405**, 537-543 (2000).
182. K. S. Campbell, A. K. Purdy, Structure/function of human killer cell immunoglobulin-like receptors: lessons from polymorphisms, evolution, crystal structures and mutations. *Immunology* **132**, 315-325 (2011).
183. N. M. Valiante *et al.*, Functionally and structurally distinct NK cell receptor repertoires in the peripheral blood of two human donors. *Immunity* **7**, 739-751 (1997).
184. D. Pende *et al.*, Killer Ig-Like Receptors (KIRs): Their Role in NK Cell Modulation and Developments Leading to Their Clinical Exploitation. *Front Immunol* **10**, 1179 (2019).
185. S. G. Marsh *et al.*, Killer-cell immunoglobulin-like receptor (KIR) nomenclature report, 2002. *Immunogenetics* **55**, 220-226 (2003).
186. J. Feng, M. E. Call, K. W. Wucherpfennig, The assembly of diverse immune receptors is focused on a polar membrane-embedded interaction site. *PLoS Biol* **4**, e142 (2006).
187. L. L. Lanier, B. C. Corliss, J. Wu, C. Leong, J. H. Phillips, Immunoreceptor DAP12 bearing a tyrosine-based activation motif is involved in activating NK cells. *Nature* **391**, 703-707 (1998).
188. A. Kikuchi-Maki, T. L. Catina, K. S. Campbell, Cutting edge: KIR2DL4 transduces signals into human NK cells through association with the Fc receptor gamma protein. *J Immunol* **174**, 3859-3863 (2005).
189. S. Yusa, K. S. Campbell, Src homology region 2-containing protein tyrosine phosphatase-2 (SHP-2) can play a direct role in the inhibitory function of killer cell Ig-like receptors in human NK cells. *J Immunol* **170**, 4539-4547 (2003).
190. P. Bruhns, P. Marchetti, W. H. Fridman, E. Vivier, M. Daeron, Differential roles of N- and C-terminal immunoreceptor tyrosine-based inhibition motifs during inhibition of cell activation by killer cell inhibitory receptors. *J Immunol* **162**, 3168-3175 (1999).
191. E. Cisneros, M. Moraru, N. Gomez-Lozano, M. Lopez-Botet, C. Vilches, KIR2DL5: An Orphan Inhibitory Receptor Displaying Complex Patterns of Polymorphism and Expression. *Front Immunol* **3**, 289 (2012).
192. P. Hansasuta *et al.*, Recognition of HLA-A3 and HLA-A11 by KIR3DL2 is peptide-specific. *Eur J Immunol* **34**, 1673-1679 (2004).
193. J. P. Goodridge, A. Burian, N. Lee, D. E. Geraghty, HLA-F and MHC class I open conformers are ligands for NK cell Ig-like receptors. *J Immunol* **191**, 3553-3562 (2013).
194. S. Sivori *et al.*, A novel KIR-associated function: evidence that CpG DNA uptake and shuttling to early endosomes is mediated by KIR3DL2. *Blood* **116**, 1637-1647 (2010).
195. R. Biassoni *et al.*, The human leukocyte antigen (HLA)-C-specific "activatory" or "inhibitory" natural killer cell receptors display highly homologous extracellular domains but differ in their transmembrane and intracytoplasmic portions. *J Exp Med* **183**, 645-650 (1996).

196. G. David *et al.*, Large spectrum of HLA-C recognition by killer Ig-like receptor (KIR)2DL2 and KIR2DL3 and restricted C1 SPECIFICITY of KIR2DS2: dominant impact of KIR2DL2/KIR2DS2 on KIR2D NK cell repertoire formation. *J Immunol* **191**, 4778-4788 (2013).
197. C. A. Stewart *et al.*, Recognition of peptide-MHC class I complexes by activating killer immunoglobulin-like receptors. *Proc Natl Acad Sci U S A* **102**, 13224-13229 (2005).
198. K. van der Ploeg *et al.*, Modulation of Human Leukocyte Antigen-C by Human Cytomegalovirus Stimulates KIR2DS1 Recognition by Natural Killer Cells. *Front Immunol* **8**, 298 (2017).
199. M. M. Naiyer *et al.*, KIR2DS2 recognizes conserved peptides derived from viral helicases in the context of HLA-C. *Sci Immunol* **2**, (2017).
200. L. Thiruchelvam-Kyle *et al.*, The Activating Human NK Cell Receptor KIR2DS2 Recognizes a beta2-Microglobulin-Independent Ligand on Cancer Cells. *J Immunol* **198**, 2556-2567 (2017).
201. M. J. W. Sim *et al.*, Human NK cell receptor KIR2DS4 detects a conserved bacterial epitope presented by HLA-C. *Proc Natl Acad Sci U S A* **116**, 12964-12973 (2019).
202. M. Della Chiesa *et al.*, Evidence that the KIR2DS5 gene codes for a surface receptor triggering natural killer cell function. *Eur J Immunol* **38**, 2284-2289 (2008).
203. B. Husain *et al.*, A Platform for Extracellular Interactome Discovery Identifies Novel Functional Binding Partners for the Immune Receptors B7-H3/CD276 and PVR/CD155. *Mol Cell Proteomics* **18**, 2310-2323 (2019).
204. H. G. Hilton *et al.*, Mutation at positively selected positions in the binding site for HLA-C shows that KIR2DL1 is a more refined but less adaptable NK cell receptor than KIR2DL3. *J Immunol* **189**, 1418-1430 (2012).
205. A. K. Moesta *et al.*, Synergistic polymorphism at two positions distal to the ligand-binding site makes KIR2DL2 a stronger receptor for HLA-C than KIR2DL3. *J Immunol* **180**, 3969-3979 (2008).
206. H. G. Hilton *et al.*, Polymorphic HLA-C Receptors Balance the Functional Characteristics of KIR Haplotypes. *J Immunol* **195**, 3160-3170 (2015).
207. H. G. Hilton, P. Parham, Missing or altered self: human NK cell receptors that recognize HLA-C. *Immunogenetics* **69**, 567-579 (2017).
208. P. M. Saunders *et al.*, Killer cell immunoglobulin-like receptor 3DL1 polymorphism defines distinct hierarchies of HLA class I recognition. *J Exp Med* **213**, 791-807 (2016).
209. S. Rajagopalan, E. O. Long, A human histocompatibility leukocyte antigen (HLA)-G-specific receptor expressed on all natural killer cells. *J Exp Med* **189**, 1093-1100 (1999).
210. S. Rajagopalan *et al.*, Activation of NK cells by an endocytosed receptor for soluble HLA-G. *PLoS Biol* **4**, e9 (2006).
211. S. Rajagopalan, J. Fu, E. O. Long, Cutting edge: induction of IFN-gamma production but not cytotoxicity by the killer cell Ig-like receptor KIR2DL4 (CD158d) in resting NK cells. *J Immunol* **167**, 1877-1881 (2001).
212. M. P. Martin *et al.*, Epistatic interaction between KIR3DS1 and HLA-B delays the progression to AIDS. *Nat Genet* **31**, 429-434 (2002).
213. A. Lopez-Vazquez *et al.*, Protective effect of the HLA-Bw4I80 epitope and the killer cell immunoglobulin-like receptor 3DS1 gene against the development of hepatocellular carcinoma in patients with hepatitis C virus infection. *J Infect Dis* **192**, 162-165 (2005).
214. V. Beziat *et al.*, NK cell responses to cytomegalovirus infection lead to stable imprints in the human KIR repertoire and involve activating KIRs. *Blood* **121**, 2678-2688 (2013).

215. A. Poggi *et al.*, Extrathymic differentiation of T lymphocytes and natural killer cells from human embryonic liver precursors. *Proc Natl Acad Sci U S A* **90**, 4465-4469 (1993).
216. M. C. Mingari *et al.*, Interleukin-15-induced maturation of human natural killer cells from early thymic precursors: selective expression of CD94/NKG2-A as the only HLA class I-specific inhibitory receptor. *Eur J Immunol* **27**, 1374-1380 (1997).
217. J. Yu, A. G. Freud, M. A. Caligiuri, Location and cellular stages of natural killer cell development. *Trends Immunol* **34**, 573-582 (2013).
218. P. Vacca *et al.*, CD34+ hematopoietic precursors are present in human decidua and differentiate into natural killer cells upon interaction with stromal cells. *Proc Natl Acad Sci U S A* **108**, 2402-2407 (2011).
219. A. M. Abel, C. Yang, M. S. Thakar, S. Malarkannan, Natural Killer Cells: Development, Maturation, and Clinical Utilization. *Front Immunol* **9**, 1869 (2018).
220. K. Karre, H. G. Ljunggren, G. Piontek, R. Kiessling, Selective rejection of H-2-deficient lymphoma variants suggests alternative immune defence strategy. *Nature* **319**, 675-678 (1986).
221. H. G. Ljunggren, K. Karre, In search of the 'missing self': MHC molecules and NK cell recognition. *Immunol Today* **11**, 237-244 (1990).
222. N. Anfossi *et al.*, Human NK cell education by inhibitory receptors for MHC class I. *Immunity* **25**, 331-342 (2006).
223. M. Yawata *et al.*, MHC class I-specific inhibitory receptors and their ligands structure diverse human NK-cell repertoires toward a balance of missing self-response. *Blood* **112**, 2369-2380 (2008).
224. J. L. Petersen, C. R. Morris, J. C. Solheim, Virus evasion of MHC class I molecule presentation. *J Immunol* **171**, 4473-4478 (2003).
225. N. C. Fernandez *et al.*, A subset of natural killer cells achieves self-tolerance without expressing inhibitory receptors specific for self-MHC molecules. *Blood* **105**, 4416-4423 (2005).
226. N. T. Joncker, N. C. Fernandez, E. Treiner, E. Vivier, D. H. Raulet, NK cell responsiveness is tuned commensurate with the number of inhibitory receptors for self-MHC class I: the rheostat model. *J Immunol* **182**, 4572-4580 (2009).
227. V. Beziat, H. G. Hilton, P. J. Norman, J. A. Traherne, Deciphering the killer-cell immunoglobulin-like receptor system at super-resolution for natural killer and T-cell biology. *Immunology* **150**, 248-264 (2017).
228. S. Kim *et al.*, Licensing of natural killer cells by host major histocompatibility complex class I molecules. *Nature* **436**, 709-713 (2005).
229. J. P. Goodridge *et al.*, Remodeling of secretory lysosomes during education tunes functional potential in NK cells. *Nat Commun* **10**, 514 (2019).
230. D. H. Raulet, R. E. Vance, Self-tolerance of natural killer cells. *Nat Rev Immunol* **6**, 520-531 (2006).
231. P. Brodin, T. Lakshmikanth, S. Johansson, K. Karre, P. Hoglund, The strength of inhibitory input during education quantitatively tunes the functional responsiveness of individual natural killer cells. *Blood* **113**, 2434-2441 (2009).
232. E. Narni-Mancinelli *et al.*, Tuning of natural killer cell reactivity by NKp46 and Helios calibrates T cell responses. *Science* **335**, 344-348 (2012).
233. D. H. Raulet, R. E. Vance, C. W. McMahon, Regulation of the natural killer cell receptor repertoire. *Annu Rev Immunol* **19**, 291-330 (2001).
234. X. Y. Zhao *et al.*, Donor and host coexpressing KIR ligands promote NK education after allogeneic hematopoietic stem cell transplantation. *Blood Adv* **3**, 4312-4325 (2019).

235. P. Haas *et al.*, NK-cell education is shaped by donor HLA genotype after unrelated allogeneic hematopoietic stem cell transplantation. *Blood* **117**, 1021-1029 (2011).
236. J. Robinson *et al.*, The IPD and IMGT/HLA database: allele variant databases. *Nucleic Acids Res* **43**, D423-431 (2015).
237. L. Ruggeri *et al.*, Effectiveness of donor natural killer cell alloreactivity in mismatched hematopoietic transplants. *Science* **295**, 2097-2100 (2002).
238. A. Saad, L. S. Lamb, Ex vivo T-cell depletion in allogeneic hematopoietic stem cell transplant: past, present and future. *Bone Marrow Transplant* **52**, 1241-1248 (2017).
239. L. Ruggeri *et al.*, NK cell alloreactivity and allogeneic hematopoietic stem cell transplantation. *Blood Cells Mol Dis* **40**, 84-90 (2008).
240. M. Bosch, F. M. Khan, J. Storek, Immune reconstitution after hematopoietic cell transplantation. *Curr Opin Hematol* **19**, 324-335 (2012).
241. L. Minculescu *et al.*, Early Natural Killer Cell Reconstitution Predicts Overall Survival in T Cell-Replete Allogeneic Hematopoietic Stem Cell Transplantation. *Biol Blood Marrow Transplant* **22**, 2187-2193 (2016).
242. D. Pende *et al.*, Anti-leukemia activity of alloreactive NK cells in KIR ligand-mismatched haploidentical HSCT for pediatric patients: evaluation of the functional role of activating KIR and redefinition of inhibitory KIR specificity. *Blood* **113**, 3119-3129 (2009).
243. S. Cooley *et al.*, Donors with group B KIR haplotypes improve relapse-free survival after unrelated hematopoietic cell transplantation for acute myelogenous leukemia. *Blood* **113**, 726-732 (2009).
244. S. Cooley *et al.*, Donor killer cell Ig-like receptor B haplotypes, recipient HLA-C1, and HLA-C mismatch enhance the clinical benefit of unrelated transplantation for acute myelogenous leukemia. *J Immunol* **192**, 4592-4600 (2014).
245. J. M. Venstrom *et al.*, HLA-C-dependent prevention of leukemia relapse by donor activating KIR2DS1. *N Engl J Med* **367**, 805-816 (2012).
246. G. Pittari *et al.*, NK cell tolerance of self-specific activating receptor KIR2DS1 in individuals with cognate HLA-C2 ligand. *J Immunol* **190**, 4650-4660 (2013).
247. F. Babor *et al.*, Presence of centromeric but absence of telomeric group B KIR haplotypes in stem cell donors improve leukaemia control after HSCT for childhood ALL. *Bone Marrow Transplant* **54**, 1847-1858 (2019).
248. H. Zhou *et al.*, Donor selection for killer immunoglobulin-like receptors B haplotype of the centromeric motifs can improve the outcome after HLA-identical sibling hematopoietic stem cell transplantation. *Biol Blood Marrow Transplant* **20**, 98-105 (2014).
249. L. Oevermann *et al.*, KIR B haplotype donors confer a reduced risk for relapse after haploidentical transplantation in children with ALL. *Blood* **124**, 2744-2747 (2014).
250. H. J. Symons *et al.*, Improved survival with inhibitory killer immunoglobulin receptor (KIR) gene mismatches and KIR haplotype B donors after nonmyeloablative, HLA-haploidentical bone marrow transplantation. *Biol Blood Marrow Transplant* **16**, 533-542 (2010).
251. A. Mancusi *et al.*, Haploidentical hematopoietic transplantation from KIR ligand-mismatched donors with activating KIRs reduces nonrelapse mortality. *Blood* **125**, 3173-3182 (2015).
252. M. R. Verneris *et al.*, Investigation of donor KIR content and matching in children undergoing hematopoietic cell transplantation for acute leukemia. *Blood Adv* **4**, 1350-1356 (2020).

253. A. Shimoni *et al.*, Killer cell immunoglobulin-like receptor ligand mismatching and outcome after haploidentical transplantation with post-transplant cyclophosphamide. *Leukemia* **33**, 230-239 (2019).
254. C. Willem *et al.*, Impact of KIR/HLA Incompatibilities on NK Cell Reconstitution and Clinical Outcome after T Cell-Replete Haploidentical Hematopoietic Stem Cell Transplantation with Posttransplant Cyclophosphamide. *J Immunol* **202**, 2141-2152 (2019).
255. A. Moffett-King, Natural killer cells and pregnancy. *Nat Rev Immunol* **2**, 656-663 (2002).
256. P. Le Bouteiller, J. Tabiasco, Killers become builders during pregnancy. *Nat Med* **12**, 991-992 (2006).
257. A. King *et al.*, Surface expression of HLA-C antigen by human extravillous trophoblast. *Placenta* **21**, 376-387 (2000).
258. R. Hackmon *et al.*, Definitive class I human leukocyte antigen expression in gestational placentation: HLA-F, HLA-E, HLA-C, and HLA-G in extravillous trophoblast invasion on placentation, pregnancy, and parturition. *Am J Reprod Immunol* **77**, (2017).
259. J. Hanna *et al.*, Decidual NK cells regulate key developmental processes at the human fetal-maternal interface. *Nat Med* **12**, 1065-1074 (2006).
260. S. Verma, A. King, Y. W. Loke, Expression of killer cell inhibitory receptors on human uterine natural killer cells. *Eur J Immunol* **27**, 979-983 (1997).
261. A. Moffett, O. Chazara, F. Colucci, M. H. Johnson, Variation of maternal KIR and fetal HLA-C genes in reproductive failure: too early for clinical intervention. *Reprod Biomed Online* **33**, 763-769 (2016).
262. P. R. Kennedy *et al.*, Activating KIR2DS4 Is Expressed by Uterine NK Cells and Contributes to Successful Pregnancy. *J Immunol* **197**, 4292-4300 (2016).
263. M. Shiroishi *et al.*, Human inhibitory receptors Ig-like transcript 2 (ILT2) and ILT4 compete with CD8 for MHC class I binding and bind preferentially to HLA-G. *Proc Natl Acad Sci U S A* **100**, 8856-8861 (2003).
264. C. W. Redman, I. L. Sargent, Latest advances in understanding preeclampsia. *Science* **308**, 1592-1594 (2005).
265. D. Alecsandru *et al.*, Maternal KIR haplotype influences live birth rate after double embryo transfer in IVF cycles in patients with recurrent miscarriages and implantation failure. *Hum Reprod* **29**, 2637-2643 (2014).
266. S. E. Hiby *et al.*, Maternal activating KIRs protect against human reproductive failure mediated by fetal HLA-C2. *J Clin Invest* **120**, 4102-4110 (2010).
267. S. E. Hiby *et al.*, Combinations of maternal KIR and fetal HLA-C genes influence the risk of preeclampsia and reproductive success. *J Exp Med* **200**, 957-965 (2004).
268. S. E. Hiby *et al.*, Association of maternal killer-cell immunoglobulin-like receptors and parental HLA-C genotypes with recurrent miscarriage. *Hum Reprod* **23**, 972-976 (2008).
269. S. E. Hiby *et al.*, Maternal KIR in combination with paternal HLA-C2 regulate human birth weight. *J Immunol* **192**, 5069-5073 (2014).
270. A. Nakimuli *et al.*, A KIR B centromeric region present in Africans but not Europeans protects pregnant women from pre-eclampsia. *Proc Natl Acad Sci U S A* **112**, 845-850 (2015).
271. J. H. Blokhuis *et al.*, KIR2DS5 allotypes that recognize the C2 epitope of HLA-C are common among Africans and absent from Europeans. *Immun Inflamm Dis* **5**, 461-468 (2017).
272. T. Ichinohe *et al.*, Feasibility of HLA-haploidentical hematopoietic stem cell transplantation between noninherited maternal antigen (NIMA)-mismatched family

members linked with long-term fetomaternal microchimerism. *Blood* **104**, 3821-3828 (2004).
273. T. Ichinohe, T. Teshima, K. Matsuoka, E. Maruya, H. Saji, Fetal-maternal microchimerism: impact on hematopoietic stem cell transplantation. *Curr Opin Immunol* **17**, 546-552 (2005).
274. M. Noris *et al.*, Thymic microchimerism correlates with the outcome of tolerance-inducing protocols for solid organ transplantation. *J Am Soc Nephrol* **12**, 2815-2826 (2001).
275. M. S. Kimpo, B. Oh, S. Lee, The Role of Natural Killer Cells as a Platform for Immunotherapy in Pediatric Cancers. *Curr Oncol Rep* **21**, 93 (2019).
276. J. E. Rubnitz *et al.*, NKAML: a pilot study to determine the safety and feasibility of haploidentical natural killer cell transplantation in childhood acute myeloid leukemia. *J Clin Oncol* **28**, 955-959 (2010).
277. A. Curti *et al.*, Successful transfer of alloreactive haploidentical KIR ligand-mismatched natural killer cells after infusion in elderly high risk acute myeloid leukemia patients. *Blood* **118**, 3273-3279 (2011).
278. U. Koehl *et al.*, Advances in clinical NK cell studies: Donor selection, manufacturing and quality control. *Oncoimmunology* **5**, e1115178 (2016).
279. S. Cooley *et al.*, First-in-human trial of rhIL-15 and haploidentical natural killer cell therapy for advanced acute myeloid leukemia. *Blood Adv* **3**, 1970-1980 (2019).
280. W. Hu, G. Wang, D. Huang, M. Sui, Y. Xu, Cancer Immunotherapy Based on Natural Killer Cells: Current Progress and New Opportunities. *Front Immunol* **10**, 1205 (2019).
281. N. Vey *et al.*, A phase 1 trial of the anti-inhibitory KIR mAb IPH2101 for AML in complete remission. *Blood* **120**, 4317-4323 (2012).
282. D. M. Benson, Jr. *et al.*, A Phase I Trial of the Anti-KIR Antibody IPH2101 and Lenalidomide in Patients with Relapsed/Refractory Multiple Myeloma. *Clin Cancer Res* **21**, 4055-4061 (2015).
283. M. Carlsten *et al.*, Checkpoint Inhibition of KIR2D with the Monoclonal Antibody IPH2101 Induces Contraction and Hyporesponsiveness of NK Cells in Patients with Myeloma. *Clin Cancer Res* **22**, 5211-5222 (2016).
284. J. L. Shirley, Y. P. de Jong, C. Terhorst, R. W. Herzog, Immune Responses to Viral Gene Therapy Vectors. *Mol Ther* **28**, 709-722 (2020).
285. J. D. Suerth, V. Labenski, A. Schambach, Alpharetroviral vectors: from a cancer-causing agent to a useful tool for human gene therapy. *Viruses* **6**, 4811-4838 (2014).
286. J. D. Suerth *et al.*, Efficient generation of gene-modified human natural killer cells via alpharetroviral vectors. *J Mol Med (Berl)* **94**, 83-93 (2016).
287. M. Yamashita, M. Emerman, Retroviral infection of non-dividing cells: old and new perspectives. *Virology* **344**, 88-93 (2006).
288. R. S. Mitchell *et al.*, Retroviral DNA integration: ASLV, HIV, and MLV show distinct target site preferences. *PLoS Biol* **2**, E234 (2004).
289. T. Sutlu *et al.*, Inhibition of intracellular antiviral defense mechanisms augments lentiviral transduction of human natural killer cells: implications for gene therapy. *Hum Gene Ther* **23**, 1090-1100 (2012).
290. J. D. Brandstadter, Y. Yang, Natural killer cell responses to viral infection. *J Innate Immun* **3**, 274-279 (2011).
291. L. L. Lanier, Evolutionary struggles between NK cells and viruses. *Nat Rev Immunol* **8**, 259-268 (2008).

292. S. Muller *et al.*, High Cytotoxic Efficiency of Lentivirally and Alpharetrovirally Engineered CD19-Specific Chimeric Antigen Receptor Natural Killer Cells Against Acute Lymphoblastic Leukemia. *Front Immunol* **10**, 3123 (2019).
293. E. C. Sayitoglu *et al.*, Boosting Natural Killer Cell-Mediated Targeting of Sarcoma Through DNAM-1 and NKG2D. *Front Immunol* **11**, 40 (2020).
294. Y. H. Chang *et al.*, A chimeric receptor with NKG2D specificity enhances natural killer cell activation and killing of tumor cells. *Cancer Res* **73**, 1777-1786 (2013).
295. T. Kamiya, Y. H. Chang, D. Campana, Expanded and Activated Natural Killer Cells for Immunotherapy of Hepatocellular Carcinoma. *Cancer Immunol Res* **4**, 574-581 (2016).
296. C. M. Artlett, J. B. Smith, S. A. Jimenez, Identification of fetal DNA and cells in skin lesions from women with systemic sclerosis. *N Engl J Med* **338**, 1186-1191 (1998).
297. U. Mahmood, K. O'Donoghue, Microchimeric fetal cells play a role in maternal wound healing after pregnancy. *Chimerism* **5**, 40-52 (2014).
298. M. Paximadis *et al.*, Human leukocyte antigen class I (A, B, C) and II (DRB1) diversity in the black and Caucasian South African population. *Hum Immunol* **73**, 80-92 (2012).
299. S. Rajagopalan, E. O. Long, Understanding how combinations of HLA and KIR genes influence disease. *J Exp Med* **201**, 1025-1029 (2005).
300. F. Cichocki, J. S. Miller, S. K. Anderson, Killer immunoglobulin-like receptor transcriptional regulation: a fascinating dance of multiple promoters. *J Innate Immun* **3**, 242-248 (2011).
301. S. Cooley, P. Parham, J. S. Miller, Strategies to activate NK cells to prevent relapse and induce remission following hematopoietic stem cell transplantation. *Blood* **131**, 1053-1062 (2018).
302. M. A. Rizzo, G. H. Springer, B. Granada, D. W. Piston, An improved cyan fluorescent protein variant useful for FRET. *Nat Biotechnol* **22**, 445-449 (2004).
303. R. Y. Tsien, The green fluorescent protein. *Annu Rev Biochem* **67**, 509-544 (1998).
304. K. Weber, U. Bartsch, C. Stocking, B. Fehse, A multicolor panel of novel lentiviral "gene ontology" (LeGO) vectors for functional gene analysis. *Mol Ther* **16**, 698-706 (2008).
305. G. Maki, H. G. Klingemann, J. A. Martinson, Y. K. Tam, Factors regulating the cytotoxic activity of the human natural killer cell line, NK-92. *J Hematother Stem Cell Res* **10**, 369-383 (2001).
306. W. R. Beyer, M. Westphal, W. Ostertag, D. von Laer, Oncoretrovirus and lentivirus vectors pseudotyped with lymphocytic choriomeningitis virus glycoprotein: generation, concentration, and broad host range. *J Virol* **76**, 1488-1495 (2002).
307. V. Sandrin *et al.*, Lentiviral vectors pseudotyped with a modified RD114 envelope glycoprotein show increased stability in sera and augmented transduction of primary lymphocytes and CD34+ cells derived from human and nonhuman primates. *Blood* **100**, 823-832 (2002).
308. D. Fenard *et al.*, Vectofusin-1, a new viral entry enhancer, strongly promotes lentiviral transduction of human hematopoietic stem cells. *Mol Ther Nucleic Acids* **2**, e90 (2013).
309. C. Radek *et al.*, Vectofusin-1 Improves Transduction of Primary Human Cells with Diverse Retroviral and Lentiviral Pseudotypes, Enabling Robust, Automated Closed-System Manufacturing. *Hum Gene Ther* **30**, 1477-1493 (2019).
310. D. Drandi *et al.*, Minimal Residual Disease Detection by Droplet Digital PCR in Multiple Myeloma, Mantle Cell Lymphoma, and Follicular Lymphoma: A Comparison with Real-Time PCR. *J Mol Diagn* **17**, 652-660 (2015).
311. B. J. Hindson *et al.*, High-throughput droplet digital PCR system for absolute quantitation of DNA copy number. *Anal Chem* **83**, 8604-8610 (2011).

312. W. Ye *et al.*, Accurate quantitation of circulating cell-free mitochondrial DNA in plasma by droplet digital PCR. *Anal Bioanal Chem* **409**, 2727-2735 (2017).
313. E. D'Aversa *et al.*, Non-invasive fetal sex diagnosis in plasma of early weeks pregnants using droplet digital PCR. *Mol Med* **24**, 14 (2018).
314. H. Do, A. Dobrovic, Sequence artifacts in DNA from formalin-fixed tissues: causes and strategies for minimization. *Clin Chem* **61**, 64-71 (2015).
315. D. G. Wang *et al.*, Large-scale identification, mapping, and genotyping of single-nucleotide polymorphisms in the human genome. *Science* **280**, 1077-1082 (1998).
316. M. Grskovic *et al.*, Validation of a Clinical-Grade Assay to Measure Donor-Derived Cell-Free DNA in Solid Organ Transplant Recipients. *J Mol Diagn* **18**, 890-902 (2016).
317. J. Kim, I. S. Hwang, S. Shin, J. R. Choi, S. T. Lee, SNP-based next-generation sequencing reveals low-level mixed chimerism after allogeneic hematopoietic stem cell transplantation. *Ann Hematol* **97**, 1731-1734 (2018).
318. H. Andrikovics *et al.*, Current Trends in Applications of Circulatory Microchimerism Detection in Transplantation. *Int J Mol Sci* **20**, (2019).
319. L. S. Loubiere *et al.*, Maternal microchimerism in healthy adults in lymphocytes, monocyte/macrophages and NK cells. *Lab Invest* **86**, 1185-1192 (2006).
320. H. S. Gammill *et al.*, Pregnancy, microchimerism, and the maternal grandmother. *PLoS One* **6**, e24101 (2011).
321. K. Khosrotehrani, D. W. Bianchi, Multi-lineage potential of fetal cells in maternal tissue: a legacy in reverse. *J Cell Sci* **118**, 1559-1563 (2005).
322. F. Prosper, D. Stroncek, C. M. Verfaillie, Phenotypic and functional characterization of long-term culture-initiating cells present in peripheral blood progenitor collections of normal donors treated with granulocyte colony-stimulating factor. *Blood* **88**, 2033-2042 (1996).
323. A. H. Yin *et al.*, AC133, a novel marker for human hematopoietic stem and progenitor cells. *Blood* **90**, 5002-5012 (1997).
324. Y. J. Summers *et al.*, AC133+ G0 cells from cord blood show a high incidence of long-term culture-initiating cells and a capacity for more than 100 million-fold amplification of colony-forming cells in vitro. *Stem Cells* **22**, 704-715 (2004).
325. P. R. Gordon *et al.*, Large-scale isolation of CD133+ progenitor cells from G-CSF mobilized peripheral blood stem cells. *Bone Marrow Transplant* **31**, 17-22 (2003).
326. R. Handgretinger, S. Kuci, CD133-Positive Hematopoietic Stem Cells: From Biology to Medicine. *Adv Exp Med Biol* **777**, 99-111 (2013).
327. K. Sumide *et al.*, A revised road map for the commitment of human cord blood CD34-negative hematopoietic stem cells. *Nat Commun* **9**, 2202 (2018).
328. A. Finkielsztein, A. C. Schlinker, L. Zhang, W. M. Miller, S. K. Datta, Human megakaryocyte progenitors derived from hematopoietic stem cells of normal individuals are MHC class II-expressing professional APC that enhance Th17 and Th1/Th17 responses. *Immunol Lett* **163**, 84-95 (2015).
329. P. Cunin, P. A. Nigrovic, Megakaryocytes as immune cells. *J Leukoc Biol* **105**, 1111-1121 (2019).
330. K. O'Donoghue *et al.*, Microchimeric fetal cells cluster at sites of tissue injury in lung decades after pregnancy. *Reprod Biomed Online* **16**, 382-390 (2008).
331. V. Cirello *et al.*, Fetal cell microchimerism in papillary thyroid cancer: a possible role in tumor damage and tissue repair. *Cancer Res* **68**, 8482-8488 (2008).
332. V. K. Gadi, Fetal microchimerism in breast from women with and without breast cancer. *Breast Cancer Res Treat* **121**, 241-244 (2010).

333. K. O'Donoghue *et al.*, Microchimerism in female bone marrow and bone decades after fetal mesenchymal stem-cell trafficking in pregnancy. *Lancet* **364**, 179-182 (2004).
334. A. Chapel *et al.*, Peptide-specific engagement of the activating NK cell receptor KIR2DS1. *Sci Rep* **7**, 2414 (2017).
335. C. T. Tiemessen *et al.*, Cutting Edge: Unusual NK cell responses to HIV-1 peptides are associated with protection against maternal-infant transmission of HIV-1. *J Immunol* **182**, 5914-5918 (2009).
336. V. Stary, G. Stary, NK Cell-Mediated Recall Responses: Memory-Like, Adaptive, or Antigen-Specific? *Front Cell Infect Microbiol* **10**, 208 (2020).
337. S. Cooley *et al.*, Donor selection for natural killer cell receptor genes leads to superior survival after unrelated transplantation for acute myelogenous leukemia. *Blood* **116**, 2411-2419 (2010).
338. M. Pfeiffer *et al.*, Intensity of HLA class I expression and KIR-mismatch determine NK-cell mediated lysis of leukaemic blasts from children with acute lymphatic leukaemia. *Br J Haematol* **138**, 97-100 (2007).
339. D. A. Lee *et al.*, Haploidentical Natural Killer Cells Infused before Allogeneic Stem Cell Transplantation for Myeloid Malignancies: A Phase I Trial. *Biol Blood Marrow Transplant* **22**, 1290-1298 (2016).
340. A. Romanski *et al.*, Mechanisms of resistance to natural killer cell-mediated cytotoxicity in acute lymphoblastic leukemia. *Exp Hematol* **33**, 344-352 (2005).
341. M. Gamliel *et al.*, Trained Memory of Human Uterine NK Cells Enhances Their Function in Subsequent Pregnancies. *Immunity* **48**, 951-962 e955 (2018).
342. T. E. C. Kieffer, A. Laskewitz, S. A. Scherjon, M. M. Faas, J. R. Prins, Memory T Cells in Pregnancy. *Front Immunol* **10**, 625 (2019).
343. L. Ruggeri *et al.*, Tregs Suppress GvHD at the Periphery and Unleash the Gvl Effect in the Bone Marrow. *Blood* **124**, 842-842 (2014).
344. I. Odak *et al.*, Focusing of the regulatory T-cell repertoire after allogeneic stem cell transplantation indicates protection from graft-versus-host disease. *Haematologica* **104**, e577-e580 (2019).
345. I. Choi *et al.*, Donor-derived natural killer cells infused after human leukocyte antigen-haploidentical hematopoietic cell transplantation: a dose-escalation study. *Biol Blood Marrow Transplant* **20**, 696-704 (2014).
346. M. Stern *et al.*, Pre-emptive immunotherapy with purified natural killer cells after haploidentical SCT: a prospective phase II study in two centers. *Bone Marrow Transplant* **48**, 433-438 (2013).
347. D. Finkelshtein, A. Werman, D. Novick, S. Barak, M. Rubinstein, LDL receptor and its family members serve as the cellular receptors for vesicular stomatitis virus. *Proc Natl Acad Sci U S A* **110**, 7306-7311 (2013).
348. Y. Gong *et al.*, Rosuvastatin Enhances VSV-G Lentiviral Transduction of NK Cells via Upregulation of the Low-Density Lipoprotein Receptor. *Mol Ther Methods Clin Dev* **17**, 634-646 (2020).
349. J. E. Rasko, J. L. Battini, R. J. Gottschalk, I. Mazo, A. D. Miller, The RD114/simian type D retrovirus receptor is a neutral amino acid transporter. *Proc Natl Acad Sci U S A* **96**, 2129-2134 (1999).
350. H. Jensen, M. Potempa, D. Gotthardt, L. L. Lanier, Cutting Edge: IL-2-Induced Expression of the Amino Acid Transporters SLC1A5 and CD98 Is a Prerequisite for NKG2D-Mediated Activation of Human NK Cells. *J Immunol* **199**, 1967-1972 (2017).

351. R. Bari *et al.*, A Distinct Subset of Highly Proliferative and Lentiviral Vector (LV)-Transducible NK Cells Define a Readily Engineered Subset for Adoptive Cellular Therapy. *Front Immunol* **10**, 2001 (2019).
352. A. B. L. Colamartino *et al.*, Efficient and Robust NK-Cell Transduction With Baboon Envelope Pseudotyped Lentivector. *Front Immunol* **10**, 2873 (2019).
353. D. Hoffmann *et al.*, Detailed comparison of retroviral vectors and promoter configurations for stable and high transgene expression in human induced pluripotent stem cells. *Gene Ther* **24**, 298-307 (2017).
354. F. Herbst *et al.*, Impaired Lentiviral Transgene Expression In Vivo Caused by Massive Methylation of SFFV Promoter Sequences. *Blood* **116**, 3760-3760 (2010).
355. A. Kaminski, M. T. Howell, R. J. Jackson, Initiation of encephalomyocarditis virus RNA translation: the authentic initiation site is not selected by a scanning mechanism. *EMBO J* **9**, 3753-3759 (1990).
356. A. L. Szymczak, D. A. Vignali, Development of 2A peptide-based strategies in the design of multicistronic vectors. *Expert Opin Biol Ther* **5**, 627-638 (2005).
357. Z. Liu *et al.*, Systematic comparison of 2A peptides for cloning multi-genes in a polycistronic vector. *Sci Rep* **7**, 2193 (2017).
358. W. R. Frazier, N. Steiner, L. Hou, S. Dakshanamurthy, C. K. Hurley, Allelic variation in KIR2DL3 generates a KIR2DL2-like receptor with increased binding to its HLA-C ligand. *J Immunol* **190**, 6198-6208 (2013).
359. R. Godal *et al.*, Natural killer cell killing of acute myelogenous leukemia and acute lymphoblastic leukemia blasts by killer cell immunoglobulin-like receptor-negative natural killer cells after NKG2A and LIR-1 blockade. *Biol Blood Marrow Transplant* **16**, 612-621 (2010).
360. K. Zwolinska *et al.*, The effects of killer cell immunoglobulin-like receptor (KIR) genes on susceptibility to HIV-1 infection in the Polish population. *Immunogenetics* **68**, 327-337 (2016).
361. S. Aranda-Romo *et al.*, Killer-cell immunoglobulin-like receptors (KIR) in severe A (H1N1) 2009 influenza infections. *Immunogenetics* **64**, 653-662 (2012).
362. L. Zhi-ming *et al.*, Polymorphisms of killer cell immunoglobulin-like receptor gene: possible association with susceptibility to or clearance of hepatitis B virus infection in Chinese Han population. *Croat Med J* **48**, 800-806 (2007).
363. L. G. Alves, R. Rajalingam, F. Canavez, A novel real-time PCR method for KIR genotyping. *Tissue Antigens* **73**, 188-191 (2009).
364. C. Vilches, J. Castano, N. Gomez-Lozano, E. Estefania, Facilitation of KIR genotyping by a PCR-SSP method that amplifies short DNA fragments. *Tissue Antigens* **70**, 415-422 (2007).
365. C. Frohn *et al.*, DNA typing for natural killer cell inhibiting HLA-Cw groups NK1 and NK2 by PCR-SSP. *J Immunol Methods* **218**, 155-160 (1998).
366. B. Fehse, O. S. Kustikova, M. Bubenheim, C. Baum, Pois(s)on--it's a question of dose. *Gene Ther* **11**, 879-881 (2004).
367. H. Luthman, G. Magnusson, High efficiency polyoma DNA transfection of chloroquine treated cells. *Nucleic Acids Res* **11**, 1295-1308 (1983).

8. Appendix

8.1 List of hazardous substances according to GHS classification

Substances	GHS symbol	H Statement	P Statement
2-Propanol	02, 07	H225, H319, H336	P210, P280, P305+P351+P338,
Ampicillin	08	H334, H317	P261, P272, P280, P284, P302+P352, P304+P341, P321, P333+P313, P342+P311, P363, P501
BD Golgi Stop™ Protein Transport Inhibitor	02, 07,	H225, H302	P210, P233, P240, P241, P242, P243, P280, P264, P270, P303+P361+P353, P301+P312, P330, P370+P378, P304, P235
Calcium chloride ($CaCl_2$)	07	H319	P280, P305+P351+P338+P313
Chloroquine	07	H302	
Ethanol (pure)	02, 07	H225, H319	P210, P233, P305+P351+P338
Ethidium bromide	06, 08	H302, H330, H341	P201, P260, P280, P304+P340, P308+P311
Formaldehyde (37%)	05, 06, 08	H301+H311+H331, H314, H317, H335, H341, H350, H370	P260, P280, P303, P361, P353, P304+P340, P305+P351+P338, P308+P311
Ionomycin, calcium salt	07	H302	P301+P312, P264, P330, P270
Penicillin/Streptomycin	07	H302, H317	P280
QIAprep Spin Miniprep Kit	02, 05, 07, 08	H315, H319, H290, H225, H336, H334	P210, P261, P280, P284, P290, P304+P340, P342+P311
QIAquick Gel Extraction Kit	05, 07	H302, H318, H412	P280, P305+P351+P338+P310
Sodium hydroxide (NaOH)	05	H290	P234, P390
Triton X-100	05, 07, 09	H302, H318, H411	P270, P273, P280, P305+P351+P338, P310
TRIzol™ Reagent	05, 06, 08	H301, H311, H331, H314, H335, H341, H373, H412	P201, P261, P264, P280, P273, P301+P310, P302+P352, P303+P361+P353, P204+P340, P305+P351+P338, P403+P233, P501

8.2 Primer sequences

8.2.1 KIR genotyping primer sequences

Table 33: Primer sequences for KIR genotyping described by (*364*). FW: forward primer; Rev reverse primer.

KIR	Orientation	Sequence 5'→3'	bp	TM	SD
2DL1	Fw	GTT GGT CAG ATG TCA TGT TTGA A	142	83.62	0.25
	Rev	CCT GCC AGG TCT TGC G			
2DL2	Fw	AAA CCT TCT CTC TCA GCC CA	142	87.05	0.25
	Rev	GCC CTG CAG AGA ACC TAC A			
2DL3	Fw	AGA CCC TCA GGA GGT GA	156	82.536	0.22
	Rev	CAG GAG ACA ACT TTG GAT CA			

2DL4	Fw	TCA GGA CAA GCC CTT CTG C	131	85.92	0.32
	Rev	GGA CAG GGA CCC CAT CTT TC			
2DL5	Fw	ATC TAT CCA GGG AGG GGA G	147	86.81	0.33
	Rev	CAT AGG GTG AGT CAT GGA G			
2DP1	Fw	CGA CAC TTT GCA CCT CAC G	141	84.69	0.23
	Rev	GGA GCT GAC AAC TGA TG			
2DS1	Fw	TCT CCA TCA GTC GCA TGA A	96	82.78	0.18
	Rev	GGT CAC TGG GAG CTG AC			
2DS2	Fw	TGC ACA GAG AGG GGA AGT A	110	82.72	0.17
	Rev	CCC TGC AAG GTC TTG CA			
2DS3	Fw	AAA CCT TCT CTC TCA GCC CA	158	84.88	0.54
	Rev	GCA TCT GTA GGT TCC TCC T	213	87.45	0.10
2DS4	Fw	GGT TCA GGC AGG AGA GAA T	133	85.2	0.27
	Rev	CTG GAA TGT TCC GTK GAT G	111		
2DS5	Fw	AGA GAG GGG ACG TTT AAC C	147	84.47	0.18
	Rev	CTG ATA GGG GGA GTG AGT			
3DL1	Fw	TCC ATC GGT CCC ATG ATG TT	109	83.94	0.19
	Rev	CCA CGA TGT CCA GGG GA			
3DL2	Fw	CAT GAA CGT AGG CTC CG	131	88.08	0.22
	Rev	GAC CAC ACG CAG GGC AG			
3DL3	Fw	AAT GTT GGT CAG ATG TCA G	196	87.01	0.25
	Rev	GCY GAC AAC TCA TAG GGTA			
3DP1f	Fw	GTA CGT CAC CCT CCC ATG ATG TA	398	90.53	0.21
	Rev	GAA AAC GGT GTT TCG GAA TAC			
3DS1	Fw	CAT CAG TTC CAT GAT GCG	107	84.25	0.18
	Rev	CCA CGA TGT CCA GGG GA			
Control 1 Necdin. MAGE	Fw	GGC TGC ACC TGA GGC TAA	335	91.41	0.14
family member	Rev	GCC CCA AAA GAA CTC GTA TTC			
Control 2	Fw	TTA CCC AGA GCC CTA TCG TTC T	352	78.75	0.05
galactocerebrosidase	Rev	GTC TGC CCA TCA CCA CCT ATT			

8.2.2 HLA-C genotyping primer sequences

Table 34: Primer sequences for HLA-C genotyping.

Name	Sequence 5'→3'	Specification	Described
NK1	GTT GTA GTA GCC GCG CAG T	C2 allele	
NK2	GTT GTA GTA GCC GCG CAG G	C1 allele	
NK common	CGC CGC GAG TCC RAG AGG	C1 and C2 allele	(*365*)
CRP fw	CCA GCC TCT CTC ATG CTT TTG GCC AGA CAG	C-reactive protein	
CRP rev	GGG TCG AGG ACA GTT CCG TGT AGA AGT GGA	C-reactive protein	

8.2.3 KIR cloning primer sequences

Table 35: Primer sequences for KIR cloning.

Primer	Sequence 5'→3'	Used for

2DL1_N1_fw	GTC GCG GCT GCC TGT CT	2DL1 nested PCR 1
2DL1_N1_rev	CCG GTT TTG AGA CAG GGC TGT TG	2DL1 nested PCR 1
2DL1_N2_fw	TGC TCC GGC AGC ACC ATG	2DL1 nested PCR 2
2DL1_N2_rev	CTA GAA GAC GCC CTC AAG GCC	2DL1 nested PCR 2
2DS1_N1_fw	CAC CGG CAG CAC CAT GTC	2DS1 nested PCR 1
2DS1_N1_rev	CCT CTC AGA AGG GCG AGTG	2DS1 nested PCR 1
2DS1_N2_fw	AGC ACC ATG TCG CTC ACG	2DS1 nested PCR 2
2DS1_N2_fw	AGC ACC ATG TCG CTCA CG	2DS1 nested PCR 2
2DS1_N2_rev	CTC TGT GTG AAA ACA CAG TGA TCC	2DS1 nested PCR 2
2DL2_N1_fw	GGC CGC CTG TCT GCA CA	2DL2 nested PCR 1
2DL2_N1_rev	TGA GAC AGG GCT GTT GTC TCC C	2DL2 nested PCR 1
2DL2_N2_fw	GTC TGC ACA GAC AGC ACC ATG T	2DL2 nested PCR 2
2DL2_N2_rev	GAA GAC GCC CTC AAG GCC T	2DL2 nested PCR 2
2DS2_N1_fw	CCG CCT GTC TGC ACA GAC	2DS2 nested PCR 1
2DS2_N1_rev	CCT CTC AGA AGG GCG AGT GAT T	2DS2 nested PCR 1
2DS2_N2_fw	GCA CAG ACA GCA CCA TGT C	2DS2 nested PCR 2
2DS2_N2_rev	CTC TGT GTG AAA ACA CAG TGA TCC	2DS2 nested PCR 2
Alpha_ampl	TGC GGC TTA GGG AGG CAG AAG	Sequencing primer
rev_after IRES	CGG AAT TTA CGT AGC GGC CG	Sequencing primer

8.2.4 Primer and probe sequences for marker selection and ddPCR

Table 36: Primer and probes for marker selection and ddPCR.

Name	Primer	Sequence 5'->3'	Label for ddPCR
01b	Fw	GTA CCG GGT CTC CAC CAG G	-
01ab	Rev	GGG AAA GTC ACT CAC CCA AGG	-
01ab	Probe	CTG GGC CAG AAT CTT GGT CCT CAC A	5'-FAM 3'-BHQ1
3	Fw	CTT TTG CTT TCT GTT TCT TAA GGG C	-
3	Rev	TCA ATC TTT GGG CAG GTT GAA	-
3	Probe	CAT ACG TGC ACA GGG TCC CCG AGT	5'-FAM 3'-BHQ1
04ab	Fw	CTG GTG CCC ACA GTT ACG CT	-
04a	Rev	AAG GAT GCG TGA CTG CTA TGG	-
04b	Rev	AGG ATG CGT GAC TGC TCC TC	-
04ab	Probe	TCC TGG CAG TGT GGT CCC TTC AGA A	5'-FAM 3'-BHQ1
05b	Fw	AGT TAA AGT AGA CAC GGC CTC CC	-
05ab	Rev	CAT CCC CAC ATA CGG AAA AGA	-
05ab	Probe	CCC TGG ACA CTG AAA ACA GGC AAT CCT	5'-FAM 3'-BHQ1
6	Fw	CAG TCA CCC CGT GAA GTC CT	-
6	Rev	TTT CCC CCA TCT GCC TAT TG	-
6	Probe	CCC ATC CAT CTT CCC TAC CAG ACC AGG	5'-FAM 3'-BHQ1
07a	Fw	TGG TAT TGG CTT TAA AAT ACT GGG	-
07b	Fw	GGT ATT GGC TTT AAA ATA CTC AAC C	-
07a	Rev	TGT ACC CAA AAC TCA GCT GCA	-
07b	Rev	CAG CTG CAA CAG TTA TCA ACG TT	-
07ab	Probe	TCC TCA CTT CTC CAC CCC TAG TTA AAC A	5'-FAM 3'-BHQ1

08b	Fw	GCT GGA TGC CTC ACT GAT GTT	-
08ab	Rev	TGG GAA GGA TGC ATA TGA TCT G	-
08ab	Probe	CTC CCA ACC CCC ATT TCT GCC TG	5'-FAM 3'-BHQ1
09ab	Fw	GGG CAC CCG TGT GAG TTT T	-
09b	Rev	CAG CTT GTC TGC TTT CTG CTG	-
09ab	Probe	TGG AGG ATT TCT CCC CTG CTT CAG ACA G	5'-FAM 3'-BHQ1
10a	Fw	GCC ACA AGA GAC TCA G	-
10b	Fw	TTA GAG CCA CAA GAG ACA ACC AG	-
10ab	Rev	TGG CTT CCT TGA GGT GGA AT	-
10ab	Probe	CAG TGT CCC ACT CAA GTA CTC CTT TGG CA	5'-FAM 3'-BHQ1
11a	Fw	TAG GAT TCA ACC CTG GAA GC	-
11ab	Rev	CCA GCA TGC ACC TGA CTA ACA	-
11ab	Probe	CAA GGC TTC CTC AAT TCT CCA CCC TTC C	5'-FAM 3'-BHQ1
12b	Fw	TGG ATG CCT CAC TGA TCC	-
12ab	Rev	TGA TCT GAC AGG CAG AAA TGG G	-
12ab	Probe	CTA CTT CCA CAG CTT CAA CTA TGT TGT TTA CCT TGC C	5'-FAM 3'-BHQ1
16a	Fw	GAT TAA TTC ATG TGT GAT CTG CT	-
16ab	Rev	TGT GGC CCC ATT TCC AGA	-
16ab	Probe	TTC ACT AGC AAG CAG TGA CAC AGA TAC AAC AGG	5'-FAM 3'-BHQ1
17b	Fw	ACA GAA ATG ATT TGG GAG GAT	-
17ab	Rev	CCA GCA CAC TGA ACA TTT GCT CTT	-
17ab	Probe	CCT GCA TGA CTT CTG AGG CTT TCT TGC C	5'-FAM 3'-BHQ1
24b	Fw	GTC ACA TTT TCA GGC CCT TCT AAT AG	-
24ab	Rev	TTG GGA GGG TTC AAG ACT TCA G	-
24ab	Probe	CCT TTT GCT GTT TCT GCC ATA TTT GTA GTT ACT TCC TC	5'-FAM 3'-BHQ1
mbl	Fw	TTT GTT CTC ACT GCC ACC	-
mbl	Rev	GGC ACT ATG ATG AGC AGT GGG	-
mbl	Probe	AAA GCA TGT TTA TAG TCT TCC AGC AGC AAC G	5'-FAM 3'-BHQ1
HCK	Fw	TAT TAG CAC CAT CCA TAG GAG GCT T	-
HCK	Rev	GTT AGG GAA AGT GGA GCG GAA G	-
HCK	Probe	TAA CGC GTC CAC CAA GGA TGC GAA	5'-HEX 3'-BHQ1
Y	Fw	AAC TCA CCT CCA ACA CAT ACT CCA C	-
Y	Rev	TTC ATG ATG AAA TCT GCT TTT TGT TT	-
Y	Probe	CAG CCA CCA GAA TTA TCT CCA AGC TCT CTG CA	5'-FAM 3'-BHQ1
eGFP/Cer	Fw	CAG GAG CGC ACC ATC TTC TT	-
eGFP/Cer	Rev	AGG GTG TCG CCC TCG AAC	-
eGFP/Cer	Probe	CTA CAA GAC CCG CGC CGA GGT GA	5'-FAM 3'-BHQ1

8.3 Gating strategies

8.3.1 Gating strategy sort maternal NK cells into subgroups

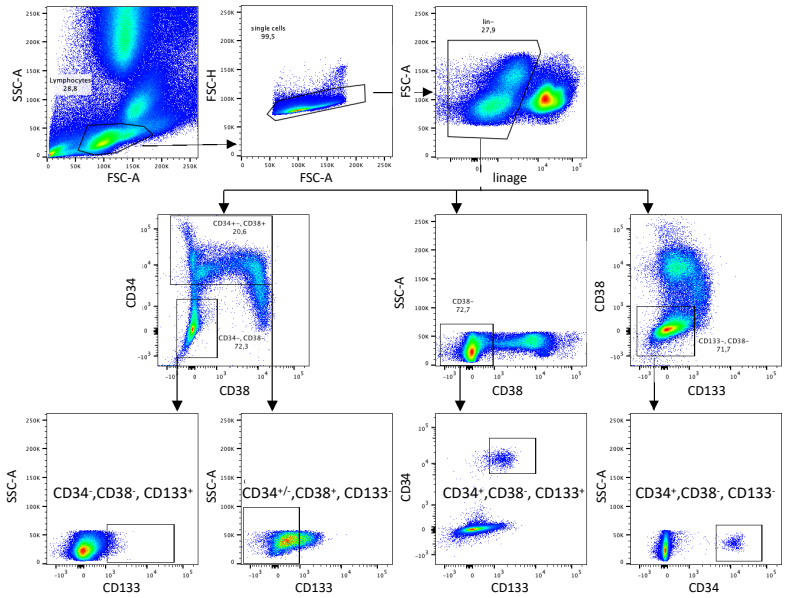

Figure 31: Gating strategy for sort of maternal NK cells into subgroups. Depicted is one representative example.

8.3.2 Gating strategy KIR phenotyping

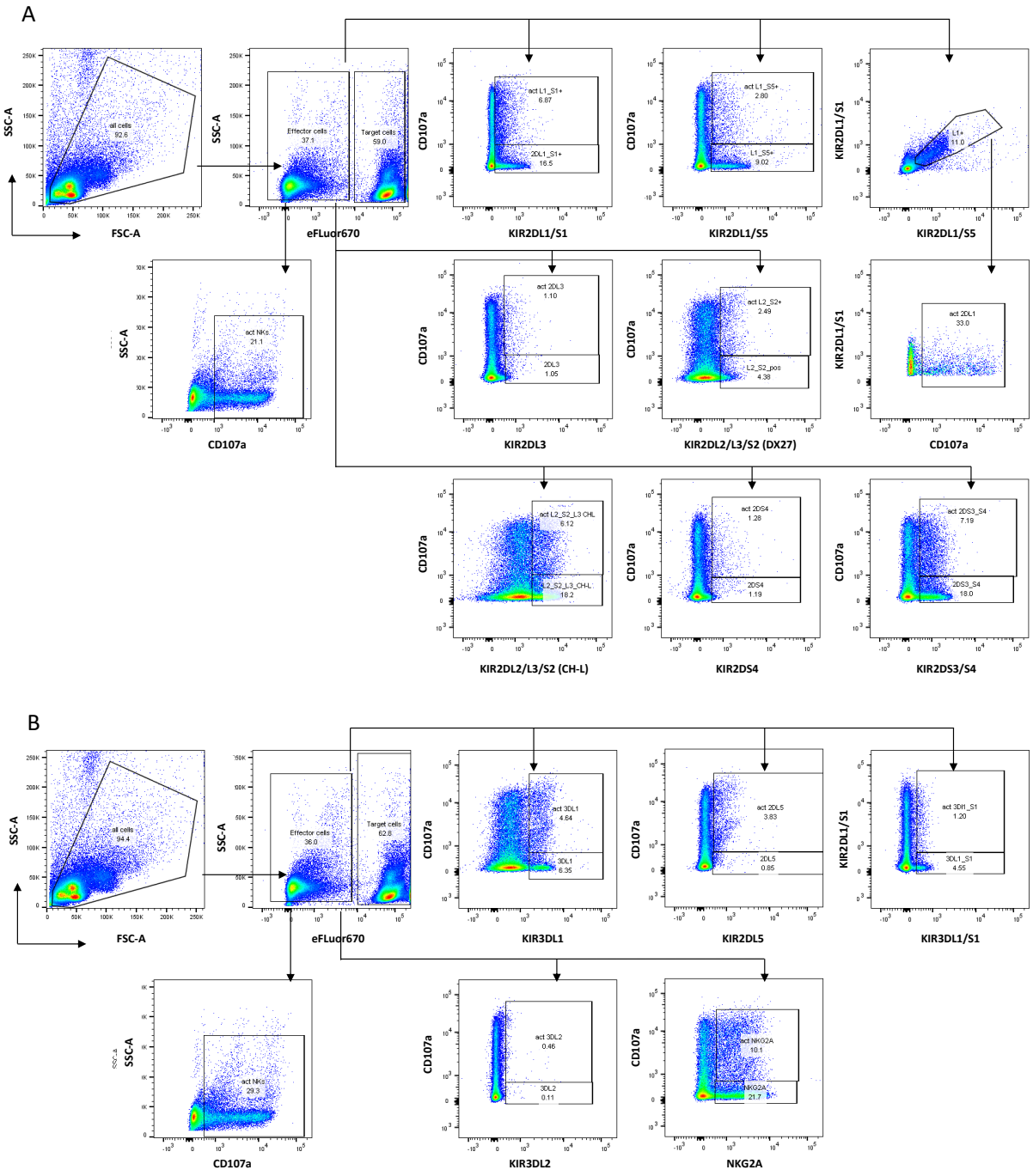

Figure 32: Gating strategy for determination of KIR phenotypes. Depicted is one representative example for gating of (A) KIR2DL panel and (B) KIR3DL panel.

8.4 List of n values from statistical analyses.

Table 37: n values to figure 10 - 15.

Figure	Group	N		
10 A	Female	23		
	Male	28		
10 C	AML	2		
	c-ALL	28		
	T-ALL	2		
	B-ALL	9		
	other	10		
11 A	HLA-C	Child	Mother	Father
	C1/C1	23	24	16
	C1/C2	37	38	13
	C2/C2	10	7	4
11 B	FM+/-	Child	Mother	Father
	FM-	32	32	13
	FM+	19	19	7
11 D	FM+/-	Match	Mismatch	
	FM- mother	11	21	
	FM+ mother	14	4	
	FM- father	7	6	
	FM+ father	4	3	
11 E	FM+/-	non-self	missing-self	
	FM-	8	13	
	FM+	1	3	
11 F	Child	C1/C1	C1/C2	C2/C2
	Mother C1/C1	11	4	0
	Mother C1/C2	10	15	7
	Mother C2/C2	0	4	1
11 G	Match	26		
	Mismatch	25		
11 H	C1/C1 match	11		
	C1/C2 match	15		
	non-self	9		
	missing self	16		
12 A	FM +/-	2DL3+	2DL3-	
	FM-	31	2	
	FM+	16	6	
12 B	All	51		
12 C	2DL2 only	14		
	2DL2 and 2DL3	29		
	2DL3 only	8		

Figure	Group	N			
12 D+E	FM +/-	Child		Mother	
	FM-	32		32	
	FM+	19		19	
12 F	KIR gene motif	Child		Mother	
	A/A cen	13		16	
	A/B cen	29		31	
	B/B cen	9		4	
	A/A tel	25		27	
	A/B tel	24		23	
	B/B tel	2		1	
13B	FM +/-	Child		Mother	
	FM-	32		32	
	FM+	19		19	
13 C	B content score	Child	Mother	Father	
	0	15	10	8	
	1	27	30	14	
	2	26	26	3	
	3+4	2	4	3	
13 D + E	B content score	Child		Mother	
	0	9		5	
	1	21		21	
	2	20		21	
	3+4	1		4	
16 A+B	FM-	23			
	FM+	10			
16 C		Match		Mismatch	
	FM-	11		12	
	FM+	8		2	
14	KIR	FM-	FM+	FM- activated	FM+ activated
	All act	-	-	42	10
	2DL1/S1	42	10	42	10
	2DL1/S5	30	8	30	8
	2DL1	39	9	39	9
	2DL2/3/S2(DX27)	36	10	36	10
	2DL3	42	10	42	10
	2DL2/3/S2(CH-L)	18	3	18	3
	2DL5	31	9	31	9
	2DS4	41	10	41	10
	2DS3/S4	31	9	31	9
	NKG2A	26	7	26	7

Table 38: n values to figure 16 and 17.

Figure	Group	N					
		C1/C1 match		C1/C2 match		mismatched	
		FM-	FM+	FM-	FM+	FM-	FM+
15	All act	2	7	9	2	16	2
	Act 2DL1/S1	2	7	9	2	16	2
	Act 2DL1/S5	1	6	9	1	13	2
	Act 2DL1	1	7	9	1	16	2
	Act 2DL2/L3/S2DX27	2	7	7	2	13	2
	Act 2DL3	2	7	9	2	16	2
	Not activated	-	-	-	-	-	-
	2DL1/S1	2	7	9	2	16	2
	2DL1/S5	1	6	9	1	13	2
	2DL1	1	7	9	1	16	2
	2DL2/L3/S2 DX27	2	7	7	2	13	2
	2DL3	2	7	9	2	16	2
18 A	Mother	36					
	Father	15					
18 B	FM-	23					
	FM+	13					
18 C		Mother		Father			
	Match	25		12			
	Mismatch	20		9			
18 D		FM-		FM+			
	Match	11		10			
	Mismatch	12		2			
18 E		Blast		K562			
	HLA-C1/C1	19		15			
	HLA-C1/C2	16		15			
	HLA-C2/C2	4		4			
18 F	Cen A/A	16					
	Cen A/B	23					
	Cen B/B	5					
	Tel A/A	23					
	Cel A/B	21					
	Tel B/B	0					
18 G	2DL2+	4					
	2DL2/L3+	19					
	2DL3+	12					
18 H	0	7					
	1	21					
	2	15					
	3+4	1					
18 I	0	0					
	1	4					
	2	7					
	3+4	1					
18 J	0	4					
	1	13					
	2	6					
	3+4	1					
18 K	Haplotype	FM-		FM+			
	A	4		0			
	Bx	19		12			

9. Curriculum vitae

Der Lebenslauf entfällt aus datenschutzrechtlichen Gründen.

10. Acknowledgement

Zuerst möchte ich mich ganz besonders bei Prof Dr. Ingo Müller dafür bedanken, dass ich dieses interessante und abwechslungsreiche Thema bearbeiten durfte. Danke, für die anregenden und hilfreichen Diskussionen, sowie für die Möglichkeit, mich durch die Teilnahme an nationalen und auch internationalen Kongressen wissenschaftlich weiter zu entwickeln.
Ganz besonders möchte ich mich auch bei Prof. Dr. Wolfram Brune bedanken, für die Begutachtung meiner Arbeit, sowie die hilfreichen Anregungen.

Besonders herzlich möchte ich mich bei Dr. Anne Kruchen bedanken. Zuerst für das mir entgegengebrachte Vertrauen, dass ich das von ihr begonnen Projekt weiter erforschen durfte. Des Weiteren danke ich ihr für ihre Geduld, Zeit und motivierenden/aufmunternden Worte, wenn die NK Zellen mal wieder nicht so wollten wie sie „doch“ sollten.
Ein großes Danke geht auch an PD Dr. Kerstin Cornils, für die Unterstützung bei Fragen jegliche Art bezüglich Klonierungen und viralen Vektoren.

Ein großes Danke geht an die gesamte AG Müller (Annika, Bernd, Frauke, Johannes, Jaqui, Kerstin S., Laura, Luise, Marianne, Stefan und Vany) für die tolle und hilfsbereite Atmosphäre in der Gruppe. Danke für die unterhaltsamen Stunden (mit guter Musik) in der rechten Zellkultur oder auch im Geräteraum/Büro, die für den nötigen Spaß und die gute Stimmung im Laboralltag gesorgt haben. Auch bei allen im Geräteraum, den Schüllers, hierbei ganz besonders Dörthe, möchte ich mich herzlich bedanken. Vor allem für die Hilfsbereitschaft, die netten Mittagspausen und insgesamt tolle und schöne Zeit, sowie den Spaß bei den Unternehmungen außerhalb des Instituts.

Bei dem gesamten Team des Forschungsinstitut Kinderkrebs-Zentrum Hamburg möchte ich mich für die nette und stets hilfsbereite Atmosphäre bedanken, sowie der Else Kröner-Fresenius-Stiftung und der Fördergemeinschaft Kinderkrebs-Zentrum Hamburg e. V. für die weitere Finanzierung.
Prof. Dr. Boris Fehse und Anita Badbaran danke ich für ihre Unterstützung mit der ddPCR Etablierung. Der Routine Diagnostik danke ich für die Möglichkeit zur Nutzung der Labore und der AG Altfeld für die Hilfe bei dem Erstellen des KIR Panels, sowie für die HLA-C Zelllinien.

Zu guter Letzt möchte ich mich sehr bei meiner Familie und meinen Freunden bedanken. Besonders Mama, Papa, Anni, Becci und Chrisi, sowie Marc danke ich von ganzem Herzen für ihre Unterstützung, die nötige Ablenkung, sowie die ermunternden Worte!

11. Eidesstattliche Versicherung

Hiermit versichere ich an Eides statt, die vorliegende Dissertation selbst verfasst und keine anderen als die angegebenen Hilfsmittel benutzt zu haben. Die eingereichte schriftliche Fassung entspricht der auf dem elektronischen Speichermedium. Ich versichere, dass diese Dissertation nicht in einem früheren Promotionsverfahren eingereicht wurde.

24.09.2020

Datum	Unterschrift